EPFL

Aliphatic Carboxylic Acids as Coupling Partners in Carbon-Heteroatom Bond-Forming Reactions

Runze MAO

■ École
polytechnique
fédérale
de Lausanne

2020

"Among what matters the most

is matter itself"

K. C. Nicolaou

Acknowledgments

Abstract

Carboxylic acids are one of the most suitable starting materials for synthesis. They are readily available and therefore inexpensive, stable and non-toxic. Many carboxylic acids can be obtained directly from natural resources, thus avoiding the extraction of fossil resources, such as oil or natural gas, in the production of chemicals. Furthermore, renewable carboxylic acids derived from biomass have a wide structural diversity (e.g., amino acids, fatty acids and sugar acids), which not only holds greater potential for the synthesis of complex molecules, but also advances the development of green chemistry.

In this context, this thesis aims at establishing new carbon-heteroatom coupling reactions with carboxylic acids as versatile coupling partners. These reactions are hitherto unknown, which not only fill some of the gaps in synthetic organic chemistry, but also provide solutions for the rapid assembly of bioactive molecules.

In order to overcome the challenge of forming $C(sp^3)$-heteroatom bonds, Chapters 4, 5 and 6 detail the development of photoredox/copper bi-catalytic systems and their applications in decarboxylative $C(sp^3)$-N and $C(sp^3)$-O coupling reactions. These methods are not only compatible with numerous functional groups, but also allow for rapid late-stage functionalization. More importantly, these methods can simplify the pathway for building drug core skeletons, highlighting the potential of these methods to expedite drug discovery.

To bridge the disconnection in the synthesis of trifluoromethylthioesters from carboxylic acids, Chapter 7 describes the establishment of a "umpolung" strategy and its application in the conversion of carboxylic acids to trifluoromethylthioesters. This approach provides the most concise synthetic pathway to date for the synthesis of trifluoromethylthioesters, which not only accommodates a variety of functional groups, but also allows for the rapid functionalization of carboxylic acid-containing natural products and drug molecules.

In summary, this thesis illustrates how novel catalytic methods can be used to convert inexpensive, readily available and environmentally benign aliphatic carboxylic acids into high value-added compounds.

Résumé

Les acides carboxyliques sont l'une des matières premières les plus appropriées pour la synthèse. Ils sont facilement disponibles et donc peu coûteux, stables et non toxiques. De nombreux acides carboxyliques peuvent être obtenus directement à partir de ressources naturelles, ce qui permet d'éviter l'extraction de ressources fossiles, comme le pétrole ou le gaz naturel, dans la production de produits chimiques. En outre, les acides carboxyliques renouvelables dérivés de la biomasse présentent une grande diversité structurelle (par exemple, des acides aminés, des acides gras et des acides de sucre), ce qui non seulement offre un plus grand potentiel pour la synthèse de molécules complexes, mais fait également progresser le développement de la chimie verte.

Dans ce contexte, cette thèse vise à établir de nouvelles réactions de couplage carbone-hétéroatome avec les acides carboxyliques comme partenaires de couplage polyvalents. Ces réactions sont jusqu'à présent inconnues, qui non seulement comblent certaines lacunes de la chimie organique synthétique, mais fournissent également des solutions pour l'assemblage rapide de molécules bioactives.

Afin de surmonter le défi de la formation de liaisons $C(sp^3)$-hétéroatomes, les chapitres 4, 5 et 6 détaillent le développement de systèmes bi-catalytiques photorédox/cuivre et leurs applications dans les réactions de couplage $C(sp^3)$-N et $C(sp^3)$-O décarboxylatives. Ces méthodes sont non seulement compatibles avec de nombreux groupes fonctionnels, mais elles permettent également une fonctionnalisation rapide en phase avancée. Plus important encore, ces méthodes peuvent simplifier la voie de construction des squelettes de base des médicaments, ce qui met en évidence le potentiel de ces méthodes pour accélérer la découverte de médicaments.

Pour combler la déconnexion dans la synthèse des trifluorométhylthioesters des acides carboxyliques, le chapitre 7 décrit l'établissement d'une stratégie de "umpolung" et son application dans la conversion des acides carboxyliques en trifluorométhylthioesters. Cette approche fournit la voie de synthèse la plus concise à ce jour pour la synthèse des trifluorométhylthioesters, qui non seulement prend en compte une variété de groupes fonctionnels, mais permet également la transformation rapide de produits naturels contenant des acides carboxyliques et de molécules médicamenteuses.

En résumé, cette thèse illustre comment de nouvelles méthodes catalytiques peuvent être utilisées pour convertir des acides carboxyliques aliphatiques peu coûteux, facilement disponibles et sans danger pour l'environnement en composés à haute valeur ajoutée.

Mots-clés: catalyse photoredox, catalyse au cuivre, acides carboxyliques, decarboxylation, chimie radicalaire, couplage C-N, couplage C-O, désoxygénation, trifluorométhylthiolation, umpolung, thioesters de trifluorométhyle.

List of Symbols and Abbreviations

Ac	acetyl
acac	acetylacetonate
Ad	adamantyl
Ar	aryl
BDE	bond-dissociation energy
bpy	2,2'-bipyridine
Bn	benzyl
Boc	*tert*-butyloxycarbonyl
Bu	*n*-butyl
cat.	catalyst
cod	1,4-cyclooctadiene
CV	cyclic voltammetry
Cy	cyclohexyl
DABCO	1,4-diazabicyclo[2.2.2]octane
DBU	1,8-diazabicyclo(5.4.0)undec-7-ene
DCE	1,2-dichloroethane
DCM	dichloromethane
DFT	density-functional theory
diglyme	bis(2-methoxyethyl) ether
dtbpy	4,4'-di-*tert*-butyl-2,2'-bipyridine
DMA	*N,N*-dimethylacetamide
DME	1,2-dimethoxyethane
DMF	*N,N*-dimethylformamide

dppe	1,2-bis(diphenylphosphino)ethane	
dppf	1,1′-bis(diphenylphosphino)ferrocene	
d.r.	diastereomeric ratio	
ee	enantiomeric excess	
equiv.	equivalent	
ESI	electrospray Ionization	
Et	ethyl	
eT	energy transfer	
EWG	electron-withdrawing group	
g	gram	
GC	gas chromatography	
h	hour	
HRMS	high-resolution mass spectrometry	
i-	*iso-*	
LED	light-emitting diode	
m	meter	
m-	*meta-*	
Me	methyl	
min	minute	
N-	nitrogen-	
NHPI	*N*−(acyloxy)phthalimides	
NMP	*N*-methylpyrrolidone	
NMR	nuclear magnetic resonance	
Nu	nucleophile	
o-	*ortho*	

O-	oxygen-
p-	*para-*
PC	photocatalyst
phen	1,10-phenanthroline
ppy	phenylpyridine
Pr	propyl
Py	pyridine
RT	room temperature
SET	single electron transfer
SCE	saturated calomel electrode
Tf	trifluoromethanesulfonyl
THF	tetrahydrofuran
TLC	thin-layer chromatography
Tol	tolyl

x

Table of Content

Chapter 1

Introduction

1.1   Introduction

Among what matters the most is matter itself.[1] It is, therefore, not a surprise that chemistry, the science of matter, is considered by many as the central science bridging physics and biology. Its power stems from its ability to analyze and synthesize materials from atoms and other, more or less complex, molecules. The latter practice, synthesis, is of paramount importance to our well-being, underpinning several fields of science, including drug discovery, chemical biology or materials science. Innovations in synthetic chemistry have enabled the discovery of many breakthroughs in science and technology, which have been critical in fostering economic growth and improving our quality of life. In modern society, continued innovations in synthetic chemistry are required to support and drive the discovery of science's next wave.[2]

Beginning in the 1960s, E. J. Corey formalized the concept of retrosynthetic analysis: beginning with the product and choosing suitable disconnections recursively.[3] Not surprisingly, novel synthetic methods not only allow us to achieve previously unattainable transformations, but also expand how we design and construct molecules. Therefore, attracted by the art of molecular architecture, our group's long-term scientific interests have focused on developing new synthetic methodologies to obtain high value-added molecules from readily available and inexpensive raw materials.

Over the past century, carbon-heteroatom bonds, especially carbon-nitrogen, carbon-oxygen, and carbon-sulfur bonds, have been gaining attention from chemists due to their prevalence in many scientific fields. At the same time, aliphatic carboxylic acids are regarded as an ideal set of starting materials due to their easy availability, low cost, and environmental friendliness. Applying one of the golden rules of synthetic methods - the production of complex or high value-added organic compounds from readily available and inexpensive feedstocks - the use of aliphatic carboxylic acids to construct $C(sp^3)$-heteroatom bonds should be very useful. Surprisingly, however, as of 2016, the use of aliphatic carboxylic acids as coupling partners in carbon-heteroatom bond-forming reactions was still in its infancy. This served as an inspiration to initiate related work with great motivation.

Following this lead, Chapter 2 focuses on the background and significance of the relevant fields to demonstrate the latest advances in such areas. Followed by Chapter 3, which introduces the goals of my Ph.D. research. Consequently, the establishment of two synthetic systems, namely (1) decarboxylative $C(sp^3)$-heteroatom bond-forming reactions catalyzed by synergistic

photoredox and copper catalysis (Chapters 4-6) and (2) deoxygenative trifluoromethylthiolation of carboxylic acids (Chapter 7), will be described in detail. Also, we will detail the applications of the former strategy in the construction of diverse chemical bonds, including (1) decarboxylative C(sp^3)-N coupling reactions (Chapter 4); (2) cross-coupling of alkyl redox-active esters with benzophenone imines (Chapter 5); and (3) decarboxylative C(sp^3)-O cross-coupling reactions (Chapter 6). Finally, a general conclusion will be given in Chapter 8, outlining the problems addressed in the thesis as well as the applications. Besides, future perspectives and possible follow-up studies will be further elaborated in Chapter 8.

Chapter 2

Background and Significance

2.1 *N*-hydroxyphthalimide esters as redox-active esters in cross-coupling reactions

2.1.1 Introduction

Transition metal-catalyzed cross-coupling reactions represent one of the most widely used methods in synthetic organic chemistry. The power of these transformations has mostly been demonstrated by utilizing diverse $C(sp^2)$-aryl and alkenyl electrophiles (typically their halides and pseudo halides).[4] However, transition metal-catalyzed cross-coupling reactions using alkyl halides are largely underdeveloped and remain challenging, probably due to difficulties in oxidative addition or reductive elimination, as well as the possibility of undergoing β-hydrogen elimination (Figure 1).[5-7]

In this regard, aliphatic carboxylic acids and their derivatives (typically redox-active esters) have emerged as more attractive coupling partners with a distinct nature compared to alkyl halides. Carboxylic acids are inexpensive, stable, and are among the most ubiquitous organic molecules in nature. More importantly, carboxylic acids and their derivatives are activated in a very different way than aryl and alkyl halides.[8]
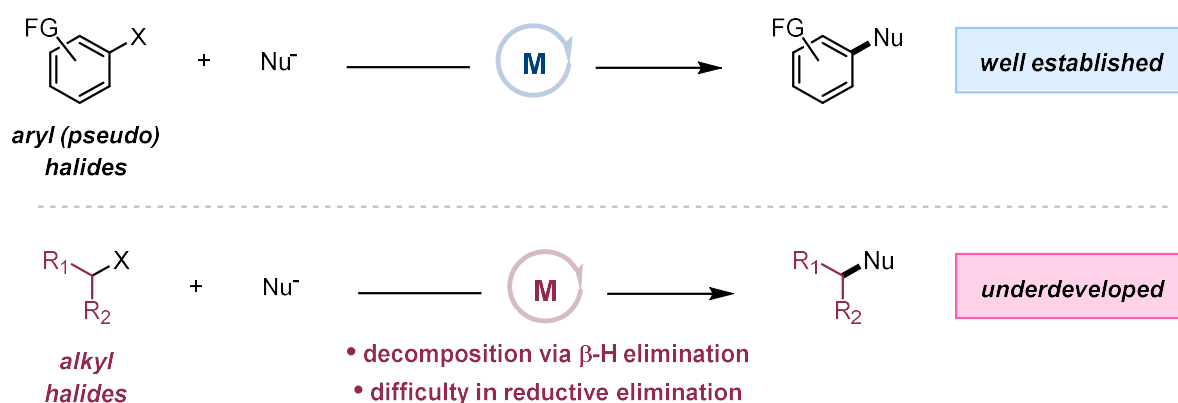
Figure 1 Comparison of transition metal-catalyzed cross-coupling of aryl (pseudo) halides (top) and alkyl electrophiles (bottom).

Recent years have witnessed a resurgence of interest in the field of decarboxylative cross-coupling reactions.[8-10] In particular, aryl and alkenyl carboxylic acids and their salts have been well-established as carbanion precursors in a large number of decarboxylative cross-coupling

reactions.[11-14] These transformations are usually mediated by a nucleophilic organometallic intermediate that is formed by transition metal-catalyzed CO_2 extrusion.[15] Apart from decarboxylative cross-couplings with carbanion intermediates, radical-mediated couplings have also been well explored. The latter includes two common types of activation: (1) Direct oxidative decarboxylation of carboxylic acids in the presence of strong oxidants.[16-20] (2) Reductive decarboxylation using redox-active esters derived from carboxylic acids as substrates.[15] The former is more straightforward, but the use of strong oxidants tends to narrow the scope and may lead to more side products. In contrast, while the latter requires an additional step to activate the substrate, it has significant advantages over the former such as milder reaction conditions, broader substrate scopes, and more potential applications to use such methods to modify natural products and drug molecules.
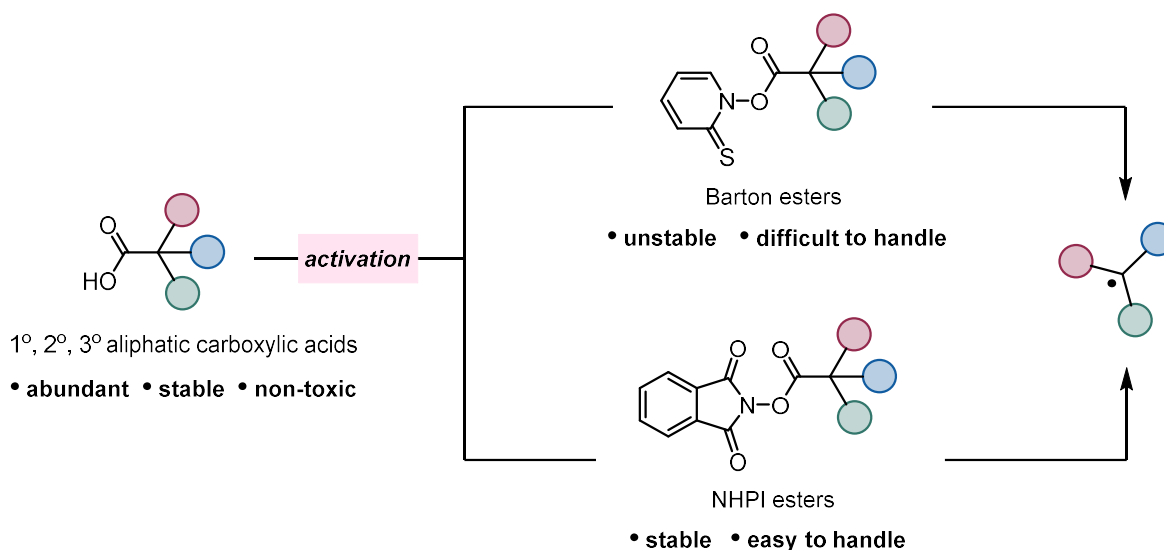
Figure 2 Representative radical precursors of reductive decarboxylative transformations.

In this context, Barton decarboxylation reactions that utilize *N*-hydroxy-2-thiopyridone esters (Barton esters) as substrates represent one of the earliest reductive decarboxylation methods. This reaction is named after its developer, the British chemist and Nobel laureate Sir Derek Barton (1918–1998).[21-23] However, such redox-active esters are frequently unstable and difficult to handle and store (Figure 2). Alternatively, in 1988, Okada, Okamoto, and Oda first demonstrated the use of *N*-(hydroxy)phthalimide (NHPI) esters, via reductive decarboxylation, to deliver alkyl

radicals (Figure 2).[24-25] NHPI esters are stable and can be prepared from the corresponding carboxylic acids and *N*-(hydroxy)phthalimide (NHPI) in one step. NHPI esters can be activated by reduction, via single-electron transfer (SET), to generate carbon dioxide, phthalimidyl anion, and the corresponding sp^3 carbon-centered radicals that can be used in several transformations (Figure 3). Interestingly, after the pioneering reports from Okada and co-workers, this field remained unexplored for almost two decades until a recent surge of interest in using NHPI esters as electrophiles in decarboxylative coupling reactions. Recently, significant advances have been achieved to demonstrate the utility of NHPI esters as efficient radical precursors in forging C-C and C-X (X = B, Si, Se, S, N) bonds. In this section, we detail the progress that has been made since the groundbreaking work reported by Okada and his colleagues in 1988. It is noteworthy that this section is divided into photoredox-catalyzed cross-couplings and transition metal-catalyzed cross-couplings based on the method of activation of NHPI esters. Within these broad categories, subsections are further divided according to the type of bond formation.
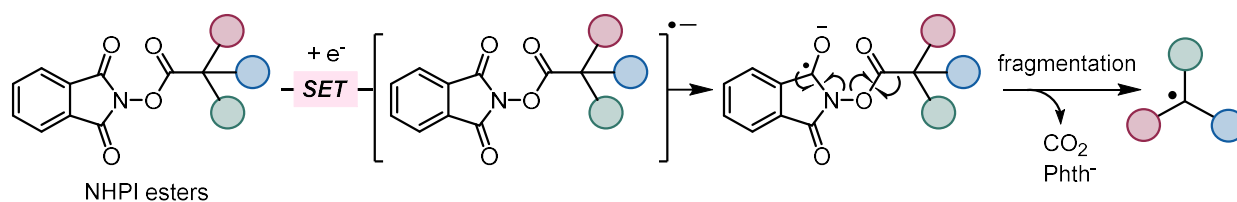
Figure 3 Redox reactivity of NHPI esters via single-electron transfer.

2.1.2   Activation modes and their mechanisms

It is important to understand the possible activation modes before elaborating on the cross-coupling reactions using *N*-(hydroxy)phthalimide (NHPI) esters as substrates. In this section, a brief description of the activation mode of NHPI esters will be demonstrated.

In the regime of photoredox-catalyzed and transition metal-catalyzed activation of NHPI esters, the activation mode of NHPI esters can be subdivided into four types: (1) photoredox-catalyzed reductive cross-coupling reactions; (2) redox-neutral photocatalytic cross-coupling reactions; (3) cross-coupling reactions via synergetic photoredox and metal catalysis; (4) transition-metal catalyzed cross-coupling reactions.

Notably, these four modes of activation cover almost all types of cross-coupling reactions of NHPI esters. Therefore, we will illustrate each coupling reaction of NHPI esters that occurs thereafter (sections 2.1.3 and 2.1.4) based on these modes. Moreover, a representative example of each reaction will be presented.

2.1.2.1 Photoredox-catalyzed reductive cross-coupling reactions (Mode A)

In this activation mode (Figure 4), the photoredox catalyst (PC) is initially transformed into its excited state PC* under visible light irradiation. The excited PC* can reduce NHPI esters via single-electron transfer (SET), delivering the oxidized PC$^+$ and the corresponding radical anion intermediate of the NHPI ester. Upon decarboxylation, a carbon-centered radical can be released from the radical anion intermediate with the removal of carbon dioxide and a phthalimidyl anion. In the meantime, the PC$^+$ cation can be reduced by an additional reductant (using Hantzsch ester for example) resulting in the release of a radical cation and regeneration of the PC. Finally, a hydrogen atom of the Hantzsch ester radical cation can be abstracted by the aforementioned carbon-centered radical or its derivatives (for example, using an olefin as a radical trap) to obtain the final product.
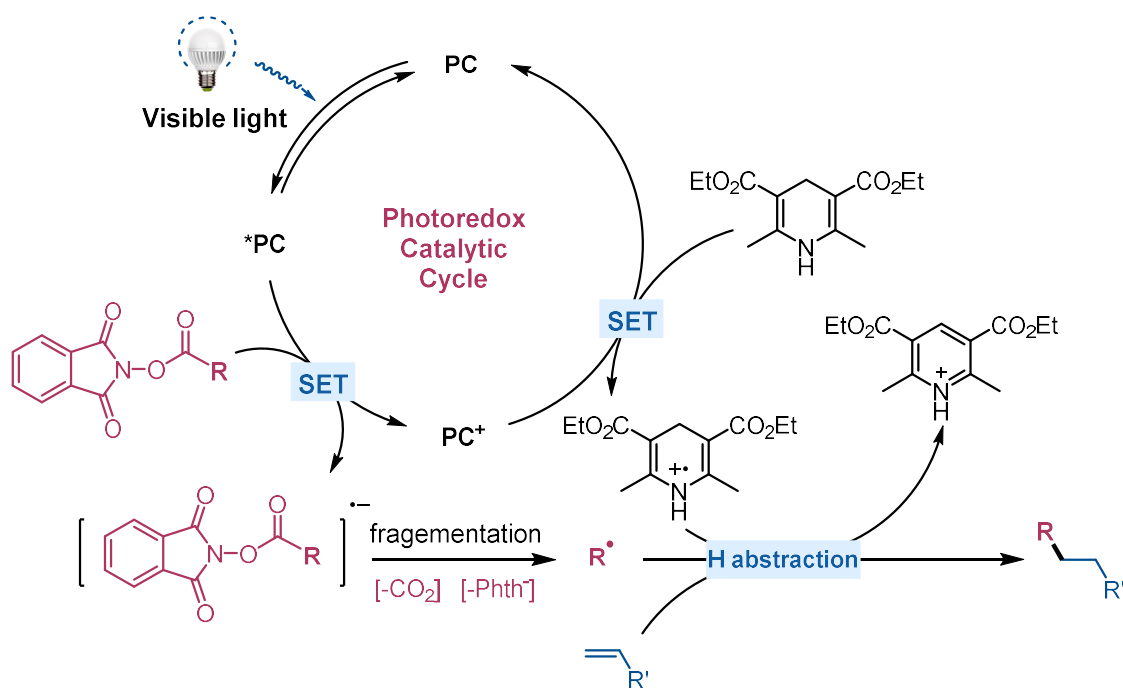
Figure 4 Mechanistic pathway of Photoredox-catalyzed reductive cross-coupling reaction

2.1.2.2 Cross-couplings via synergetic photoredox and metal catalysis (Mode B)

In this process, a tandem catalysis approach is applied (Figure 5). The generation of a carbon-centered radical and PC$^+$ proceeds in the same way as detailed in Mode A. Afterwards, a low-valent transition metal **I** can coordinate a nucleophile to form a metal complex **II**. Then PC$^+$ can interact with this low-valent metal complex **II** via single-electron transfer, regenerating PC and an oxidized M$^+$ complex **III**. The latter can trap the carbon-centered radical produced by the NHPI ester, giving an M^{2+} complex **IV**. The M^{2+} complex **IV** can consequently perform reductive elimination, delivering the final product **V** and regenerating the low-valent transition metal **I** as the precatalyst.
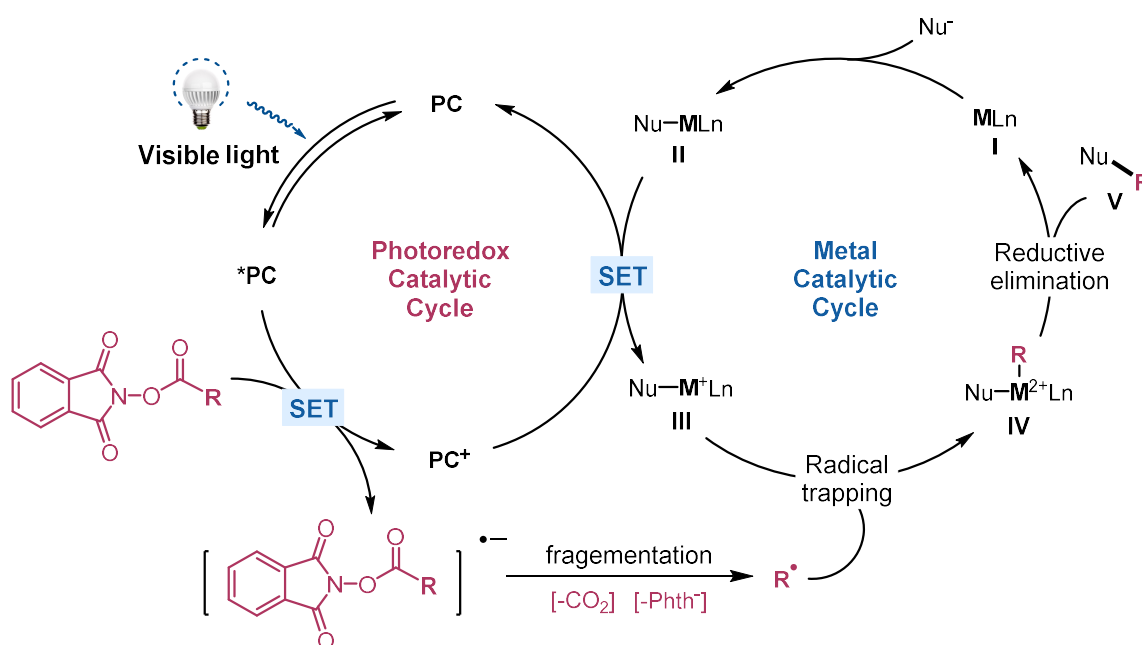
Figure 5 Mechanistic pathway of cross-couplings via synergetic photoredox and metal catalysis.

2.1.2.3 Redox-neutral photocatalytic cross-coupling reactions (Mode C)

In this activation mode (Figure 6), the most important feature is that the overall reaction is redox neutral. Upon irradiation of visible light, PC can be excited to PC*, the latter can then reduce an NHPI ester to generate a carbon-center radical and PC$^+$. The PC$^+$ can further oxidize the carbon-

center radical, forming a carbocation and regenerating the PC. Meanwhile, the carbocation can be trapped by additional nucleophiles to deliver the desired products **V**.

2.1.2.4   Transition-metal catalyzed cross-coupling reactions (Mode D)

Instead of using photoredox-catalyzed modes to activate the NHPI ester, Mode D uses a low-valent metal complex **II**, which is obtained via transmetalation of low-valent metal **I** with a nucleophile. Complex **II** then interacts with an NHPI ester and after transferring an electron from the low-valent metal complex **II** to an NHPI ester, M^+ complex **III** and a carbon-centered radical can be generated. The M^+ complex can be oxidized by the radical to form an M^{2+} complex **IV**. Finally, the high-valent metal complex **IV** performs reductive elimination to give the final product **V** and liberate the pre-catalyst **I** for the next catalytic cycle (Figure 6).
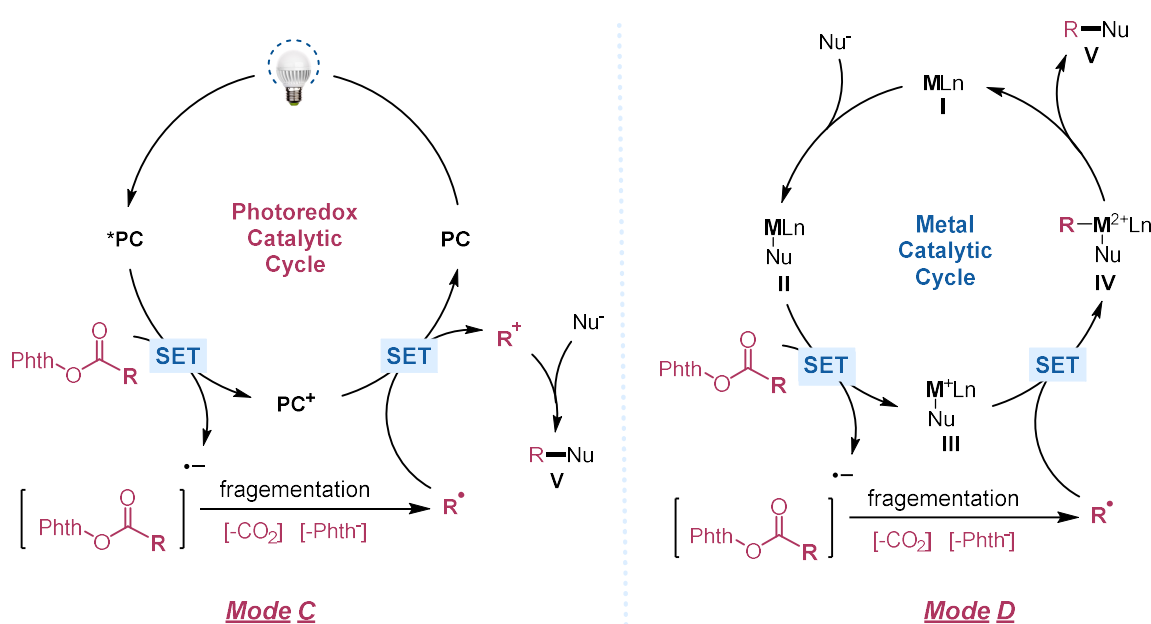
Figure 6   Mode C: Mechanistic pathway of cross-couplings via synergetic photoredox and metal catalysis; Mode D: Mechanistic pathway of transition-metal catalyzed cross-coupling reactions.

2.1.3   Photoredox-catalyzed decarboxylative cross-coupling reactions

2.1.3.1   C(sp^3)-C(sp^3) bond formation

In 1991, Okada and co-workers reported that NHPI esters can act as alkyl radical precursors via photoredox-catalyzed decarboxylation and undergo radical-mediated Michael addition to electron-deficient olefins. The reaction proceeds in the presence of visible light, photocatalyst [Ru(bpy)$_3$]Cl$_2$ (bpy=2,2'-bipyridine) and the hydrogen donor 1-benzyl-1,4-dihydronicotinamide (BNAH) to deliver the desired products in moderate yields (Table 1, entry 1).[25]

Consequent studies of NHPI esters as free radical precursors in cross-coupling reactions stalled for two decades. In 2012, Overman and co-workers rediscovered the potential of NHPI esters and applied NHPI ester **2.4** in constructing the key skeleton **2.6** of (-)-aplyviolene with α-chlorocyclopentenone **2.5** under slightly modified Okada conditions (Table 1, entry 2).[26] Importantly, under Okada's conditions, an unsatisfactory yield was obtained due to the formation of byproducts via reduction and hydrolysis. Modified conditions using 1 mol% [Ru(bpy)$_3$](BF$_4$)$_2$ as the photocatalyst, Hantzsch ester (1.5 equiv.) as the hydrogen donor, Hünig's base (*i*Pr$_2$EtN, 2.25 equiv.) as the reductive quencher, DCM as the solvent, under irradiation of blue LEDs, enable the formation of **2.6** in 61% yield and with d.r. value >20:1.

Besides reductive decarboxylative coupling with electron-deficient olefins, Overman and co-workers further expanded the strategy to vinylation and allylation with allylic and vinylic halides, affording new quaternary carbon centers in moderate to good yields (Table 1, entry 3). It is important to mention that even in the absence of the photocatalyst, the reaction still occurred without diminished yields, but with a significantly slower reaction rate.[27]

In a similar fashion, Hu and co-workers reported a photoredox-catalyzed decarboxylative allylation utilizing allyl sulfones as the allylating agent (Table 1, entry 4). The scope of this methodology is broad and tolerant to a variety of primary, secondary, tertiary, and α-heteroatom-substituted aliphatic acid-derived NHPI esters. Interestingly, the reaction can be conducted in both aqueous solutions and organic solvents under mild conditions at a fast rate (complete reaction within 30 min).[28]

In 2016, König and co-workers reported a metal-free photoredox-catalyzed decarboxylative alkylation of NHPI esters with electron-deficient alkenes. In the presence of organic photocatalyst (**OPC**) eosin Y and green light (535 nm), NHPI esters can be reduced to give alkyl radicals that are trapped by electron-deficient alkenes to forge new C(sp^3)-C(sp^3) bonds. Noteworthily, the

NHPI esters are made from biomass-derived chemical compounds, including naturally abundant amino acids, α-oxyacids, and fatty acids (Table 1, entry 5) which are available from renewable resources.[29]

Table 1   Photoredox-catalyzed C(sp3)-C(sp3) bond formation.

Entry	Representative substrates	Conditions	Product	Mode
1	**2.1** + **2.2**	[Ru(bpy)₃]Cl₂ (cat.) BNAH (1 equiv.) THF/H₂O or tBuOH/H₂O hv (> 460 nm)	**2.3** 68%	**A** Okada, 1991[25]
2	**2.4** + **2.5**	[Ru(bpy)₃](BF₄)₂ (1mol%) Hantzsch ester (1.5 equiv.) iPr₂NEt (2.25 equiv.) DCM, blue LEDs	**2.6** 61% (d.r.>20:1)	**A** Overman, 2012[26]
3	**2.7** + **2.8**	[Ru(bpy)₃](PF₆)₂ (1 mol%) Hantzsch ester (1.5 equiv.) iPr₂NEt (2.2 equiv.) DCM, RT, blue LEDs, 18 h	**2.9** 81%	**A** Overman, 2015[27]
4	**2.10** + **2.11**	[Ru(bpy)₃](PF₆)₂ (1 mol%) Hantzsch ester (1.5 equiv.) iPr₂NEt (1 equiv.) HCO₂H (1 equiv.) DCM, blue LEDs RT, 30 min	**2.12** 67%	**A** Hu, 2015[28]

5	**2.13** + **2.14**	Eosin Y (10 mol%) iPr$_2$NEt (2 equiv.) DCM (dry), RT 535 nm, air, 18 h	**2.15** 76%	**A** König, 2016[29]
6	**2.16** + **2.17** 1.5 equiv	[Ir(ppy)$_2$dtbpy]PF$_6$ (2.5 mol%) H$_2$O (25 equiv.) MeCN, 5 W blue LEDs RT, 12 h	**2.18** 78% (from dehydrocholic acid)	**C** Song, 2018[30]
7	**2.19** + **2.20**	[Ir(ppy)$_2$dtbpy]PF$_6$ (2 mol%) TsOH·H$_2$O (20 mol%) MeCN, 5 W blue LEDs RT, Ar, 24 h	**2.21** 77%	**C** Pan, 2017[31]
8	**2.22** + **2.23**	[Ir(ppy)$_2$dtbpy]PF$_6$ (1 mol%) H$_2$O (10 equiv.) pyridine (1.2 equiv.) MeCN, RT, blue LEDs	**2.24** 75%	**C** Xiao, 2018[32]
9	**2.22** + **2.25**	Eosin Y (2 mol%) TMEDA (1.5 equiv.) DMF, CFL (15 W) RT, 24 h	**2.26** 75%	**C** Guo, 2018[33]

[Ru(bpy)$_3$](PF$_6$)$_2$ [IrdF(CF$_3$)ppy$_2$](dtbpy)PF$_6$ [Ir(dtbbpy)(ppy)$_2$]PF$_6$

BNAH   TMEDA   Hantzsch ester
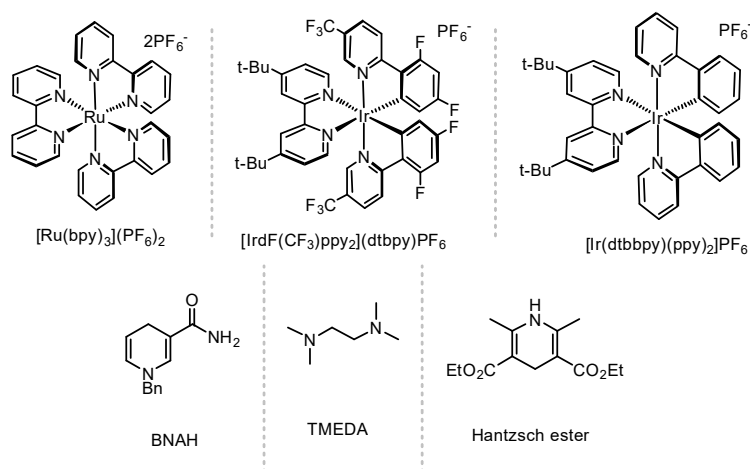
In 2018, Song and co-workers reported a photoredox-catalyzed decarboxylative alkylation of NHPI esters with silyl enol ethers. This method enables the synthesis of a diverse set of functionalized aryl alkyl ketones using NHPI esters as versatile alkyl radical source and tolerates primary, secondary, and tertiary aliphatic acid-derived NHPI esters (Table 1, entry 6). Moreover, the late-stage functionalization of natural products (the synthesis of **2.18** from **2.16** as representative transformation) and drug molecules showcases the practicality of this method.[30]

Cascade reactions can be designed to build complex molecules using NHPI esters as radical precursors as well. Pan and co-workers developed a methodology via a tandem alkylation-lactonization process, mediated by alkyl radicals generated from NHPI esters, towards the synthesis of alkyl-substituted lactones in moderate to good yields (Table 1, entry 7). This method tolerates a range of alkenoic acids and NHPI esters derived from primary, secondary, and tertiary aliphatic carboxylic acids.[31] Meanwhile, Xiao and co-workers also documented a facile and elegant cascade method to build various benzazepine derivatives from NHPI esters and acrylamide-tethered styrene derivatives (Table 1, entry 8).[32] Similarly, Guo and co-workers reported a photoredox-catalyzed decarboxylative cyclization of NHPI esters with vinyl azides to generate substituted phenanthridines (Table 1, entry 9).[33]

2.1.3.2 C(sp^3)-C(sp^2) bond formation

Natural α-amino acids and nitrogen-containing heterocycles are both readily available building blocks to demonstrate diverse biological activities. Conjugating these attractive subunits provide a great chance to discover bio-active molecules. In this regard, Fu and co-workers

documented a novel method to introduce *N*-protected α-amino acids and peptides to phenanthridine derivatives via radical addition (Table 2, entry 1).[34]

In a similar fashion, Fu and co-workers applied the merger of photoredox and phosphoric acid catalysis in the alkylation reactions of diverse nitrogen heteroarenes using α-amino acid-derived NHPI esters. Several examples utilizing dipeptide- and tripeptide-based NHPI esters were demonstrated to undergo alkylation reactions at the C-terminus smoothly, producing potentially bioactive molecules. Iridium-based photocatalyst (Ir cat.) with suitable redox potential and phosphoric acid as an acid co-catalyst (PA cat.) are crucial components for the success of this alkylation process (Table 2, entry 2).[35]

Building on previous work, the Fu group has further developed a photoredox-catalyzed Minisci-type alkylation approach. Such a method enables the use of primary, secondary, and tertiary aliphatic carboxylic acid-based NHPI esters as versatile alkyl radical precursors for the alkylation of nitrogen heteroarenes. A stoichiometric amount of Brønsted acid or catalytic amount of Lewis acid was required to promote the reaction (Table 2, entry 3).[36]
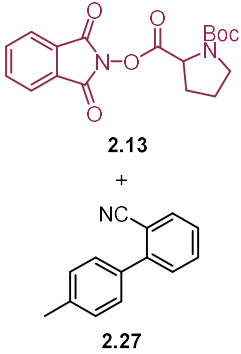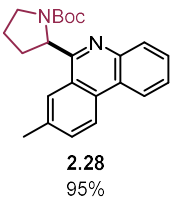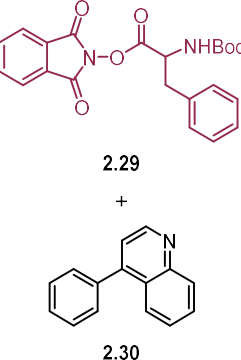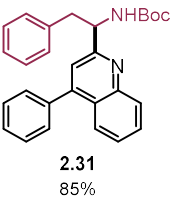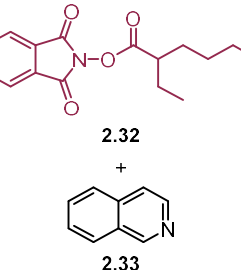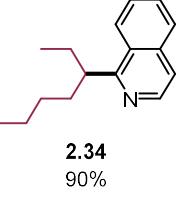
Duan and co-workers recently documented a photoredox-catalyzed decarboxylative cross-coupling of NHPI esters with cinnamic acids. This method allows for the couplings of a range of NHPI esters and cinnamic acids, yielding substituted alkenes in moderate to good yields and good stereoselectivity (the (*E*)-isomers dominate). Mild reaction conditions, ease of handling, and good tolerance of functional groups are the most important features of this method. However, these reactions require a stoichiometric amount of Lewis acid ($Mg(ClO_4)_2$) to activate the NHPI esters (Table 2, entry 4).[37]

Meanwhile, Xu, Zhang and co-workers reported a Ruthenium-based photoredox-catalyzed and 1,4-diazabicyclo[2.2.2]octane (DABCO)-promoted cross-coupling of aliphatic acid-derived NHPI esters and cinnamic acids, affording substituted alkene in decent yields and good stereoselectivity (the (*E*)-isomers dominate). Apart from primary, secondary, and tertiary aliphatic acid-derived NHPI esters, α-amino acids derivatives were also viable substrates to give the corresponding allylic amines in high stereoselectivity (Table 2, entry 5).[38]

Recently, Fu and co-workers documented a photoinduced palladium-catalyzed decarboxylative Heck-type reaction between aliphatic NHPI esters and styrene derivatives. The combination of $Pd(PPh_3)_2Cl_2$ with 4,5-bis(diphenylphosphino)-9,9-dimethylxanthene (Xantphos) can catalyze the reaction upon irradiation of blue LEDs, thus affording the desired Heck products

with high yields and stereoselectivity. A wide range of aliphatic acid-derived NHPI esters were suitable substrates that can be activated via a single-electron transfer from the palladium complex (Table 2, entry 6).[39]

Table 2 Photoredox-catalyzed $C(sp^3)$-$C(sp^2)$ bond formation.

Entry	Representative substrates	Conditions	Product	Mode
1	**2.13** + **2.27**	[Ru(bpy)$_3$]Cl$_2$ (1 mol%) iPr$_2$NEt (0.4 equiv.) K$_2$CO$_3$ (1.2 equiv.) DMF, RT, 2 h CFL (40 W)	**2.28** 95%	**A** Fu, 2016[34]
2	**2.29** + **2.30**	[Ir(dF(CF$_3$)ppy)$_2$dtbpy]PF$_6$ (2 mol%) **PA cat.** (10 mol%) DMA, blue LEDs (36 W) RT, Ar, 3 h	**2.31** 85%	**C** Fu, 2017[35]
3	**2.32** + **2.33**	[Ir(dF(CF$_3$)ppy)$_2$dtbpy]PF$_6$ (2 mol%) TFA (2 equiv.) DMA, blue LEDs (36 W) RT, Ar, 6 h	**2.34** 90%	**C** Fu, 2017[36]

4	**2.35** + **2.36**	*fac*-Ir(ppy)₃ (1 mol%) Mg(ClO₄)₂ (2 equiv.) NMP, CFL(23 W) RT, N₂, 36 h	**2.37** 75% (E/Z>99:1)	**C** Duan, 2017[37]
5	**2.22** + **2.38**	[Ru(bpy)₃]Cl₂·6H₂O (1 mol%) DABCO (50 mol%) DMA, blue LEDs (36 W) RT, 12 h	**2.39** 92% (E/Z=98:2)	**A** Xu and Zhang, 2017[38]
6	**2.22** + **2.40**	Pd(PPh₃)₂Cl₂ (5 mol%) Xantphos (6 mol%) K₂CO₃ (1.2 equiv.) H₂O (1 equiv.) DMA, blue LEDs (36 W) RT, Ar, 24 h	**2.39** 96% (E/Z=99:1)	**B** Fu, 2018[39]

fac-Ir(ppy)₃   [IrdF(CF₃)ppy₂)(dtbpy)PF₆   [Ir(dtbbpy)(ppy)₂]PF₆

(PA cat.)   Xantphos   DABCO

2.1.3.3 C(sp³)-C(sp) bond formation

Photoredox-catalyzed cross-coupling reactions between aliphatic acid-derived NHPI esters and alkynylation reagents have also been explored to construct C(sp³)-C(sp) bonds. In 2015, the Chen group reported a photoredox-catalyzed reductive cross-coupling method between NHPI

esters and alkynyl phenyl sulfones (for example, **2.42**), delivering alkyl-, aryl-, and silyl-substituted alkynes upon irradiation of blue LEDs at room temperature (Table 3, entry 1).[40]

Alternatively, Fu and co-workers developed a synergetic photoredox and copper catalysis to perform alkynylation of aliphatic acid-derived NHPI esters with aliphatic and aromatic terminal alkynes. This method is highlighted by its mild reaction conditions, high efficiency and no addition of additives or bases. However, the scope of the NHPI esters is limited to α-amino acid derivatives (Table 3, entry 2).[41]

Table 3   Photoredox-catalyzed C(sp^3)-C(sp) bond formation.

Entry	Representative substrates	Conditions	Product	Mode
1	**2.41** + **2.42**	[Ru(bpy)$_3$](PF$_6$)$_2$ (1 mol%) *i*Pr$_2$NEt (2.0 equiv.) Hantzsch ester (1.5 equiv.) DCM, RT, N$_2$, 0.5 h blue LEDs	**2.43** 76%	**A** Chen, 2015[40]
2	**2.44** + **2.45**	[Ru(bpy)$_3$]Cl$_2$ (1 mol%) CuI (10 mol%) DCM, RT, Ar, 6 h CFL (40 W)	**2.46** 89%	**B** Fu, 2017[41]
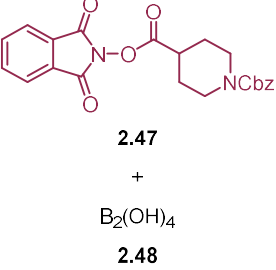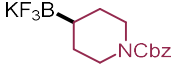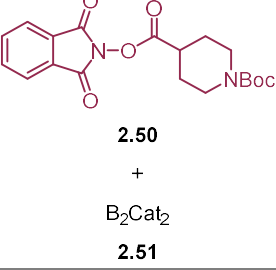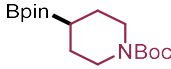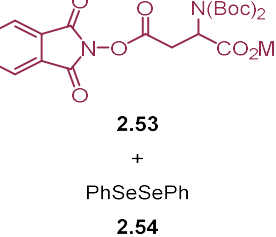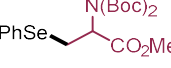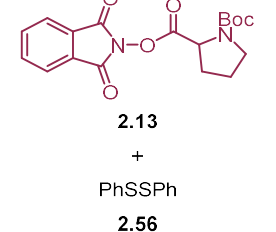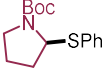
2.1.3.4   C(sp^3)-X (X=B, Se, S) bond formation

Although alkylboron compounds rarely exist in nature, they are an important class of building blocks and are widely used in the synthesis of complexes and functional materials. In this regard, the transformation of versatile aliphatic carboxylic acids to alkylboron compounds is of great interest to synthetic chemists. In 2017, Li and co-workers developed an elegant photoredox-

catalyzed decarboxylative borylation of aliphatic acid-derived NHPI esters in mild conditions. A set of primary and secondary alkyl tetrafluoborates and boronates were synthesized in good yields. The authors proposed a mechanistic pathway where the alkyl radicals derived from the corresponding NHPI esters react with the base-activated diboron species to give the desired organo-boron compounds (Table 4, entry 1).[42]

Table 4   Photoredox-catalyzed C(sp^3)-X (X=B, Se, S) bond formation.

Entry	Representative substrates	Conditions	Product	Mode
1	**2.47** + B$_2$(OH)$_4$ **2.48**	[Ir(ppy)$_2$dtbpy]PF$_6$ (1 mol%) DMF, 12 h, then KHF$_2$ CFL (45 W)	**2.49** 85%	**A** Li, 2017[42]
2	**2.50** + B$_2$Cat$_2$ **2.51**	Blue LEDs, DMA, 14 h then pinacol, Et$_3$N	**2.52** 91%	**A** Aggarwal, 2017[43]
3	**2.53** + PhSeSePh **2.54**	[Ru(bpy)$_3$](PF$_6$)$_2$ (1 mol%) iPr$_2$NEt (2.5 equiv.) Hantzsch ester (1.5 equiv.) THF/DCM, Ar, RT, 5 h, CFL (45 W)	**2.55** 82%	**A** Fu, 2016[44]
4	**2.13** + PhSSPh **2.56**	Cs$_2$CO$_3$ (1.5 equiv.) DMF, Ar, RT 0.5-48 h 40 W CFL	**2.57** 93%	**A** Fu, 2016[45]

Shortly after, Aggarwal and co-workers documented a conceptually similar photoredox-catalyzed metal-free decarboxylative borylation of aliphatic acid-derived NHPI esters, using bis(catecholato)diboron as the borylating reagent and *N,N*-dimethylacetamide (DMAc) as the solvent under irradiation of blue LEDs, and performing at room temperature. After the completion of the reaction, a simple work-up with pinacol and trimethylamine allows for the isolation of more stable pinacol borates via ligand exchange. This method can tolerate a broad range of primary, secondary, and tertiary aliphatic acid-derived NHPI esters as potential alkyl radical precursors (Table 4, entry 2).[43]

Carbon–sulfur bond formation is of great importance in organic synthesis because sulfur-containing compounds widely occur in natural products, bio-active molecules, and functional materials. In 2016, Fu and co-workers demonstrated a photoredox-catalyzed decarboxylative coupling strategy of using aliphatic acid-derived NHPI esters in the synthesis of chiral α-selenoamino acid derivatives (Table 4, entry 3).[44] Subsequentially, the same group developed a visible light-promoted arylthiolation of aliphatic acid-derived NHPI esters with aryl thiols. Notably, photocatalysts are not required in such transformations, and a wide range of aliphatic acid-derived NHPI esters, including amino acid-derived NHPI esters, are compatible under the standard conditions (Table 4, entry 3).[45]

In 2017, Fu and co-workers reported an intramolecular decarboxylative C(sp^3)-N bond cross-coupling of NHPI esters.[46] Upon irradiation of blue LEDs, a solution of NHPI esters in the presence of 10 mol % CuCN, 5 mol % 2,9-dimethyl-1,10-phenanthroline (neocuproine), and 15 mol % xantphos in 1,2-dichloroethane (DCE) at 5−10 °C can furnish the desired protected amine in moderate to high yields (Figure 7). Control experiments underlined the importance of light, CuCN, dmp, and xantphos for efficient C−N bond formation. Diverse functional groups were tolerated including olefins, halides, ethers, ketones, carbamates, and thiophenes. This method enables the transformation of primary (**2.58**, **2.59** and **2.62**), secondary (**2.60**), and natural product-derived NHPI esters (**2.61** and **2.63**) into protected amines, and representative examples are shown in Figure 7. However, this method seems to be very sensitive to steric bulk, showing no transformations of tertiary NHPI esters, and exhibiting sluggish transformations using sterically bulkier primary NHPI esters as substrates.
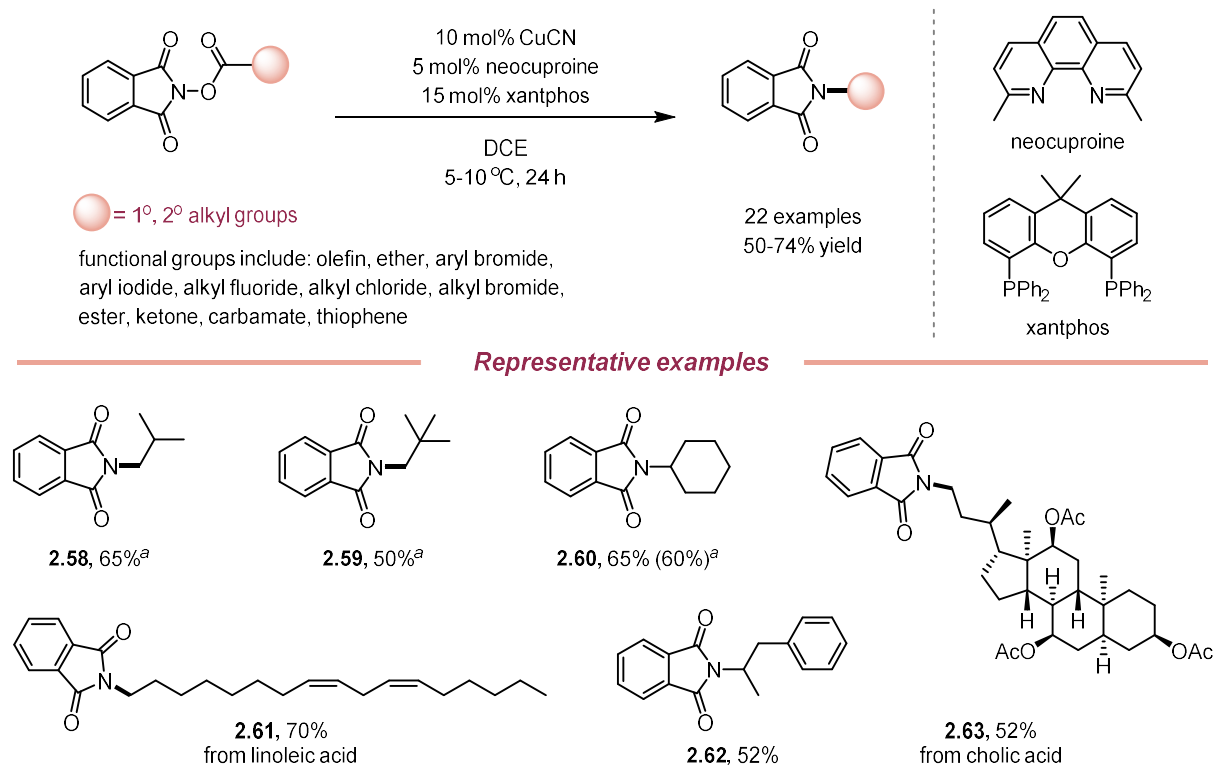
Figure 7 Photoinduced intramolecular decarboxylative C(sp³)–N bond formation of NHP ester. [a]Catalyst loading: 20 mol% CuCN, 10 mol% dmp, 30 mol % xantphos.

A proposed mechanism of this decarboxylative C(sp³)-N coupling transformation is shown in Figure 8. Initially. the precatalyst Cu^I complex **2.68** can absorb visible light, reaching its excited state **2.69**. The excited species Cu^I* (**2.69**) has a higher reduction potential that can reduce the NHPI ester to generate an alkyl radical and a Cu^{II}(phthalimide) complex **2.70**. Afterwards, the alkyl radical can react, either through a rebound process or via a cross-coupling pathway, with Cu^{II}(phthalimide) complex **2.70**, to obtain the desired product and regenerate the precatalyst Cu^I complex **2.68**.
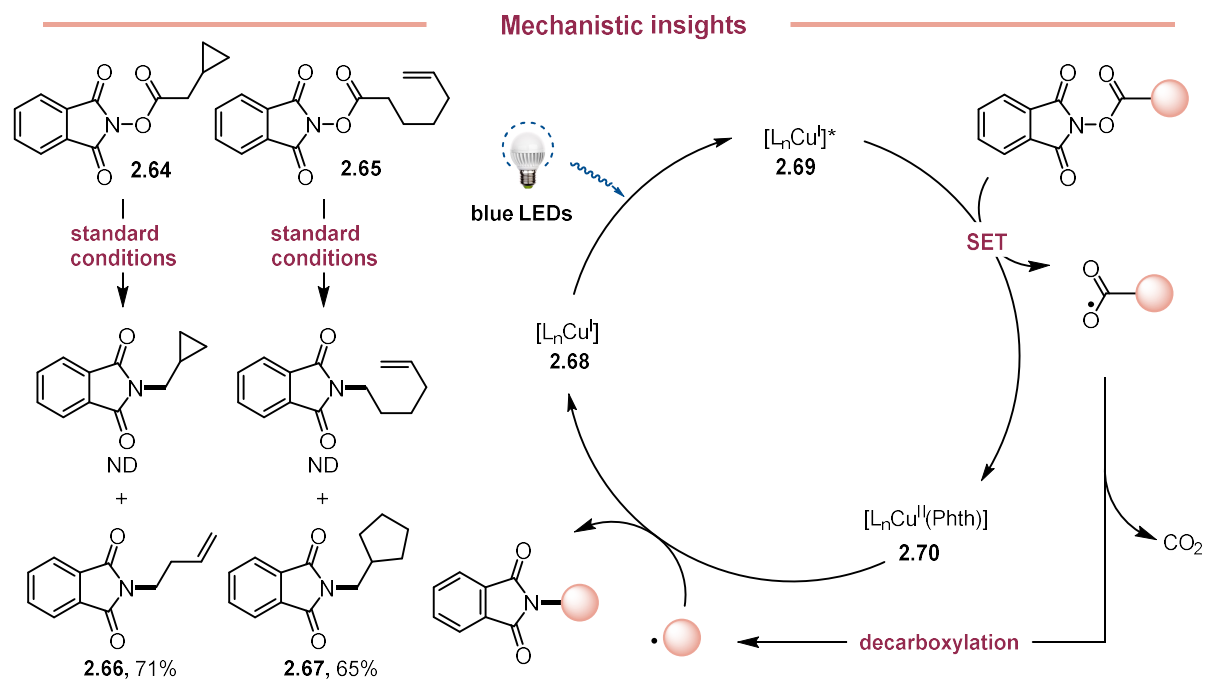
Figure 8 Mechanistic studies on the photoinduced intramolecular decarboxylative C(sp³)–N bond formation of NHP ester.

This approach nicely complements the classic Curtius rearrangement by avoiding the use of toxic and explosive azide reagents, which provides a safe and effective alternative. However, the limitations of intramolecular transformation and the inaccessibility of tertiary alkyl groups underline the limitations of this method.

2.1.4 Transition metal-catalyzed decarboxylative cross-coupling reactions

In 2016, the groups of Baran and Weix independently reported transition metal-catalyzed decarboxylative cross-couplings of NHPI esters without the use of photoredox catalysis. Since then, great progress has been made in the field of transition metal-catalyzed decarboxylative cross-coupling reactions using NHPI esters as versatile electrophiles. In this section, all these developments will be classified and described in detail according to the nature of bond formation, including 1. C(sp³)-C(sp²) bond formation; 2. C(sp³)-C(sp³) bond formation; 3. C(sp³)-C(sp) bond formation; 4. C(sp³)-X (X=B, Si) bond formation.

2.1.4.1   C(sp^3)-C(sp^2) bond formation

In 2016, Baran and co-workers developed a nickel catalyzed reductive decarboxylative cross-coupling reaction between aliphatic acid-derived NHPI esters and aryl zinc reagents to forge C(sp^3)-C(sp^2) bonds. Aliphatic acid-derived NHPI esters derived from aliphatic carboxylic acids were used as alkyl halide surrogates in this transformation because of their earth-abundant, nontoxic, and inexpensive nature. The reactions were conducted under mild conditions and presented good functional group tolerance (Table 5, entry 1).[47]

Meanwhile, Weix and co-workers reported the use of nickel as a catalyst and zinc powder as a reducing agent in cross-electrophile coupling reactions between aliphatic acid-derived NHPI esters and aryl iodides to construct C(sp^3)-C(sp^2) bonds. In contrast to Baran's work using aryl zinc reagents, Weix's method uses aryl iodide and zinc powder. The former tolerates only secondary radicals, while the latter can tolerate more types of radical precursors, including methyl, primary and secondary radicals (Table 5, entry 2).[48]
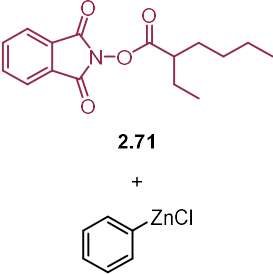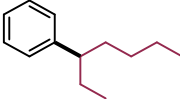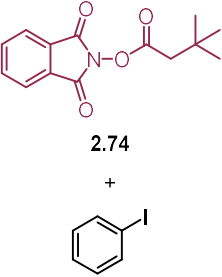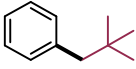
Following the establishment of C(sp^3)-C(sp^2) bonds by nickel-catalyzed cross-coupling reactions, the Baran group extended this concept to reaction conditions very similar iron-catalyzed cross-coupling reactions. Compared to the nickel-catalyzed strategy, iron catalysis exhibits several advantages: 1. Lower catalyst loading and shorter reaction times are required; 2. The iron catalysis can tolerate a wide range of aliphatic acid-derived NHPI esters, including primary, secondary and tertiary, whereas nickel catalysis is applicable only to secondary NHPI esters; 3. Iron catalysis can be used for in situ prepared (activation with HATU or HBTU) and isolated (NHPI esters) redox-active esters, and both scenarios proceeded smoothly; 4. The iron-catalyzed strategy can even tolerate highly nucleophilic arylmagnesium reagents, which is attributed to the fast kinetic profile of this transformation (Table 5, entry 3).[49]

Shortly after, the group of Baran replaced the sensitive aryl-zinc organometallic reagents with bench-stable arylboronic acids. By applying the concept of Suzuki-type cross-coupling, a decarboxylative cross-coupling of primary and secondary aliphatic acid-derived *N*-hydroxytetrachlorophthalimide (TCNHPI) esters with arylboronic acid was reported. Interestingly, this transformation is only effective for more reactive TCNHPI esters, whereas simple unsubstituted NHPI esters were either shown to be less effective or did not work at all (Table 5, entry 4).[50]

In a following study, the same group applied the nickel-catalyzed system to couple aliphatic acid-derived NHPI esters with alkenyl Grignard reagents. This Negishi-type cross-coupling enables the formation of versatile $C(sp^3)$-$C(sp^2)$ bonds. This strategy is viable to a wide range of substrates, including primary, secondary, and tertiary carboxylic acid-derived TCNHPI esters, enabling the synthesis of a diverse set of olefins–from mono-substituted to fully substituted ones– with exquisite control of olefin geometry. The authors also showcased late-stage olefinations of several natural products and drug molecules (Table 5, entry 5).[51]
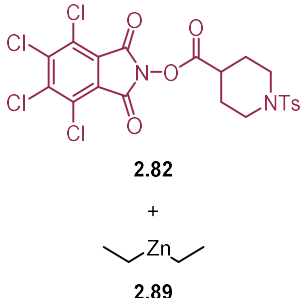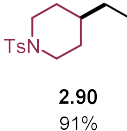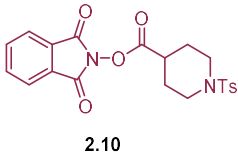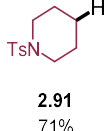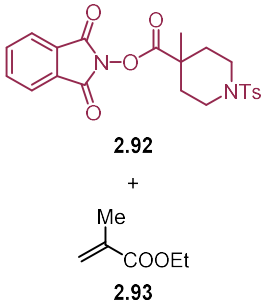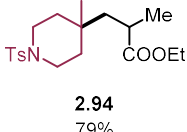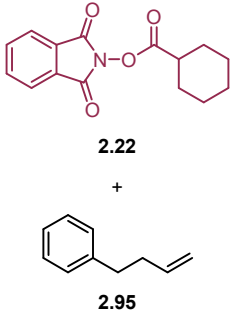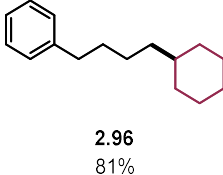
Reisman and co-workers reported the first Ni-catalyzed asymmetric cross-coupling between aliphatic NHPI esters and (E)-vinyl bromides. The reaction was carried out under mild conditions in the presence of nickel-indaBOX derived chiral catalyst **2.87** and tetrakis-(N,N-dimethylamino)ethylene (TDAE) as a terminal organic reductant. The presented methodology tolerates multiple functional groups and gives the desire products in good yields and with high enantioselectivity (Table 5, entry 6).[52]

Table 5   Transition metal-catalyzed $C(sp^3)$-$C(sp^2)$ bond formation.

Entry	Representative substrates	Conditions	Product	Mode
1	**2.71** + ZnCl **2.72**	NiCl₂·6H₂O (20 mol%) dtbpy (40 mol%) THF/DMF, RT, 16 h	**2.73** 92%	**D** Baran, 2016[47]
2	**2.74** + I **2.75**	Ni(dtbpy)Br₂ (10 mol%) Zn powder (2.0 equiv.) DMA, RT, 20 h	**2.76** 60%	**D** Weix, 2016[48]

3	**2.22** + **2.77**	Fe(acac)$_3$ (10 mol%) dppBz (12 mol%) THF, RT, 1 h	**2.78** 78% **D** Baran, 2016[49]
4	**2.79** + **2.80**	NiCl$_2$·6H$_2$O (20 mol%) dtbpy (20 mol%) Et$_3$N (10.0 equiv.) 1,4-dioxane/DMF 75 ºC, 12 h	**2.81** 82% **D** Baran, 2016[50]
5	**2.82** + **2.83**	Ni(acac)$_2$·xH$_2$O (10 mol%) dtbpy (10 mol%) THF/DMF, RT	**2.84** 80% **D** Baran, 2017[51]
6	**2.85** + **2.86**	**2.87** (NiL*, 10 mol%) TDAE (3.0 equiv.) NaI (0.5 equiv.) TMSBr (1.0 equiv.) DMA, -7 ºC, N$_2$, 16 h	**2.88** 80% (96% ee) **D** Reisman, 2017[52]

dtbpy

dppBz

DMPU

NiL* **2.87**
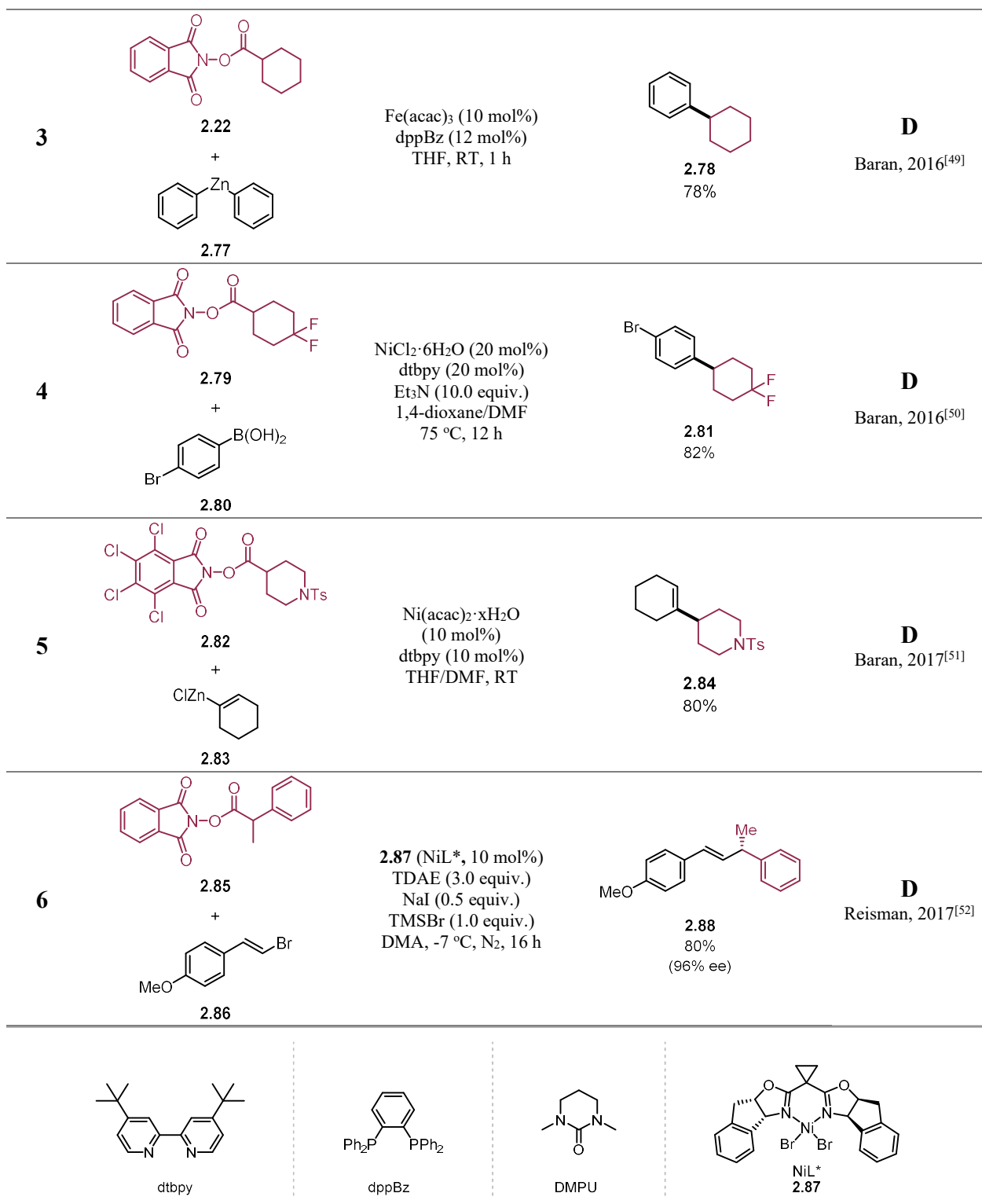
2.1.4.2   C(sp³)-C(sp³) bond formation

Table 6   Transition metal-catalyzed C(sp³)-C(sp³) bond formation.

Entry	Representative substrates	Conditions	Product	Mode
1	**2.82** + **2.89**	NiCl₂·glyme (20 mol%) 2,2'-bibpy (40 mol%) THF/DMF, RT, N₂	**2.90** 91%	**D** Baran, 2017[53]
2	**2.10**	PhSiH₃ (3 equiv.) NiCl₂·6H₂O (10 mol%) dtbpy (20 mol%) THF/DMF/iPrOH 40 °C, 1 h	**2.91** 71%	**D** Baran, 2017[54]
3	**2.92** + **2.93**	Ni(ClO₄)₂·6H₂O (20 mol%) Zn (2 equiv.), LiCl (3 equiv.) MeCN, RT, 12 h	**2.94** 79%	**D** Baran, 2017[54]
4	**2.22** + **2.95**	Ni(PPh₃)Cl₂ (10 mol%) dtbpy (15 mol%) Mg(OAc)₂·4H₂O (3 equiv.) polymethylhydrosiloxane DMA, 40 °C, 3 h	**2.96** 81%	**D** Fu, 2016[55]

In 2016, Baran and co-workers documented a decarboxylative cross-coupling of alkyl NHPI esters with primary and secondary dialkylzinc reagents in the presence of an inexpensive nickel catalyst to build C(sp³)-C(sp³) bonds (Table 6, entry 1). This reaction is robust, site-specific, and proceeds under mild conditions, providing a broad scope that covers primary, secondary, and tertiary aliphatic acid-derived NHPI esters. More importantly, this method allows the late-stage

functionalization of a broad range of natural products and drugs, showcasing its potential in drug discovery.[53]

Shortly after, the concept was expanded again by the Baran group to realize a Barton-type decarboxylative cross-coupling and a Giese-type addition reaction (Table 6, entries 2-3). These two reactions were conducted under mild conditions using $NiCl_2 \cdot 6H_2O$/dtbpy as the catalyst and zinc as the reductant, in the presence of either a hydrogen atom source or an electron-deficient olefin, leading to the desired products in moderate to good yields.[54]

Olefins and carboxylic acids are among the most accessible feedstock compounds. They are ubiquitous in both natural products and drug molecules. In 2016, Fu and co-workers developed a novel and elegant nickel-catalyzed decarboxylative hydroalkylation of olefins (Table 6, entry 4). This reaction provided a practical strategy to form $C(sp^3)$-$C(sp^3)$ bonds of alkyl NHPI esters with inactivated olefins. This method has an excellent functional group tolerance and exhibits good chemo- and regioselectivity. Notably, a stoichiometric amount of $Mg(OAc)_2 \cdot 4H_2O$ (3 equiv.) is required.[55]
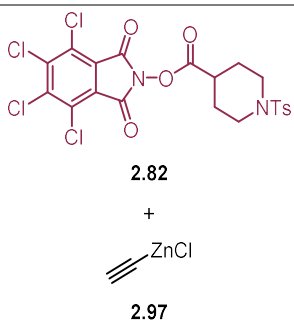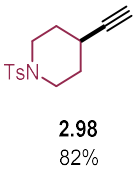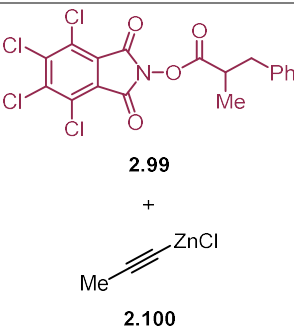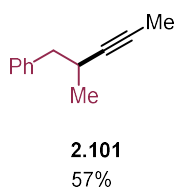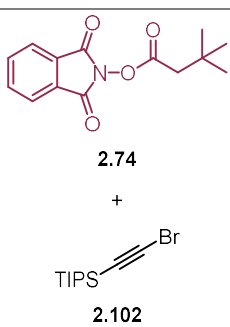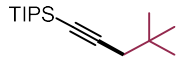
2.1.4.3   C(sp³)-C(sp) bond formation

Recently, Baran's group has succeeded in extending its strategy, using metal (Ni or Fe) catalyzed decarboxylative cross-couplings of NHPI esters, to the synthesis of alkylated alkynes (Table 7, entries 1-2).[56] Accordingly, by using highly activated TCNHPI esters, via nickel catalysis or iron catalysis, terminal alkynes or internal alkynes were afforded in the presence of ethynylzinc reagents or alkynylmagnesium compounds, respectively. Similar to previous cross-couplings of NHPI esters, the authors evidenced that this alkynylation reaction proceeds via a free radical pathway. At present, the differences in reactivity between nickel and iron catalysis remain ambiguous and require further in-depth investigations. Nevertheless, as the authors presented, both protocols are simple to operate and have a broad scope.

In parallel with Baran's report, Weix and co-workers developed a nickel-catalyzed decarboxylative cross-coupling of aliphatic NHPI esters with bromoalkynes to afford terminal and internal alkynes (Table 7, entry 3).[57] This cross-electrophilic coupling allows the simple and straightforward synthesis of a wide range of alkynes in satisfactory yields. Importantly, the addition of manganese as a reducing agent and lithium bromide as an additive is essential to inhibit the formation of the undesired diyne products. Based on preliminary mechanistic studies, the

authors ruled out the possibility of any alkynylmanganese intermediates, and provided evidence to support the nickel catalytic pathway.

Table 7   Transition metal-catalyzed C(sp^3)-C(sp) bond formation.
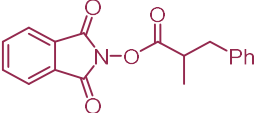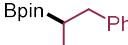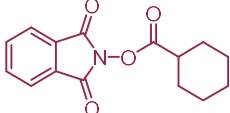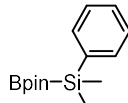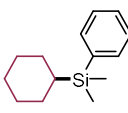
Entry	Representative substrates	Conditions	Product	Mode
1	**2.82** + **2.97**	NiCl$_2$·6H$_2$O (20 mol%) dtbpy (20 mol%) THF/DMF, RT, 12 h	**2.98** 82%	**D** Baran, 2017[56]
2	**2.99** + **2.100**	FeBr$_2$·H$_2$O (20 mol%) dtbpy (20 mol%) THF/NMP, -15 °C, 15 min	**2.101** 57%	**D** Baran, 2017[56]
3	**2.74** + **2.102**	Ni(dme)Br$_2$ (10 mol%) dtbpy (10 mol%) Mn (2.0 equiv.) LiBr (1.0 equiv.) NMP, RT, overnight	**2.103** 89%	**D** Weix, 2017[57]

2.1.4.4 C(sp^3)-X (B, Si) bond formation

To further demonstrate the robustness of nickel-catalyzed decarboxylative cross-coupling of NHPI esters, Baran and co-workers developed an elegant and scalable nickel-catalyzed decarboxylative borylation of NHPI esters that can transform ubiquitous aliphatic carboxylic acids into their corresponding boronic esters (Table 8, entry 1).[58] By employing an inexpensive nickel

catalyst together with a dimethoxy-substituted bipyridine ligand in the presence of B_2pin_2 **2.105** (Bpin=pinacol boronate) under mild conditions, a series of aliphatic carboxylic acid-derived NHPI esters successfully coupled with B_2pin_2 to provide the corresponding boronic esters in moderate to good yields (see **2.106** as an example). Notably, the premixing of methyllithium with B_2pin_2 was crucial to activate the diboron moiety for transmetalation. Moreover, this method found applications in the direct synthesis of a range of borates that would otherwise require multiple steps, including the functionalization of natural products and drugs.

Table 8   Transition metal-catalyzed $C(sp^3)$-X (B, Si) bond formation.

Entry	Representative substrates	Conditions	Product	Mode
1	**2.104** + B_2pin_2 **2.105**	NiCl$_2$·6H$_2$O (10 mol%) di-OMebpy (13 mol%) MgBr$_3$·Et$_2$O (1.5 equiv.) MeLi (3.0 equiv.) THF/DMF, 0 °C-RT, 2 h	**2.106** 67%	**D** Baran, 2017[58]
2	**2.22** + **2.107**	CuTC (10 mol%) dtbpy/Cy$_3$P (10 mol%) NaOEt (1.0 equiv.) THF/NMP, RT	**2.108** 91%	**D** Oestreich, 2017[59]

Recently, the Oestreich group has successfully explored a copper-catalyzed decarboxylative silylation reaction of NHPI esters with a Si-B reagent (Table 8, entry 2).[59] Interestingly, this is the first example where NHPI esters can be activated and used as electrophiles in copper catalysis. A diverse set of primary and secondary aliphatic carboxylic acid-derived NHPI esters were smoothly silylated in good yields (see **2.108** as an example). Although an adamantyl-substituted silane was afforded from 1-adamantane carboxylic acid in moderate yields (40%), other tertiary alkyl NHPI esters were coupled sluggishly probably due to the steric hindrance. Using this method,

α-silylated amines can be synthesized in one step from the corresponding α-amino acids. Supported by the radical clock and radical trapping experiments, the authors showed that the reaction follows a radical pathway.

2.1.5 Conclusion and outlook

In this section, we have detailed the progress made in the field of cross-coupling reactions using NHPI esters as surrogates for alkyl halides since their initial discovery. Decarboxylative cross-coupling reactions employing NHPI esters have been applied to achieve a variety of previously unattainable transformations. These new methodologies have been widely used in the late-stage functionalization and construction of natural products and drugs. They have not only provided a shortcut to known molecules, but more importantly, paved the way for the discovery of new chemical transformations. Despite these advances and achievements, there are still more challenges and opportunities to be explored. Future research into reaction mechanisms should lead to more in-depth studies to advance the field's rapid development. In the meantime, we can also expect the development of a series of asymmetric cross-coupling reactions involving NHPI esters. As such, we anticipate that the field of using NHPI esters as versatile coupling partners will continue to grow at a remarkable pace, providing the synthetic organic community with new synthetic tools for streamlined access to high value-added products.

2.2 The merger of photoredox and copper catalysis

2.2.1 Introduction

The scientific and societal impact of transition metal catalysis has long been recognized. The Nobel Prizes awarded in 2001 (to Knowles, Noyori, and Sharpless for the development of asymmetric catalytic synthesis),[60] 2005 (to Chauvin, Grubbs, and Schrock for the development of the metathesis method in organic synthesis),[61] and 2010 (to Heck, Negishi, and Suzuki for palladium-catalyzed cross couplings in organic synthesis)[62] are cases in point. Although these studies span more than 40 years, they all share a common feature: applying simple and readily available raw materials to construct high value-added molecules. More importantly, transition metal catalysis provides new modes of chemical activation, allowing bond-forming or bond-breaking pathways that were hitherto unimaginable in the synthetic organic community. This remarkable capability makes transition metal catalysis invaluable for organic synthesis and, more broadly, for the production of organic molecules to benefit society.

The success of these transition metal-catalyzed transformations typically relies on transition metal catalysts to activate the electrophiles (for example haloarenes) via an oxidative addition step, followed by a reductive elimination step to construct the desired bonds. This paradigm is well exemplified especially in modern palladium and nickel catalysis. For more than 40 years, palladium and nickel catalysts have been designed to make these steps (oxidative addition and reduction elimination) universally effective, leading to significant developments in building carbon-carbon, carbon-nitrogen, carbon-sulfur, and carbon-oxygen bonds.[6, 63]

In contrast, the diverse use of copper catalysts in cross-coupling chemistry has been far less successful than that of palladium or nickel catalysts, despite the potential economic and operational advantages of copper catalysts. The disadvantage of copper catalysis is mainly due to the relatively low rate of its oxidative addition step, which is usually the rate-determining step for this type of catalysis (Figure 9).[64-66] As such, the most widely used copper-catalyzed cross-coupling reactions have been limited to transmetalling reagents such as organoboronic acids, primarily to bypass the challenge of oxidative addition.[67] Nevertheless, copper catalysis also has very distinct advantages. The biggest advantage is that for most coupling partners, reductive elimination from the corresponding high-valent copper complexes is facile and robust.[68] For example, it is known that copper-catalyzed reductive elimination to build C-X bonds (X = highly electronegative atoms or

groups, such as F and CF$_3$) is more advantageous and faster than that of Pd and Ni (Figure 9).[67, 69-70] Therefore, if a novel copper-catalyzed mode can be developed such that it can not only bypass or overcome the difficulties of the challenging oxidative addition step but also fully exploit the advantages of copper catalysis, it would be of great value for the development of synthetic organic chemistry. At the same time, such an approach could significantly enhance the scope and practicality of copper-catalyzed cross-coupling reactions.
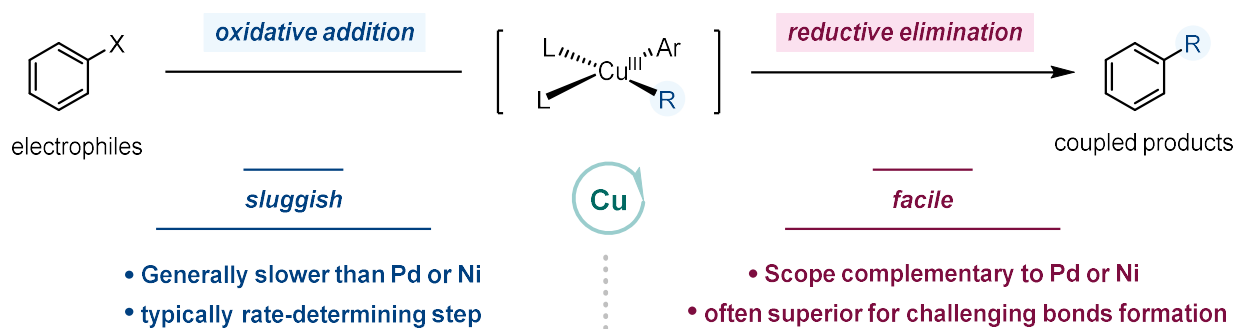
Figure 9 Advantages and disadvantages of copper catalysis compared to palladium and nickel catalysis in cross-coupling reactions.

Notably, no matter which transition metal catalysis is studied, three fundamental aspects of the catalyst have consistently been the focus of attention: ligand design, manipulation of available oxidation states, and electronic excitation. It is also true for copper catalysis, wherein diverse ligands have been developed to enhance the reactivity of copper catalysis.[67] Electronic excitation has also been investigated to overcome the harsh operating conditions of some traditional non-light-mediated copper-catalyzed reactions.[71-72]

In the prior decade, photoredox catalysis has shown its superior performance in obtaining high-energy oxidative and electronic excited states of transition metal complexes. This catalytic approach, terms as metallophotocatalysis, offers new mechanistic paradigms and provides access to elusive reactivity.[73] This mode of catalysis is of tremendous help to conventional transition metal catalysis, in particular, copper catalysis. Indeed, the merger of photoredox and copper catalysis has recently emerged as an efficient dual catalytic system for cross-coupling reactions.[74] In this section, we focus on the advances in the merger of photoredox and copper catalysis. Before that, a brief photoredox catalysis tutorial is necessary.

2.2.2   Photoredox catalysis tutorial

Over the past century, photocatalysis has contributed significantly to the advance of synthetic organic chemistry, developing a range of transformations that were previously unattainable. Broadly speaking, photocatalysis refers to the conversion of photon energy into usable chemical energy, with common pathways including energy transfer and single electron transfer (SET). Recently, the rapid development of photoredox catalysis has received increasing attention and has been applied to a range of transformations.[75-78] In this mode of catalysis, a light-absorbing catalyst, when excited, can either accept or provide an electron from an organic or organometallic substrate. This single-electron transfer process both facilitates the acquisition of highly reactive radical species under mild conditions and effectively "activates" other catalysts, which are unable to function in the absence of photocatalysts and visible light.

Interestingly, the most commonly used photocatalysts in organic synthesis were originally developed more than half a century ago for applications such as water splitting,[79] carbon dioxide reduction,[80] and new solar cell materials.[81] Although there were some early reports demonstrating the use of photoredox catalysis to forge organic bonds, this mode of catalysis has only recently become widely used. Seminal reports by the groups of MacMillan,[82] Yoon,[83] Stephenson[84] and others helped initiate interest in the field of organic photoredox catalysis. Since then, many research groups have reported on the application of photoredox catalysis in synthetic organic chemistry over the past decade. A search of the Web of Science database for the keywords "photoredox catalysis" (and derivatives) has resulted in our conservative estimate of over 700 published articles on this topic to date.[73]

The key discovery in the field of photoredox catalysis was the realization that metal-polypyridyl complexes and organic dyes have unique electronic properties in their excited states. Irradiation with low-energy visible light (wavelengths that are not absorbed by common organic molecules) can selectively excite these catalytic chromophores to their excited states. For commonly used metal-polypyridyl complexes, absorption corresponds to a metal-to-ligand charge transfer (MLCT) event in which an electron is promoted from a non-bonding metal-centered orbital to ligand-centered LUMO of the ligand framework (Figure 10). A subsequent intersystem crossing (ISC) may lead to the formation of long-lived triplet excited states. In this configuration, the catalyst possesses a high-energy electron in the ligand-centered LUMO and a low-energy hole in the metal-centered HOMO. Thus, these excited-state catalysts are both reducing and oxidizing,

and this unusual electronic property provides a powerful tool for developing new reactions. Indeed, the excited state can simply donate a high-energy electron from the ligand π^* orbital (functioning as a reducing agent) or accept an electron into a low-energy metal-center hole (functioning as an oxidizing agent) (Figure 10). The resulting reduced or oxidized catalyst retains a strong thermodynamic drive to return to its original oxidation state. As a consequence, a second electron-transfer event can occur, allowing for a redox-neutral transformation (Figure 10). Importantly, there is a clear relationship between the photocatalyst's structural characteristics and its redox properties, and these catalysts can be rationally designed by modifying the ligand framework and the metal center.[85]
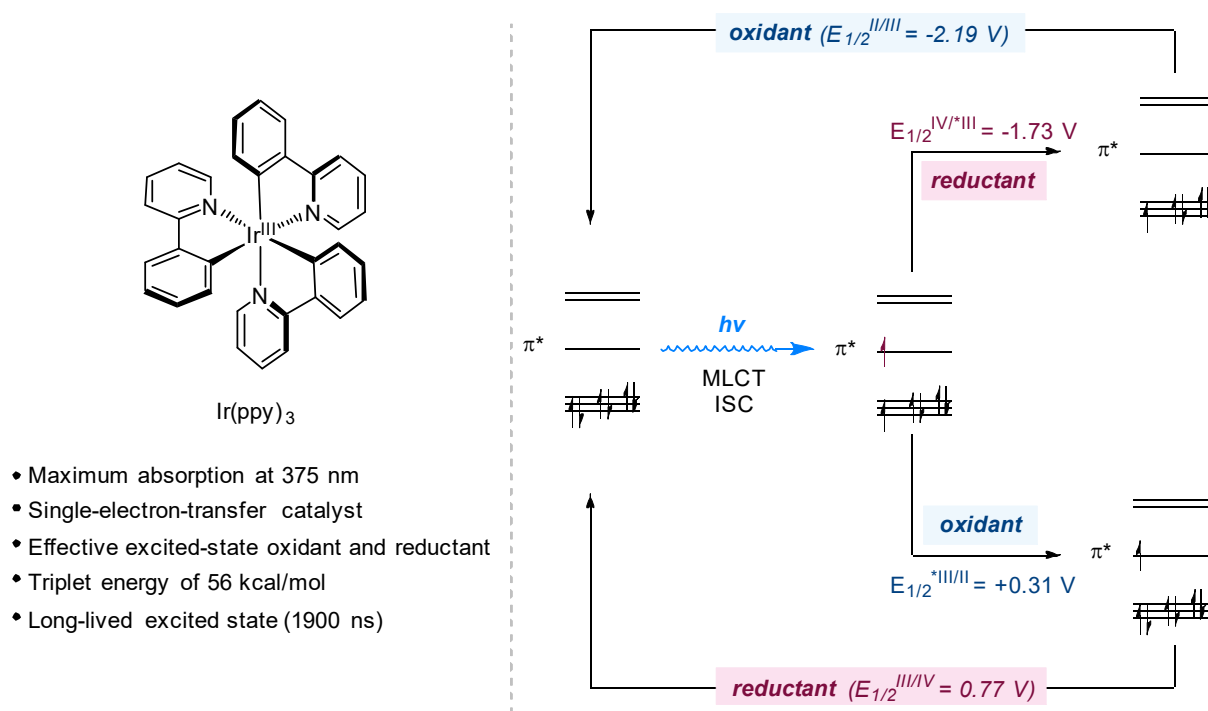
Figure 10 Key features of a representative photoredox catalyst. All potentials are given in volts versus the saturated calomel electrode (SCE). Measurements were performed in acetonitrile at room temperature unless otherwise noted. MLCT, metal-to-ligand charge transfer; ISC, intersystem crossing; ppy, 2-phenylpyridine.

Photoredox catalysis provides a unique reaction mode in which the oxidation and reduction of organic molecules and organometallic metals can occur simultaneously. This duality contrasts with conventional redox reactions, which are typically singly neutral, oxidative or reductive

processes. Thanks to rapid electron transfer and the facile generation of high-energy intermediates, photoredox catalysis can achieve previously unattainable transformations. Another major advantage of photoredox catalysis is the continuous generation of excited-state catalysts. Thus, fruitless electron transfer events or quenching pathways may not lead to lower yields because the photocatalyst can be re-excited at the sole expense of the quantum yield of the reaction (the ratio of photons absorbed per reaction turnover).

2.2.3 Recent advances in the merger of photoredox and copper catalysis

2.2.3.1 Co-operative photoredox-copper catalysis: capturing radicals with copper
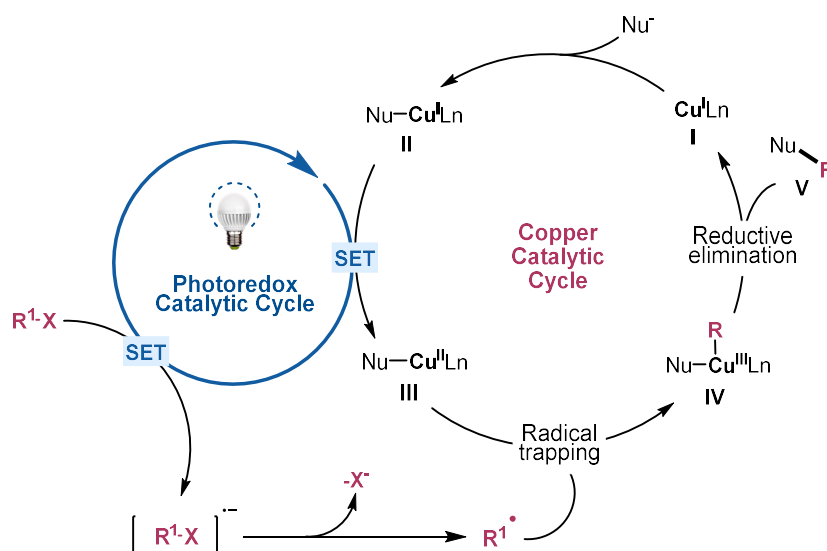
Figure 11 A general mechanistic pathway of co-operative photoredox-copper catalysis: capturing radical with copper.

Recently, the combination of copper(I) or copper(II) salts with conventional Ir-based, Ru-based, or organic photocatalysts has shown striking advantages in synthetic organic chemistry. In particular, due to the persistent radical effect (PRE) exhibited by copper, organic radical intermediates generated by photoredox catalysis can be efficiently captured and thus stabilized by the metal center. The resulting organocopper intermediates show diverse reactivities, enabling a range of follow-up chemistry. The mechanistic paradigm includes the following generic steps (Figure 11, in no particular order): (1) a photocatalyst, upon excitation, aids to generate a radical species ($R^1\cdot$) by single-electron reduction of an electrophile; (2) the anionic ligand (Nu$^-$) replaces

one of the reaction counterparts to form complex **II** or in some cases Transmetalation (Figure 11); (3) the oxidized photocatalyst oxidizes the complex **II**, via single-electron transfer, to complex **III** (Figure 11); (4) complex **III** can trap the radical species ($R^1\cdot$) and forms the highly reactive Cu^{III} species **IV**; (5) reductive elimination of **IV** occurs to generate the desired products and regenerate the initial Cu^I species **I**. Notably, the carbophilic nature of copper enables the acquisition of various Cu-C species, such as Cu-aryl and Cu-alkyl, which lays the groundwork for efficient building of various important bonds, such as $C(sp^2)$-$C(sp^3)$, $C(sp^2)$-$C(sp^2)$, $C(sp^3)$- $C(sp)$ and $C(sp^3)$-$C(sp^3)$ bonds.
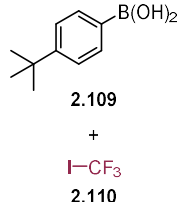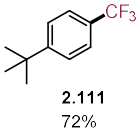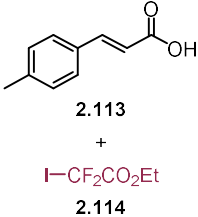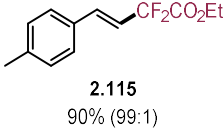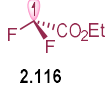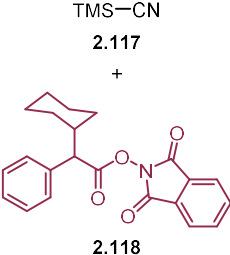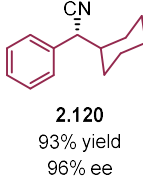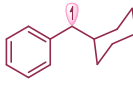
In a seminal study published in 2012, Sanford and co-workers laid the groundwork for the combined use of copper and photoredox catalysis.[86] Inspired by their previously developed photoredox and palladium-catalyzed dual catalytic systems,[92] this time they have successfully and elegantly applied similar ideas to the development of a synergistic photoredox and copper-catalyzed perfluoroalkylation method. Selective perfluoroalkylation strategies are highly desirable because the modification of drug-like molecules with such functional groups often exhibits more excellent metabolic stability. In this regard, this methodology provides a mild and general approach for the coupling between perfluoroalkyl iodides and arylboronic acids. In the proposed mechanism, the photoexcitation of $Ru(bpy)_3^{2+}$ to $Ru(bpy)_3^{2+}*$ is followed by a single-electron reduction by Cu^I species to produce $Ru(bpy)^{3+}$ and Cu^{II} species. Reduction of CF_3I by $Ru(bpy)_3^+$ gives $CF_3\cdot$ radical **2.112** (Table 9, entry 1), I^- and $Ru(bpy)_3^{2+}$. Then, $CF_3\cdot$ radical (**2.112**) can be trapped by Cu^{II} species to produce the $Cu^{III}(CF_3)$ intermediate. Subsequent base-promoted transmetalation between $Cu^{III}(CF_3)$ complex and arylboronic acid would produce $Cu^{III}(aryl)(CF_3)$ intermediate, which can undergo reductive elimination efficiently to furnish the desired trifluoromethylated products, liberating the precatalyst Cu^I and closing the catalytic cycle.

In 2016, Liu and co-workers documented a synergetic copper and photoredox-catalyzed decarboxylative difluoroalkylation of α,β-unsaturated carboxylic acids with iododifluoroacetate, enabling the introduction of difluoroalkyl groups into substituted cinnamic acids.[87] This protocol is applicable to a wide range of substituted cinnamic acids and provides a method for the efficient preparation of difluoroalkylated alkenes (Table 9, entry 2).

Enantioselective cross-coupling can be achieved by using chiral ligands in the synergistic Cu/photoredox catalysis system. In 2017, Liu and co-workers reported an enantioselective decarboxylative cyanation using this system.[88] The secondary benzylic NHPI ester was used

together with trimethylsilyl cyanide (TMSCN) to generate benzyl nitriles in the presence of [Ir(ppy)$_3$] (0.5 mol%), CuBr (1 mol%) and chiral In-BOX **2.119** (1.2 mol%) ligand (Table 9, entry 3). The key step is the combination of the radical that is obtained from an NHPI ester via photoreduction, with the chiral L*Cu^{II}CN complex. The latter originates from the L*Cu^{I}CN complex through photooxidation. Reductive elimination from the resulting Cu^{III} species can furnish the products in good yields and with excellent enantioselectivities. Inspired by this work, in 2018, Mei, Han and co-workers expanded this strategy to achieve enantioselective bifunctionalization-cyanoalkylation of olefins using chiral ligand In-BOX **2.125** (Table 9, entry 4).

Table 9   Cooperative photoredox and copper dual catalysis: capturing radical with copper.

Entry	Representative substrates	Conditions	Product	Radical species generated	Contributor(s)
1	**2.109** + I—CF$_3$ **2.110**	[Ru(bpy)$_3$]Cl$_2$·6H$_2$O (1 mol%) CuOAc (20 mol%) K$_2$CO$_3$ (1.0 equiv.) DMF, 60 °C, 12 h 26 W light bulb	**2.111** 72%	**2.112**	Sanford, 2012[86]
2	**2.113** + I—CF$_2$CO$_2$Et **2.114**	[Ru(bpy)$_3$]Cl$_2$·6H$_2$O (2 mol%) [Cu(MeCN)$_4$]PF$_6$ (10 mol%) Et$_3$N (1.5 equiv.) DCM, Ar, RT blue LEDs, 12 h	**2.115** 90% (99:1)	**2.116**	Liu, 2016[87]
3	TMS—CN **2.117** + **2.118**	Ir(ppy)$_3$ (0.5 mol%) CuBr (1 mol%) In-BOX **2.119** (1.2 mol%) DMF/p-xylene (4/6) Ar, blue LEDs, 24 h	**2.120** 93% yield 96% ee	**2.121**	Liu, 2017[88]

4	TMS—CN **2.122** + (styrene with Br) **2.123** + (phthalimide cyclopentyl ester) **2.124**	Ir(ppy)₃ (0.5 mol%) CuBr (1 mol%) In-BOX **2.125** (1.2 mol%) NMP/PhCl (4/6) blue LEDs, 24 h	**2.126** 72% yield 94% ee	**2.127**	Mei and Han, 2018[89]
5	(Cl/Br benzene) **2.128** + (sulfonium CF₃ OTf) **2.129**	[Ir(dFMeppy)₂(4,4'-dCF₃bpy)]PF₆ **2.130** (0.125 mol%), CuBr₂·2LiBr (20 mol%), (Me₃Si)₂SiOH **2.131** (1.5 equiv.), K₃PO₄ (4.0 equiv.), acetone, 35 °C, blue LEDs, 24 h	**2.132** 96%	**2.133** / **2.112**	MacMillan, 2017[90]
6	(indane acid) **2.134** + (benziodoxole CF₃) **2.135**	[Ir(dF(CF₃)ppy)₂(4,4'-dCF₃bpy)]PF₆ **2.136** (0.125 mol%), CuCN (20 mol%), Bphen (30 mol% BTMG (0.5 equiv.) EtOAc, H₂O blue LEDs, 6 h	**2.137** 82%	**2.138**	MacMillan, 2017[91]

In-BOX **2.119**

In-BOX **2.125**

2.130 [Ir(dFMeppy)₂(4,4'-dCF₃bpy)]PF₆

2.131 tris(trimethylsilyl)silanol

2.136 [Ir(dF(CF3)ppy)₂(4,4'-dCF₃bpy)]PF₆

Bphen

BTMG

As mentioned earlier, while high-valent Cu^{III} species can undergo facile reductive elimination, the oxidative addition of C(sp^2)-halogen bonds to low-valent Cu^I species was a long-standing problem in copper chemistry, hindering the widespread use of Cu as an efficient cross-coupling catalyst. In 2018, MacMillan and co-workers proposed a solution to this issue by combining Ir-based photocatalyst with a copper catalyst in the presence of tris(trimethylsilyl)silanol **2.131**, which can successfully couple aryl bromides with trifluoromethylating agents **2.219** (Table 9, entry 5)[90]. This transformation is an overall redox-neutral process. In their proposed mechanism, upon irradiation with visible light, the excited photocatalyst can oxidize tris(trimethylsilyl)silanol to generate a reactive silyl radical and a reduced photocatalyst. The former can abstract the bromine from an aryl bromide to generate an aryl radical, while the latter can reduce the trifluoromethylating reagent to generate a trifluoromethyl radical. Thereafter, the Cu^I complex can capture the aforementioned trifluoromethyl radical and aryl radical in turn to form a highly reactive ArCu^{III}CF$_3$ complex, which enables facile reductive elimination to deliver the desired trifluoromethylated arenes in excellent yields.
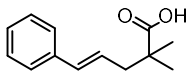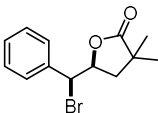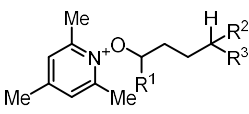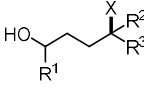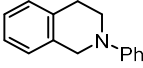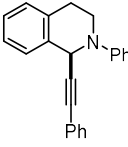
Given the importance of trifluoromethylated compounds, in 2018, MacMillan and co-workers reported a decarboxylative trifluoromethylation of aliphatic carboxylic acids using dual photoredox and copper catalysis (Table 9, entry 6).[91] According to their proposed mechanism, initially, the free carboxylic acid would coordinate a Cu^{II} catalyst to form a Cu^{II}-carboxylate complex, this complex can be oxidized to the corresponding Cu^{III}-carboxylate complex via photooxidation by excited photocatalyst Ir^{III}*. Subsequent carbon dioxide extrusion and recombination of an alkyl radical with the Cu^{II} catalyst would generate an Cu^{III}-alkyl intermediate, which would oxidize Ir^{II} to ground state photocatalyst Ir^{III} and generate a Cu^{II}-alkyl intermediate. This intermediate would react with the Togni reagent 3,3-dimethyl-1-(trifluoromethyl)-1,2-benzoiodoxole **2.135** to provide the target alkyl-CF$_3$ product in good yield and regenerate the Cu^{II} catalyst to close one catalytic cycle.
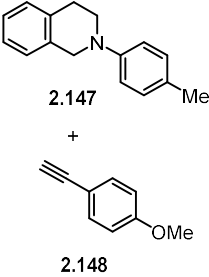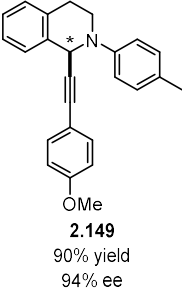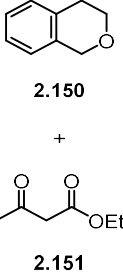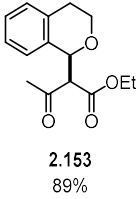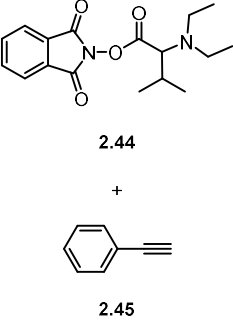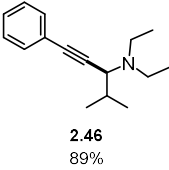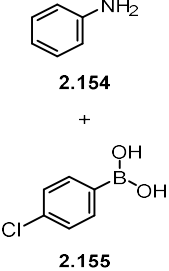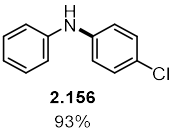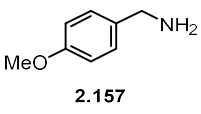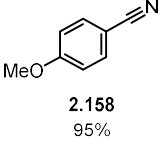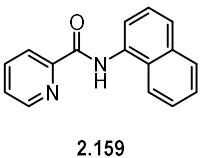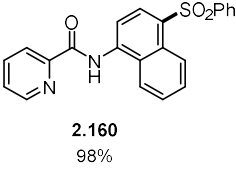
2.2.3.2 Miscellaneous roles of copper in metallaphotocatalysis
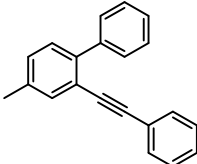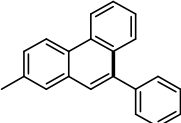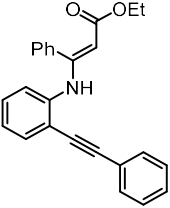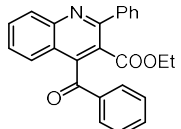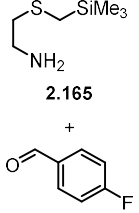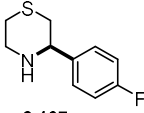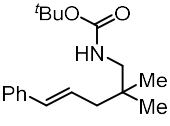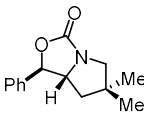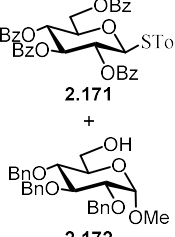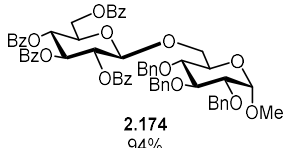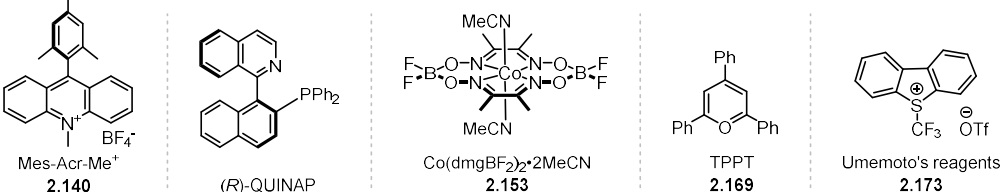
In addition to capturing radicals, copper can also play a variety of roles to enrich the field of metallaphotocatalysis. For example, in 2017, Nicewicz and co-workers reported a regioselective halogenation of unsaturated carboxylic acids.[93] This transformation begins with the

photooxidation of an olefin by an acridinium photocatalyst. The resulting carbon radical cations can trigger an intramolecular ring closure via nucleophilic substitution by the carboxylic acid group, generating a carbon-centered radical. The Cu^{II} catalyst can then transfer the halide from an external halide source to the newly generated carbon-centered radical to furnish a halide product (Table 10, entry 1). In 2019, Zhu and co-workers reported a remote C(sp^3)-H functionalization of *N*-alkoxypyridinium salts with silyl reagents via photoredox/copper synergetic catalysis.[94] This conversion was achieved by reducing *N*-alkoxypyridinium salts using excited photocatalyst Ir^{III}*, to generate an alkoxy radical that would undergo 1,5-hydrogen atom transfer to produce a carbon-centered radical. In the meantime, a silicon-based reagent (such as trimethylsilyl- azide (TMSN$_3$), cyanide (TMSCN) and isothiocyanate (TMSSCN)) can transmetallate to a Cu^{II} catalyst and successfully transfer these functional groups to the carbon-centered radical to produce various δ-functionalized alcohols (Table 10, entry 2).

Table 10 Miscellaneous roles of copper in synergetic copper/photoredox catalysis.

Entry	Representative substrates	Conditions	Product	Roles of Cu-salts	Contributor(s)
1	2.139	Mes-Acr-Me$^+$ **2.140** (5 mol%) CuBr$_2$/bpy (10 mol%) diethyl bromomalonate (1.0 equiv.) CH$_3$CN, RT, 18 h blue LEDs	2.141 94%, 2.1:1 dr	halogen-atom transfer (X = Br, Cl)	Nicewicz, 2017[93]
2	2.142	Ir(ppy)$_3$ (2 mol%) Cu(OAc)$_2$ (20 mol%) Phen (30 mol%) TMSX CH$_3$CN, RT blue LEDs	2.143	pseudohalogen-group transfer (X = N$_3$, CN, SCN)	Zhu, 2019[94]
3	2.144 + 2.145	[Ru(bpy)$_3$](PF$_6$)$_2$ (1 mol%) [Cu(MeCN)$_4$]PF$_6$ (10 mol%) CH$_2$Cl$_2$ 5 W fluorescent bulb	2.146 88%	activation of alkynes	Rueping, 2012[95]

	Substrates	Conditions	Product	Role of Cu	Reference
4	2.147 + 2.148	[Ir(ppy)$_2$dtbpy]PF$_6$ (1 mol%) Cu(OTf)$_2$ (10 mol%) (R)-QUINAP (15 mol%) (BzO)$_2$ (1.2 equiv.) THF/CH$_3$CN (1/1) -20 ºC, 2 d visible light	2.149 90% yield 94% ee	activation of alkynes and asymmetric induction	Li, 2015[96]
5	2.150 + 2.151	Mes-Acr-Me$^+$ (5 mol%) Cu(OTf)$_2$ (10 mol%) Co(dmgBF$_2$)$_2$·2MeCN **2.152** (10 mol%) CH$_3$CN blue LEDs, 24 h, Ar	2.153 89%	activation of alkynes	Wu, 2015[97]
6	2.44 + 2.45	[Ru(bpy)$_3$]Cl$_2$ (1 mol%) CuI (10 mol%) DCM, RT, Ar, 6 h CFL (40 W)	2.46 89%	activation of alkynes	Fu, 2017[98]
7	2.154 + 2.155	Ir(ppy)$_3$ (1 mol%) Cu(OAc)$_2$ (10 mol%) myristic acid (20 mol%) 2,6-lutidine PhMe/MeCN (1:1) 35 ºC, blue LEDs open air, 20 h	2.156 93%	ligand exchange and transmetalation	Kobayashi, 2015[99]
8	2.157	[Ru(bpy)$_3$]Cl$_2$ (2 mol%) CuBr (10 mol%) LiO^{t}Bu (20 mol%) DMSO, O$_2$ blue LEDs	2.158 95%	ligating co-oxidant	Tao, 2017[100]
9	2.159	[Ru(bpy)$_3$](PF$_6$)$_2$ (3 mol%) Cu(OAc)$_2$·H$_2$O (20 mol%) PhSO$_2$Na (2 equiv.) K$_2$S$_2$O$_8$ (2 equiv.) acetone/H$_2$O (1:1), RT 26 W household light	2.160 98%	co-oxidant	Wu, 2017[101]

10	2.161	Eosin Y (3 mol%) Cu(OTf)₂ (5 mol%) CH₂Cl₂, RT, 72 h 23 W household light	2.162 100%	triple bond activation	Guo, 2016[102]
11	2.163	Mes-Acr-Me⁺ (5 mol%) CuCl₂ (20 mol%) Phen (20 mol%) TBHP (3.0 equiv.) O₂ (1 atm), DMF blue LEDs, RT, 24 h	2.164 65%	triple bond activation	Zhu, 2017[103]
12	2.165 + 2.166	[Ir(ppy)₂dtbpy]PF₆ (1 mol%) Cu(OTf)₂ (1.0 equiv.) Bi(OTf)₃ (50 mol%) MeCN, RT, 16 h blue LEDs	2.167 47%	Lewis acidity	Bode, 2017[104]
13	2.168	TPPT 2.169 (2.5 mol%) Cu(TFA)₂ (1.2 equiv.) CH₂Cl₂, RT, 15 h blue LEDs	2.170 82%	oxidant	Yoon, 2018[105]
14	2.171 + 2.172	[Ru(bpy)₃](PF₆)₂ (5 mol%) Umemoto's reagents 2.173 (2.6 equiv.) Cu(OTf)₂ (1.5 equiv.) CH₂Cl₂, RT, 4 h blue LEDs	2.174 94%	additives	Ye, 2016[106]

In 2012, Rueping and co-workers developed a photooxidative acetylation reaction of tetrahydroisoquinolines. By using [Ru(bpy)₃](PF₆)₂ as a photooxidant under oxygen atmosphere and acetyl copper species as active nucleophilic reagents that generated from the interaction of [Cu(MeCN)₄]PF₆ with terminal alkynes, they successfully obtained 1-alkynyl tetrahydroisoquinoline derivatives in moderate to excellent yields (Table 10, entry 3).[95] Later, Li

and co-workers further extended this strategy to its asymmetric version by applying chiral Cu-QUINAP complex.[96] This complex enables the formation of chiral Cu-QUINAP-acetyl species by reacting with terminal alkynes. The chiral Cu-QUINAP-acetyl complex can, therefore, act as an active nucleophilic reagent to attack an iminium intermediate and produce 1-alkynyl tetrahydroisoquinoline derivatives with excellent enantioselectivity (Table 10, entry 4). In a similar fashion, Wu and co-workers disclosed that this strategy could also be successfully expanded to the functionalization of isochromans with β-keto esters.[97] In this reaction, a catalytic amount of Cu(OTf)$_2$ can be used to activate the nucleophiles, assisting them to attack oxonium intermediates (Table 10, entry 5). In 2017, Fu and co-workers documented a photoredox-catalyzed decarboxylation and alkynylation of NHPI esters derived from α-amino acids with terminal alkynes.[41] Similar to the aforementioned reaction mechanisms, in which a catalytic amount of CuI is necessary to generate nucleophilic reagents in the form of copper acetylates. Notably, this reaction is overall redox-neutral, in which the photo-reduction process can reduce the NHPI esters to generate carbon-centered radicals, while the photo-oxidation process enables the oxidation of the carbon radicals to the corresponding carbon cations (Table 10, entry 6).

In 2015, Kobayashi and co-workers developed an improved Chan-Lam coupling reaction between electron-deficient aryl boronic acids and anilines by applying a combined copper/photoredox catalytic system to the Chan-Lam coupling reactions.[99] In this reaction, initially, the Cu^{II} catalyst can form a Cu^{II}-amido complex by sequential ligand exchange with an aniline and transmetalation with an aryl boronic acid. The Cu^{II}-amido complex can be oxidized by Ir^{IV} to form a Cu^{III} intermediate, which can undergo reductive elimination to furnish the desired product. The reaction successfully employs the interaction between the photocatalyst and the copper catalyst, which effectively facilitates the C-N coupling reaction by modulating the valence state of the copper intermediate (Table 10, entry 7). In 2017, Tao and co-workers successfully oxidized a variety of primary amines to nitriles using the [Ru(bpy)$_3$]Cl$_2$/CuBr dual catalytic system (Table 10, entry 8).[100] The mechanistic pathway includes (1) initial ligand exchange of Cu^I with a primary amine to form a Cu^I-amido intermediate. (2) Single-electron transfer from the Cu^I-amido intermediate to excited photocatalyst Ru^{II}*. (3) Sequential deprotonation by superoxide radical anion and hydrogen peroxide anion can occur, respectively, to form a copper amido intermediate. (4) Then, another similar catalytic cycle is performed to obtain the desired nitrile products. In another study, Wu and coworkers discovered a mild and efficient approach for C4–H sulfonylation

of 1-naphthylamine derivatives using sodium sulfonates. This C4-H sulfonylation can be realized under mild conditions using dual photoredox/copper catalysis and could tolerate various functional groups. Preliminary studies disclosed that the copper catalyst can assist a single-electron transfer of the substrate in the presence of an external oxidant (Table 10, entry 9).[101]

The Lewis acidity of copper has also been leveraged in activating C≡C triple bonds via the formation of a π-complex between an internal alkyne and Cu^{II} complex. This three-center two-electron (3c-2e) system can be oxidized by an exogenous photocatalyst to form a 3c-1e system. In 2016, Guo and co-workers disclosed that this 3c-1e system could undergo an areneyne cyclization reaction to produce phenanthrene derivatives in good yields (Table 10, entry 10).[102] In addition, Cu^{II} salts have also been used to build polysubstituted quinolines via an intramolecular oxidative cyclization/oxygen insertion of aromatic enamines under mild reaction conditions (Table 10, entry 11).[103] In 2017, Bode and co-workers reported the usage of stoichiometric $Cu(OTf)_2$ as the Lewis acid to lower oxidation potentials of imine substrates, which can then participate in photocatalytic syntheses of various aza-heterocycles by using the silicon amine protocol (SLAP) (Table 10, entry 12).[104] Stoichiometric Cu^{II} salts have also been investigated and applied to other photocatalyzed synthetic applications. For example, in 2018, Yoon and co-workers employed Cu^{II} salts as terminal oxidants in a study for the oxyamination of alkenes (Table 10, entry 13).[105] In 2016, Ye and coworkers reported their unique role to serve as additives in *O*-glycosylation (Table 10, entry 14).[106]

2.2.4   Conclusion and outlook

Over the past decade, the merger of photoredox and copper catalysis has emerged as a highly versatile platform for developing new synthetic methodologies. By combining these respective powerful catalytic approaches, synthetic organic chemists can access to elusive reactivity that were previously unattainable using a single catalytic system. Therefore, we anticipate that the field of metallaphotocatalysis, particularly synergistic copper and photoredox catalysis, will continue to evolve at a significant rate, expanding the toolbox for the synthetic organic community to simplify the acquisition of valuable chemical building blocks.

2.3 Decarboxylative C(sp³)-N and C(sp³)-O cross-coupling reactions

2.3.1 Importance of nitrogen- and oxygen-containing compounds

Nitrogen- and oxygen-containing functional groups are ubiquitous in molecules relevant to medicine, agriculture, and materials science.[107-112] Not only do they play a pivotal role in regulating physical properties such as lipophilicity and basicity, but can also effectively modulate the efficacy of drugs through hydrogen bonding interactions and conformational effects. Due to the widespread use of these functional groups, the construction of C-O and C-N bonds is of paramount importance in the synthetic organic chemistry community, and the transformation to form these bonds occupies 7 out of the 20 most commonly used reactions in medicinal chemistry alone.[113-114]

Transition metal-catalyzed cross-coupling reactions are the most widely used method for constructing C-N and C-O bonds. Its high efficiency, broad substrate applicability, and tolerance to numerous functional groups make this method widely used in industry and academia. Among the numerous transition metal-catalyzed cross-coupling reactions, the palladium-catalyzed Buchwald-Hartwig reactions,[109, 115-118] the copper-catalyzed Ullman-type reactions[119-120] and Chan-Evans-Lam-type reactions[121] have virtually dominated the field over the past few decades. [116, 122-125] Nevertheless, the use of transition metal-catalyzed cross-coupling reactions for the construction of C-N and C-O bonds also has limitations. For example., while $C(sp^2)$-N and $C(sp^2)$-O cross-couplings of aryl electrophiles can be achieved by the aforementioned protocols, $C(sp^3)$-N and $C(sp^3)$-O cross-couplings of alkyl electrophiles have posed a major challenge.[5-7] The most important issues are as follows: (1) The generation of $C(sp^3)$-metal species by oxidative addition of metal and alkyl electrophiles is sluggish. (2) $C(sp^3)$-metal species that generated via oxidative addition of metal and alkyl electrophiles are susceptible to β-hydrogen elimination. (3) The reductive elimination of $C(sp^3)$-metal intermediates is more difficult to form $C(sp^3)$-N and $C(sp^3)$-O bonds than $C(sp^2)$-N and $C(sp^2)$-O bonds due to the smaller orbital overlap.

In addition to the transition metal-catalyzed reactions, other reaction methods, such as nucleophilic substitution with alkyl halides,[126-128] nucleophilic aromatic substitution (S_NAr).[129] reductive amination,[130] the Curtius rearrangement,[131] and the Mitsunobu reaction[132] can also construct the corresponding $C(sp^3)$-N and $C(sp^3)$-O bonds. However, the drawbacks of these reactions cannot be ignored. For example, the reliance on expensive and toxic reagents, the

generation of harmful quantitative byproducts, and the inability to use sterically bulky alkyl groups. Therefore, scientists have long pursued a novel and robust approach to the construction of $C(sp^3)$-N and $C(sp^3)$-O bonds using inexpensive substrates under mild conditions while allowing the introduction of sterically bulky alkyl groups.
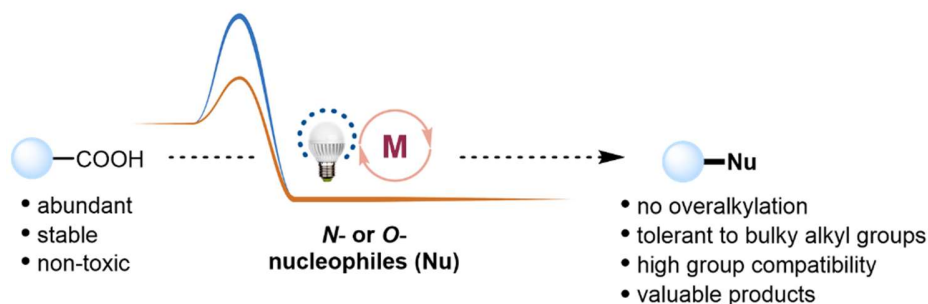
Figure 12 Advantages of photoredox (and metal) catalyzed decarboxylative $C(sp^3)$–N, O bond formation.

Aliphatic carboxylic acids, as a class of raw materials, are ideal starting materials for synthetic organic chemistry by virtue of their low price, stability, and non-toxic nature. These properties are in stark contrast to commonly used electrophiles, such as alkyl (pseudo) halides. In addition, the only by-product of the decarboxylative process is CO_2, which is environmentally benign, non-flammable, and non-toxic. Besides, carboxylic acids are a highly characterized class of scaffolds that promote high chemoselectivity as well as regioselectivity of the reaction. Precisely because of the potential advantages of aliphatic carboxylic acids as feedstocks in organic synthetic transformations, several precedents of decarboxylative $C(sp^3)$-N and $C(sp^3)$-O couplings have been reported.[133-137] However, they are limited to specific substrates or intramolecular couplings. Therefore, the development of a general strategy for mild and efficient decarboxylative $C(sp^3)$-N and $C(sp^3)$-O couplings is highly desirable (Figure 12).

Recent rapid developments in the field of photocatalysis have contributed to the evolution of catalytic methods and, to a large extent, to the innovation of synthetic methods. The essence of photoredox catalysis is the conversion of light energy, by means of single-electron transfer (SET) or energy transfer (ET), into chemical energy. Compared to conventional methods, photoredox catalysis is not only green, safe, clean, and easy to control, but more importantly, renders

previously impossible organic transformations possible. At the same time, the rapidly growing field of visible light catalysis has recently been able to combine the mildness, selectivity, and activity of reactions and take them to a new level. In the last decade, the field of synthetic organic chemistry has made many breakthroughs in photocatalyzed reactions.[74, 78, 85, 138-139] In this context, we will focus on the advances in intra- and intermolecular decarboxylative $C(sp^3)$-N and $C(sp^3)$-O formation using photocatalysis in this section.

2.3.2 Intramolecular decarboxylative $C(sp^3)$-N bond formation

Fu and co-workers reported an intramolecular decarboxylative $C(sp^3)$-N cross-coupling of NHPI esters (Figure 7).[46] Interestingly, the method applies the bifunctionality of the copper catalyst, both as a photocatalyst and as a cross-coupling metal catalyst. As an alternative to the Curtius rearrangement reaction, this method is not only safe but also mild. However, as mentioned previously, the substrate scope of this method is limited and is neither suitable for sterically bulky alkyl groups nor for more N-nucleophilic reagents.

2.3.3 Intermolecular decarboxylative $C(sp^3)$-N bond formation

2.3.3.1 Hypervalent iodine[III]-mediated decarboxylative Ritter-type amination

In 2017, Minakata and co-workers reported a Ritter-type amination reaction of aliphatic carboxylic acids to construct $C(sp^3)$-N bonds.[140] This reaction utilizes $PhI(OAc)_2$ and molecular iodine (I_2) to activate the carboxylic acid under irradiation of ultraviolet light and generate the corresponding amination products in moderate to high yields (Figure 13). This approach has expanded the range of feedstocks for Ritter-type amination, i.e., from alkenes, alkanes, and alcohols to carboxylic acid substrates, while avoiding the use of strong acids and high temperatures and, to some extent, expanding substrate compatibility. It should be noted, however, that this reaction is similar to the classical Ritter-type amination reaction, where the substrate scope is limited to tertiary radical sources, namely tertiary aliphatic carboxylic acids (**2.175**-**2.180**, Figure 13). Mechanistic studies suggest that the reaction may sequentially undergo aliphatic carboxylic acid activation/oxidation/nucleophilic substitution/hydrolysis, in which the formation of alkyl iodides and the corresponding alkyl-λ^3-iodanes are the key intermediates of the reaction. In addition, fluorescence irradiation can effectively activate molecular iodide while facilitating the decarboxylation process.
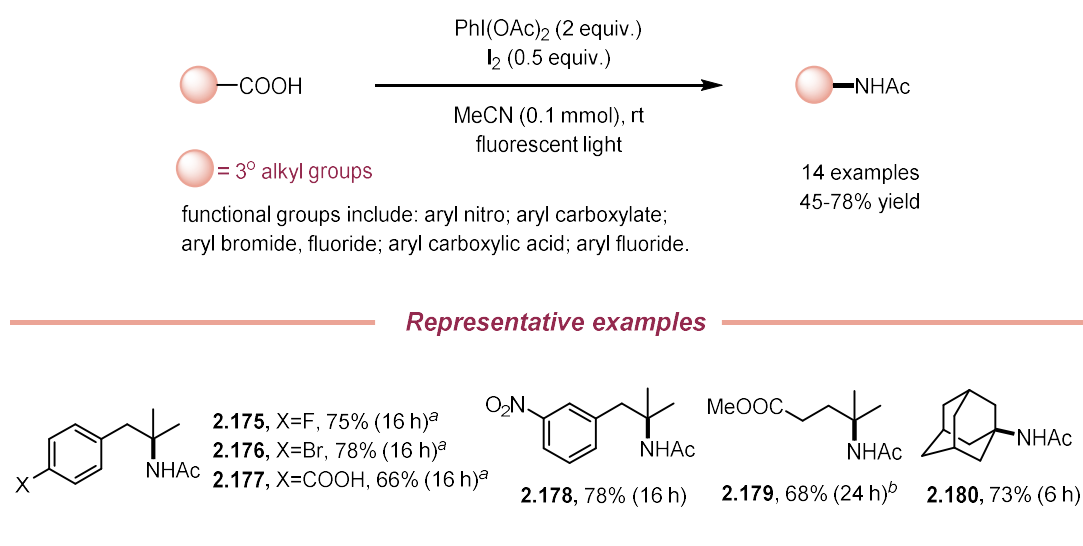
Figure 13 Hypervalent iodine^{III}-mediated decarboxylative Ritter-type amination. ^{a}PhI(OAc)$_2$ (1.5 equiv.) was used. ^{b}PhI(OAc)2 (2.5 equiv.) was used.

2.3.3.2 Decarboxylative imidation of arylacetic acids

In 2018, Itami and co-workers reported a C(sp3)-N bond-forming reaction via photoredox-catalyzed decarboxylative imidation of aryl acetic acids (Figure 14)[141] The optimized reaction conditions using [Ru(bpy)$_3$]Cl$_2$·6H$_2$O (2.5 mol%) as the photocatalyst, 1-butoxy-1λ^3-benzo[d][1,2]iodaoxol-3(1H)-one (IBB) (2.5 equiv.) as a hypervalent-iodine-based oxidant and dichloromethane as the solvent at 40 °C under irradiation of blue LEDs. The method exhibits good functional group compatibility and could also be applied to the late-stage functionalization of drug molecules, such as indomethacin (**2.181**), flurbiprofen (**2.182**) and ibuprofen (**2.183**). However, the scope is limited to aryl acetic acids, and the nitrogen nucleophile is restricted to disulfonimides, which, in some extent, confines the application of this methodology.
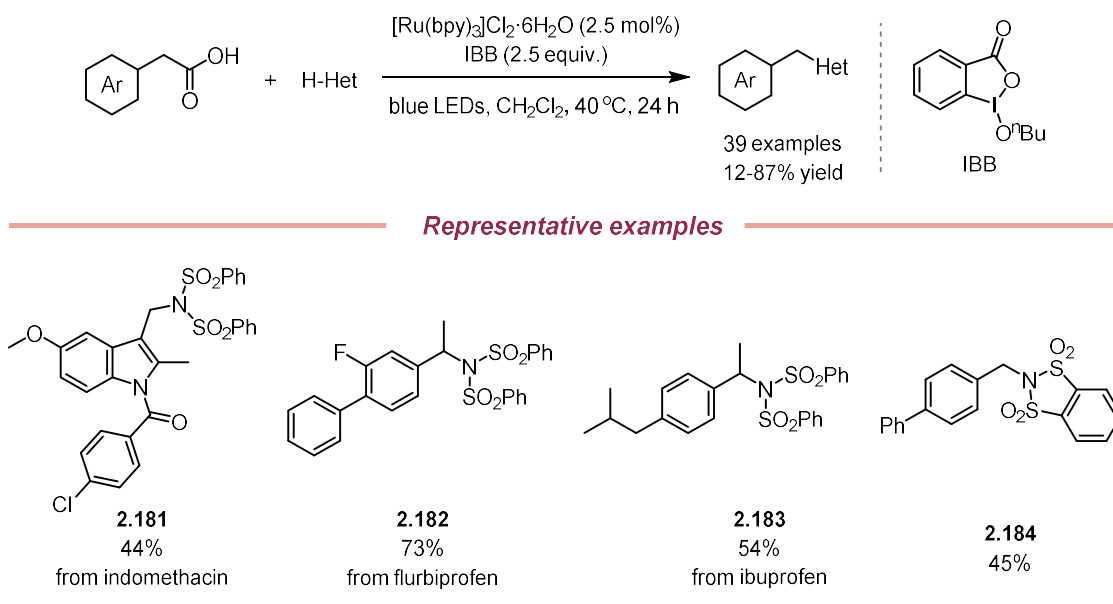
Figure 14 Photoreodx-catalyzed decarboxylative C(sp^3)–N couplings using aryl acetic acids.

2.3.3.3 Decarboxylative azidation of cyclic amino acids

In 2019, Leonori and co-workers[142] reported a method for photoredox-catalyzed decarboxylative azidation of cyclic amino acids. The optimized conditions included the use of rhodamine 6G (Rh6G), a low-cost and readily available organic dye, as a photocatalyst, green LEDs as light source, CsOBz as base and DCE as solvent (Figure 15). Notably, Rhodamine 6G as a photocatalyst seems to be essential for the functionalization of cyclic amino acids and dipeptides to ensure the efficiency of the reaction. Nevertheless, the method has significant limitations, such as the carboxylic acid substrates being restricted to cyclic amino acids (**2.185-2.186**) and a limited number of tertiary aliphatic carboxylic acids (**2.189-2.190**). Moreover, the reaction cannot convert acyclic amino acids (**2.187-2.188**) under optimized conditions.
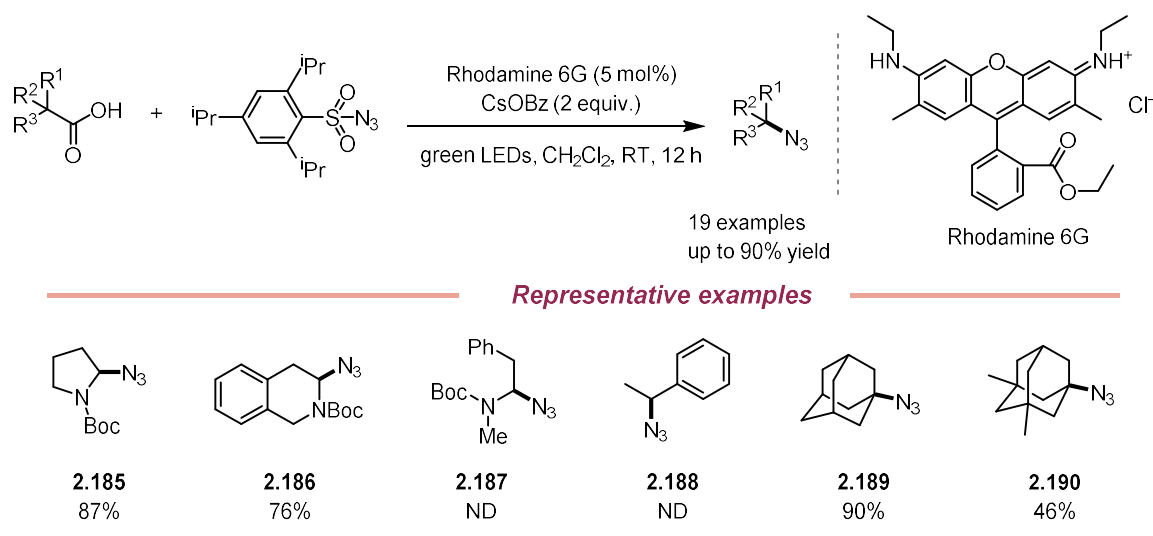
Figure 15 Intermolecular decarboxylative azidation of cyclic amino acids with rhodamine 6G as the photocatalyst.

2.3.4 Decarboxylative C(sp³)-O bond formation

The C(sp^3)-O fragments are highly valuable for various applications. However, obtaining them by conventional S$_N$1 or S$_N$2 methods is problematic because of their poor functional group compatibility and the required harsh reaction conditions. Furthermore, using transition metals as catalysts to construct carbon-heteroatom bonds is another efficient approach. However, in this case, the formation of C(sp^3)-O bonds may be difficult due to slow oxidative addition/reduction elimination and β-hydrogen elimination. Recently, Nagao, Ohmiya, and co-workers demonstrated a photocatalytic approach to construct such important groups (Figure 16).[143] They reported the formation of C(sp^3)-O bonds between several nucleophiles, especially oxygen nucleophiles, and redox-active alkyl esters (NHPI esters) catalyzed by an organic photocatalyst **2.191** alone. The photoredox catalyzed reaction exhibits a unique tandem reduction and oxidation process, which makes full use of the oxidizing and reducing properties of the photocatalyst and makes the whole reaction redox-neutral. This reaction does not require external oxidants, reductants, or even bases, demonstrating a cost-effective approach. With respect to the range of substrates, it is very similar to the Ritter-type reactions, only NHPI esters that generate stabilized carbon cations can be used to obtain good to excellent yields of the corresponding products (**2.192-2.195**).
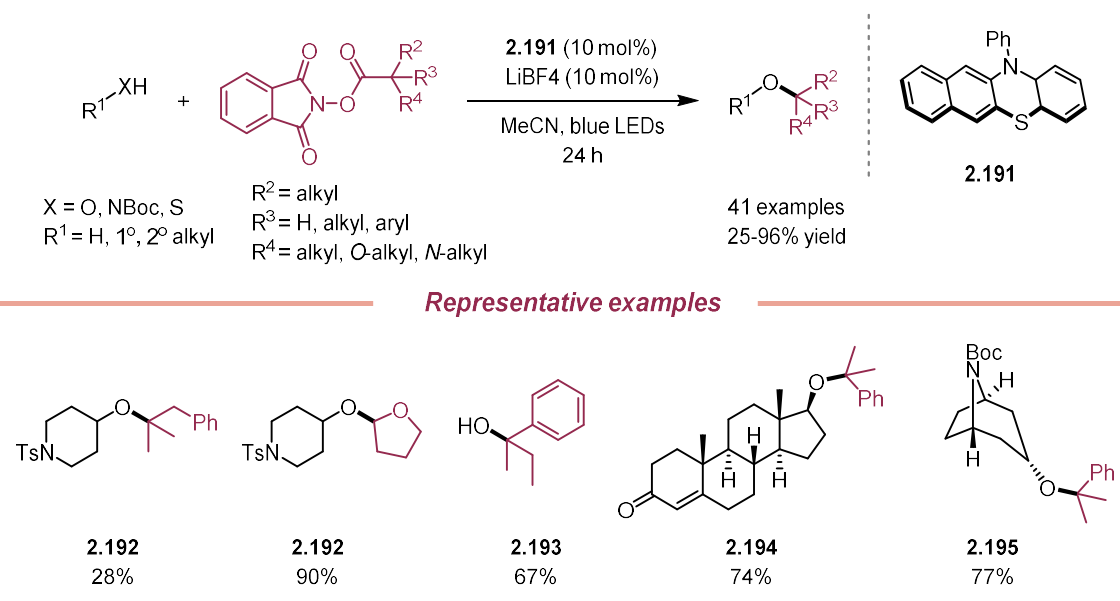
Figure 16 Decarboxylative C(sp³)-O cross-coupling using organo-photocatalyst.

2.3.5 Conclusion and outlook

This section summarizes recent advances in the photoredox-catalyzed C(sp³)-N and C(sp³)-O decarboxylative coupling reactions. This strategy has recently received extensive attention from the synthetic organic community, as this approach not only takes full advantage of photocatalysis and the use of aliphatic carboxylic acids as substrates, but also the construction of high value-added products is attractive.

However, despite the inherent advantages of this strategy, the field is still in its infancy and the reported relevant work shows clear limitations. For example, all reactions shown in this section are restricted to intramolecular reactions or specific carboxylic acid substrates (e.g., tertiary aliphatic carboxylic acids).

We anticipate that a versatile, efficient photocatalytic method for decarboxylative C(sp³)-N and C(sp³)-O coupling could be developed in the future. We expect that such an approach will not only avoid the drawbacks of conventional methods but also allow for a broader application potential.

2.4   Recent developments in using benzophenone imines as ammonia equivalents

2.4.1   Introduction

Most of the 200 best-selling small-molecule drugs of 2018 contain nitrogen atoms, with unprotected primary amines accounting for nearly 25% of them.[144] Therefore, the importance of primary amines in the drug molecule is significant. As a result, synthetic organic chemists have shown great interest in developing new methods to obtain primary amines.[145]
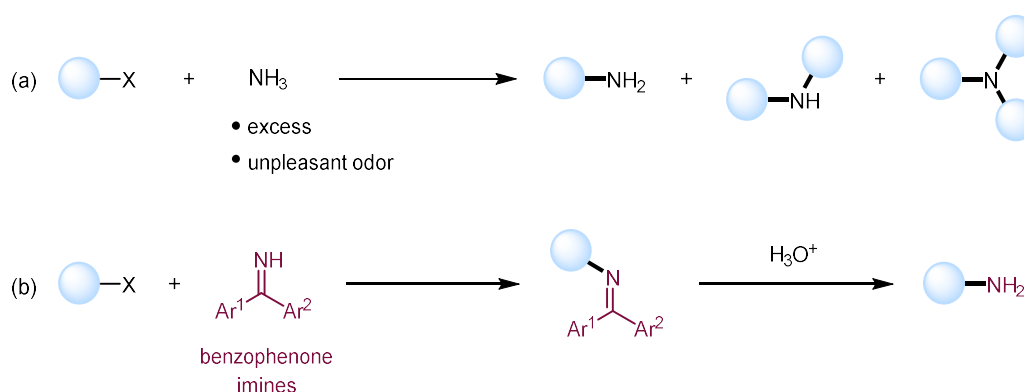
Figure 17 Synthetic routes to primary amines. (a) using ammonia as nitrogen source; (b) using benzophenone imines as ammonia equivalents.

Ammonia represents one of the most readily available nitrogen sources, and it has been widely used to generate primary amines.[146] However, the direct use of ammonia has obvious limitations (Figure 17), such as (1) the difficulty in controlling the number of substitutions, leading to the formation of by-products, such as secondary and tertiary amines; (2) the fact that a large excess of ammonia is usually required to inhibit the formation of side reactions; and (3) the unpleasant odor and toxicity are problems in use that cannot be ignored. Therefore, to overcome these issues, chemists have been searching for an effective and efficient alternative to ammonia. Among all the candidates, benzophenone imine and its derivatives show great potential (Figure 17).

Benzophenone imine or (diphenylmethylene)amine is an important reagent in organic synthesis. It is a commercially available liquid that is easily prepared by adding phenylmagnesium

bromide to benzonitrile and hydrolyzing it with methanol or by reacting benzophenone with ammonia. Initially, synthetic applications of benzophenone imine have been historically associated with peptide chemistry, particularly as a masked primary amine in the preparation of optically active α-amino acids.[147] Benzophenone imine and derivatives can not only serve as ammonia equivalents, but can also readily synthesize masked primary amines avoiding over functionalization. Furthermore, the masked primary amines can be converted to their deprotected form by simple hydrolysis, which not only ensures high yields but also preserves enantioselectivity.[148] More importantly, benzophenone imines are simple and readily available, and their analogues can also be obtained from nitrile compounds in one step using Grignard's reagent[149].

In this context, we summarize in this section recent advances in the use of benzophenone imines as ammonia equivalents.

2.4.2 Palladium- or nickel-catalyzed cross-coupling reactions

In a 2016 review, Buchwald and co-workers have summarized palladium-catalyzed cross-coupling reactions using benzophenone imines as ammonia surrogates.[109] Therefore, in this section, we will only list the representative results reported after this review.

2.4.2.1 Cross-coupling reactions with aryl (pseudo) halides

In 2017, Rueping and co-workers reported a nickel-catalyzed Buchwald-Hartwig-type amination between phenol derivatives and benzophenone imines (Figure 18).[150] Under optimal conditions, pivalates, carbonates, carbamates, and sulfamates can all be efficiently activated. Under optimal conditions with Ni(cod)$_2$ as the metal source and dcpe(1,2-bis(dicyclohexylphosphino)ethane) as the ligand, pivalate is the best activating group. When benzophenone imines were used as nucleophiles, a series of primary aromatic amines (via hydrolysis, 21 examples, 40-92% yield) or secondary amines (via reduction, 3 examples, 71-88% yield) were obtained in moderate to excellent yields.
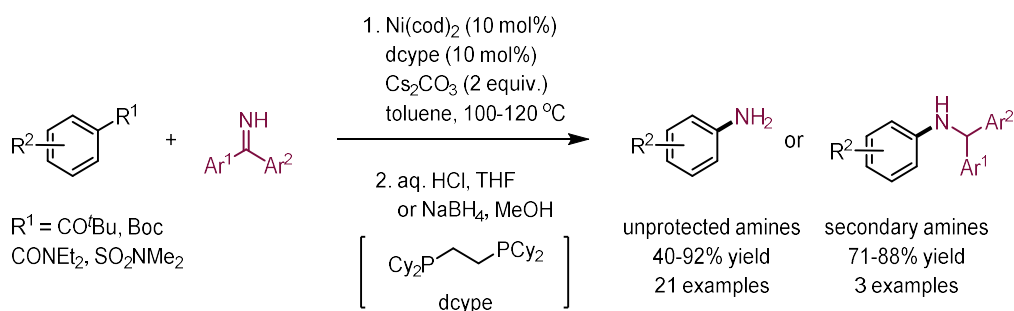
Figure 18 Nickel-catalyzed Buchwald-Hartwig-type amination between phenol derivatives and benzophenone imines.

Although Buchwald-Hartwig amination reactions using aryl monohalides are well established, one-pot chemoselective cross-coupling using aryl dihalides is still limited. In 2018, the Colacot group developed a method for the synthesis of aminoanilines between aryl dihalides, benzophenone imine, and amines (Figure 19).[151] Theoretically, this three-component, one-pot reaction could yield various products simultaneously. However, by modulating the nucleophilic reagents and the catalyst system (catalyst system: **2.196**+**2.197** or **2.196**+**2.198**), they succeeded in obtaining only one product.
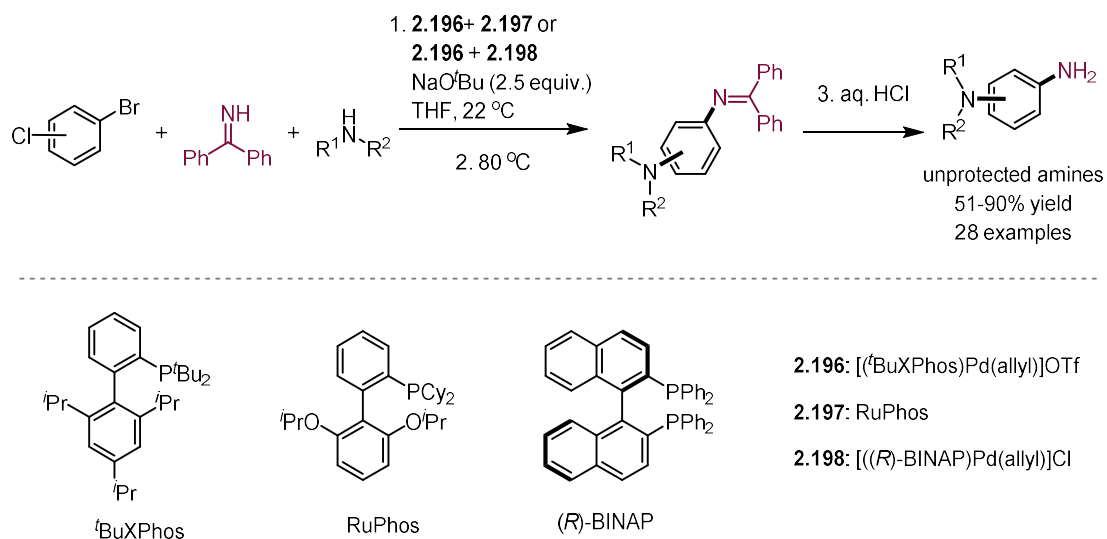
Figure 19 Palladium-catalyzed three-component, one-pot synthesis of aminoanilines.

Transition metal-catalyzed cross-coupling reactions of benzophenone imines with alkyl halides, especially those containing sterically bulky alkyl groups, are challenging and of great practical interest. In 2016, Hartwig's group reported an elegant work to efficiently construct $C(sp^3)$-N bonds by coupling between benzophenone imines and secondary or tertiary alkyl bromides using a palladium-based catalyst.[149] After evaluating a range of phosphine ligands, they found that the sterically bulky trialkylphosphine ligand ^{t}BuCy$_2$P gave the highest yield of *N*-alkylated products (Figure 20). In addition, the method can tolerate different functional groups, giving the corresponding products in moderate to excellent yields. However, the elevated temperature and unreactive primary alkyl bromides exhibit some limitations of this methodology. To shed light on this reaction mechanism, both radical clock and racemization experiments were conducted to support a radical process. Besides, when *exo*- (**2.199**) and *endo*- (**2.200**) 2-bromonorbornane were employed simultaneously as the starting materials, only product in the *exo* form (**2.201**) could be detected in >97% yield (Figure 20), further evidencing the existence of a radical intermediate (**2.202**).
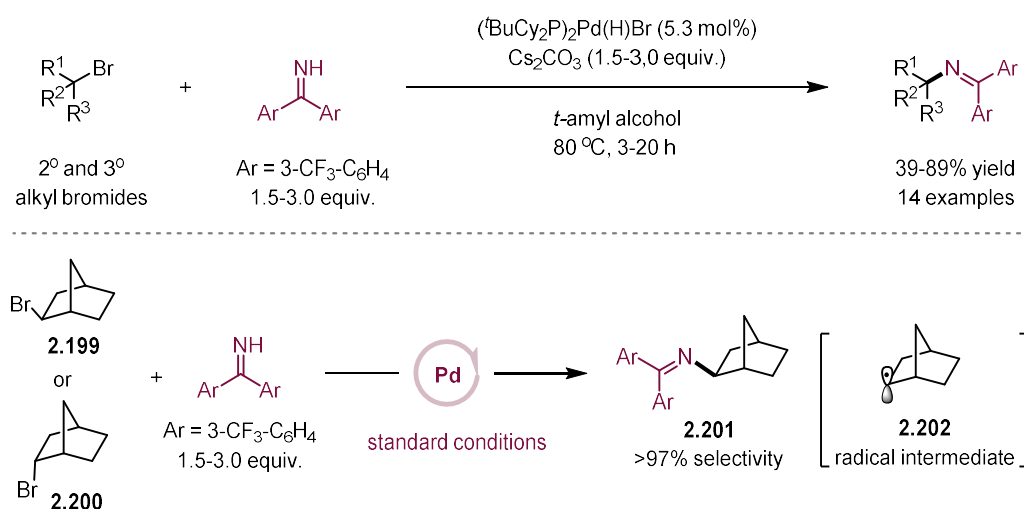
Figure 20 Palladium-catalyzed cross-coupling reaction with alkyl bromides.

2.4.3   Other cross-coupling reactions

In addition to palladium- and nickel-catalyzed cross-coupling reactions, benzophenone imines are widely used as unique ammonia equivalents in other types of cross-coupling reactions. In this section, we will present the latest advances.

2.4.3.1   Iodide-catalyzed oxidative cross-dehydrogenative cross-coupling

In 2015, Li and co-workers reported a method for oxidative amination with benzophenone imines.[152] This method utilizes catalytic amounts of iodide source, potassium iodide (KI, 10 mol%), or tetra-*n*-butylammonium iodide (TBAI, 10 mol%), and *tert*-butyl hydroperoxide (TBHP, 3 equivalents) to achieve several interesting oxidative amination reactions with benzophenone imines. With the optimal reaction conditions, the method was successfully applied to the synthesis of a variety of products to efficiently introduce amino groups and to obtain biologically active products in satisfactory yields (Figure 21).
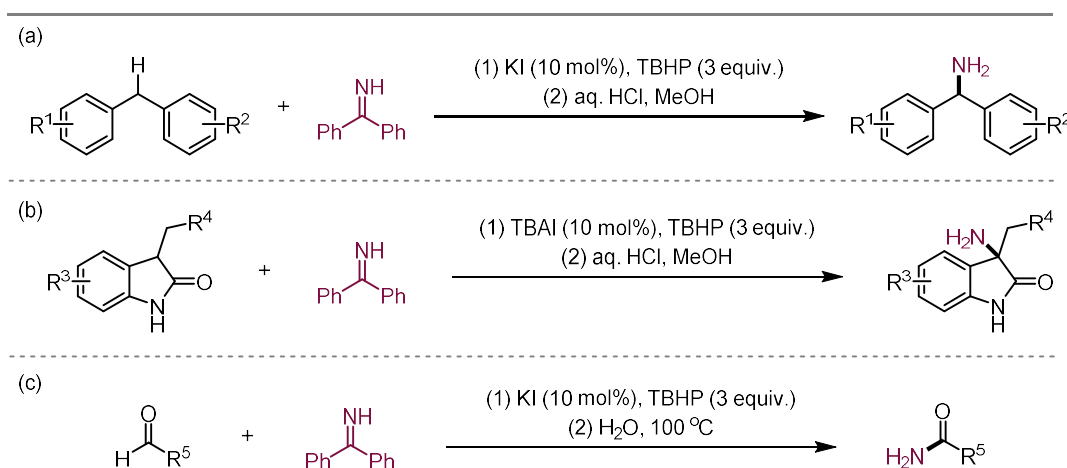
Figure 21 Iodide-catalyzed oxidative cross-coupling reaction.

2.4.3.2   Copper-catalyzed cross-dehydrogenative coupling of alkyl arenes

In 2019, Kramer and co-workers reported a copper-catalyzed cross-dehydrogenative coupling method, which enables the transformation of alkyl arenes and benzophenone imines into α-substituted primary benzylamines.[153] The highest efficiency can be obtained when using CuI (1 mol%) as the metal source, 1,10-phenanthroline (2 mol%) as the ligand, di-*tert*-butyl peroxide

(4.0 equiv.) as the oxidant and chlorobenzene as the solvent under 90 °C for 48 hours. The standard conditions can tolerate various secondary and tertiary alkyl arenes (16 examples), obtaining synthetically useful yields (20-70%). As observed by the authors, under the standard conditions, both ethylbenzene and benzophenone imine can undergo dimerization, which favors a free radical pathway. In addition, kinetic isotope effect experiments showed that the hydrogen-atom transfer process was the rate-determining step (Figure 22).
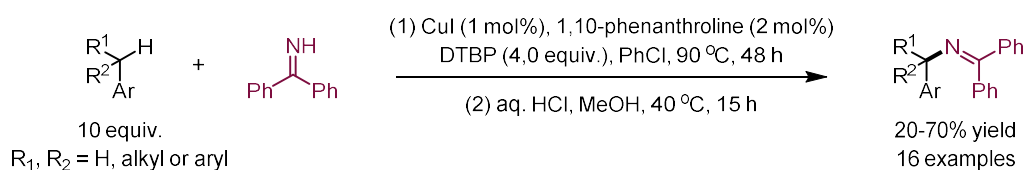
Figure 22 Copper-catalyzed cross-dehydrogenative coupling reaction of alkylarenes.

2.4.3.3 Oxidative α-amination of esters using benzophenone imine-derived hypervalent iodine reagents

The umpolung of benzophenone imine is of great interest as it allows the conversion of a masked amine from a nucleophile to an electrophile. In 2019, Minakata and co-workers reported the synthesis of benzophenone imine-derived hypervalent iodine reagents and the successful applications of such reagents in oxidative α-amination of esters.[154] The hypervalent iodine reagent can be prepared by ligand exchange between a benzophenone imine and an acetoxyiodine, and the product was confirmed by X-ray crystallography, while the method allows for gram-scale synthesis of the reagent. The hypervalent iodine reagent can be applied to an oxidative amination reaction of ketene silyl acetals and various α-amino acid derivatives were obtained (Figure 23). Mechanistic studies indicated that a single-electron transfer from the silyl ketene acetal to the hypervalent iodine reagent occurred during this transformation.
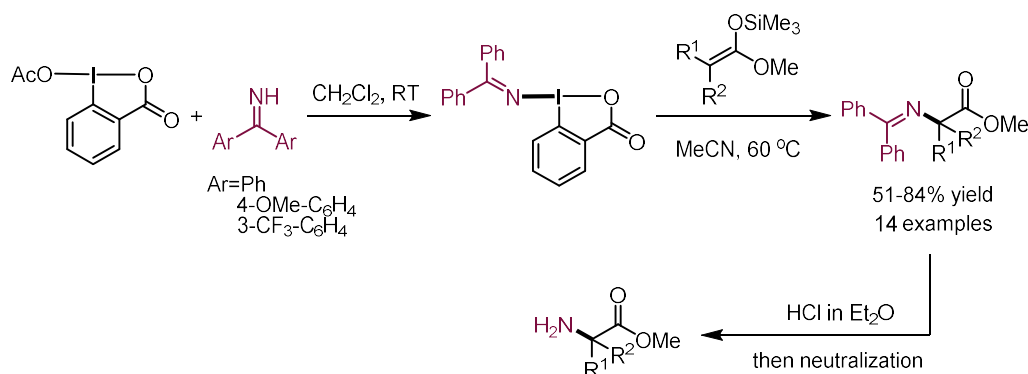
Figure 23 Oxidative α-amination of esters with hypervalentiodine reagents.

2.4.4 Catalytic nucleophilic ring-opening of epoxides

Nucleophilic ring-opening of epoxides with nitrogen nucleophiles represents a class of efficient approaches to synthesize 1,2-amino alcohols. Such transformations are widely used to build valuable compounds, such as chiral ligands. In 2008, the groups of Mai and Schneider reported an enantioselective ring-opening method between *meso*-epoxides and benzophenone imine that catalyzed by scandium triflate-chiral bipyridine complex (Sc(OTf)$_3$ and **2.203**) (Figure 24).[155] However, the scope of this method is narrow (3 examples) and yields are moderate (48-56% yield). Later, Lim and Leitch also reported Lewis acid-catalyzed nucleophilic ring-opening of epoxides with benzophenone imine.[156] After a screening of nearly 50 Lewis acids, Y(OTf)$_3$ gave the best result Notably, a synthetic application was also presented to synthesize the skeleton of PRMT5 inhibitor[157] in a gram scale without isolating the intermediates.
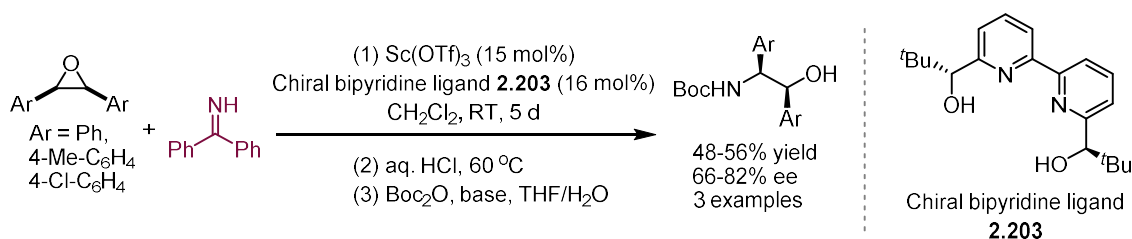
Figure 24 Lewis acid-catalyzed nucleophilic substitution of epoxides.

2.4.5   Catalytic N-H insertion of carbenes

Transition metal-catalyzed enantioselective insertion of α-diazo carbonyl compounds into N-H bonds supplies an effective approach to build α-amino acids.[158-160] In this context, the group of Liu developed enantioselective insertion of carbenes into the N-H bond of benzophenone imines (Figure 25). The previously reported catalyst system (Rh₂(OAc)₄ and chiral guanidine **2.204** in O-H insertion)[161] has successfully found a new application for inserting N-H bonds.[162] After systematic screening, it was finally found that Rh₂(esp)₂ and an *L*-Ramipril-derived chiral guanidine could yield the desired product in high yields and with good enantioselectivity. The use of 4,4'-difluorobenzophenone imine can further enhance the effectiveness. The authors also examined the scope of substrates and showed that both aryl- and alkyl-substituted α-diazo esters could be used for the transformation, with satisfactory yields and enantioselectivity.
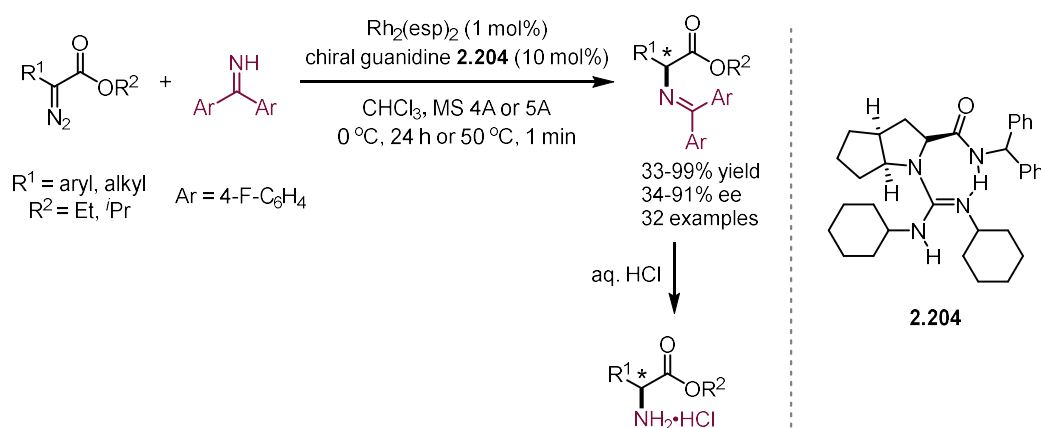
Figure 25 Rhodium/chiral guanidine-catalyzed NH insertion of carbenes.

2.4.6   Catalytic enantioselective nucleophilic additions

Benzophenone imines can be used not only in cross-coupling reactions but also in nucleophilic addition reactions due to their nucleophilic nature. In this section, we present their recent applications in the field of catalytic enantioselective amination of unsaturated compounds.

2.4.6.1   Addition to nitroalkenes

The enantioselective 1,4-addition reactions of ammonia and nitroalkenes provide an efficient way to obtain chiral β-amino nitroalkanes.[163] In previously reported work, the deprotection

process of the protected amine was a major problem. Unsurprisingly, an easily removed protected group can greatly simplify subsequent conversions and make the process of obtaining high value-added chiral amines easier. To solve these difficulties, Jørgensen and coworkers applied benzophenone imine as an ammonia equivalent for a 1,4-addition with nitroalkenes (Figure 26).[164] The optimization results showed that the best enantioselectivity of the reaction could be obtained at low temperatures when a thiourea **2.205** was used as catalyst and *n*-heptane as a solvent. A study of the scope of substrate applicability revealed that both alkyl- and aryl-substituted nitroalkenes are viable substrates. More importantly, the deprotection could be carried out in the same pot and the corresponding primary amine hydrochloride products were obtained in high yields.
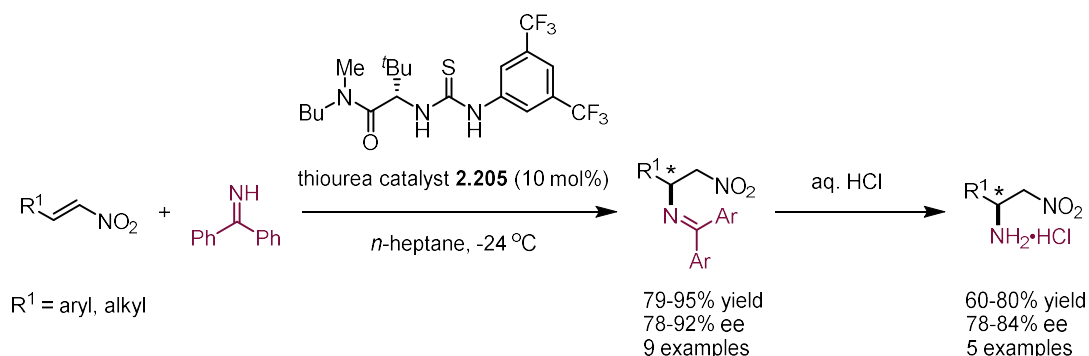
Figure 26 Organocatalyzed 1,4-addition to nitroalkenes.

2.4.6.2   Addition to Mirita-Baylis-Hillman carbonates

Enantioselective amination of Morita-Baylis-Hillman (MBH) carbonates enables a concise route to optically active β-aminocarbonyl compounds. Although the use of phthalimides as nitrogen nucleophiles has been reported and achieved 90% enantiomeric excess (ee) in most cases,[165-166] applying benzophenone imine as a nitrogen nucleophile would simplify the subsequent deprotection step. In 2011, Cheng and co-workers disclosed the usage of benzophenone imine as an ammonia equivalent for enantioselective amination with MBH carbonates (Figure 27).[167] Catalyzed by a chiral organocatalyst (DHQD)₂AQN **2.206**, various MBH carbonates were transformed with high enantioselectivity (in most cases more than 95% ee). Subsequently, the products were deprotected under acidic conditions to obtain unprotected amines without corroding the stereoselectivity.
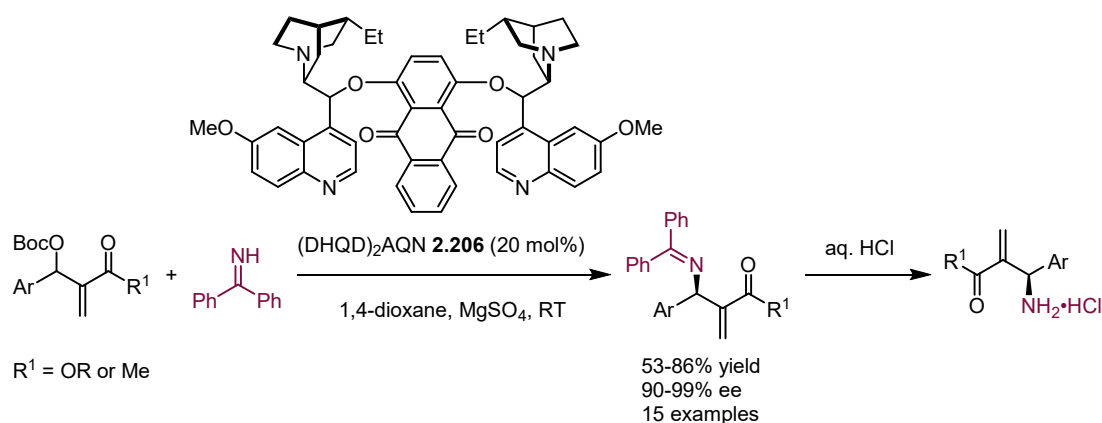
Figure 27 Organocatalytic addition to Morita-Baylis-Hillman carbonates.

2.4.6.3 Hydroamination of allenes

Chiral allylic amines are important as intermediates for obtaining biologically active compounds.[168] Although ammonia can theoretically be transformed into allylic amines by direct amination, this atom-economic approach does not proceed efficiently. However, benzophenone imines can overcome the disadvantages of ammonia as a nucleophilic reagent. It is for this reason that in 2016 Breit and co-workers developed a rhodium-catalyzed enantioselective hydroamination of terminal allenes with benzophenone imine (Figure 28).[169] The authors chose cyclohexylallene as a substrate to optimize reaction conditions. It was found that the combination of rhodium catalyst [Rh(cod)Cl]₂, Josiphos ligand, and pyridinium *p*-toluenesulfonate (PPTS) gave the best yields and enantioselectivity. With the optimal conditions in hand, the authors examined the scope of substrate applicability and found that the method could be successfully applied to the conversion of various terminal olefins (17 examples), yielding the products in good yields (60-91% yield) and with high enantioselectivities (84-97% ee). It is noteworthy that this method also allows gram-scale synthesis without affecting the yield and enantioselectivity. More importantly, primary amines can be obtained without loss of enantioselectivity after simple acidic deprotection.
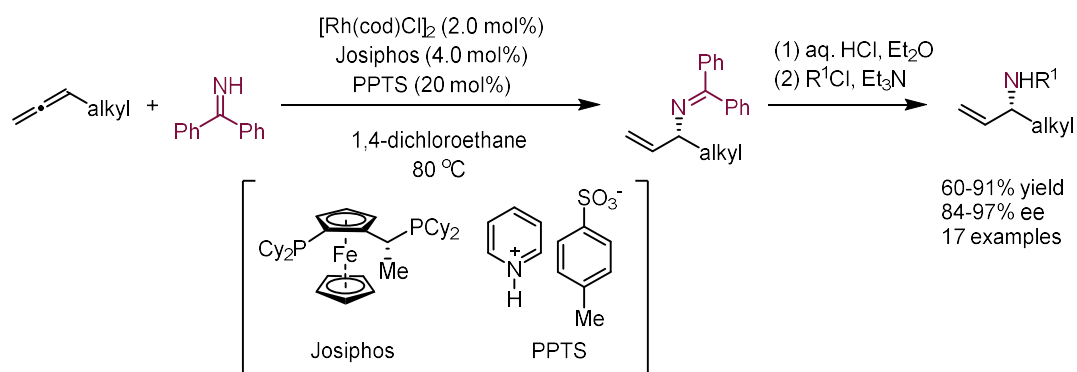
Figure 28 Rhodium-catalyzed hydroamination of allenes.

2.4.6.4   Addition to α, β-unsaturated aldehydes

Catalytic nucleophilic addition of nitrogen nucleophiles to α, β-unsaturated aldehydes offers a concise path to 1,3-amino alcohols and derivatives.[170-171] However, a facile route to unprotected amine has not been reported yet. The use of benzophenone imine can provide an alternative approach. In 2018, Alemán and co-workers showed the usage of benzophenone imine as ammonia equivalents for prolinol (**2.207**)-catalyzed addition to α, β-unsaturated aldehydes.[172] In this reaction, an intramolecular hydrogen bonding in the imine nucleophile is vital for both the yield and enantioselectivity (Figure 29). DFT calculations showed the acidity of the N-H proton could be enhanced due to the hydrogen-bonding effect, thus, increasing the yields and enantioselectivities. Encouraged by these results, the optimized conditions were applied to more substrates to enrich diversity. Unprotected δ-amino-esters could be obtained after simple hydrolysis.
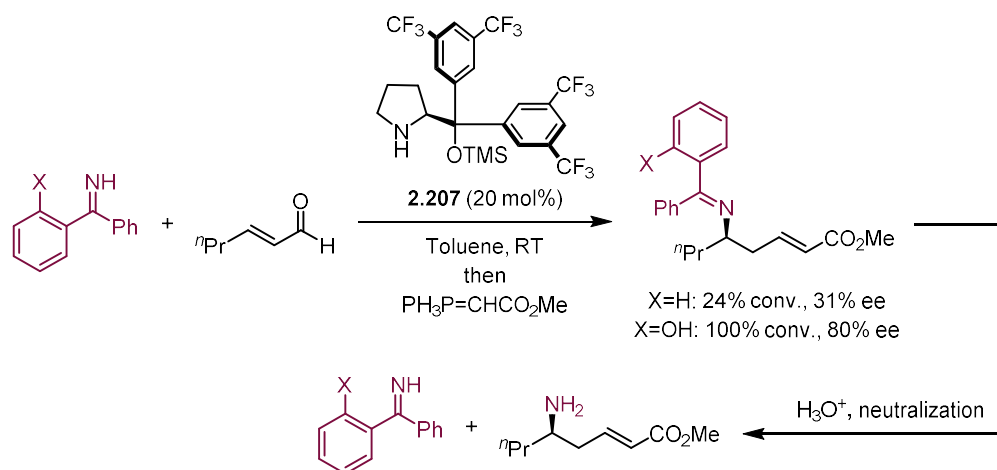
Figure 29 Diarylprolinol-catalyzed addition of 2-hydroxybenzophenone imines to α,β-unsaturated aldehydes.

2.4.7 Conclusion and outlook

In summary, in this section, we have presented recent developments in the amination reaction of using benzophenone imines as nucleophiles. In contrast to the direct use of ammonia as nucleophilic reagents, benzophenone imines can be used as a class of efficient ammonia equivalents by virtue of their excellent reactivity and chemoselectivity as well as their easy deprotection. Such reagents can effectively assist chemists in developing methods to obtain primary aryl- and alkyl-amines that are important in medicinal chemistry. In addition, the generated primary amines can be easily converted subsequently, laying the foundation for efficient synthesis of other amine compounds. We anticipate that this reagent will drive the discovery of more amination reactions to facilitate the rapid synthesis of more bioactive compounds.

2.5   Recent advances in the synthesis trifluoromethylthioesters

2.5.1   Introduction
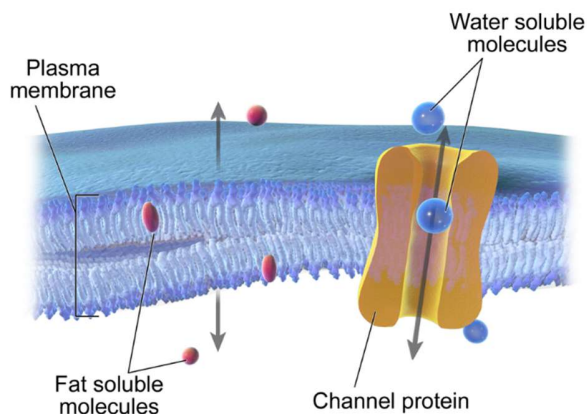
Figure 30 Demonstration of the passive diffusion and transmembrane of small molecules through a typical cell membrane.[173]

Fluorine is the most abundant halogen element in the Earth's crust and ranks 13th in the abundance ranking of all elements.[174] In terms of fluorine element distribution, fluorine is widespread in most igneous and sedimentary rocks (270-740 ppm), but most of this class of fluorine is an insoluble form and is not available for effective natural circulation. In contrast, however, organic fluorine compounds have significant applications in human society. For example, the introduction of fluorine-containing groups into organic molecules tends to significantly alter their chemical, physical, and biological properties, making fluorinated compounds very widely used in medicine, agriculture, and material sciences.[175-178] Despite the pivotal importance of organic fluorine compounds, however, there are barely more than ten organic fluorine compounds that have been identified in nature. Therefore, synthetic fluorine chemistry has become a critical field, building a bridge from nature to human society.

One example of the importance of fluorine chemistry in human society is the contribution of fluorine to medicinal chemistry. One of the most important applications of fluorine in medicinal chemistry is to modulate the lipophilicity of drugs in order to enhance the membrane permeability of drugs. Membrane permeability refers to the rate of passive diffusion of molecules through a

membrane and is an important property to evaluate during the drug design process. This property is particularly important when studying small molecule drugs with intracellular targets, as the efficacy of small molecules is highly dependent on their ability to penetrate membranes (Figure 30).[179] In this context, fluorinated groups can significantly increase the lipophilicity of small-molecule drugs, thus enhancing their membrane permeability.

Hansch lipophilicity parameter (π_R) is an important indicator of functional groups. In medicinal chemistry, the addition of highly lipophilic electron-withdrawing groups to bioactive molecules may improve their metabolic stability. Among all the fluorine-containing groups, in contrast to trifluoromethyl (-CF$_3$, π_R =0.88) and trifluoromethoxy (-OCF$_3$, π_R =1.04) groups, trifluoromethylthio groups (-SCF$_3$, π_R =1.44) are of considerable interest due to their superior properties.[180-182] Because of this, many pharmaceutical and agrochemical compounds that have been marketed contain -SCF$_3$ groups (Figure 31). Precisely because of the growing interest in -SCF$_3$ groups, in recent years, the development of trifluoromethylthiolation has attracted more and more attention from chemists and has led to a number of significant advances in synthetic methodologies.[178, 183-197] However, the diversity of such field is lacking. For example, although the synthesis of trifluoromethylthioethers is very well established, the study of trifluoromethylthioesters is still in its infancy, not only academically but also in terms of practical applications. Despite the fact that trifluoromethylthioesters may have greater pharmaceutical potential in terms of properties such as lipophilicity.
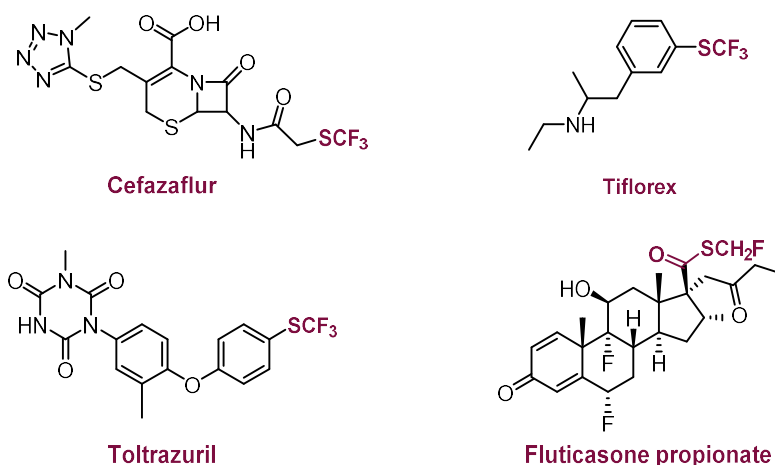
Figure 31 Examples of bio-active compounds containing a trifluoromethylthio (-SCF$_3$) group.

In this section, we will focus on advances in the synthesis of trifluoromethylthioesters. Notably, since Man and co-workers first reported on the synthesis of trifluoromethylthioesters in 1959,[198] all reported methods have used either acid chlorides or aldehydes as starting materials. Therefore, we have divided this section based on the use of the substrates.

2.5.2 Synthesis of trifluoromethylthioesters from acid chlorides

Trifluoromethylthioesters can be synthesized by halide substitution reactions from corresponding acid chlorides with various nucleophilic trifluoromethylthiolating reagents. In 1959, Man and co-workers reported the first example using $Hg(SCF_3)_2$ as a trifluoromethylthiolating reagent for the synthesis of trifluoromethylthioesters.[198] Three acid chlorides, acetyl chloride, propionyl chloride, and 2,2,2-trifluoroacetyl chloride, were converted to the corresponding trifluoromethylthioesters in 23-51% yields at 40 ℃ or 50 ℃ using diethyl ether as a solvent and stoichiometric amounts of $Hg(SCF_3)_2$ as the trifluoromethanethiolating reagent (Figure 32). However, the limitations are evident for this method: the use of stoichiometric amounts of a toxic heavy metal reagent has posed a significant issue for this conversion.
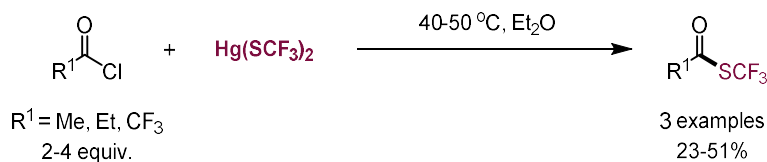
Figure 32 Using $Hg(SCF_3)_2$ as a trifluoromethylthiolating reagent for the synthesis of trifluoromethylthioesters.

After the pioneering work reported by Man's group, the field remained dormant for nearly half a century until 2004, when Yagupolskii and co-workers reported the use of tetramethylammonium trifluoromethylthiolate (NMe_4SCF_3) as a reagent for the synthesis of trifluoromethylthioesters.[199] This method smoothly converted a set of acid chlorides into the corresponding products under the standard conditions in 63-82% yields (**2.208-2.213**, Figure 33). It is noteworthy that the addition of NMe_4SCF_3 should be performed slowly and dropwise at -30 ℃, demonstrating the high activity of this trifluoromethylthiolating reagent.
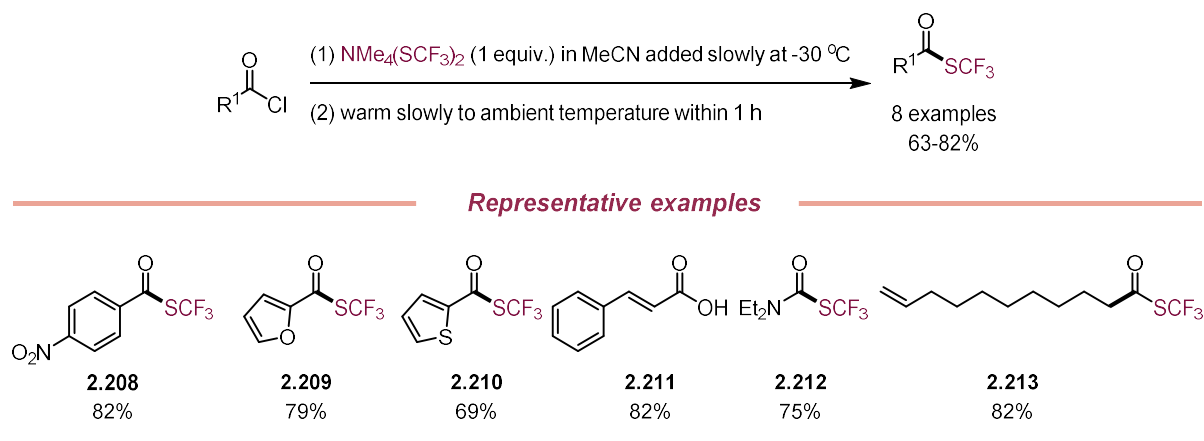
Figure 33 Using NMe$_4$SCF$_3$ as a trifluoromethylthiolating reagent for the synthesis of trifluoromethylthioesters.

Subsequently in 2016, Weng and co-workers developed a copper-mediated trifluoromethylthiolation method for acid chlorides using (bpy)CuSCF$_3$ as the trifluoromethythiolating reagent.[196] This method enables the synthesis of a variety of trifluoromethylthioesters in good to excellent yields and with good tolerance to various functional groups such as cyano, ether, ester, halide, and nitro groups (Figure 34). More importantly, the reaction conditions can tolerate both aryl-, cinnamic-, alkyl- acid chlorides, providing a general approach to synthesize these valuable products. However, the use of stoichiometric amounts of metal reagent (bpy)CuSCF$_3$ poses a problem for this methodology.
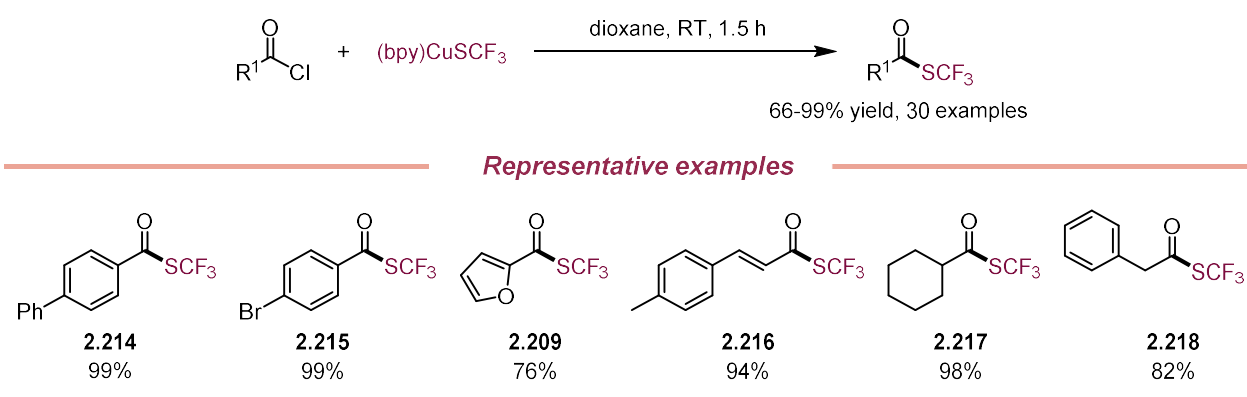
Figure 34 Using (bpy)CuSCF$_3$ as a trifluoromethylthiolating reagent for the synthesis of trifluoromethylthioesters.

2.5.3   Synthesis of trifluoromethylthioesters from aldehydes

The synthesis of trifluoromethylthioesters from aldehydes is an efficient method for obtaining these valuable products. Usually, this method requires a hydrogen-atom transfer (HAT) reagent to achieve the conversion of aldehydes to trifluoromethylthioesters. A general mechanistic pathway of this strategy is depicted in Figure 35. Specifically, the C-H bond in the aldehyde group has a relatively low bond dissociation energy (BDE) (~94 kcal/mol),[200] which allows a diverse selection of HAT reagents to abstract this weak C-H bond and form the key intermediate, a carbonyl radical. Since carbonyl radicals are nucleophilic radicals they can be rapidly captured in the presence of electrophilic trifluoromethylthiolating reagents and smoothly generate the final trifluoromethylthioester. The main advantages of this method over the previous one include the mild conditions, good tolerance of functional groups, and better chemoselectivity.
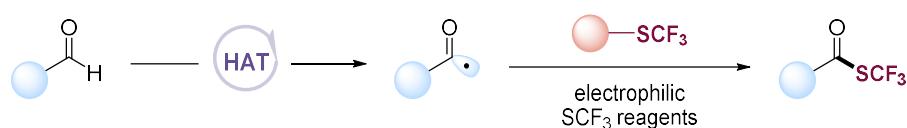
Figure 35 A general mechanistic pathway of the conversion of aldehydes to trifluoromethylthioesters via hydrogen-atom transfer (HAT).

In 2018 Glorius and co-workers developed a synergistic catalytic strategy by combining photoredox catalysts with hydrogen atom transfer (HAT) reagents for the efficient synthesis of trifluoromethylthioesters from aldehydes.[187] The method exhibits a wide range of substrate applicability and good functional group tolerance under mild and redox-neutral conditions (Figure 36). Moreover, the synthetic utility of the method is reflected in the late functionalization of three bioactive molecules (**2.219**) making it amenable to drug discovery. Mechanistically, the authors proposed that upon irradiation the excited state of the Ir-based photocatalyst can oxidize the sodium benzoate generating a hydridophilic benzoyloxy radical PhCOO·. Such radicals can abstract the hydrogen atom from the aldehyde and form a carbonyl radical. Then the carbonyl radicals can react with the electrophilic trifluoromethylthiolating reagent Phth-SCF$_3$ and furnish the desired product. In the meantime, the phthalimide radical Phth· can oxidize the reduced photocatalyst to regenerate it and close one catalytic cycle.
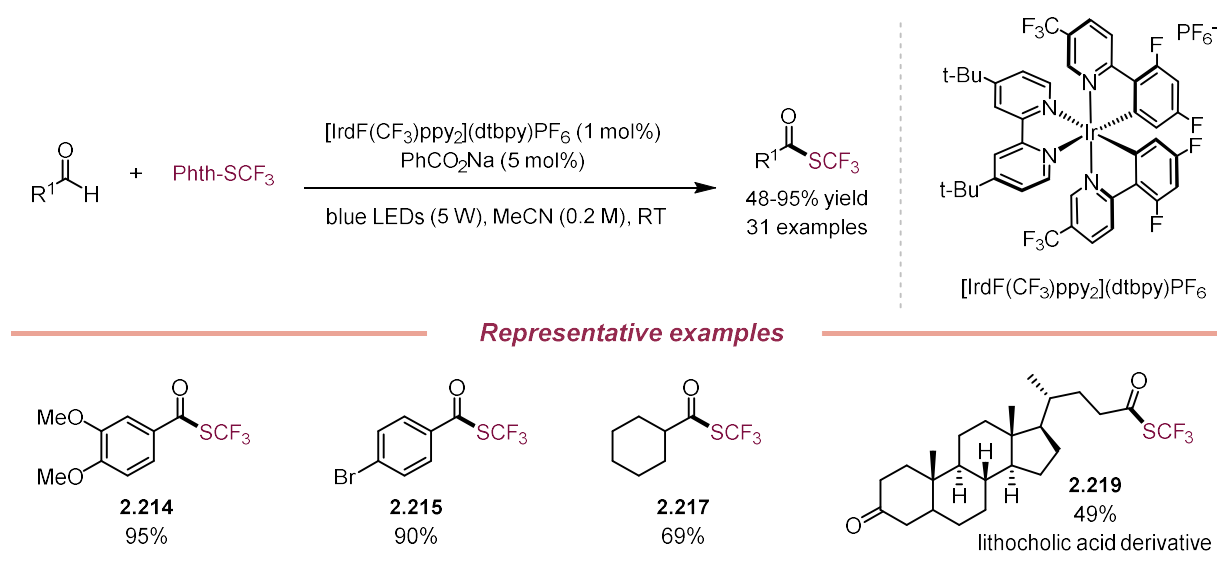
Figure 36 Synergistic catalytic strategy using combined photoredox/HAT catalysis, for the efficient synthesis of trifluoromethylthioesters from aldehydes.

Shortly after, Shen and co-workers disclosed a general method for the preparation of fluoroalkylthioesters including trifluoromethylthio-, pentafluoroethylthio-, difluoromethylthio-, monofluoromethylthio-esters from aldehydes and the corresponding fluoroalkylthiolating reagents was reported (Figure 37).[193] The reactions were conducted under mild conditions and, using in situ generated azide radical (N_3·) as a HAT reagent, various functional groups such as fluorine, chloride, bromide, iodide, and ester groups were compatible. Mechanistically, the authors proposed that an azide radical could be generated by combining sodium azide and [Bis(trifluoroacetoxy)iodo]benzene (PIFA). The azide radicals can abstract the H atom of the aldehyde to form a carbonyl radical, which reacts with $PhSO_2SR_f$ to give the corresponding fluoroalkylthioester (refer to the model shown in Figure 35).
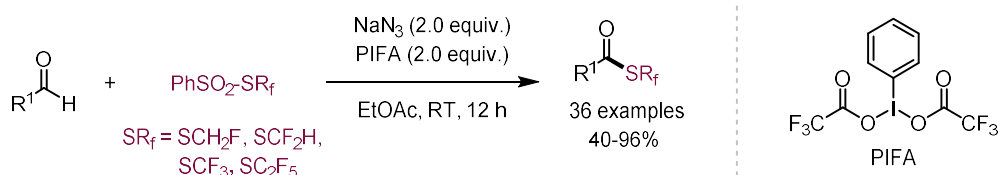
Figure 37 A general method for the preparation of fluoroalkylthioesters from aldehydes.

2.5.4 Conclusion and outlook

In summary, direct trifluoromethylthiolation via halide substitution reactions of acid chlorides or hydrogen atom transfer (HAT) of aldehydes is effective in supplying trifluoromethylthioesters, providing two reliable methods for generating these high value-added products. However, the drawbacks of the existing methods are also evident: (1) The generation of considerable amounts of metal by-products is a significant problem for most halide substitution reactions of acid chlorides. (2) Both strategies use unstable, less available organic compounds as substrates, posing sustainability and economic issues for the reactions. In the future, we expect a method to be developed using inexpensive, non-toxic and abundant chemical feedstocks as starting materials, which would greatly alleviate the current problems. Furthermore, the decomposition of nucleophilic trifluoromethylthiolating reagents is another problem that plagues many chemists. Therefore, a method that can in situ generate the SCF_3^- anion would effectively solve this problem and contribute to the improvement of chemoselectivity.

Chapter 3

Thesis Goals

Chapter 3

3.1 Thesis goals

3.1.1 Decarboxylative C(sp^3)-N and C(sp^3)-O cross-coupling reactions
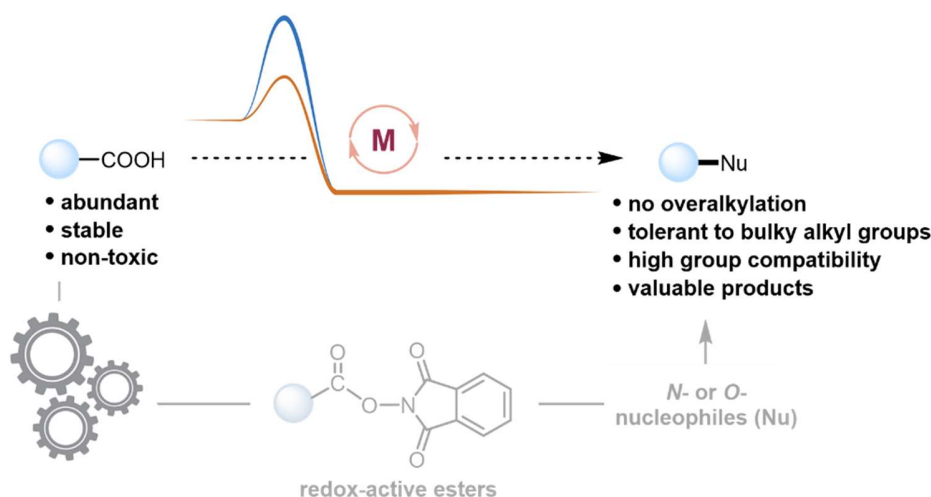
Figure 38 Transition metal-catalyzed C(sp^3)-N and C(sp^3)-O cross-couplings of redox-active esters (RAEs).

In Chapter 2.3, we mentioned that although the transition metal-catalyzed C(sp^2)-N and C(sp^2)-O cross-coupling reactions have been well developed and applied in various fields, the development of transition metal-catalyzed C(sp^3)-N and C(sp^3)-O cross-coupling reactions has lagged behind and the related bottlenecks need to be urgently overcome. In fact, one of the major problems of the conversion is the insufficient capacity of transition metal-catalysts to perform oxidative addition of traditional alkyl electrophiles (e.g., alkyl halides). It is for this reason that in Chapter 2.1 we presented in detail the application of *N*-(hydroxy)phthalimide (NHPI) esters as a novel alkyl electrophilic reagent in various coupling reactions. Indeed, with the redox-active properties of NHPI esters and the incomparable attributes of their parent - aliphatic carboxylic acids (e.g., accessibility, stability, and non-toxicity), a series of efficient and unprecedented coupling reactions have been developed. However, to date, transition metal-catalyzed decarboxylative C(sp^3)-N and C(sp^3)-O cross-coupling reactions using NHPI esters have been rarely reported with the only example being the intramolecular C(sp^3)-N coupling of NHPI esters developed by Fu and co-workers.[46]

Given the importance of developing a general, efficient method of using NHPI esters as coupling partners for transition metal-catalyzed intermolecular C(sp^3)-N and C(sp^3)-O couplings (Figure 38), my Ph.D.'s first goal was to develop such a method to fill a gap in the field.

However, the development of such a method is very challenging (1) How to efficiently generate alkyl radicals from NHPI esters? (2) After generating an alkyl radical, how to capture the active species? (3) How to make the method an overall redox-neutral process? (4) How can the valence state of the metal center be effectively tuned to facilitate a smooth catalytic cycle? (5) How to selectively achieve reductive elimination of C(sp^3)-metal species (instead of β-hydrogen elimination)?

Being fully aware of the difficulties of the subject, we also hoped that the method has some unique advantages (Figure 38), such as avoidance of overalkylation, universality to functional groups and tolerance to sterically bulky alkyl groups, ability to rapidly modify natural products and drug molecules; and potential to speed up the drug discovery process.

In addition, preliminary mechanistic studies will benefit the understanding of the reaction itself, while helping more laboratories to understand the reaction and to inspire the development of more relevant methods to address additional questions.

3.1.2 Deoxygenative trifluoromethylthiolation of carboxylic acids
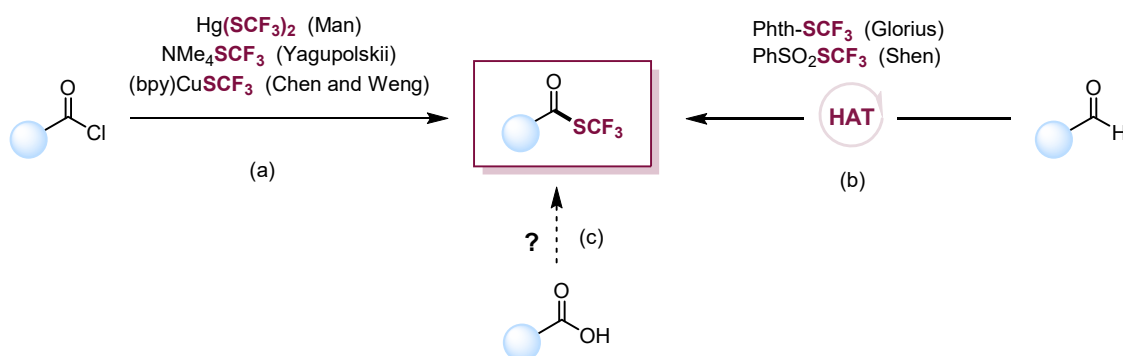
Figure 39 Synthesis of trifluoromethylthioesters.

As described in Chapter 2.5, despite the potential of trifluoromethylthioester compounds in medicinal chemistry to modulate the properties of small molecules, approaches to synthesize such

compounds are very limited. The existing methods are limited to halide substitution reactions of acid chlorides or hydrogen atom transfer (HAT) reactions of aldehydes.[187, 193, 196, 198-199] However, both methods have fundamental problems, the biggest of which are the unavailability, toxicity and instability of the starting materials. Therefore, a major problem can be solved by simply using carboxylic acids as a coupling partner by virtue of their ready availability, stability and non-toxicity (Figure 39).

In addition, previous reports showed that the nucleophilic CF_3S^- anion could readily dissociate into F^- anion and carbonothioic difluoride CSF_2 in the reaction solution. The F^- anion can compete with the CF_3S^- anion during the reaction, leading to the formation of fluorinated byproducts.[185, 201] Considering this problem, if there is a method that can generate CF_3S^- anion in situ, the aforementioned by-product can be effectively inhibited, yielding the desired products in high efficiency and better chemoselectivities.

In this context, the second goal of my Ph.D. is to develop a method for deoxygenative trifluoromethylthiolation of carboxylic acids via a umpolung process. We expect that this method will provide a novel strategy for the synthesis of trifluoromethylthioesters. At the same time, we hope to provide a scheme for the slow, in situ generation of CF_3S^- anions in a reaction system to address the inherent issue with the use of nucleophilic trifluoromethylthiolating reagents. Our longer-term vision is that the reaction will allow for efficient modification of drugs and natural products, paving the way for their potential applications in various fields.

Chapter 4

Decarboxylative C(sp^3)-N Cross-Coupling via Synergetic Photoredox and Copper Catalysis

Chapter 4

4.1 Reaction design and optimization

This chapter details our process of establishing a synergistic photoredox and copper-catalyzed platform, as well as its application for decarboxylative C(sp^3)-N bond-forming reactions and related mechanistic studies. In this section, we elaborate on the reaction design and the optimization of the decarboxylative C(sp^3)-N cross-couplings via synergistic photoredox/copper catalysis.

4.1.1 Reaction design
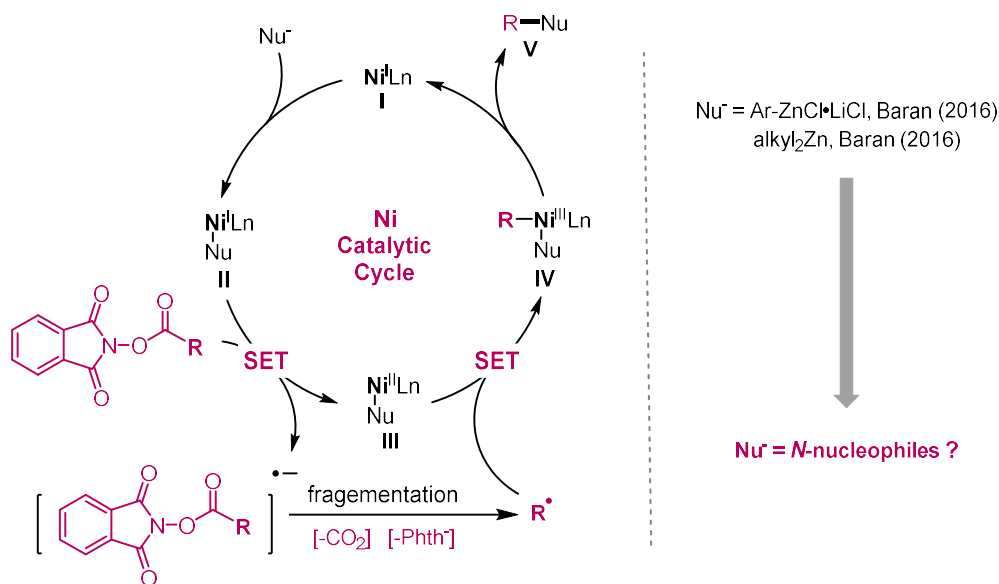
Figure 40 Initial reaction design for the decarboxylative C(sp^3)-N cross-coupling reactions.

In 2016, Baran and co-workers developed a nickel-catalyzed decarboxylative coupling reaction between aliphatic acid-derived NHPI esters and aryl zinc reagents to forge C(sp^3)-C(sp^2) bonds.[47] Mechanistically, after forming the precatalyst Ni^I complex **I**, it can transmetalate with an aryl zinc reagent (Nu$^-$ = aryl zinc reagent) to produce aryl−Ni^I complex **II** (Figure 40). Next, **II** would then donate an electron to an NHPI ester, thus generating the radical anion of the activated ester with concomitant formation of Ni^{II} complex **III**. Fragmentation of the former followed by the release of CO$_2$ would generate the phthalimide anion and the alkyl radical species. At this point, recombination of the radical species and the phthalimide anion with complex **III** would furnish

the Ni^{III} intermediate **VI**, which upon reductive elimination would give the desired cross-coupling product and close the catalytic cycle.
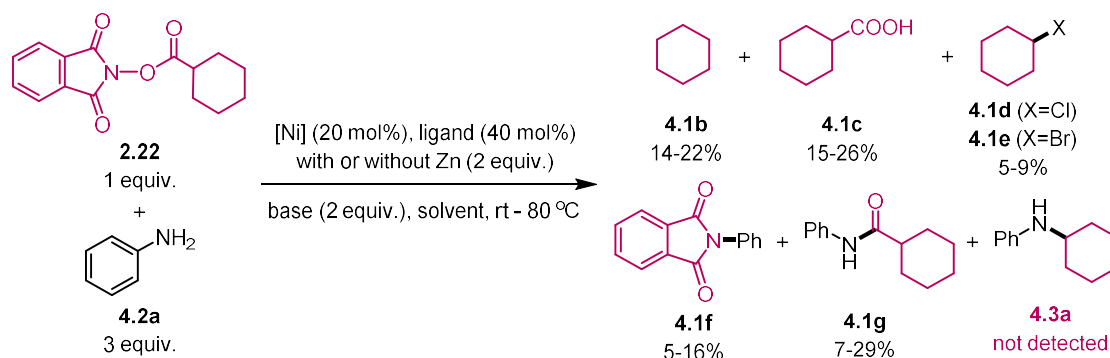
Figure 41 A preliminary test of cyclohexyl NHPI ester **2.22** with aniline **4.2a** under Baran's conditions.[47] [Ni] = NiCl$_2$·glyme or NiCl$_2$·6H$_2$O; ligand = di-*t*Bubipy; base = Cs$_2$CO$_3$, Et$_3$N, NaO^{t}Bu etc.; solvent = DMF, MeCN, DMA, etc.

Immediately after noticing this work, the thought occurred to us: by simply replacing the aryl zinc reagents with *N*-nucleophiles, could the same or similar reaction conditions be feasible to construct the C(sp^3)-N bonds? However, a preliminary test of cyclohexyl NHPI ester **2.22** with aniline **4.2a** under similar conditions completely failed to yield the desired aminated product **4.3a**. Instead, by-products derived from **2.22** (**4.1b**-**4.1e**), the amidated product (**4.1g**), and aniline substitution of *N*-phenylphthalimide (**4.1f**) were observed (Figure 41). After analyzing the obtained products, we sought to rationalize the causes for the unsuccessful experiments and came to preliminary conclusions: (1) NHPI esters tend to form amide bonds rather than amine bonds in the presence of *N*-nucleophiles; (2) single-electron transfer initiated by an organometallic nickel or iron species is crucial for activating NHPI esters. However, the analogous electron transfer from metal amido species is hitherto unknown, probably due to their sluggish nature of donating electrons in the ground state. (3) since the metal amido species can not be efficiently oxidized to its high-valent state, the subsequent reductive elimination step becomes very slow. In order to overcome the above issues, improvements in two aspects were needed: (1) the alkyl NHPI ester needs to be rapidly reduced and produce C-centered radicals, this is crucial to overcome the main amidated byproduct **4.1g**. (2) An oxidant is needed to oxidize the metal amido species to its high-valent state to facilitate the reductive elimination step.
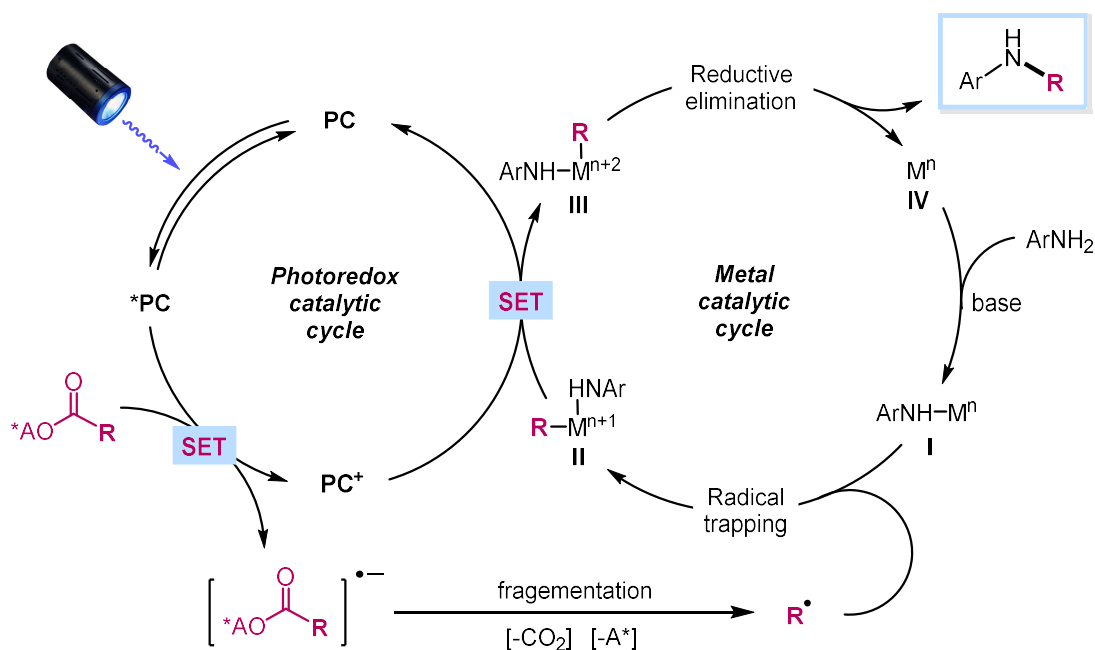
Figure 42 Mechanistic design for decarboxylative amination via synergetic photoredox and transition metal catalysis.

Based on the above-mentioned considerations, we believed that the introduction of photoredox catalysis to metal catalysis could solve the existing issues. In this way, the oxidizing and reducing agents will be combined into one photocatalyst. More importantly, by simply adjusting the photocatalyst, we can easily tune the redox potentials of the oxidizing and reducing ends to achieve better reactivity. Thus, we proposed a dual catalysis system and expected that this would help overcome the difficulties in developing such a decarboxylative C(sp^3)-N cross-coupling method (Figure 42).

Initially, visible-light excitation of a photocatalyst generates an excited-state complex, which reduces a redox-active ester via a single-electron transfer (SET). The reduced ester then undergoes decarboxylation to give an alkyl radical, which is trapped by a low-valent metal amido complex **I** to give intermediate **II** (Figure 42). The photocatalytic cycle is closed by a single-electron transfer from intermediate **II** to the oxidized photocatalyst, yielding at the same time a high-valent metal alkyl amido complex **III**. C-N reductive elimination from **III** then gives the desired amine product and liberates a low-valent metal species **IV**. The latter reacts with an aniline to give complex **I** and

completes the metal catalytic cycle. This type of relay between photoredox catalysis with nickel catalysis has been exploited for C-C coupling,[202-204] and electron-transfer via photoredox catalysis is reported to promote C(sp^2)-N reductive elimination on Ni and Cu.[205-206] However, a similar strategy has not been demonstrated for C(sp^3)-N coupling.

4.1.2 Optimization

4.1.2.1 First approach and preliminary results
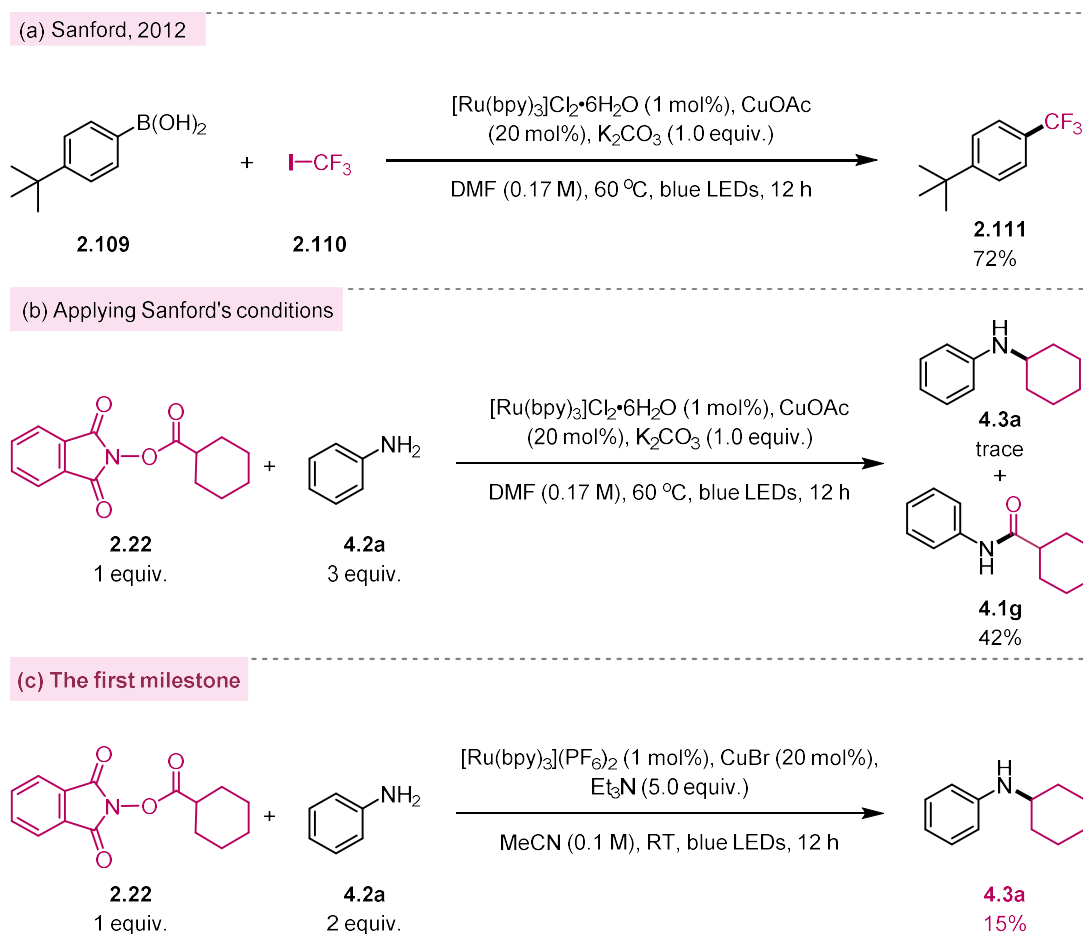
Figure 43 (a) Synergistic photoredox and copper-catalyzed trifluoromethylation reaction reported by the Sanford group in 2012; (b) Experimental exploration: applying Sanford's conditions to our reaction design; (c) The first milestone in our exploration of the decarboxylative C(sp^3)-N cross-coupling method.

After careful review of the reported cooperative photoredox/copper-catalyzed work (see Chapter 2.2), we found that the synergistic photoredox and copper-catalyzed trifluoromethylation

strategy reported by the Sanford group in 2012[86] is similar to our designed reaction route (Figure 43a). Therefore, we envisioned that their reaction conditions could be applied to our designed route. To try this idea, based on Sanford's conditions, we replaced the nucleophilic reagent from 4-*tert*-butylphenylboronic acid **2.109** to aniline **4.2a**, and the electrophilic reagent from trifluoromethyl iodide **2.110** to cyclohexyl NHPI ester **2.22**, while retaining the remaining original conditions (Figure 43b). However, by applying their conditions to our reaction, we could only observe trace amounts of the aminated product **4.3a**, suggesting that Sanford's conditions are not effective in our reaction. Interestingly, we noted that the amidated product **4.1g** was obtained in 42% yield, suggesting that the amidation reaction was much faster than the amination process under Sanford's conditions.

From this initial trial, we realized that it was critical to inhibit the rapid formation of amidated product in order to enable the amination reaction to proceed smoothly. Based on this idea, we believed that adjusting the base, solvent, and temperature could inhibit the rapid amidation reaction to some extent. Encouragingly, after some preliminary experiments, we found that when Ru(bpy)$_3$(PF$_6$)$_2$ (1 mol%) was used as a photocatalyst, CuBr (20 mol%) as a transition metal catalyst, Et$_3$N (5 equiv.) as an organic base, and MeCN (0.1 M) as a solvent, and after 12 h of blue LED irradiation at room temperature, 15% of **4.3a** could be obtained (Figure 43c). This result provided a solid basis for our subsequent screening of the reaction conditions.

It is important to note that in order to ensure sufficient photon flux density and a suitable reaction temperature, the light source we applied to the reaction was 40W blue LEDs (which we purchased from Kessil Co., Ltd., product number A160WE). A table fan was used to maintain room temperature during the irradiation process (table fan purchased from Galaxus Co., Ltd., and max. power 35W).

4.1.2.2 Further optimization of reaction conditions

Ligands can play a magical role in transition metal-catalyzed reactions. We first studied the effects of different ligands on the reactivity based on the preliminary conditions previously obtained (Figure 43c).

Since this reaction is somewhat similar to the copper-catalyzed Ullman-type amination reaction, we believed that the ligands that performed well in the Ullman amination reaction were potentially capable of facilitating our reaction. Besides, early studies have shown that different

types of bidentate ligands appear to be more effective than monodentate ligands. This is because a bidentate ligand can occupy two adjacent coordination sites, thus bringing the two coupling partners closer together and facilitating the reaction.[207] Also, the ligands used in Ullmann-type reactions are generally *N*-donors, *O*-donors or a mixture of *N*- and *O*-donors, whereas *P*- based ligands are generally less effective.[208]
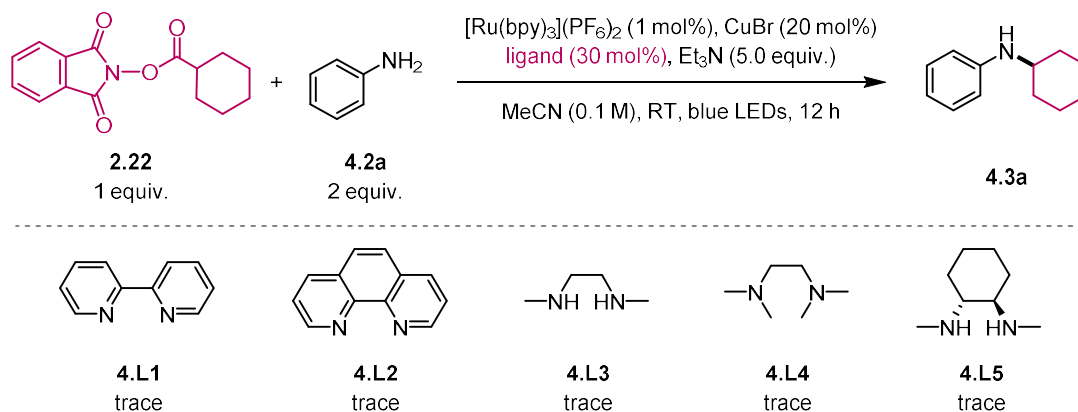
Figure 44 Reactivity of *N,N'*-ligands to the decarboxylative C(sp^3)-N cross-coupling reactions.

To begin with, we tested a class of readily available *N, N'*-bidentate ligands (Figure 44) such as bipyridine **4.L1**, 1,10-phenanthroline **4.L2**, *N, N'*-dimethylethylenediamine (DMEDA) **4.L3**, tetramethylethylenediamine (TMEDA) **4.L4**, trans-*N, N'*-dimethylcyclohexane-1,2-diamine **4.L5**. However, all of these ligands failed to facilitate the reaction indicating the ineffectiveness of *N,N'*-bidentate ligands for the reaction.

Next, we screened a wide range of ligands and tested their reactivity in the decarboxylative C(sp^3)-N cross-coupling reaction. Unfortunately, we found that the *P*-type ligands (**4.L6** and **4.L7**, Figure 45), 8-quinolinol *N*-oxide (**4.L8**), and 2,2'-bisphenol (**4.L9**) were not effective ligands in this reaction. To our delight, when we tried the diol-type ligands (**4.L10** and **4.L11**) and the diketone ligands (**4.L12**), we were able to improve the reactivity to 44%-50% yields/conversions. In view of the good reactivity presented by diketone ligands and the easy accessibility and diversity of this class of ligands, we next focused on ligand optimization based on diketone ligands. After screening a series of diketone-based ligands, we discovered that electron-donating nature and the bulkiness may play a key role. The best results were achieved when electron-donating and

sterically bulky groups were introduced into the ligand skeleton. The template reaction using **4.L16** as a ligand resulted in the highest yield of 58% (Figure 45). Compared to the reaction conditions without ligand, this ligand can enhance the reactivity by 43%.
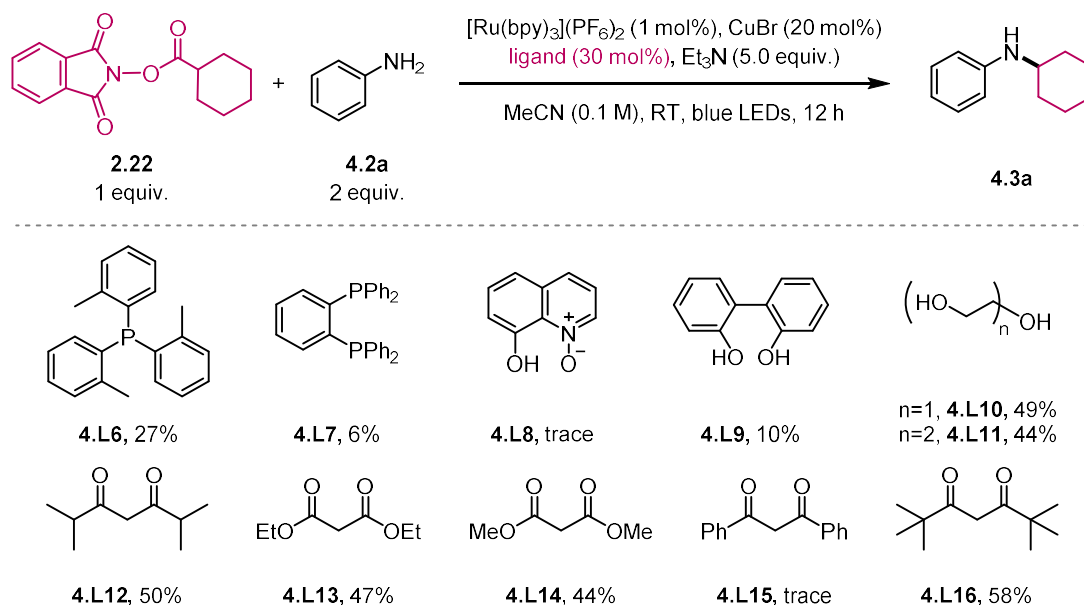
Figure 45 Reactivity of various classes of ligands to the decarboxylative C(sp^3)-N cross-coupling reactions.

After a round of ligand screening and evolution, we found that anionic ligands, such as 1,3-diol and 1,3-diketone ligands, were generally better yielding than other types of ligands. Inspired by these findings, we concluded the preliminary hypothesis that anionic ligands with both electron-donating and sterically bulky groups could facilitate the reaction. Based on this hypothesis, more simple and easily tunable anionic ligand skeletons needed to be selected for in-depth ligand optimization.

In 2012, Ma and co-workers developed 2-(2,6-dimethylphenylamino)-2-oxoacetic acid (DMPAO) as a superior ligand for copper-catalyzed *N*-arylation of acyclic secondary amines.[209] Later, by employing oxoacetic acid- and oxalic diamide- based ligands, Ma and co-workers achieved very challenging transformations, namely Cu-catalyzed amination and etherification reactions of aryl chlorides.[210-211] Inspired by these results, we sought to investigate the reactivity of these ligands in our reactions.

To begin with, oxalamide-based ligands were tested in the reaction, however, only low to moderate yields could be obtained, probably due to their poor solubility and less electron-donating effect (**4.L17-4.L24**, 18-45%, Figure 46). To our surprise, when 2-((2,6-dimethyl)phenylamino)-2-oxoacetic acid (DMPAO, **4.L25**) was used in this reaction, the yield dramatically increased to 71% (Figure 46). Encouraged by this result, we systematically modulated the substituents in the aromatic ring of **4.L25**, such as introducing one, two or three electron-donating group(s) with diverse substituted positions to the aromatic ring (**4.L26-4.L29**). Eventually, we found that the best yield at 91% was obtained using 2-((2,6-dimethoxyphenyl)amino)-2-oxoacetic acid **4.L26** as a ligand (Figure 46). After preliminary analysis, we attributed the success of **4.L26** as a ligand to the *o*-dimethoxy groups on its aromatic ring, which can not only effectively increase the steric hindrance of the ligand to accelerate the reductive elimination process, but also induce a electron-rich copper center to facilitate the "oxidative addition" process (Cu^I complex to Cu^{III} complex).
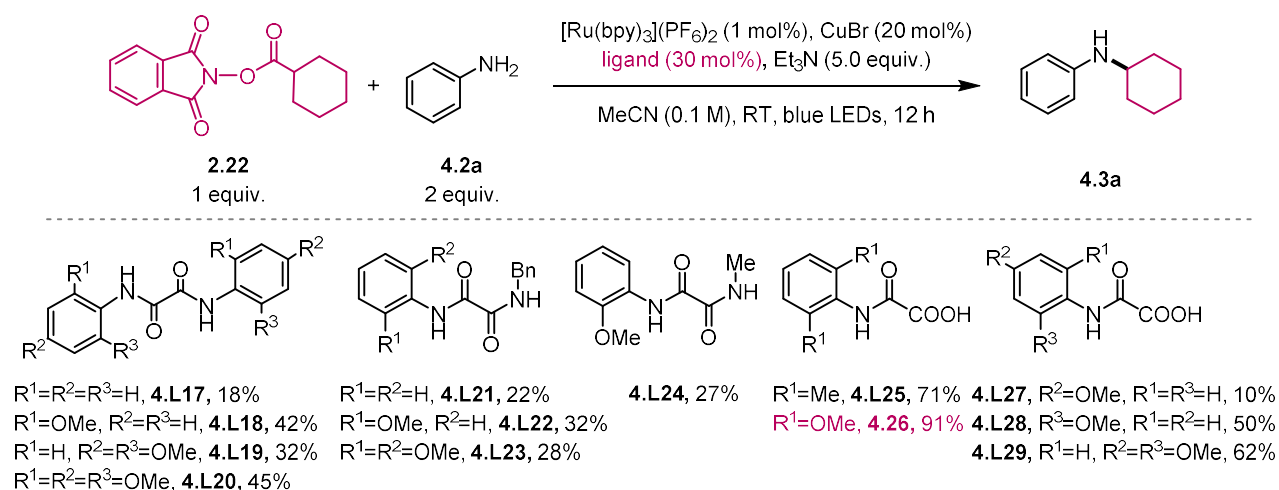
Figure 46 Reactivity of oxoacetic acid- and oxalic diamide- based ligands to the decarboxylative C(sp^3)-N cross-coupling reactions.

Different catalyst loadings were evaluated, and lowering the catalyst loadings led to lower yields (Table 11, entries 1-3). Considering the reduction potential of NHPI esters ($E_{1/2}$ < -1.28 V vs. SCE in MeCN),[212] the addition of an appropriate amount of Lewis acid can enhance the reduction efficiency by coordination. Since the copper catalyst can also act as a Lewis acid, an increase of free copper anions in solution would be beneficial. Therefore, we increased the metal/ligand ratio to ensure the liberation of sufficient "free" copper ions (Table 11, entries 4-6),

and these changes proved to be beneficial. When changing the metal/ligand ratio to 20/7.5, the product yield increased to 94% (Table 11, entry 4).

Table 11 Optimization of the Cu cat./ligand ratio
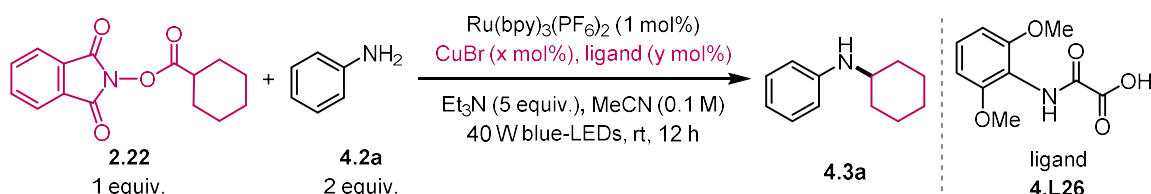
entry	CuBr/ligand (x/y ratio)	GC yield^a
1	20/30	91%
2	10/15	70%
3	5/7.5	48%
4	20/7.5	94%
5	20/5	81%
6	20/0	15%

^{a}Corrected GC yield using *n*-dodecane as an internal standard.

Table 12 Optimization of various transition metal catalysts
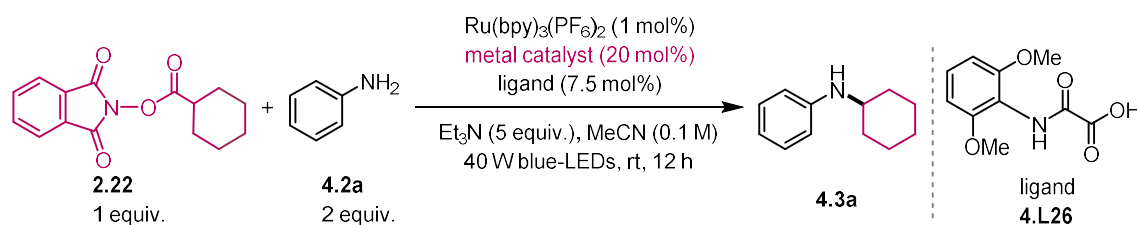
entry	transition metal	GC yield^a
1	CuBr	94%
2	CuCl	35%
3	CuI	76%
4	Cu	trace
5	CuBr$_2$	43%
6	NiCl$_2$•6H$_2$O, CoCl$_2$•6H$_2$O, FeCl$_2$	ND

^{a}Corrected GC yield using *n*-dodecane as an internal standard; ND = not detected.

Table 13 Optimization of different temperatures

2.22 1 equiv. + 4.2a 2 equiv. → Ru(bpy)$_3$(PF$_6$)$_2$ (1 mol%), CuBr (20 mol%), ligand (7.5 mol%), Et$_3$N (5 equiv.), MeCN (0.1 M), temperature, 40 W blue-LEDs, 12 h → 4.3a; ligand 4.L26
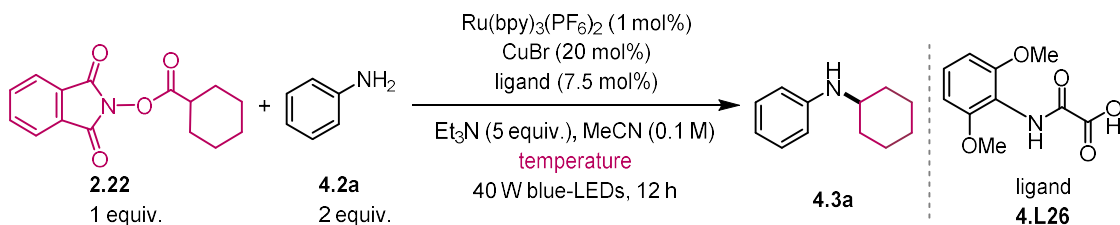
entry	temperature	GC yield[a]
1	RT	94%
2	55 °C	35%
3	0 °C	68%

[a]Corrected GC yield using *n*-dodecane as an internal standard.

Next, we screened different metal catalysts. Although palladium catalysis has been widely used for C-N coupling with great success, we believe that non-precious metal catalysts, such as Fe, Co, Ni and Cu-based catalysts, may be more advantageous for the application by virtue of their inexpensive and readily available nature. In this reaction, however, we found only copper catalysts to be effective (Table 12). Among the copper catalysts we examined, Cu(I) salts could give better yields than Cu metal and Cu(II) salts (Table 12, entries 1-5).

In addition, we screened different reaction temperatures (Table 13). Unlike previous copper-catalyzed amination reactions that required either low[71] or high temperatures[119] to ensure better chemoselectivity or efficient conversion, this method gave the best yields at room temperature.

The pivotal role of photocatalysts in photocatalytic reactions is evident. After screening a set of photocatalysts, we found that Ru(bpy)$_3$(PF$_6$)$_2$ was the most suitable one for the reaction and gave the best result under standard conditions (Figure 47). We attributed the catalyst's excellent performance to its long excited-state lifetime (τ=1100 ns), suitable absorption wavelength (λ_{max}=452 nm), and strong redox potential at the oxidizing and reducing ends ($E_{1/2}$ (Ru^{3+}/Ru^{2+}*) = -0.81V; $E_{1/2}$ (Ru^{3+}/Ru^{2+}) = 1.29V vs. SCE in MeCN at RT).[78]
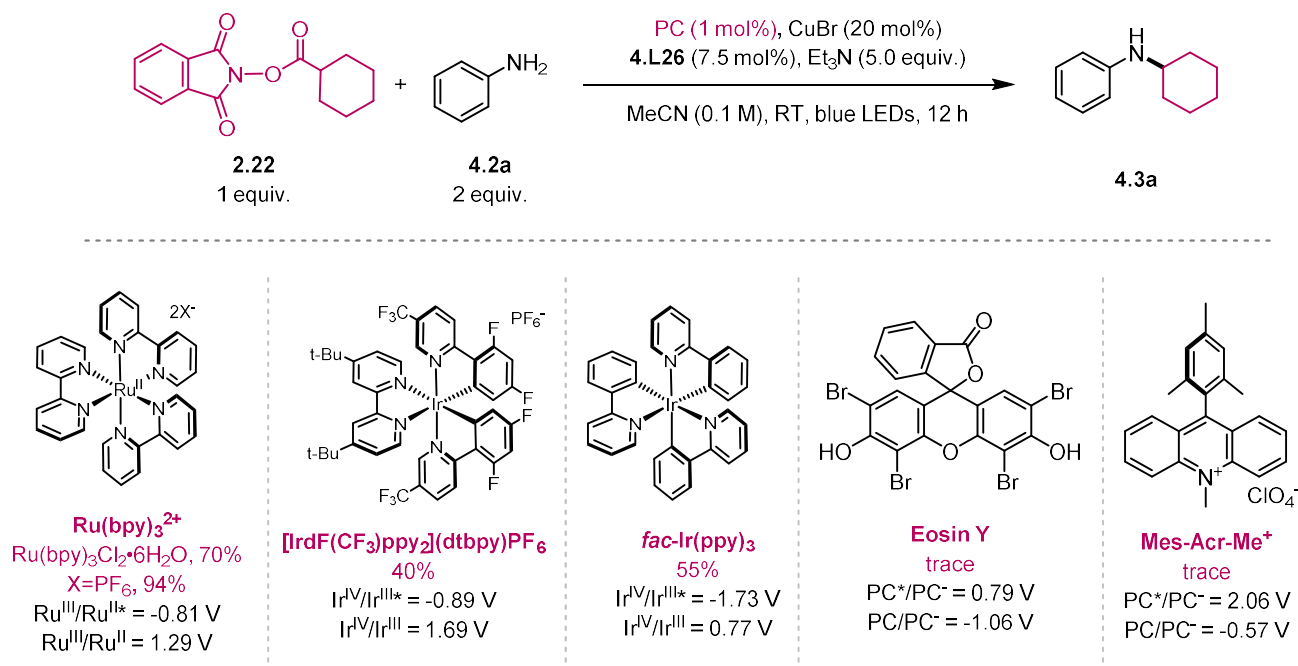
Figure 47 Optimization of different photocatalysts

The influence of bases on the reaction is dramatic and decisive. Of all the organic and inorganic bases that were tried, the aminated product could be produced only when triethylamine was used as a base (Table 14). We speculated that triethylamine acts as more than a base in this reaction, and the important role of triethylamine in this reaction will be discussed in the mechanistic investigations section. Furthermore, a preliminary evaluation of different solvents showed that MeCN performed best and had the highest yield under standard conditions (Table 15). Finally, control experiments showed that light, Ru(bpy)₃(PF₆)₂, and a copper salt are all essential. Without any of the three, no amination products were observed (Table 16). At this point, we had obtained the optimal reaction conditions for the coupling of secondary NHPI ester **2.22** with aniline **4.2a**: using Ru(bpy)₃PF₆ (1 mol%) as a photocatalyst, CuBr (20 mol%) as a copper salt, **4.L26** (7.5 mol%) as a ligand, Et₃N (5 equiv.) as a base, and MeCN (0.1 M) as a solvent, and irradiation with blue LEDs (Kessile 40 W) for 12 h at room temperature.

Primary aliphatic carboxylic acids are inexpensive and abundant reagents. The decarboxylative C(sp³)-N cross-coupling of NHPI esters derived from primary alkyl carboxylic acids would yield high value-added linear alkyl aryl amine products. However, with the reaction conditions as mentioned above, the efficiency is very low, only giving the desired product in a 28%

Table 14 Optimization of different bases
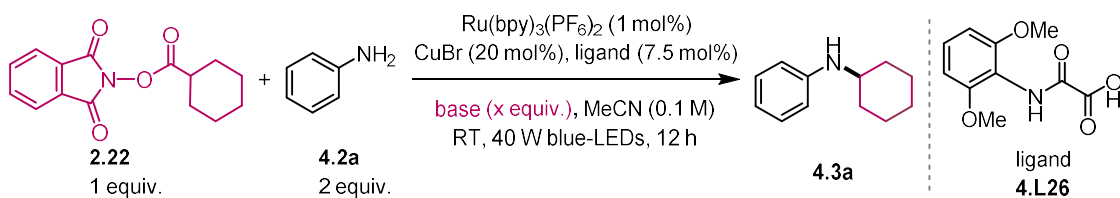
entry	base	GC yield[a]
1	Et$_3$N[b]	94%
2	DIPEA, DABCO, triethanoamine, Na$_2$CO$_3$, K$_2$CO$_3$, K$_3$PO$_4$, KO^{t}Bu, NaO^{t}Bu, KOH, Cs$_2$CO$_3$[c]	trace

[a]Corrected GC yield using *n*-dodecane as an internal standard. [b]using 5 equiv. base. [c]using 1 equiv. base.

Table 15 Optimization of different solvents
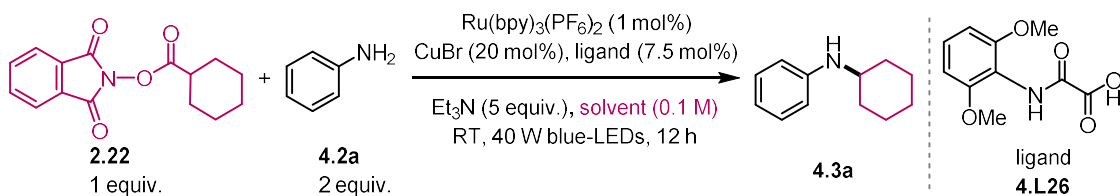
entry	solvent	GC yield[a]
1	MeCN	94%
2	benzene	21%
3	DMA	32%
4	dioxane	trace
5	toluene	trace

[a]Corrected GC yield using *n*-dodecane as an internal standard.

Table 16   Control experiments
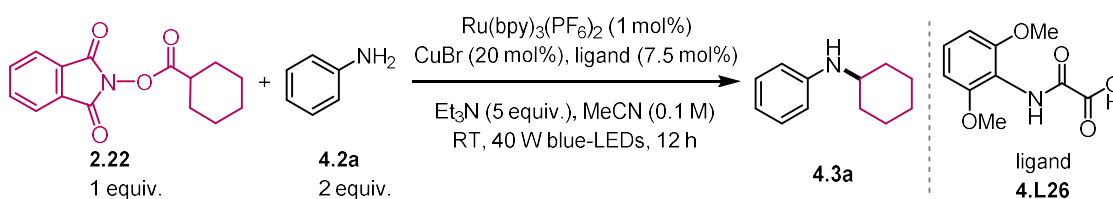
entry	variants	GC yield[a]
1	none	94%
2	no light	ND
3	no Ru(bpy)$_2$(PF$_6$)$_2$	ND
4	no CuBr	ND
5	no ligand	15%

[a]Corrected GC yield using *n*-dodecane as an internal standard; ND = not detected.

Table 17   Optimization of reaction parameters for primary NHPI ester
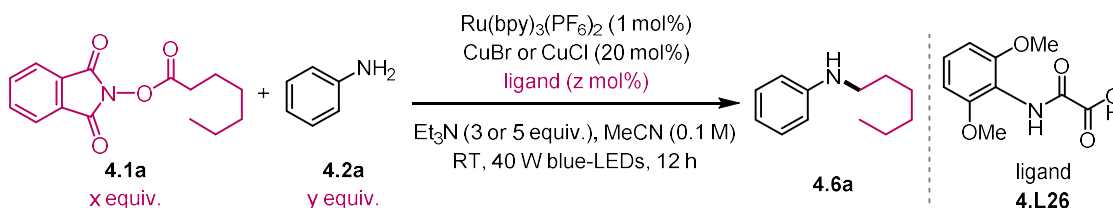
entry	4.1a/4.2a (x/y)	copper cat.	ligand (z mol%)	base	GC yield[a]
1	1/2	CuBr	**4.L26** (7.5 mol%)	5 equiv.	28%
2	2/1	CuBr	**4.L26** (7.5 mol%)	3 equiv.	39%
3	2/1	CuBr	-	3 equiv.	46%
4	2/1	CuCl	-	3 equiv.	64%

[a]Corrected GC yield using *n*-dodecane as an internal standard; ND = not detected.

yield (Table 17, entry 1). We attributed this to the very high activity of the primary alkyl radicals and the rapid rate of the dimerization reaction (14% of the homocoupling product could be observed by GC) and other side reactions (e.g. Barton-type decarboxylation). Therefore, we adjusted the ratio of NHPI ester **4.1a** to aniline **4.2a** from 1/2 to 2/1 and correspondingly adapted

the equivalents of triethylamine from 5 to 3 equivalents. As expected, the yield of the reaction increased by 11% to 39% (Table 17, entry 2). To our surprise, the reaction yield could be increased by 7% when the auxiliary ligand was removed (Table 17, entry 3). We credited this to the high activity of the primary alkyl radical, which enabled the coupling reaction in a smooth manner without the aid of an external ligand. Further screening of copper salts showed that CuCl was more suitable for the coupling of primary alkyl NHPI esters (Table 17, entry 4).

Thus far, we had achieved the optimum reaction conditions for the coupling between primary NHPI ester **4.1a** and aniline **4.2b**: using Ru(bpy)$_3$PF$_6$ (1 mol%) as a photocatalyst, CuCl (20 mol%) as a copper salt, Et$_3$N (3 equiv.) as a base, and MeCN (0.1 M) as a solvent, and irradiation with blue LEDs (Kessile 40 W) for 12 h at room temperature.

4.2   Scope of the decarboxylative C(sp^3)-N coupling reaction

With the optimized reaction conditions in hand, we then turned our attention to the scope of the reaction. First, we explored the scope of anilines and other *N*-nucleophiles followed by different alkyl NHPI esters.

4.2.1   Scope of anilines
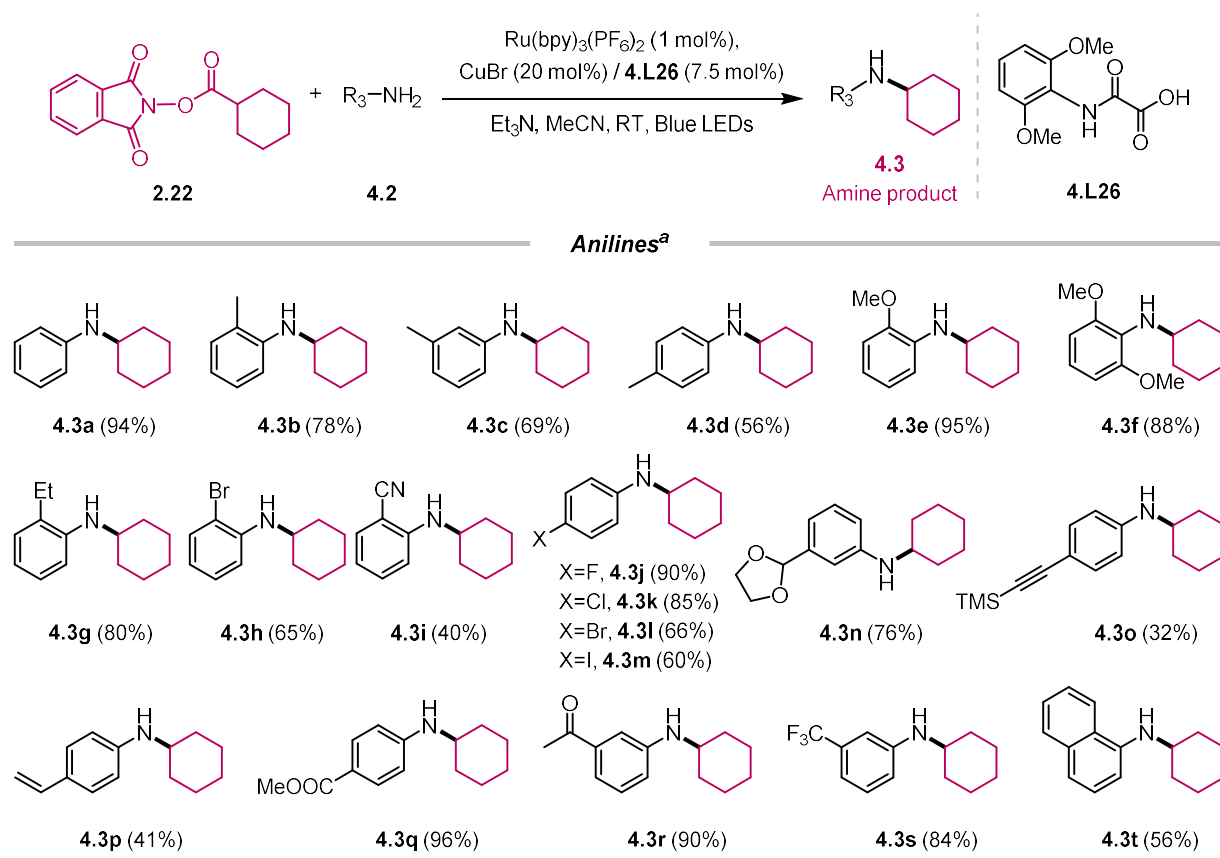
Figure 48 Scope of anilines. ^{a}General conditions: NHPI ester **2.22** (1 equiv.), anilines **4.2** (2 equiv.), Ru(bpy)$_3$(PF6)$_2$ (1 mol%), CuBr (20 mol%), **4.L26** (7.5 mol%) and Et$_3$N (5 equiv.) in MeCN (0.1 M), irradiated at room temperature for 12 h, isolated yield.

The optimal reaction conditions (Table 16, entry 1) were successfully applied for the coupling of secondary alkyl NHPI ester **2.22** with a broad set of anilines **4.2** (Figure 48). Gratefully, *ortho*-, *meta*-, and *para*-toluidine coupled with **2.22** to afford the corresponding alkyl aryl amines in moderate to excellent yields (Figure 48, **4.3b-4.3d**). Sterically hindered *ortho*-substituted anilines are commonly poor nucleophiles for C-N cross-coupling reactions. However, anilines with

ortho-substitution, such as mono-methoxy (**4.3e**), di-methoxy (**4.3f**), ethyl (**4.3g**), bromo (**4.3h**), or cyano (**4.3i**) groups were all suitable substrates in the current methodology. C(sp^2)-halogen atom bonds are important scaffolds in cross-coupling reactions. To our delight, halogen-substituted anilines with various halogens were well-tolerated, delivering the products in decent yields (**4.3j**-**4.3m**). Synthetically useful functional groups, such as cyano (**4.3i**), masked aldehyde (**4.3n**), acetylene (**4.3o**), vinyl (**4.3p**), ester (**4.3q**), ketone (**4.3r**), trifluoromethyl (**4.3s**), were all compatible. Naphthyl group-containing compound **4.3t** could also be achieved with ease.

4.2.2   Scope of other *N*-nucleophiles
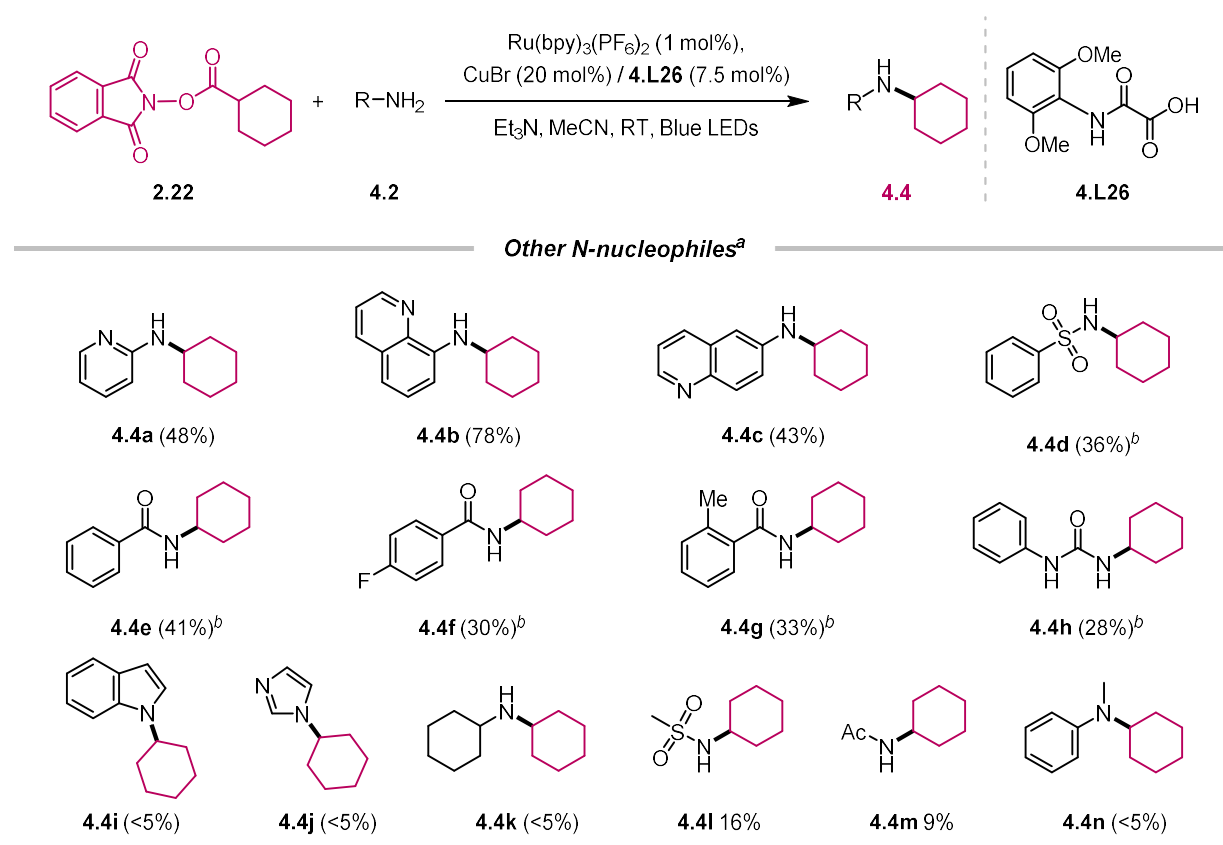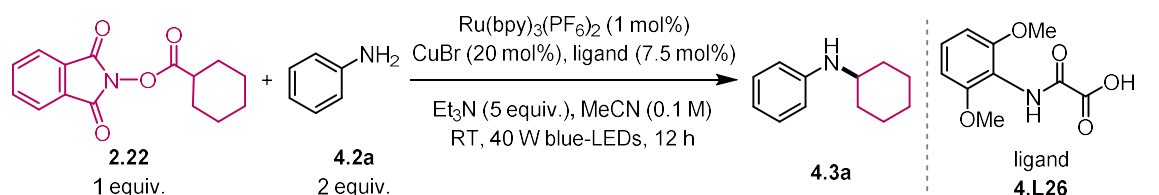
Figure 49 Scope of other *N*-nucleophiles. [a]General conditions: NHPI ester **2.22** (1 equiv.), *N*-nucleophiles **4.2** (2 equiv.), Ru(bpy)$_3$(PF6)$_2$ (1 mol%), CuBr (20 mol%), **4.L26** (7.5 mol%) and Et$_3$N (5 equiv.) in MeCN (0.1 M), irradiated at room temperature for 12 h, isolated yield. [b]Cu(MeCN)$_4$PF$_6$ (50 mol%), **L3** (30 mol%), 20 h, isolated yield.

The use of different *N*-nucleophilic reagents is valuable in expanding the substrate scope for C-N coupling reactions. However, our reaction enables the transformation of challenging anilines (Figure 49), such as **4.4a** (pyridine), **4.4b** (sterically hindered quinoline), and **4.4c** (quinoline), to the *N*-alkylated products. The assessment of other *N*-nucleophiles revealed some limitations of the current method. While sulfonamide (**4.4d**), amide (**4.4e-4.4g**), urea (**4.4h**) were coupled in modest yields and increased loading of the copper catalyst was required (Figure 49). In addition, alkylation of nitrogen heterocyclic nucleophiles such as indole (**4.4i**) and imidazole (**4.4j**) was not feasible. Alkylamines tended to give amidation products (**4.4k**), while methanesulfonamide (**4.4l**) and acetamide (**4.4m**) were coupled in very low yields (16% and 9%, respectively). Secondary amines could only give low conversions and yields (see a representative example **4.4n**).
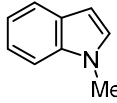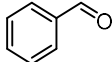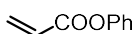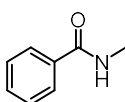
4.2.3 Rapid assessment of the applicability of functional groups

In 2013, Glorius and co-workers demonstrated a method of robustness screen for the rapid assessment of chemical reactions.[213] To further probe the limitations of the current approach regarding functional group compatibility, a range of experiments were conducted in the presence of different small-molecule additives (Table 18), including molecules containing alpha-beta unsaturated esters, aldehydes, NMe-indoles, NH-indoles, secondary alkyl amides, or unprotected alcohols. As shown in Table 18, NMe-indole (entry 2) and free alcohol (entry 3) were tolerated in the standard conditions, aldehyde (entry 4) and NH-indole (entry 5) were modestly compatible additives, and alpha-beta unsaturated ester (entry 6) and secondary alkyl amide (entry 7) inhibited the reactions to about 25% yields.

Table 18 A further test of functional-group tolerance using the screening method developed by Glorius

Entry	Additive	Yield of **4.3a** (%)^a	Additive remaining (%)^a
1	None	94	-

#	Additive	Yield			
2	N-methylindole	85	√	100	√
3	HO-(CH₂)₄-CH₃ (pentanol)	80	√	95	√
4	benzaldehyde	62	−	36	−
5	indole	49	−	64	−
6	phenyl acrylate (COOPh)	25	×	20	×
7	N-methylbenzamide	26	×	70	√

The standard reaction is undertaken in the presence of one molar equivalent of the given additive. The yield of **3a**, and the additive remaining after reaction is given. Color coding: green √: above 66%, yellow −: 34 - 66%, red ×: below 34%. [a]GC yield.

4.2.4 Scope of alkyl NHPI esters that derived from aliphatic carboxylic acids

Reaction scheme:
NHPI ester **4.1** + R⁴–NH₂ (**4.2**) → with Ru(bpy)₃(PF₆)₂ (1 mol%), CuBr (20 mol%) / **4.L26** (7.5 mol%), Et₃N, MeCN, RT, Blue LEDs → product **4.5**. Ligand **4.L26** is a 2,6-dimethoxyphenyl oxalamic acid.

Secondary and tertiary acids[a]

4.5a (81%)   **4.5b** (71%)   **4.5c** (41%)   R=H, **4.5d** (66%) / R=OMe, **4.5e** (76%)   **4.5f** (82%)

4.5g (73%)   **4.5h** (37%)   **4.5i** (60%)   **4.5j** (56%)   **4.5k** (9%)   **4.5l** (<5%)
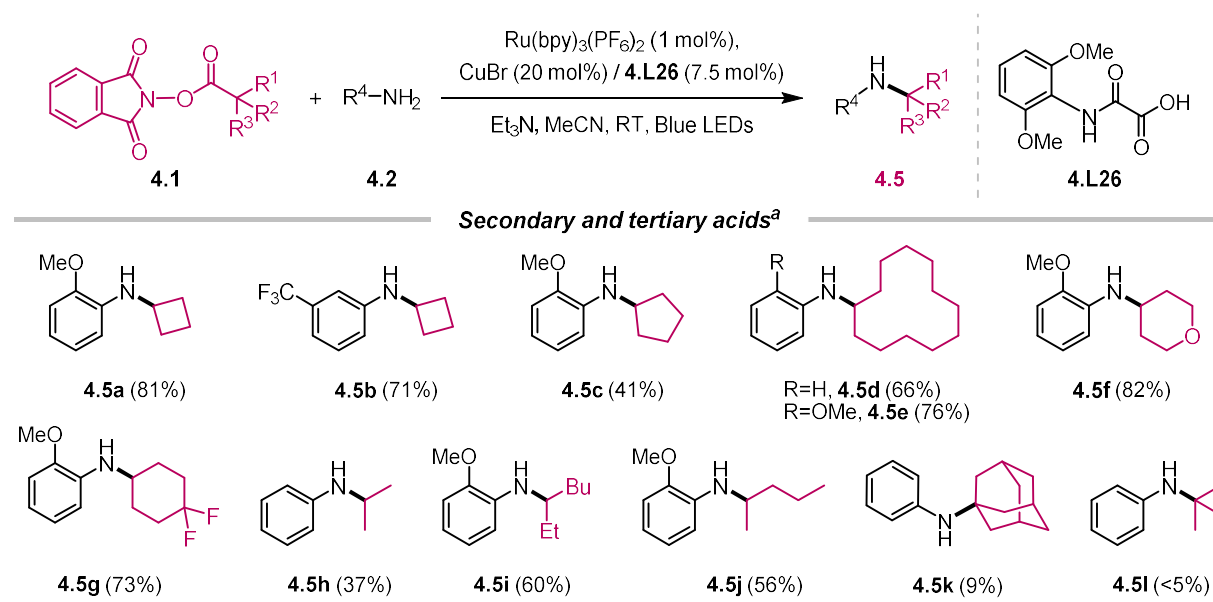
Figure 50 Scope of alkyl NHPI esters derived from secondary and tertiary carboxylic acids. [a]General conditions: NHPI ester **4.1** (1 equiv.), N-nucleophiles **4.2** (2 equiv.), Ru(bpy)₃(PF6)₂ (1 mol%), CuBr (20 mol%), **4.L26** (7.5 mol%) and Et₃N (5 equiv.) in MeCN (0.1 M), irradiated at room temperature for 12 h, isolated yield.

The scope of secondary alkyl NHPI esters was broad. Cyclic alkyl groups (Figure 50) including small and large rings (**4.5a-4.5e**), heterocyclic alkyl group (**4.5f**), and fluorinated alkyl group (**4.5g**), as well as acyclic secondary alkyl groups (**4.5h-4.5j**), were all amenable to the coupling. When a tertiary alkyl redox-active ester, which derived from 1-adamantane carboxylic acid, was coupled to aniline **4.2a**, *N*-phenyladamantan-1-amine **4.5k** was obtained only in 9% yield. Besides, the coupling between alkyl NHPI ester derived from pivalic acid and aniline was not feasible in obtaining the aminated product **4.5l**. These results are consistent with the challenge in the cross-coupling of very bulky tertiary alkyl groups.
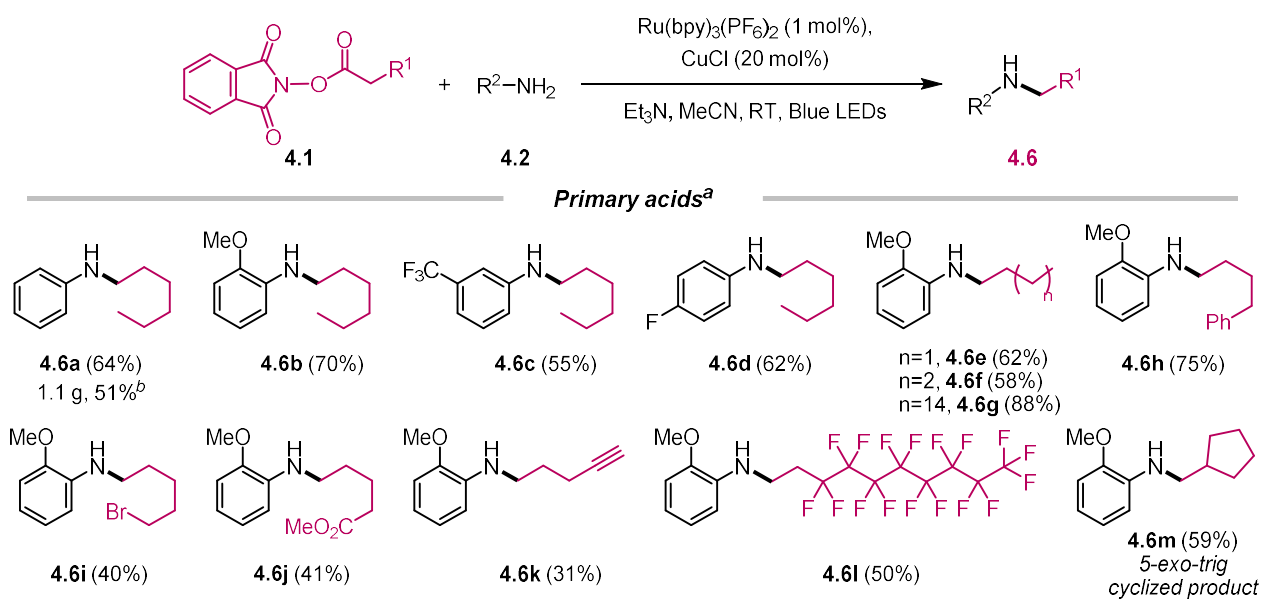
Figure 51 Scope of alkyl NHPI esters that derived from primary carboxylic acids. [a]General conditions: NHPI ester **4.1** (1 equiv.), *N*-nucleophiles **4.2** (2 equiv.), Ru(bpy)₃(PF6)₂ (1 mol%), CuCl (20 mol%), and Et₃N (3 equiv.) in MeCN (0.1 M), irradiated at room temperature for 12 h, isolated yield.

The modified conditions shown in Table 17 were successfully applied to the coupling of various primary alkyl NHPI esters (Figure 51). NHPI esters derived from readily available primary carboxylic acids coupled with different anilines in good yields (**4.6a-4.6g**). To showcase the potential of this methodology, a gram-scale reaction was performed to deliver **4.6a**. The yield of the gram-scale reaction was not significantly reduced and that the desired product **4.6a** could be obtained in 51% isolated yield. Besides, NHPI esters bearing phenyl (**4.6h**), bromo (**4.6i**), ester (**4.6j**) and acetylene (**4.6k**) groups were also examined. All the NHPI esters containing these

functional groups could smoothly couple with anilines and gave the desired products in moderate yields and with excellent chemoselectivity. A polyfluorinated alkyl group was compatible (**4.6l**) to afford polyfluorinated amines. This transformation provided a valuable and convenient route to synthesize polyfluorinated amines, which were difficult to access otherwise using conventional methods. Coupling of an activated 6-heptenoic acid (a radical-clock probe) with a cyclized rate constant of ca. 1.0×10^5 at room temperature,[214] could give the 5-exo-trig cyclized product (**4.6m**). This result was consistent with the intermediacy of alkyl radicals. Notably, no over-alkylation products were observed in any of the reactions, reflecting an important advantage of this method over other methods such as direct *N*-alkylation.

4.3   Applications of the decarboxylative C(sp³)-N coupling reactions

After studying the substrate scope of the method, we next began to investigate the applicability of this approach, including the late-stage modification of natural products and drugs and the synthesis of a drug molecular backbone.

4.3.1   Late-stage modification of natural products and drugs
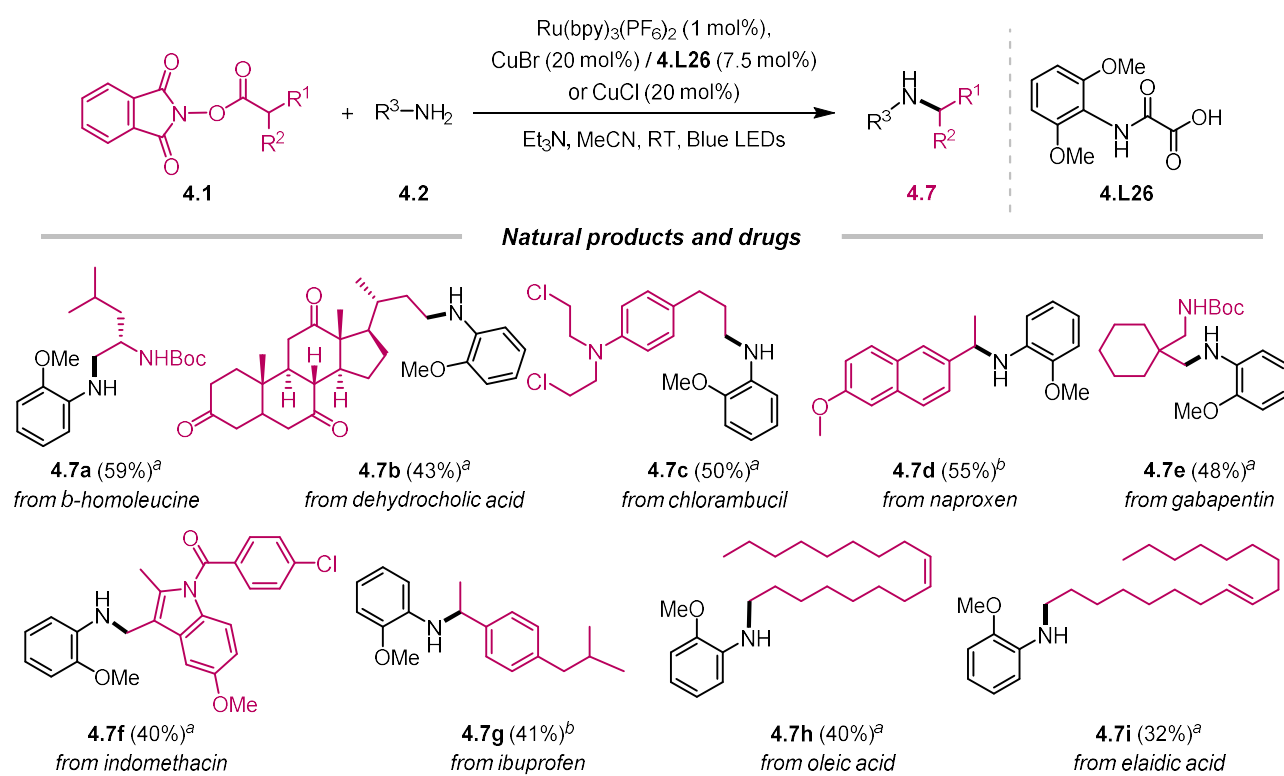
Figure 52 Late-Stage decarboxylative amination of natural products and drugs containing carboxylic acids. [a]General conditions: NHPI ester (2 equiv.), aniline (1 equiv.), Ru(bpy)₃(PF₆)₂ (1 mol%), CuCl (20 mol%) and Et₃N (3 equiv.) in MeCN (0.1 M), irradiated at room temperature for 12 h, isolated yield. [b]General conditions: NHPI ester (1 equiv.), aniline (2 equiv.), Ru(bpy)₃(PF₆)₂ (1 mol%), CuBr (20 mol%), **L3** (7.5 mol%) and Et₃N (5 equiv.) in MeCN (0.1 M), irradiated at room temperature for 12 h, isolated yield.

Carboxylic acid groups are widely occurring in natural products and drug molecules. The current method provides a versatile method for converting aliphatic carboxylic acids into alkyl arylamines. This method will have profound implications in medicinal chemistry if it can be applied to the late-stage functionalization of complex molecules. Gratefully, the method was effective to synthesize complex alkyl aryl amines with impressive chemoselectivity and functional

group compatibility (Figure 52). For example, NHPI esters from an amino acid, β-homoleucine (Figure 52, **4.7a**), and a natural product, dehydrocholic acid (**4.7b**), were aminated with ease. Drugs containing aliphatic carboxylic acid groups could be rapidly transformed into their amine derivatives in one-step (**4.7c-4.7g**), demonstrating the potential of this method for rapid, post-synthetic drug modification. NHPI esters from unsaturated fatty acids, which contain *cis*- and *trans*- double bonds, could also be used to deliver the corresponding amines without significant isomerization or oxidation of olefin groups, albeit in modest yields (**4.7h-4.7i**). The method showed a unique reactivity under very mild conditions. In particular, the current approach can tolerate a range of functional groups that are reactive in other amination methods. Indeed, chemoselectively aminating activated dehydrocholic acid and chlorambucil underscored the orthogonal feature of the current method. Specifically, in regard to reductive amination and direct *N*-alkylation, dehydrocholic acid has several carbonyl groups which are incompatible with reductive amination, while chlorambucil has two alkyl choro groups which are not tolerated to direct *N*-alkylation. Therefore, this method represents an invaluable alternative approach to conventional amination syntheses, which dramatically expands the synthetic toolbox for rapid and precise C(sp^3)-N bond formation.

4.3.2 Synthesis of the skeleton of a T. cruzi CYP51 inhibitor.
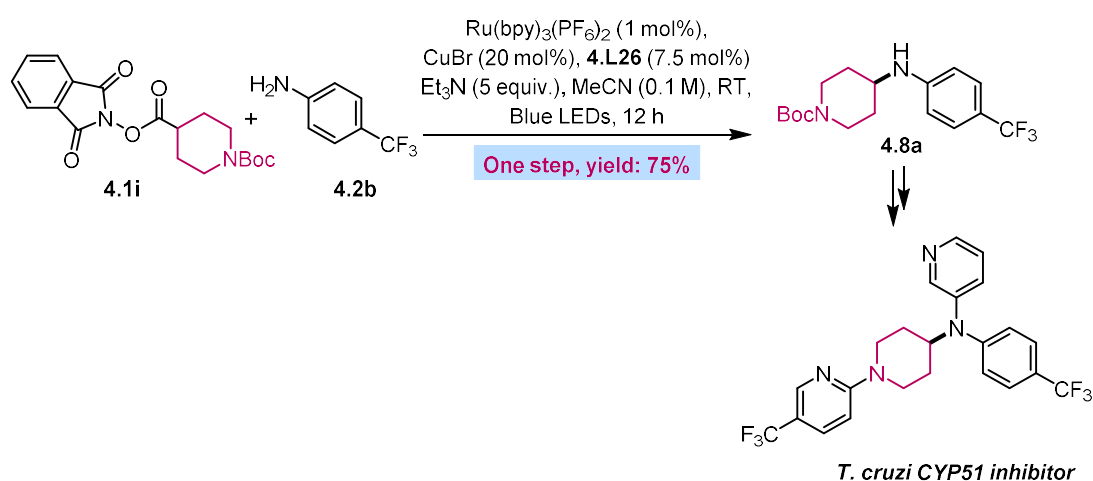
Figure 53 Synthetic applications: synthesis of **4.8a**, the skeleton of a T. cruzi CYP51 inhibitor.

To demonstrate the potential of the current method, we targeted the core skeleton of a drug candidate as a synthetic application (Figure 53). Chagas disease, caused by the protozoan parasite *Trypanosoma cruzi (T. cruzi)*, is an increasing threat to global health.[215] Analyzing the core skeleton of the *T. cruzi* CYP51 inhibitor, a disconnection of the C(sp³)-N bond dominates the retrosynthetic plan. We envisioned that the established method could enable a facile formation of this bond, therefore, streamlining the synthesis of this molecule. To our delight, when applied our method, we were able to obtain the key intermediate **4.7a** to an inhibitor of *Trypanosoma cruzi* (*T. cruzi*)[216] with a yield of 75% in only one step (Figure 53). In contrast, previously **7a** was synthesized by reductive amination via a two-step protocol and obtained in a yield of only 40%.[217]

4.4   Mechanistic investigations

4.4.1   Fluorescence quenching experiments.

While the detailed mechanism warrants a dedicated study, a few experiments gave preliminary insights. We commenced the mechanistic investigations with a series of fluorescence quenching experiments (Figure 54). The initial experiments showed that the fluorescence could only be quenched by the complex of an NHPI ester and CuBr, indicating the critical role of free copper ions in promoting single-electron transfer.
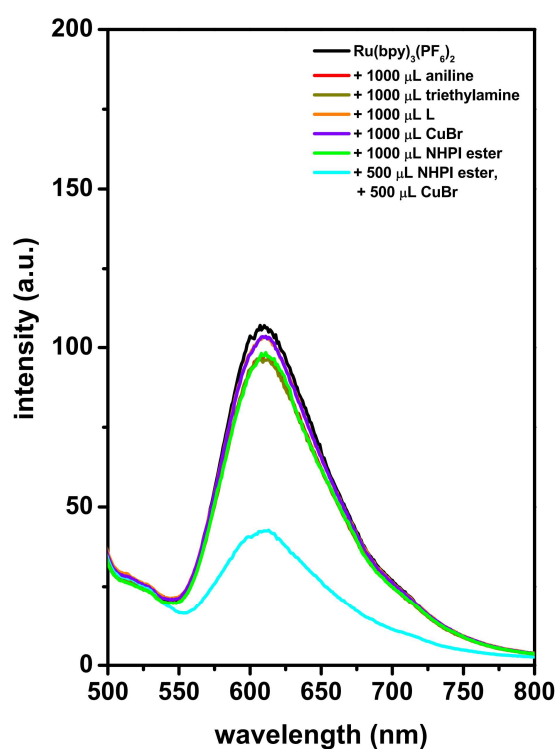
Figure 54 Fluorescence quenching experiments. Fluorescence spectra of 1000 µL [Ru(bpy)$_3$](PF$_6$)$_2$ (15 µM in MeCN) upon addition of 1000 µL aniline (100 mM in MeCN); 1000 µL triethylamine (100 mM in MeCN); 1000 µL L3 (10 mM in MeCN); 1000 µL CuBr (10 mM in MeCN); 1000 µL NHPI ester (50 mM in MeCN); 500 µL NHPI ester (50 mM in MeCN) + 500 µL CuBr (10 mM in MeCN), respectively.

4.4.2 TEMPO radical-trapping experiment
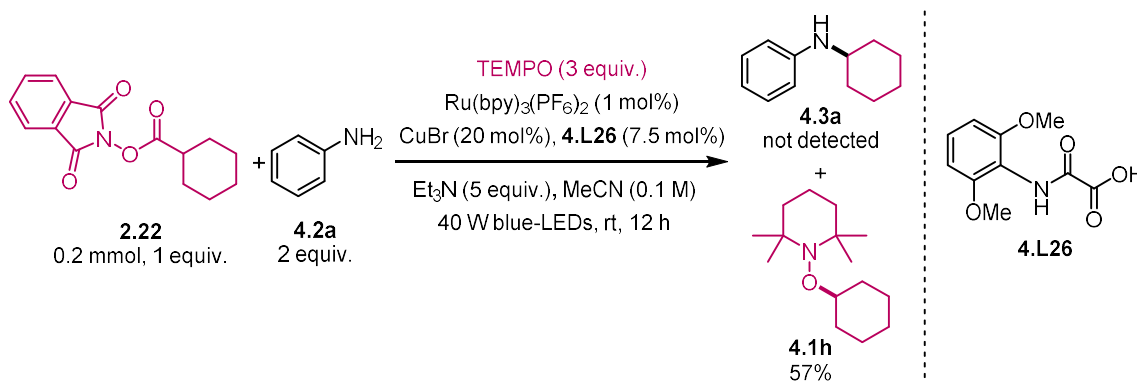
Figure 55 TEMPO trapping experiment.

In Figure 51, the radical-clock experiment (5-exo-trig cyclized product **4.6m**) showed substantial evidence of a radical-involved mechanism. Moreover, the amination reaction halted in the presence of (2,2,6,6-Tetramethylpiperidin-1-yl)oxyl (TEMPO), while *O*-alkylated TEMPO was formed and detected (Figure 55). The results of the radical-clock experiment and TEMPO radical-trapping experiments were consistent with each other, revealing that free radicals were likely involved in such reaction.

4.4.3 Reactions of an NHPI ester with and without aniline under catalytically relevant conditions

Experiments were conducted to probe whether alkyl radical reacts with Cu species prior to the formation of Cu amine/amido species (Figure 56). Under standard conditions (Figure 56a), the amination product **4.3a** had a yield of 94% in 12 h (8% in 2 h), while bromocyclohexane **4.1e** was formed in less than 1% in 12 h (trace product in 2 h). However, in the absence of aniline (Figure 56b), **4.1e** was obtained in 12% yield (1.4 % in 2 h). These results suggest that if an alkyl radical reacts with a Cu(I) species without amine coordination, then a non-negligible amount of alkyl bromide would be formed from a putative Cu(II) alkyl bromide intermediate. As only a trace amount of alkyl bromide formed in the reaction, it is more likely that a Cu amine/amido intermediate traps the alkyl radical.
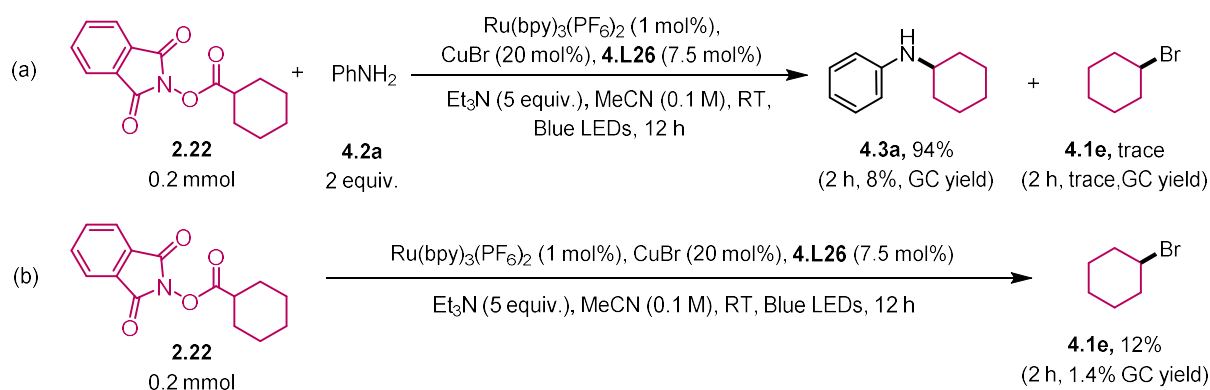
Figure 56 Reactions of **2.22** with and without aniline under catalytically relevant conditions.

4.4.4 Reactions of Cu amine complexes with an NHPI ester.

To test whether the alkyl radical is trapped by Cu(I) or Cu(II) amine/amido species, we first prepared a Cu(II) amine complex (**4.9a**) (Figure 57) and reacted with **2.22** under conditions relevant to the C-N coupling. Both in the absence and presence of **4.L26**, the amination yields were about 10% (Figure 58a). The corresponding Cu(I) amine complex could not be isolated probably due to its instability; however, an in-situ prepared Cu(I) amine species (**4.9b**) reacted with **2.22** under conditions relevant to the C-N coupling to give the amine in 41-46% yield (Figure 58b). These results suggest that the catalysis involves more likely the trapping of alkyl radical by a Cu(I) amide intermediate, which are consistent with our mechanistic proposal. However, more experiments are required to confirm this, and to elucidate the mechanistic details.
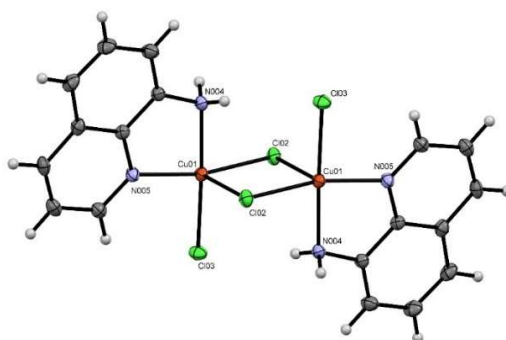
Figure 57 X-ray crystallography of 9a. Crystallographic data for the structure **4.9a** reported here has been deposited at the Cambridge Crystallographic Data Centre, under deposition number CCDC 1586680.
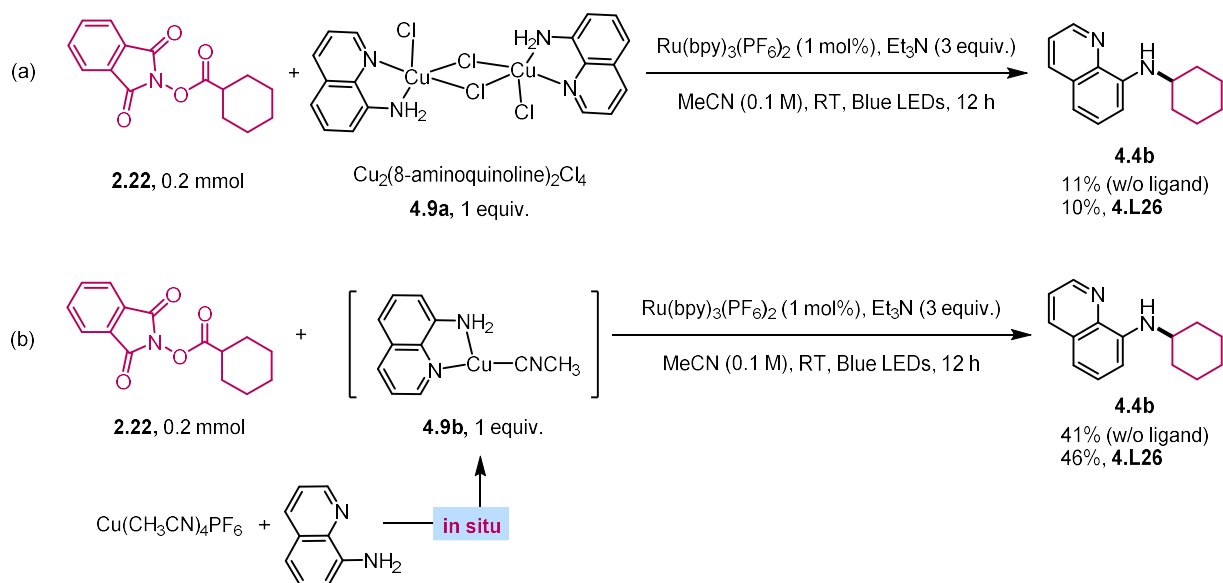
Figure 58 Reactions of Cu amine complexes with an NHPI ester.

4.4.5   DFT-based computational study[218] and proposed mechanistic pathway
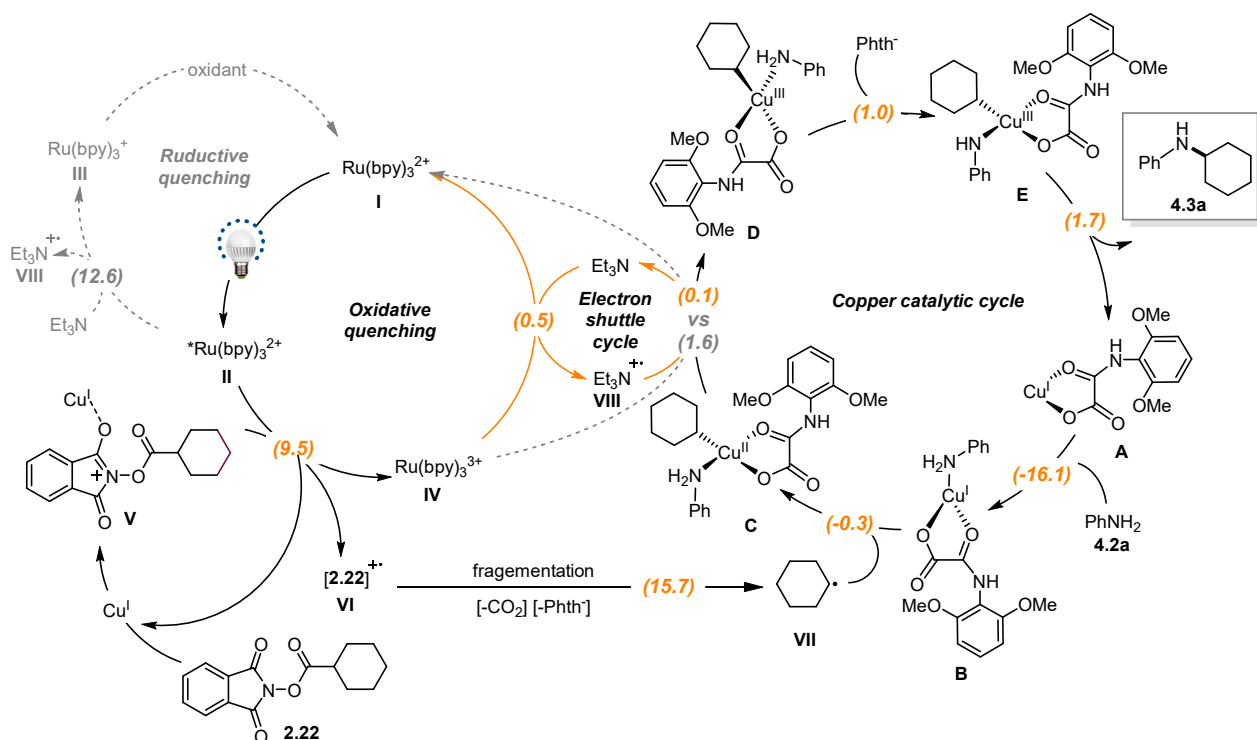
Figure 59 Proposed mechanistic pathway. The orange (possible reaction pathway) and grey values (unlikely mechanistic pathway using dashed arrows) in parentheses are the calculated Gibbs energy barriers (in kcal/mol).[218]

During the preparation of this thesis, Zhang and co-workers conducted a detailed mechanistic study of our reaction using a DFT-based computational approach.[218] The work of Zhang and co-workers inspired us and provided precious information to help us to gain a deeper understanding of the mechanism of the current method.

Based on the experimental results we obtained and the results of the theoretical computational studies by Zhang and co-workers, we speculated about a possible reaction mechanism and outlined this in Figure 59. Initially, under irradiation of blue LEDs, $Ru(bpy)_3^{2+}$ **I** can be excited to its excited state $Ru(bpy)_3^{2+*}$ **II**. At this point, according to our fluorescence quenching experiments (Figure 54) and DFT calculation[218], an oxidative quenching process by the complex **V** (forms from NHPI ester **2.22** and free Cu^I anion) is likely to happen, and enables the SET from **II** to **V**, furnishing oxidized photocatalyst $Ru(bpy)_3^{3+}$ **IV** and **VI**. Then the fragmentation of **VI** leads to the generation of cyclohexyl radical **VII**, which has been substantiated by the radical-clock experiment (Figure 51, **4.6m**) and the TEMPO trapping experiment (Figure 55). Meanwhile, the copper catalytic cycle starts from the coordination of the precatalyst **A** with aniline, and forms the Cu^I amine complex **B**, which can trap the radical **VII** to generate Cu^{II}-cyclohexyl amine complex **C**. Notably, according to the DFT calculation (Figure 59)[218], instead of the previously proposed mechanism involving the direct SET from **C** to $Ru(bpy)_3^{3+}$ **IV** with an energy barrier of 1.6 kcal/mol, we believed the process that using triethylamine as an electron shuttle is more likely. In this scenario, triethylamine can transport an electron from **C** (0.1 kcal/mol, Figure 59) to **IV** (0.5 kcal/mol, Figure 59), thus facilitate to regenerate the photocatalyst $Ru(bpy)_3^{2+}$ **I** and obtaining high-valent Cu^{III}-cyclohexyl amine complex **D**. The phthalimide anion Phth⁻ can then serve as a base to deprotonate **D** and generate a high-valence Cu^{III}-cyclohexyl amido complex **E** with a energy barrier of 1.0 kcal/mol (Figure 59). **E** can undergo reductive elimination to furnish the aminated product **4.3a** and regenerate copper catalyst **A** to close one copper catalytic cycle.

To summarize the proposed mechanism, several points are crucial. (1) Through DFT-based calculations and experiments, we found that the most likely cycling pathway for the photocatalyst is through oxidative quenching, namely the $Ru^{II}/Ru^{II*}/Ru^{III}/Ru^{II}$ cycle. (2) Et_3N has a dual role in

the reaction, not only as a base to promote the generation of the precatalyst, but also as an electron transfer reagent to promote the regeneration of the photocatalyst and to obtain high-valent copper intermediates (Figure 59). This could also explain why Et$_3$N is so unique among all the bases we optimized (Table 14). (3) The generation of alkyl radicals is considered as the rate-determining step of the reaction with an energy barrier of 15.7 kcal/mol. (4) The Cu^I salt has a dual function. Besides its ability to bind ligands to act as a catalyst in the copper-catalyzed cycle Cu^I/Cu^{II}/Cu^{III}/Cu^I, the free copper salt can also bind to NHPI esters to facilitate the oxidative quenching process.

4.5   Conclusions

In summary, the established tandem photoredox and Cu catalysis enables the decarboxylative amination of alkyl redox-active esters with anilines. This method significantly expands the scope of metal-catalyzed $C(sp^3)$-N coupling, which remains underdeveloped. Thanks to the distinct advantages of alkyl carboxylic acids over alkyl halides in availability, stability, and toxicity, the method and its underlying strategy are expected to have widespread use in amine synthesis. The unique activity of Cu-based catalysts in this decarboxylative C-N coupling contrasts the reign of Ni catalysis in analogous C-C coupling via tandem photoredox/metal catalysis,[202-204] underscoring their essential divergences.

4.6   Experimental section

4.6.1   General manipulation considerations

All manipulations for the decarboxylative $C(sp^3)$-N cross-coupling via synergetic photoredox and copper-catalyzed reactions were set up in a 15 mL Teflon-screw capped test tubes (unless otherwise noted) under an inert nitrogen (N_2) atmosphere using glove-box techniques. The test tubes were then sealed with airtight electrical tapes and the reaction mixtures were stirred under irradiation of blue LEDs with a fan cooling down the temperature. Blue LEDs were purchased from Kessil Co., Ltd. (40 W max., product No. A160WE). Table fan was purchased from Galaxus Co., Ltd. (35 W max.). Flash column chromatography was performed using silica gel (Silicycle, ultra-pure grade). Preparative thin-layer chromatography (preparative TLC) was performed using a preparative TLC plate (Merck Millipore, TLC Silica gel 60 F254, 20 x 20 cm, catalog number: 1.05715.0001) in a developing tank. Notably, the TLC plates used for the purification of amine products were washed with hexanes/triethylamine solution (volume ratio ~40:1) prior to the use in order to minimize the product loss. The eluents for column chromatography and preparative TLC were presented as ratios of solvent volumes. Yields reported in the publication are of isolated materials unless otherwise noted.

4.6.2   General procedure for *N*-hydroxyphthalimide (NHPI) ester synthesis (General procedure A)

A 100 mL round-bottom flask was charged with (if solid) carboxylic acid (1.0 equiv.), nucleophile (*N*-hydroxyphthalimide, 1.0 equiv.) and DMAP (0.1 equiv.). Dichloromethane was added (0.2 M), and the mixture was stirred vigorously. Carboxylic acid (1.0 equiv) was added via syringe (if liquid). DIC (1.1 equiv) was then added dropwise via syringe, and the mixture was allowed to stir until the carboxylic acid was consumed (determined by TLC). Typical reaction times were between 0.5 h and 12 h. After the reaction, the mixture was filtered over Celite and rinsed with additional CH_2Cl_2. The solvent was removed under reduced pressure, and purification by column chromatography afforded corresponding activated esters, which were used without further purification unless otherwise noted.

4.6.3 General procedure for branched alkyl aryl amine synthesis (General procedure B)

An oven-dried 15 mL re-sealable screw-cap test tube equipped with a Teflon-coated magnetic stir bar was sequentially charged with NHPI ester (1 equiv., 0.2 mmol), Ru(bpy)$_3$(PF$_6$)$_2$ (1 mol%), CuBr (20 mol%), **4.L26** (7.5 mol%), acetonitrile solvent (2 mL), aniline (2 equiv), Et$_3$N (5 equiv) in the glove box. The vial was sealed with a screw cap and removed from the glove box. The vigorously stirred solution was irradiated with blue LED light under table fan cooling for 12 h. After the reaction, the reaction mixture was acidified with saturated NH$_4$Cl solution and then neutralized with saturated NaHCO$_3$ solution. The crude product in the aqueous fraction was extracted with ethyl acetate. The combined organic fractions were concentrated *in vacuo* with the aid of a rotary evaporator. The crude product residue was purified by preparative thin layer chromatography (pretreated with 3% triethylamine in hexanes) using a solvent mixture (ethyl acetate, hexanes) as an eluent to afford the purified amine products.
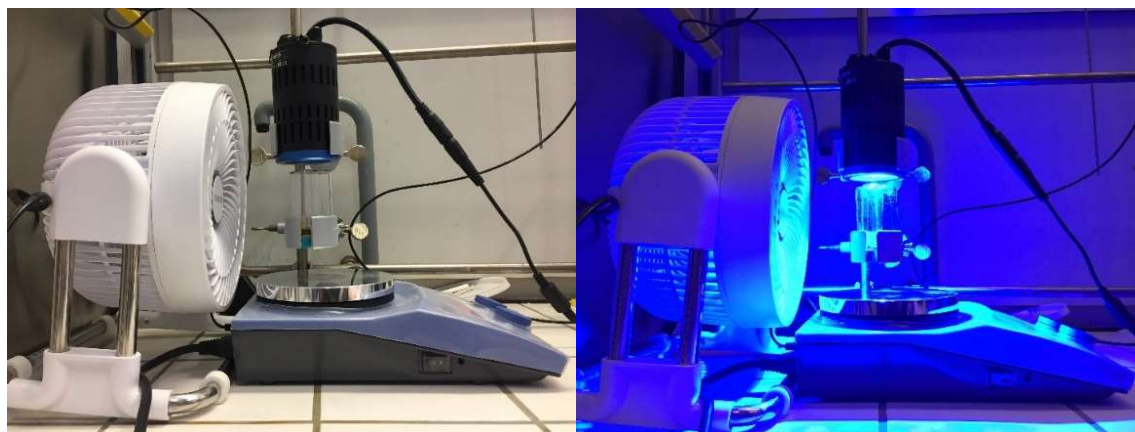
Figure 60 Reaction setup for decarboxylative C(sp^3)-N cross-coupling reactions.

4.6.4 General procedure for visible-light-mediated decarboxylative amination (Gram-scale reaction)

An oven-dried 100 mL flask equipped with a Teflon-coated magnetic stir bar was sequentially charged with aniline (12.2 mmol, 1.2 mL), 1,3-dioxoisoindolin-2-yl heptanoate (1.5 equiv, 5.1 g), Ru(bpy)$_3$(PF$_6$)$_2$ (1 mol%, 105 mg), CuCl (20 mol%, 242 mg), MeCN (61 mL), Et$_3$N (3 equiv, 5.1 mL) in the glovebox. The flask was sealed and removed from the glovebox. Then the

flask was placed 10 cm away from two blue LED, and irradiated under fan cooling (to maintain the temperature at room temperature) for 12 h. After the reaction, the resulting dark brown reaction mixture was acidified with saturated NH_4Cl solution and then neutralized with saturated $NaHCO_3$ solution. The crude product in the aqueous fraction was extracted with EtOAc. The aqueous fraction was further washed with EtOAc. The combined organic fractions were concentrated *in vacuo* with the aid of a rotary evaporator. The crude product residue was purified by column chromatography using a solvent mixture (hexanes to 20:1 hexanes:EtOAc) as an eluent to afford 1.1 g (51%) of the purified product **4.5a**.

Figure 61 Reaction setup for gram-scale decarboxylative C(sp³)-N cross-coupling reactions.

4.6.5   TEMPO trapping experiment
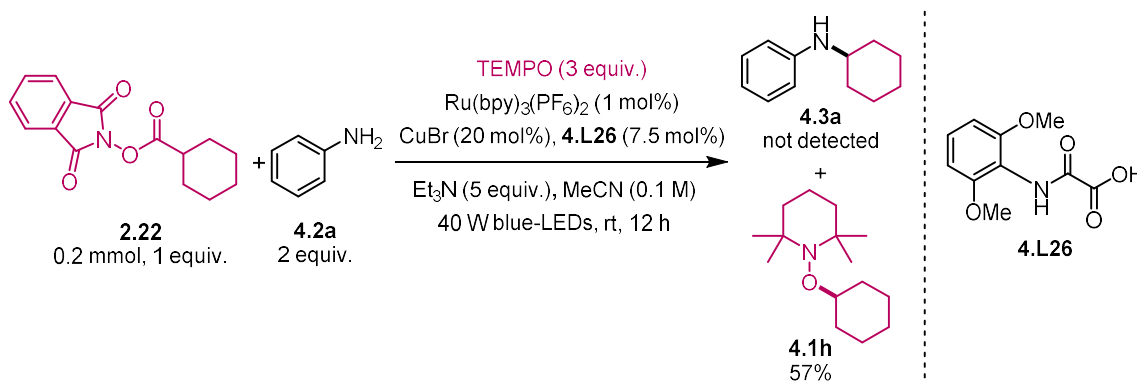
An oven-dried 15 mL vial equipped with a Teflon-coated magnetic stir bar was sequentially charged with NHPI ester **2.22** (0.2 mmol), Ru(bpy)₃(PF₆)₂ (1 mol%, 2 μmol, 1.8 mg), CuBr (20 mol%, 0.04 mmol, 5.8 mg), ligand **4.L26** (30 mol%, 0.06 mmol, 13.5 mg), MeCN (2 mL), **4.2a** (2

equiv, 0.4 mmol), Et$_3$N (5 equiv, 1 mmol, 139 μL), TEMPO (3 equiv., 0.6 mmol) in the glove box. The vial was sealed with a screw cap and removed from the glove box. Then the vial was placed 3 cm away from one blue LED, and irradiated under fan cooling (maintain the temperature at room temperature) for 12 h. After irradiation, the brown reaction mixture was submitted to mass spectrometry (LC-MS) without any further work-up. Desired product **4.3a** was not detected and TEMPO trapped product **4.1h** (57% GC yield) was found through mass spectrometry (Supplementary Figure 4).

4.6.6   Preparation of Cu(II) complex (9a)

To a test tube was added a solution of 8-aminoquinoline (0.144 g, 1.00 mmol) in CH$_2$Cl$_2$ (15 cm^3) before layer MeOH solvent (2 mL) on the top, then a methanolic solution (5 cm^3) of CuCl$_2$•2H$_2$O (0.170 g, 1.00 mmol) was carefully layered on the top, the tube was sealed and stood at room temperature for a week. Green block-like crystal **4.9a** were observed on the wall of the tube, and collected by decanting the solvent, washed with methanol and dried in air. The structure of the compound was confirmed by X-ray crystallography (Figure 57), and is identical to the literature report.[219]

4.6.7   Reactivity of Cu(II) complex 4.9a

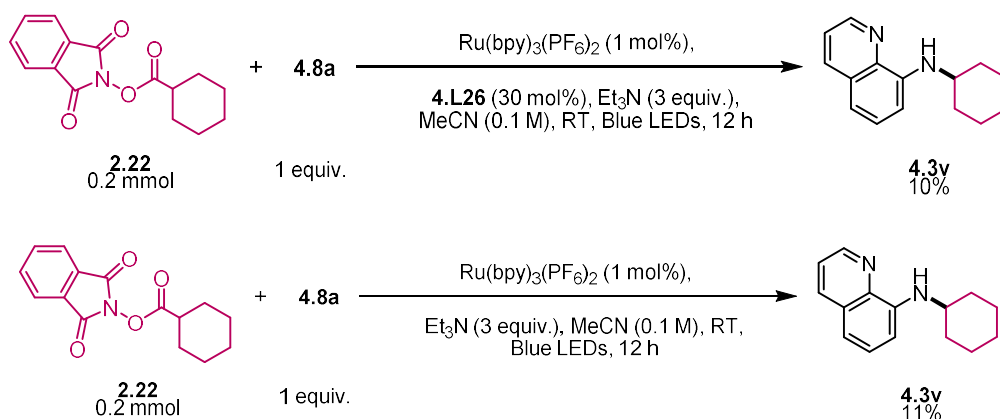

An oven-dried 15 mL vial equipped with a Teflon-coated magnetic stir bar was sequentially charged with NHPI ester **2.22** (0.2 mmol, 55 mg), Ru(bpy)$_3$(PF$_6$)$_2$ (1 mol%, 2 μmol, 1.8 mg), **4.L26** (30 mol%, 6.8 mg) or without **4.L26**, **4.9a** (1 equiv, 0.2 mmol), MeCN (2 mL), Et$_3$N (3 equiv, 80

µL), dodecane (1 equiv, 45 µL, internal standard) in the glove box. The vial was sealed with a screw cap and removed from the glove box. Then the vial was placed 3 cm away from one blue LED, and irradiated under fan cooling (maintain the temperature at room temperature) for 12 h. After the reaction, GC analysis of the mixture.

4.6.8 Preparation of Cu(I) complex 4.9b

An oven-dried 15 mL vial equipped with a Teflon-coated magnetic stir bar was charged 8-aminoquinoline (0.2 mmol, 29 mg) and CD_3CN (1 mL) in the glove box. The vial was stirring until all 8-aminoquinoline dissolved and transferred the solution to a NMR tube. Then analysis of ^{1}H NMR and ^{13}C NMR were conducted (red spectra). Afterwards, the solution was transferred to previous vial, $Cu(MeCN)_4PF_6$ (0.2 mmol, 76 mg) was added in the glove box. The vial was stirring vigorously until a transparent solution to obtain the Cu(I)-amine complex solution (solution color changed to light yellow). Then transferred the solution to a NMR tube and analysis of ^{1}H NMR and ^{13}C NMR were conducted (blue spectra).

^{1}H NMR spectra showing formation of a Cu(I) complex
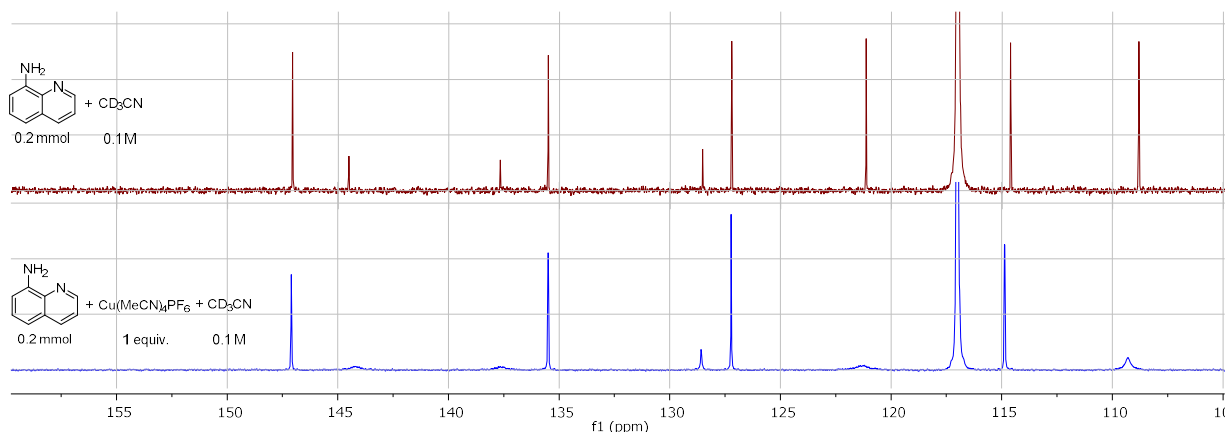
^{13}C NMR spectra showing formation of a Cu(I) complex.

4.6.9 Reactivity of in-situ generated Cu(I) complex 4.9b
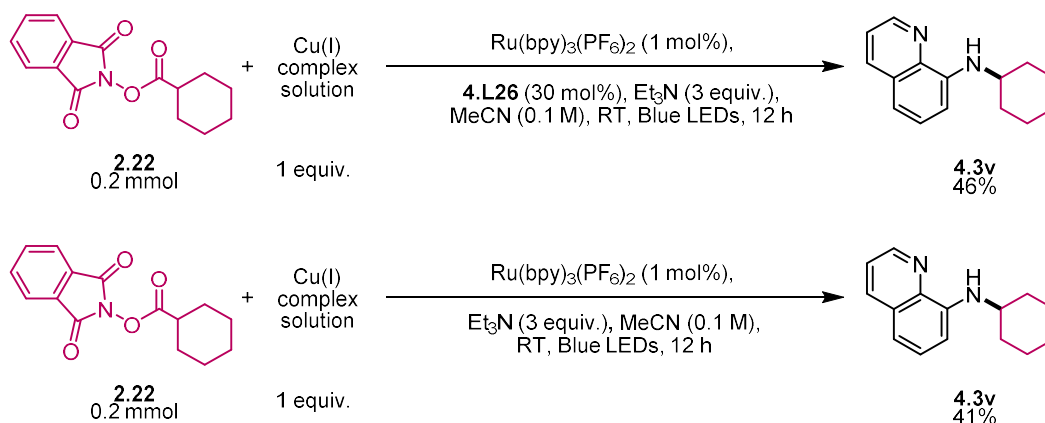
An oven-dried 15 mL vial equipped with a Teflon-coated magnetic stir bar was sequentially charged with Cu(MeCN)$_4$PF$_6$ (0.2 mmol, 76 mg), 8-aminoquinoline (1 equiv, 29 mg) and MeCN (1 mL) in the glove box, stirring vigorously for 15 min to obtain the Cu(I) com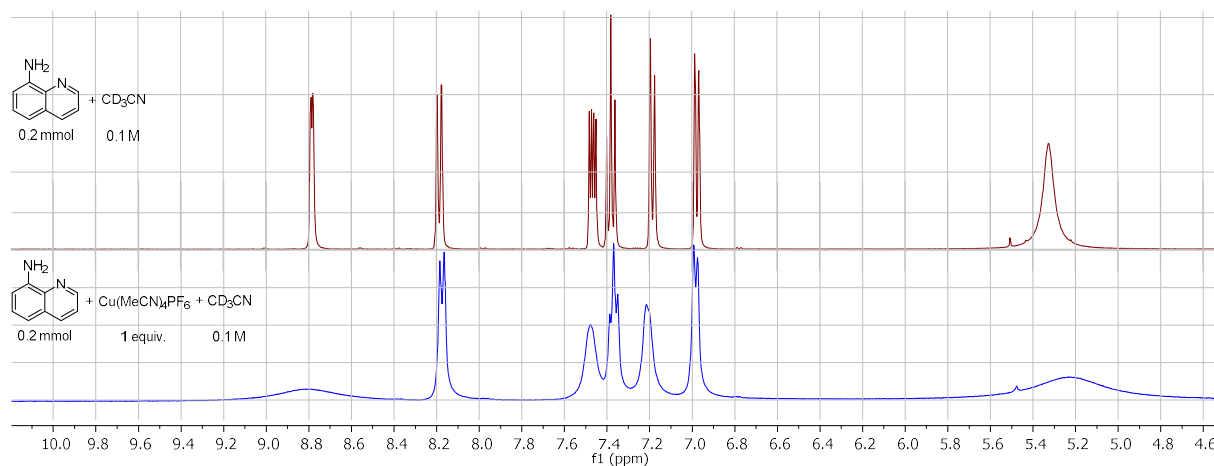plex solution (solution color changed to light yellow). Another oven-dried 15 mL vial equipped with a Teflon-coated magnetic stir bar was sequentially charged with NHPI ester **2.22** (0.2 mmol, 55 mg), Ru(bpy)$_3$(PF$_6$)$_2$ (1 mol%, 2 µmol, 1.8 mg), **4.L26** (30 mol%, 6.8 mg) or without **4.L26**, MeCN (1 mL), Et$_3$N (3 equiv, 80 µL), dodecane (1 equiv, 45 µL, internal standard) in the glove box. Then add Cu(I) complex solution into this mixture. The vial was sealed with a screw cap and removed from the glove box. Then the vial was placed 3 cm away from one blue LED, and irradiated under

fan cooling (maintain the temperature at room temperature) for 12 h. After the reaction, GC analysis of the mixture.

4.6.10 Characterization of the reaction product

***N*-cyclohexylaniline (4.3a)**
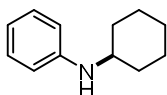
Following the General Procedure B with the corresponding NHPI ester (0.2 mmol) and aniline (0.4 mmol). The crude product was purified by preparative TLC using hexanes / EtOAc (40:1) as an eluent to afford 33 mg (94%) of the title compound **4.3a**.

^{1}H NMR (400 MHz, CD$_2$Cl$_2$): δ 7.11 (dd, *J* = 8.5, 7.3 Hz, 2H), 6.63 – 6.52 (m, 3H), 3.58 (br s, 1H), 3.28 – 3.21 (m, 1H), 2.06-2.00 (m, 2H), 1.78 – 1.62 (m, 3H), 1.41 – 1.11 (m, 5H).

^{13}C NMR (101 MHz, CDCl$_3$): δ 147.5, 129.4, 117.0, 113.3, 51.8, 33.6, 26.1, 25.2.

Spectral data match those previously reported.[220]

***N*-cyclohexyl-2-methylaniline (4.3b)**

Following the General Procedure B with the corresponding NHPI ester (0.2 mmol) and *o*-toluidine (0.4 mmol). The crude product was purified by preparative TLC using hexanes / EtOAc (30:1) as an eluent to afford 30 mg (78%) of the title compound **4.3b**.

^{1}H NMR (400 MHz, CDCl$_3$): δ 7.11 (t, *J* = 7.8 Hz, 1H), 7.05 (d, *J* = 7.3 Hz, 1H), 6.68 – 6.58 (m, 2H), 3.37 – 3.27 (m, 1H), 2.13 (s, 3H), 2.11 – 2.04 (m, 2H), 1.82 – 1.63 (m, 3H), 1.47 – 1.15 (m, 5H).

^{13}C NMR (101 MHz, CDCl$_3$): δ 145.4, 130.4, 127.2, 121.8, 116.4, 110.3, 51.7, 33.8, 26.2, 25.2, 17.7.

Spectral data match those previously reported. [220]

N-cyclohexyl-3-methylaniline (4.3c)

Following the General Procedure B with the corresponding NHPI ester (0.2 mmol) and *m*-toluidine (0.4 mmol). The crude product was purified by preparative TLC using hexanes / EtOAc (30:1) as an eluent to afford 26 mg (69%) of the title compound **4.3c**.

^{1}**H NMR** (400 MHz, CDCl$_3$): δ 7.06 (td, *J* = 7.3, 2.2 Hz, 1H), 6.50 (d, *J* = 7.5 Hz, 1H), 6.42 (d, *J* = 6.5 Hz, 2H), 3.55 (br s, 1H), 3.26 (tt, *J* = 10.2, 3.8 Hz, 1H), 2.28 (s, 3H), 2.11 – 2.00 (m, 2H), 1.82 – 1.61 (m, 3H), 1.44 – 1.32 (m, 2H), 1.28 – 1.11 (m, 3H).

^{13}**C NMR** (101 MHz, CDCl$_3$): δ 147.3, 139.2, 129.3, 118.2, 114.3, 110.6, 52.0, 33.6, 26.1, 25.2, 21.8.

Spectral data match those previously reported.[220]

N-cyclohexyl-4-methylaniline (4.3d)
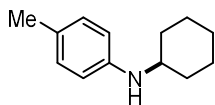
Following the General Procedure B with the corresponding NHPI ester (0.2 mmol) and *p*-toluidine (0.4 mmol). The crude product was purified by preparative TLC using hexanes / EtOAc (30:1) as an eluent to afford 21 mg (56%) of the title compound **4.3d**.

^{1}**H NMR** (400 MHz, CDCl$_3$): δ 6.98 (d, *J* = 8.1 Hz, 2H), 6.57 – 6.48 (m, 2H), 3.23 (tt, *J* = 10.1, 3.7 Hz, 1H), 2.24 (s, 3H), 2.06 (dd, *J* = 12.9, 3.9 Hz, 2H), 1.76 (dt, *J* = 13.2, 3.9 Hz, 2H), 1.65 (dt, *J* = 12.6, 3.8 Hz, 1H), 1.42 – 1.11 (m, 5H).

^{13}**C NMR** (101 MHz, CDCl$_3$): δ 145.2, 129.9, 126.2, 113.6, 52.2, 33.7, 29.8, 26.1, 25.2, 20.5.

Spectral data match those previously reported.[220]
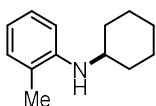
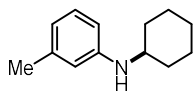### *N*-cyclohexyl-2-methoxyaniline (4.3e)

Following the General Procedure B with the corresponding NHPI ester (0.2 mmol) and *o*-anisidine (0.4 mmol). The crude product was purified by preparative TLC using hexanes / EtOAc (30:1) as an eluent to afford 39 mg (95%) of the title compound **4.3e**.

^{1}H NMR (400 MHz, CDCl$_3$): δ 6.85 (t, *J* = 7.7 Hz, 1H), 6.77 (d, *J* = 8.1 Hz, 1H), 6.69 – 6.58 (m, 2H), 4.14 (br s, 1H), 3.84 (s, 3H), 3.29 – 3.22 (m, 1H), 2.11 – 2.05 (m, 2H), 1.80 – 1.63 (m, 3H), 1.43 – 1.16 (m, 5H).

^{13}C NMR (101 MHz, CDCl$_3$): δ 150.8, 147.4, 121.5, 120.9, 116.8, 112.5, 56.1, 32.2, 25.8, 24.3. Spectral data match those previously reported.[220]

N-cyclohexyl-2,6-dimethoxyaniline (4.3f)

Following the General Procedure B with the corresponding NHPI ester (0.2 mmol) and 2,6-dimethoxyaniline (0.4 mmol). The crude product was purified by preparative TLC using hexanes / EtOAc (25:1) as an eluent to afford 42 mg (88%) of the title compound **4.3f**.

^{1}H NMR (400 MHz, CDCl$_3$): δ 6.80 (t, *J* = 8.2 Hz, 1H), 6.53 (d, *J* = 8.3 Hz, 2H), 3.83 (s, 6H), 3.50 – 3.39 (m, 1H), 3.19 (br s, 1H), 1.91 (dd, *J* = 12.4, 4.0 Hz, 2H), 1.70 (dt, *J* = 12.9, 3.7 Hz, 2H), 1.63 – 1.54 (m, 1H), 1.34 – 1.01 (m, 5H).

^{13}C NMR (101 MHz, CDCl$_3$): δ 151.5, 126.5, 119.8, 104.8, 56.1, 54.1, 34.4, 26.3, 25.3.

Physical State: reddish brown oil.

**HRMS (**ESI): calcd for C$_{14}$H$_{22}$NO$_2$ [M+H]$^+$ 236.1651; found 236.1656.

N-cyclohexyl-2-ethylaniline (4.3g)
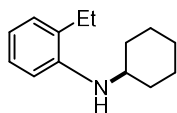
Following the General Procedure B with the corresponding NHPI ester (0.2 mmol) and 2-ethylaniline (0.4 mmol). The crude product was purified by preparative TLC using hexanes / EtOAc (30:1) as an eluent to afford 33 mg (80%) of the title compound **4.3g**.

¹H NMR (400 MHz, CDCl₃): δ 7.10 (t, *J* = 7.7 Hz, 1H), 7.07 (d, *J* = 7.4 Hz, 1H), 6.66 (t, *J* = 7.0 Hz, 2H), 3.39 – 3.28 (m, 1H), 2.47 (q, *J* = 7.5 Hz, 2H), 2.21 – 1.99 (m, 2H), 1.83 – 1.62 (m, 3H), 1.39 – 1.12 (m, 8H).

¹³C NMR (101 MHz, CDCl₃): δ 144.8, 128.2, 127.4, 127.0, 116.6, 110.7, 51.7, 33.7, 26.2, 25.2, 24.0, 13.0.
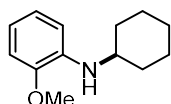
Spectral data match those previously reported.[220]
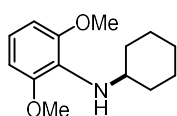
2-bromo-*N*-cyclohexylaniline (4.3h)

Following the General Procedure B with the corresponding NHPI ester (0.2 mmol) and 2-bromoaniline (0.4 mmol). The crude product was purified by preparative TLC using hexanes / EtOAc (30:1) as an eluent to afford 33 mg (65%) of the title compound **4.3h**.

¹H NMR (400 MHz, CDCl₃): δ 7.40 (dd, *J* = 7.9, 1.6 Hz, 1H), 7.14 (t, *J* = 7.8 Hz, 1H), 6.70 – 6.60 (m, 1H), 6.51 (td, *J* = 7.7, 1.5 Hz, 1H), 4.24 (br s, 1H), 3.33 – 3.28 (m, 1H), 2.07 – 2.02 (m, 2H), 1.81 – 1.75 (m, 2H), 1.68 – 1.61 (m, 1H), 1.48 – 1.18 (m, 5H).

¹³C NMR (101 MHz, CDCl₃): δ 144.3, 132.7, 128.5, 117.2, 111.9, 109.9, 51.7, 33.3, 26.0, 25.0.

Spectral data match those previously reported.[221]

2-(cyclohexylamino)benzonitrile (4.3i)

Following the General Procedure B with the corresponding NHPI ester (0.2 mmol) and 2-aminobenzonitrile (0.4 mmol). The crude product was purified by preparative TLC using hexanes / EtOAc (25:1) as an eluent to afford 16 mg (40%) of the title compound **4.3i**.

¹H NMR (400 MHz, CDCl₃): δ 7.42 – 7.31 (m, 2H), 6.71 – 6.54 (m, 2H), 4.45 (br s, 1H), 3.35 (tt, *J* = 9.8, 3.7 Hz, 1H), 2.10 – 2.00 (m, 2H), 1.85 – 1.75 (m, 2H), 1.69 – 1.59 (m, 1H), 1.46 – 1.20 (m, 5H).

¹³C NMR (101 MHz, CDCl₃): δ 149.4, 134.3, 133.1, 118.2, 116.3, 111.4, 95.8, 51.7, 33.1, 25.8, 24.9.

Spectral data match those previously reported.[222]

N-cyclohexyl-4-fluoroaniline (4.3j)

Following the General Procedure B with the corresponding NHPI ester (0.2 mmol) and 4-fluoroaniline (0.4 mmol). The crude product was purified by preparative TLC using hexanes / EtOAc (30:1) as an eluent to afford 35 mg (90%) of the title compound **4.3j**.

¹H NMR (400 MHz, CDCl₃): δ 6.87 (t, *J* = 8.7 Hz, 2H), 6.56 – 6.47 (m, 2H), 3.18 (tt, *J* = 10.2, 3.7 Hz, 1H), 2.10 – 1.98 (m, 2H), 1.76 (d, *J* = 10.4 Hz, 2H), 1.65 (d, *J* = 12.5 Hz, 1H), 1.42 – 1.31 (m, 2H), 1.26 – 1.07 (m, 3H).

¹³C NMR (101 MHz, CDCl₃): δ 156.8, 154.5, 143.9 (d, *J* = 1.8 Hz), 115.7 (d, *J* = 22.2 Hz), 114.2 (d, *J* = 7.2 Hz), 52.6, 33.6, 26.1, 25.2.

Spectral data match those previously reported.[223]

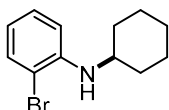### 4-chloro-*N*-cyclohexylaniline (4.3k)

Following the General Procedure B with the corresponding NHPI ester (0.2 mmol) and 4-chloroaniline (0.4 mmol). The crude product was purified by preparative TLC using hexanes / EtOAc (30:1) as an eluent to afford 36 mg (85%) of the title compound **4.3k**.

¹H NMR (400 MHz, CDCl₃): δ 7.14 – 7.03 (m, 2H), 6.56 – 6.44 (m, 2H), 3.53 (br s, 1H), 3.20 (tt, *J* = 10.1, 3.8 Hz, 1H), 2.10 – 1.98 (m, 2H), 1.80 – 1.62 (m, 3H), 1.41 – 1.08 (m, 5H).

¹³C NMR (101 MHz, CDCl₃): δ 146.1, 129.2, 121.4, 114.3, 52.0, 33.4, 26.0, 25.1.

Spectral data match those previously reported.[224]

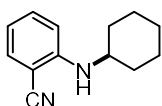### 4-bromo-*N*-cyclohexylaniline (4.3l)

Following the General Procedure B with the corresponding NHPI ester (0.2 mmol) and 4-bromoaniline (0.4 mmol). The crude product was purified by preparative TLC using hexanes / EtOAc (30:1) as an eluent to afford 34 mg (66%) of the title compound **4.3l**.

^{1}H NMR (400 MHz, CD$_2$Cl$_2$): δ 7.21 – 7.18 (m, 2H), 6.48 – 6.44 (m, 2H), 3.80 (br s, 1H), 3.22 – 3.17 (m, 1H), 2.04 – 1.09 (m, 10H).

^{13}C NMR (101 MHz, CDCl$_3$): δ 146.3, 132.1, 115.0, 108.6, 52.1, 42.5, 33.3, 26.0, 25.1, 23.6. Spectral data match those previously reported. [225]
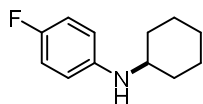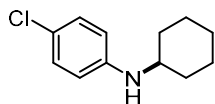
4-iodo-*N*-cyclohexylaniline (4.3m)

Following the General Procedure B with the corresponding NHPI ester (0.2 mmol) and 4-iodoaniline (0.4 mmol). The crude product was purified by preparative TLC using hexanes / EtOAc (30:1) as an eluent to afford 36 mg (60%) of the title compound **4.3m**.

^{1}H NMR (400 MHz, CDCl$_3$): δ 7.38 (d, J = 8.7 Hz, 2H), 6.36 (d, J = 8.7 Hz, 2H), 3.59 (br s, 1H), 3.23-3.17 (m, 1H), 2.02 (dd, J = 12.7, 3.1 Hz, 2H), 1.80-1.72 (m, 3H), 1.43 – 1.06 (m, 5H).

^{13}C NMR (101 MHz, CDCl$_3$): δ 147.1, 137.9, 115.5, 77.1, 51.7, 33.4, 26.0, 25.1.

Physical State: dark brown solid.

HRMS (ESI): calcd for C$_{12}$H$_{17}$IN [M+H]$^+$ 302.0406; found 302.0407.

N-cyclohexyl-3-(1,3-dioxolan-2-yl)aniline (4.3n)
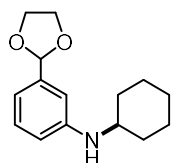
Following the General Procedure B with the corresponding NHPI ester (0.2 mmol) and 3-(1,3-dioxolan-2-yl)aniline (0.4 mmol). The crude product was purified by preparative TLC using hexanes / EtOAc (20:1) as an eluent to afford 38 mg (76%) of the title compound **4.3n**.

^{1}H NMR (400 MHz, CDCl$_3$): δ 7.16 (t, J = 7.8 Hz, 1H), 6.77 (d, J = 7.5 Hz, 1H), 6.69 (t, J = 2.0 Hz, 1H), 6.58 (dd, J = 8.2, 2.4 Hz, 1H), 5.75 (s, 1H), 4.20 – 3.94 (m, 4H), 3.59 (s, 1H), 3.28 (tt, J

= 10.1, 3.7 Hz, 1H), 2.05 (dd, *J* = 13.1, 3.9 Hz, 2H), 1.83 – 1.70 (m, 2H), 1.70 – 1.59 (m, 1H), 1.44 – 1.31 (m, 2H), 1.27 – 1.07 (m, 3H).

¹³C NMR (101 MHz, CDCl₃): δ 147.6, 139.1, 129.4, 114.8, 113.8, 111.0, 104.0, 65.3, 51.7, 33.6, 26.0, 25.1.

Physical State: light yellow oil.

HRMS (ESI): calcd for $C_{15}H_{22}NO_2$ [M+H]⁺ 248.1651; found 248.1651.

N-cyclohexyl-4-((trimethylsilyl)ethynyl)aniline (4.3o)
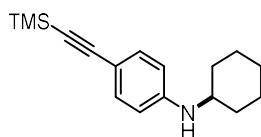
Following the General Procedure B with the corresponding NHPI ester (0.2 mmol) and methyl 4-((trimethylsilyl)ethynyl)aniline (0.4 mmol). The crude product was purified by preparative TLC using hexanes / EtOAc (20:1) as an eluent to afford 17 mg (32%) of the title compound **4.3o**.

¹H NMR (400 MHz, CDCl₃): δ 7.28 (d, *J* = 3.7 Hz, 1H), 6.47 (d, *J* = 8.2 Hz, 2H), 3.78 (br s, 1H), 3.32 – 3.20 (m, 1H), 2.08 – 2.00 (m, 2H), 1.81 – 1.62 (m, 3H), 1.45 – 1.11 (m, 5H), 0.23 (s, 9H).

¹³C NMR (101 MHz, CDCl₃): δ 147.6, 133.5, 112.6, 110.6, 106.7, 91.0, 51.6, 33.4, 26.0, 25.1.

Physical State: white solid.

HRMS (ESI): calcd for $C_{17}H_{26}NSi$ [M+H]⁺ 272.1834; found 272.1832.
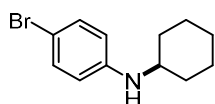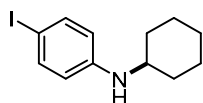
N-cyclohexyl-4-vinylaniline (4.3p)
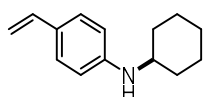
Following the General Procedure B with the corresponding NHPI ester (0.2 mmol) and 4-vinylaniline (0.4 mmol). The crude product was purified by preparative TLC using hexanes / EtOAc (25:1) as an eluent to afford 17 mg (41%) of the title compound **4.3p**.

¹H NMR (400 MHz, CDCl₃): δ 7.23 (d, *J* = 8.2 Hz, 1H), 6.65 – 6.51 (m, 3H), 5.50 (d, *J* = 17.6 Hz, 1H), 4.99 (d, *J* = 10.9 Hz, 1H), 3.58 (br s, 1H), 3.31 – 3.20 (m, 1H), 2.09 – 2.02 (m, 2H), 1.76 – 1.62 (m, 3H), 1.40 – 1.20 (m, 5H).

¹³C NMR (101 MHz, CDCl₃): δ 147.3, 136.8, 127.5, 126.8, 113.1, 109.2, 51.8, 33.6, 26.1, 25.1.

Physical State: brown oil.

HRMS (ESI): calcd for $C_{14}H_{20}N$ [M+H]$^+$ 202.1596; found 202.1600.

Methyl 4-(cyclohexylamino)benzoate (4.3q)
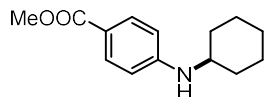
Following the General Procedure B with the corresponding NHPI ester (0.2 mmol) and methyl 4-aminobenzoate (0.4 mmol). The crude product was purified by preparative TLC using hexanes / EtOAc (25:1) as an eluent to afford 45 mg (96%) of the title compound **4.3q**.

¹H NMR (400 MHz, CD₂Cl₂): δ 7.15 – 7.03 (m, 3H), 6.70 – 6.67 (m, 1H), 3.69 (br s, 1H), 3.26 – 3.21 (m, 1H), 2.44 (s, 3H), 1.98 – 1.92 (m, 2H), 1.70 – 1.65 (m, 2H), 1.60 – 1.54 (m, 1H), 1.37 – 1.26 (m, 2H), 1.21 – 1.03 (m, 3H).

¹³C NMR (101 MHz, CD₂Cl₂): δ 198.7, 148.1, 138.7, 129.6, 117.9, 117.2, 112.0, 51.9, 33.7, 26.9, 26.3, 25.3.

Physical State: yellow solid.

HRMS (ESI): calcd for $C_{14}H_{20}NO_2$ [M+H]$^+$ 234.1489; found 234.1491.

1-(3-(cyclohexylamino)phenyl)ethan-1-one (4.3r)
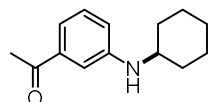
Following the General Procedure B with the corresponding NHPI ester (0.2 mmol) and 4-aminoacetophenone (0.4 mmol). The crude product was purified by preparative TLC using hexanes / EtOAc (15:1) as an eluent to afford 39 mg (90%) of the title compound **4.3r**.

¹H NMR (400 MHz, CDCl₃): δ 7.25 – 7.18 (m, 2H), 7.16 – 7.15 (m, 1H), 6.79 – 6.73 (m, 1H), 3.69 (br s, 1H), 3.31 (tt, J = 10.1, 3.8 Hz, 1H), 2.56 (s, 3H), 2.08 – 2.02 (m, 2H), 1.69 – 1.63 (m, 2H), 1.69 – 1.63 (m, 1H), 1.45 – 1.33 (m, 2H), 1.29 – 1.10 (m, 3H).

¹³C NMR (101 MHz, CDCl₃): δ 198.9, 147.7, 138.3, 129.4, 117.9, 117.4, 112.0, 51.7, 33.5, 26.9, 26.0, 25.1.

Physical State: yellow oil.

HRMS (ESI): calcd for $C_{14}H_{20}NO$ [M+H]$^+$ 218.1545; found 218.1547.

N -cyclohexyl-3-(trifluoromethyl)aniline (4.3s)

Following the General Procedure B with the corresponding NHPI ester (0.2 mmol) and 3-(trifluoromethyl)aniline (0.4 mmol). The crude product was purified by preparative TLC using hexanes / EtOAc (20:1) as an eluent to afford 41 mg (84%) of the title compound **4.3s**.

¹H NMR (400 MHz, CDCl₃): δ 7.22 (t, J = 7.7 Hz, 1H), 6.90 – 6.84 (m, 1H), 6.76 (s, 1H), 6.70 (dd, J = 8.2, 2.4 Hz, 1H), 3.74 (br s, 1H), 3.28 (tt, J = 10.1, 3.8 Hz, 1H), 2.09 – 2.00 (m, 2H), 1.81 – 1.74 (m, 2H), 1.72 – 1.63 (m, 1H), 1.46 – 1.33 (m, 2H), 1.28 – 1.13 (m, 3H).

¹³C NMR (101 MHz, CDCl₃): δ 147.6, 131.7 (q, J = 31.6 Hz), 129.8, 124.5 (q, J = 272.3 Hz), 116.1, 113.2 (q, J = 4.0 Hz), 109.2 (q, J = 3.9 Hz), 51.7, 33.4, 26.0, 25.0.

Spectral data match those previously reported.[226]

N-cyclohexylnaphthalen-1-amine (4.3t)
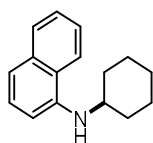
Following the General Procedure B with the corresponding NHPI ester (0.2 mmol) and naphthalen-1-amine (0.4 mmol). The crude product was purified by preparative TLC using hexanes / EtOAc (20:1) as an eluent to afford 25 mg (56%) of the title compound **4.3t**.

¹H NMR (400 MHz, CDCl₃): δ 7.83 – 7.74 (m, 2H), 7.47 – 7.39 (m, 2H), 7.34 (t, J = 7.9 Hz, 1H), 7.20 (d, J = 8.2 Hz, 1H), 6.65 (d, J = 7.6 Hz, 1H), 4.27 (br s, 1H), 3.48 (tt, J = 9.9, 3.7 Hz, 1H), 2.25 – 2.13 (m, 2H), 1.88 – 1.69 (m, 3H), 1.51 – 1.26 (m, 5H).

¹³C NMR (101 MHz, CDCl₃): δ 142.5, 134.7, 128.8, 126.8, 125.7, 124.6, 123.5, 119.9, 116.7, 104.8, 51.9, 33.4, 26.2, 25.2.

Spectral data match those previously reported.[220]

N-cyclohexylpyridin-2-amine (4.4a)

Following the General Procedure B with the corresponding NHPI ester (0.3 mmol) and 2-aminopyridine (3 equiv, 0.9 mmol). The crude product was purified by preparative TLC using hexanes / EtOAc (15:1) as an eluent to afford 26 mg (48%) of the title compound **4.4a**.

^{1}H NMR (400 MHz, CDCl$_3$): δ 8.05 (dd, J = 5.0, 1.1 Hz, 1H), 7.42 – 7.31 (m, 1H), 6.54 – 6.46 (m, 1H), 6.34 (dd, J = 8.4, 1.0 Hz, 1H), 4.44 (br s, 1H), 3.62 – 3.42 (m, 1H), 2.11 – 1.95 (m, 2H), 1.82 – 1.68 (m, 2H), 1.69 – 1.58 (m, 1H), 1.45 – 1.32 (m, 2H), 1.28 – 1.13 (m, 3H).

^{13}C NMR (101 MHz, CDCl$_3$): δ 158.25, 148.42, 137.41, 112.47, 106.80, 50.25, 33.50, 25.93, 25.02.

Spectral data match those previously reported.[227]

N-cyclohexylquinolin-8-amine (4.4b)
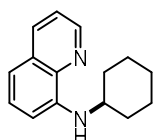
Following the General Procedure B with the corresponding NHPI ester (0.2 mmol) and quinolin-8-amine (0.4 mmol). The crude product was purified by preparative TLC using hexanes / EtOAc (20:1) as an eluent to afford 35 mg (78%) of the title compound **4.4b**.

^{1}H NMR (400 MHz, CDCl$_3$): δ 8.70 (dd, J = 4.2, 1.7 Hz, 1H), 8.04 (dd, J = 8.2, 1.7 Hz, 1H), 7.44 – 7.29 (m, 2H), 7.00 (dd, J = 8.2, 1.2 Hz, 1H), 6.77 – 6.59 (m, 1H), 6.15 (br s, 1H), 3.55 – 3.39 (m, 1H), 2.24 – 2.12 (m, 2H), 1.91 – 1.79 (m, 2H), 1.72 – 1.64 (m, 1H), 1.57 – 1.07 (m, 6H).

^{13}C NMR (101 MHz, CDCl$_3$): δ 146.5, 143.8, 136.4, 129.1, 128.0, 121.4, 113.2, 105.1, 51.5, 33.1, 26.2, 25.3.

Spectral data match those previously reported.[220]
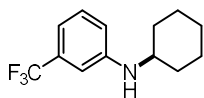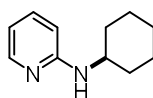
N-cyclohexylquinolin-6-amine (4.4c)
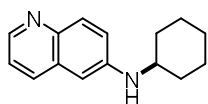
Following the General Procedure B with the corresponding NHPI ester (0.2 mmol) and quinolin-6-amine (0.4 mmol). The crude product was purified by preparative TLC using hexanes / EtOAc (20:1) as an eluent to afford 19 mg (43%) of the title compound **4.4c**.

¹H NMR (400 MHz, CDCl₃): δ 8.58 (dd, J = 4.3, 1.6 Hz, 1H), 7.93 – 7.72 (m, 2H), 7.28 – 7.24 (m, 1H), 7.07 (dd, J = 9.1, 2.6 Hz, 1H), 6.68 (d, J = 2.6 Hz, 1H), 3.96 (br s, 1H), 3.38 (tt, J = 10.1, 3.8 Hz, 1H), 2.17 – 2.10 (m, 2H), 1.80 (dt, J = 13.3, 3.9 Hz, 2H), 1.69 (dt, J = 12.8, 3.7 Hz, 1H), 1.48 – 1.17 (m, 5H).

¹³C NMR (101 MHz, CDCl₃): δ 145.6, 145.0, 142.0, 134.5, 134.4, 132.9, 130.5, 129.6, 123.7, 122.3, 121.4, 103.0, 51.9, 33.2, 26.0, 25.1.

Spectral data match those previously reported.[210]

N-cyclohexylbenzenesulfonamide (4.4d)
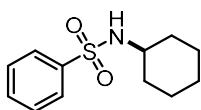
An oven-dried 15 mL vial equipped with a Teflon-coated magnetic stir bar was sequentially charged with corresponding NHPI ester (0.3 mmol), Ru(bpy)₃(PF₆)₂ (1 mol%), Cu(MeCN)₄PF₆ (50 mol%), **4.L26** (30 mol%), MeCN (0.1 M), benzenesulfonamide (0.9 mmol), Et₃N (5 equiv) in the glove box. The vial was sealed with a screw cap and removed from the glove box**.** Then the vial was placed 3 cm away from one blue LED, and irradiated under fan cooling (maintain the temperature at room temperature) for 20 h. After the reaction, the resulting dark brown reaction mixture was acidified with saturated NH₄Cl solution (~1 mL) and then neutralized with saturated NaHCO₃ solution (~1.5 mL). The crude product in the aqueous fraction was extracted with EtOAc (~10 mL). The aqueous fraction was further washed with EtOAc (3 x ~5 mL). The combined organic fractions were concentrated *in vacuo* with the aid of a rotary evaporator. The crude product residue was purified by preparative TLC (pretreated with 3% triethylamine in hexanes in order to minimize the product loss) using hexanes / EtOAc (20:1) as an eluent to afford 26 mg (36%) of the title compound **4.4d**.

¹H NMR (400 MHz, CDCl₃): δ 7.97 – 7.82 (m, 2H), 7.61 – 7.47 (m, 3H), 4.59 (d, J = 7.7 Hz, 1H), 3.20 – 3.11 (m, 1H), 1.78 – 1.70 (m, 2H), 1.66 – 1.61 (m, 2H), 1.53 – 1.47 (m, 1H), 1.27 – 1.09 (m, 5H).

¹³C NMR (101 MHz, CDCl₃): δ 141.6, 132.6, 129.2, 127.0, 52.8, 34.1, 25.3, 24.8.

Spectral data match those previously reported.[228]

N-cyclohexylbenzamide (4.4e)

An oven-dried 15 mL vial equipped with a Teflon-coated magnetic stir bar was sequentially charged with corresponding NHPI ester (0.5 mmol), Ru(bpy)$_3$(PF$_6$)$_2$ (1 mol%), Cu(MeCN)$_4$PF$_6$ (50 mol%), **4.L26** (30 mol%), MeCN (0.1 M), benzamide (1.5 mmol), Et$_3$N (5 equiv) in the glove box. The vial was sealed with a screw cap and removed from the glove box. Then the vial was placed 3 cm away from one blue LED, and irradiated under fan cooling (maintain the temperature at room temperature) for 20 h. After the reaction, the resulting dark brown reaction mixture was acidified with saturated NH$_4$Cl solution (~1 mL) and then neutralized with saturated NaHCO$_3$ solution (~1.5 mL). The crude product in the aqueous fraction was extracted with EtOAc (~10 mL). The aqueous fraction was further washed with EtOAc (3 x ~5 mL). The combined organic fractions were concentrated *in vacuo* with the aid of a rotary evaporator. The crude product residue was purified by preparative TLC (pretreated with 3% triethylamine in hexanes in order to minimize the product loss) using hexanes / EtOAc (10:1) as an eluent to afford 42 mg (41%) of the title compound **4.4e**.

^{1}H NMR (400 MHz, CDCl$_3$): δ 7.80 – 7.68 (m, 2H), 7.49 – 7.42 (m, 1H), 7.42 – 7.34 (m, 2H), 6.16 (br s, 1H), 4.04 – 3.86 (m, 1H), 2.03 – 1.95 (m, 2H), 1.80 – 1.57 (m, 3H), 1.47 – 1.09 (m, 5H).
^{13}C NMR (101 MHz, CDCl$_3$): δ 166.7, 135.2, 131.3, 128.5, 126.9, 48.8, 33.3, 25.6, 25.0.
Spectral data match those previously reported.[229]

N-cyclohexyl-4-fluorobenzamide (4.4f)

An oven-dried 15 mL vial equipped with a Teflon-coated magnetic stir bar was sequentially charged with corresponding NHPI ester (0.5 mmol), Ru(bpy)$_3$(PF$_6$)$_2$ (1 mol%), Cu(MeCN)$_4$PF$_6$ (50 mol%), **4.L26** (30 mol%), MeCN (0.1 M), 4-fluorobenzamide (1.5 mmol), Et$_3$N (5 equiv) in the glove box. The vial was sealed with a screw cap and removed from the glove box. Then the vial was placed 3 cm away from one blue LED, and irradiated under fan cooling (maintain the

temperature at room temperature) for 20 h. After the reaction, the resulting dark brown reaction mixture was acidified with saturated NH_4Cl solution (~1 mL) and then neutralized with saturated $NaHCO_3$ solution (~1.5 mL). The crude product in the aqueous fraction was extracted with EtOAc (~10 mL). The aqueous fraction was further washed with EtOAc (3 x ~5 mL). The combined organic fractions were concentrated *in vacuo* with the aid of a rotary evaporator. The crude product residue was purified by preparative TLC (pretreated with 3% triethylamine in hexanes in order to minimize the product loss) using hexanes / EtOAc (10:1) as an eluent to afford 33 mg (30%) of the title compound **4.4f**.

¹H NMR (400 MHz, CDCl₃): δ 7.84 – 7.66 (m, 2H), 7.18 – 7.02 (m, 2H), 5.93 (s, 1H), 4.05 – 3.84 (m, 1H), 2.13 – 1.93 (m, 2H), 1.80 – 1.60 (m, 3H), 1.51 – 1.35 (m, 2H), 1.31 – 1.11 (m, 3H).

¹³C NMR (101 MHz, CDCl₃): δ 165.95, 165.68, 163.46, 131.39 (d, J = 3.3 Hz), 129.25 (d, J = 8.9 Hz), 115.63 (d, J = 21.9 Hz), 48.94, 33.38, 25.70, 25.05.

Spectral data match those previously reported.[230]

N-cyclohexyl-2-methylbenzamide (4.4g)

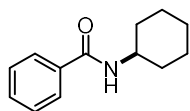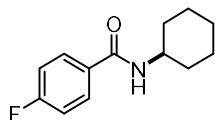An oven-dried 15 mL vial equipped with a Teflon-coated magnetic stir bar was sequentially charged with corresponding NHPI ester (0.5 mmol), Ru(bpy)₃(PF₆)₂ (1 mol%), Cu(MeCN)₄PF₆ (50 mol%), **4.L26** (30 mol%), MeCN (0.1 M), 2-methylbenzamide (1.5 mmol), Et₃N (5 equiv) in the glove box. The vial was sealed with a screw cap and removed from the glove box**.** Then the vial was placed 3 cm away from one blue LED, and irradiated under fan cooling (maintain the temperature at room temperature) for 20 h. After the reaction, the resulting dark brown reaction mixture was acidified with saturated NH_4Cl solution (~1 mL) and then neutralized with saturated $NaHCO_3$ solution (~1.5 mL). The crude product in the aqueous fraction was extracted with EtOAc (~10 mL). The aqueous fraction was further washed with EtOAc (3 x ~5 mL). The combined organic fractions were concentrated *in vacuo* with the aid of a rotary evaporator. The crude product residue was purified by preparative TLC (pretreated with 3% triethylamine in hexanes in order to minimize the product loss) using hexanes / EtOAc (10:1) as an eluent to afford 36 mg (33%) of the title compound **4.4g**.

¹H NMR (400 MHz, CDCl₃): δ 7.36 – 7.27 (m, 2H), 7.23 – 7.16 (m, 2H), 5.60 (s, 1H), 4.05 – 3.90 (m, 1H), 2.44 (s, 3H), 2.10 – 1.97 (m, 2H), 1.81 – 1.60 (m, 3H), 1.51 – 1.37 (m, 2H), 1.29 – 1.13 (m, 3H).

¹³C NMR (101 MHz, CDCl₃): δ 169.4, 137.2, 135.9, 131.0, 129.8, 126.7, 125.8, 48.6, 33.4, 25.7, 25.0, 19.8.

Spectral data match those previously reported.[231]

1-cyclohexyl-3-phenylurea (4.4h)
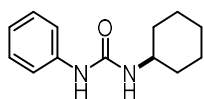
An oven-dried 15 mL vial equipped with a Teflon-coated magnetic stir bar was sequentially charged with corresponding NHPI ester (0.5 mmol), Ru(bpy)₃(PF₆)₂ (1 mol%), Cu(MeCN)₄PF₆ (50 mol%), **4.L26** (30 mol%), MeCN (0.1 M), *N*-phenylurea (1.5 mmol), Et₃N (5 equiv) in the glove box. The vial was sealed with a screw cap and removed from the glove box. Then the vial was placed 3 cm away from one blue LED, and irradia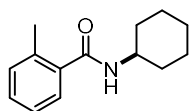ted under fan cooling (maintain the temperature at room temperature) for 20 h. After the reaction, the resulting dark brown reaction mixture was acidified with saturated NH₄Cl solution (~1 mL) and then neutralized with saturated NaHCO₃ solution (~1.5 mL). The crude product in the aqueous fraction was extracted with EtOAc (~10 mL). The aqueous fraction was further washed with EtOAc (3 x ~5 mL). The combined organic fractions were concentrated *in vacuo* with the aid of a rotary evaporator. The crude product residue was purified by preparative TLC (pretreated with 3% triethylamine in hexanes in order to minimize the product loss) using hexanes / EtOAc (10:1) as an eluent to afford 31 mg (28%) of the title compound **4.4h.**

¹H NMR (400 MHz, CDCl₃): δ 7.27 (d, *J* = 5.4 Hz, 4H), 7.15 – 6.94 (m, 1H), 6.81 (s, 1H), 4.99 (s, 1H), 3.65 (tt, *J* = 10.5, 3.9 Hz, 1H), 2.02 – 1.86 (m, 2H), 1.73 – 1.54 (m, 3H), 1.43 – 1.25 (m, 2H), 1.25 – 0.93 (m, 3H).

¹³C NMR (101 MHz, CDCl₃): δ 155.5, 138.9, 129.4, 123.7, 121.0, 49.1, 33.8, 25.7, 25.0.

Spectral data match those previously reported.[232]

N-cyclobutyl-2-methoxyaniline (4.5a)
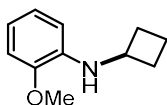
Following the General Procedure B with the corresponding NHPI ester (0.2 mmol) and *o*-anisidine (0.4 mmol). The crude product was purified by preparative TLC using hexanes / EtOAc (25:1) as an eluent to afford 29 mg (81%) of the title compound **4.5a**.

¹H NMR (400 MHz, CD₂Cl₂): δ 6.81 (td, J = 7.6, 1.4 Hz, 1H), 6.75 (dd, J = 8.0, 1.4 Hz, 1H), 6.61 (td, J = 7.7, 1.6 Hz, 1H), 6.49 (dd, J = 7.8, 1.6 Hz, 1H), 4.36 (br s, 1H), 3.95 – 3.88 (m, 1H), 3.83 (s, 3H), 2.49 – 2.37 (m, 2H), 1.90 – 1.75 (m, 4H).

¹³C NMR (101 MHz, CD₂Cl₂): δ 147.1, 137.7, 121.6, 116.6, 110.5, 109.8, 55.7, 49.1, 31.6, 15.7.

Physical State: yellow oil.

HRMS (ESI): calcd for $C_{11}H_{16}NO$ [M+H]⁺ 178.1232; found 178.1236.

N-cyclobutyl-3-(trifluoromethyl)aniline (4.5b)

Following the General Procedure B with the corresponding NHPI ester (0.2 mmol) and 2-(trifluoromethyl)aniline (0.4 mmol). The crude product was purified by preparative TLC using hexanes / EtOAc (25:1) as an eluent to afford 31 mg (71%) of the title compound **4.5b**.

¹H NMR (400 MHz, CDCl₃): δ 7.23 (t, J = 7.9 Hz, 1H), 6.92 (d, J = 7.7 Hz, 1H), 6.73 (s, 1H), 6.67 (dd, J = 8.2, 2.3 Hz, 1H), 4.13 (br s, 1H), 3.97 – 3.88 (m, 1H), 2.49 – 2.40 (m, 2H), 1.89 – 1.78 (m, 4H).

¹³C NMR (101 MHz, CDCl₃): δ 147.4, 131.7 (q, J = 31.6 Hz), 129.7, 124.5 (q, J = 272.2 Hz), 116.0 (d, J = 1.5 Hz), 113.8 (q, J = 4.0 Hz), 109.2 (q, J = 4.0 Hz), 48.9, 31.2, 15.4.

Spectral data match those previously reported. [233]

N-cyclopentyl-2-methoxyaniline (4.5c)
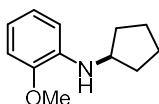
Following the General Procedure B with the corresponding NHPI ester (0.2 mmol) and *o*-anisidine (0.4 mmol). The crude product was purified by preparative TLC using hexanes / EtOAc (25:1) as an eluent to afford 16 mg (41%) of the title compound **4.5c**.

¹H NMR (400 MHz, CDCl₃): δ 6.87 (td, *J* = 7.5, 1.4 Hz, 1H), 6.76 (dd, *J* = 8.3, 1.4 Hz, 1H), 6.68 – 6.62 (m, 2H), 4.21 (s, 1H), 3.84 (s, 3H), 3.82 – 3.74 (m, 1H), 2.11 – 1.97 (m, 2H), 1.83 – 1.67 (m, 2H), 1.68 – 1.59 (m, 2H), 1.56 – 1.48 (m, 2H).

¹³C NMR (101 MHz, CDCl₃): δ 146.9, 138.1, 121.4, 116.1, 110.6, 109.4, 55.5, 54.5, 33.8, 24.3.

Physical State: brown solid.

HRMS (ESI): calcd for C₁₂H₁₈NO [M+H]⁺ 192.1388; found 192.1391.

N-phenylcyclododecanamine (4.5d)
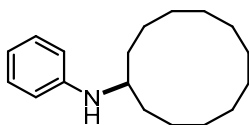
Following the General Procedure B with the corresponding NHPI ester (0.2 mmol) and aniline (0.4 mmol). The crude product was purified by preparative TLC using hexanes / EtOAc (25:1) as an eluent to afford 34 mg (66%) of the title compound **4.5d**.

¹H NMR (400 MHz, CDCl₃): δ 7.17 (t, *J* = 7.8 Hz, 2H), 6.67 (t, *J* = 7.3 Hz, 1H), 6.60 (d, *J* = 7.9 Hz, 2H), 3.57 – 3.48 (m, 1H), 3.42 (br s, 1H), 1.69 – 1.57 (m, 2H), 1.51 – 1.30 (m, 20H).

¹³C NMR (101 MHz, CDCl₃): δ 148.0, 129.4, 116.8, 113.2, 49.6, 29.9, 24.5, 24.1, 23.5, 23.4, 21.4. Spectral data match those previously reported.[234]

N-(2-methoxyphenyl)cyclododecanamine (4.5e)

Following the General Procedure B with the corresponding NHPI ester (0.2 mmol) and *o*-anisidine (0.4 mmol). The crude product was purified by preparative TLC using hexanes / EtOAc (20:1) as an eluent to afford 44 mg (76%) of the title compound **4.5e**.

¹H NMR (400 MHz, CD₂Cl₂): δ 6.82 (td, *J* = 7.6, 1.4 Hz, 1H), 6.75 (dd, *J* = 7.8, 1.4 Hz, 1H), 6.62 – 6.54 (m, 2H), 4.04 (d, *J* = 32.8 Hz, 1H), 3.82 (br s, 3H), 3.53 – 3.48 (m, 1H), 1.69 – 1.59 (m, 2H), 1.52 – 1.33 (m, 20H).

^{13}C NMR (101 MHz, CD$_2$Cl$_2$): δ 147.2, 138.3, 121.6, 115.8, 110.2, 110.0, 55.8, 49.4, 30.1, 24.8, 24.4, 23.8, 23.8, 21.8.

Physical State: pale brown solid.

HRMS (ESI): calcd for C$_{19}$H$_{32}$NO [M+H]$^+$ 290.2484; found 290.2483.

N-(2-methoxyphenyl)tetrahydro-2*H*-pyran-4-amine (4.5f)
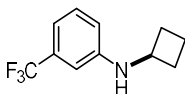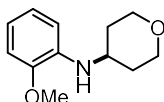

Following the General Procedure B with the corresponding NHPI ester (0.2 mmol) and *o*-anisidine (0.4 mmol). The crude product was purified by preparative TLC using hexanes / EtOAc (15:1) as an eluent to afford 34 mg (82%) of the title compound **4.5f**.

^{1}H NMR (400 MHz, CDCl$_3$): δ 6.86 (td, J = 7.6, 1.4 Hz, 1H), 6.78 (dd, J = 7.9, 1.4 Hz, 1H), 6.69 – 6.63 (m, 2H), 4.18 (br s, 1H), 4.03 – 3.99 (m, 2H), 3.85 (s, 3H), 3.57 – 3.45 (m, 3H), 2.08 – 2.02 (m, 2H), 1.58 – 1.47 (m, 2H).

^{13}C NMR (101 MHz, CDCl$_3$): δ 147.0, 136.7, 121.3, 116.6, 110.5, 109.9, 67.1, 55.5, 48.9, 33.7.

Physical State: reddish brown oil.

HRMS (ESI): calcd for C$_{12}$H$_{18}$NO$_2$ [M+H]$^+$ 208.1338; found 208.1340.

N-(4,4-difluorocyclohexyl)-2-methoxyaniline (4.5g)
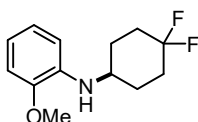
Following the General Procedure B with the corresponding NHPI ester (0.2 mmol) and *o*-anisidine (0.4 mmol). The crude product was purified by preparative TLC using hexanes / EtOAc (15:1) as an eluent to afford 35 mg (73%) of the title compound **4.5g**.

^{1}H NMR (400 MHz, CDCl$_3$): δ 6.87 (td, J = 7.6, 1.5 Hz, 1H), 6.79 (dd, J = 8.0, 1.4 Hz, 1H), 6.68 (td, J = 7.7, 1.5 Hz, 1H), 6.62 (dd, J = 7.8, 1.6 Hz, 1H), 4.16 (br s, 1H), 3.85 (s, 3H), 3.46 – 3.41 (m, 1H), 2.16 – 1.63 (m, 8H).

^{13}C NMR (101 MHz, CDCl$_3$): δ 147.0, 136.9, 121.4, 123.1, 116.7, 110.4, 109.8, 77.4, 55.6, 49.3, 32.2 (t, J = 24.2 Hz), 29.1 – 28.1 (m).

Physical State: brown oil.

HRMS (ESI): calcd for $C_{13}H_{18}F_2NO$ $[M+H]^+$ 242.1357; found 242.1362.

N-isopropylaniline (4.5h)
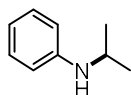
Following the General Procedure B with the corresponding NHPI ester (0.4 mmol) and aniline (0.8 mmol). The crude product was purified by preparative TLC using hexanes / EtOAc (30:1) as an eluent to afford 20 mg (37%) of the title compound **4.5h**.

^{1}H NMR (400 MHz, CD_2Cl_2): δ 7.12 (dd, J = 8.6, 7.2 Hz, 2H), 6.68 – 6.47 (m, 3H), 3.64 – 3.58 (m, 1H), 3.50 (br s, 1H), 1.20 (s, 3H), 1.18 (s, 3H).

^{13}C NMR (101 MHz, $CDCl_3$): δ 147.6, 129.4, 117.1, 113.4, 44.4, 23.1.

Spectral data match those previously reported.[235]

N-(heptan-3-yl)-2-methoxyaniline (4.5i)

Following the General Procedure B with the corresponding NHPI ester (0.2 mmol) and o-anisidine (0.4 mmol). The crude product was purified by preparative TLC using hexanes / EtOAc (25:1) as an eluent to afford 27 mg (60%) of the title compound **4.5i**.

^{1}H NMR (400 MHz, $CDCl_3$): δ 6.84 (td, J = 7.6, 1.2 Hz, 1H), 6.76 (dd, J = 7.6, 1.2 Hz, 1H), 6.60 (ddd, J = 7.6, 6.8, 1.2 Hz, 1H), 6.58 (dd, J = 6.8, 1.2 Hz, 1H), 4.06 (br s, 1H), 3.84 (s, 3H), 3.30 – 3.24 (m, 1H), 1.71 – 0.87 (m, 14H).

^{13}C NMR (101 MHz, $CDCl_3$): δ 146.8, 138.3, 121.4, 115.4, 110.0, 109.7, 55.6, 53.9, 34.3, 28.4, 27.4, 23.0, 14.2, 10.2.

Spectral data match those previously reported.[236]

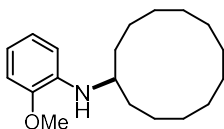**2-methoxy-N-(pentan-2-yl)aniline (4.5j)**

Following the General Procedure B with the corresponding NHPI ester (0.2 mmol) and *o*-anisidine (0.4 mmol). The crude product was purified by preparative TLC using hexanes / EtOAc (25:1) as an eluent to afford 22 mg (56%) of the title compound **4.5j**.

¹H NMR (400 MHz, CDCl₃): δ 6.87 (td, *J* = 7.6, 1.4 Hz, 1H), 6.77 (dd, *J* = 7.8, 1.4 Hz, 1H), 6.67 – 6.58 (m, 2H), 4.04 (br s, 1H), 3.85 (s, 3H), 3.48 (h, *J* = 6.3 Hz, 1H), 1.68 – 1.54 (m, 1H), 1.51 – 1.37 (m, 3H), 1.20 (d, *J* = 6.3 Hz, 3H), 0.95 (t, *J* = 7.1 Hz, 3H).

¹³C NMR (101 MHz, CDCl₃): δ 146.8, 137.8, 121.4, 115.7, 110.1, 109.6, 55.5, 48.0, 39.6, 20.9, 19.5, 14.3.

Spectral data match those previously reported.[236]

N-hexylaniline (4.6a)

Following the General Procedure C with the corresponding NHPI ester (0.4 mmol) and aniline (0.2 mmol). The crude product was purified by preparative TLC using hexanes / EtOAc (30:1) as an eluent to afford 23 mg (64%) of the title compound **4.6a**.

¹H NMR (400 MHz, CD₂Cl₂): δ 7.13 (dd, *J* = 8.6, 7.3 Hz, 2H), 6.63 (t, *J* = 7.3 Hz, 1H), 6.60 – 6.54 (m, 2H), 3.66 (br s, 1H), 3.08 (t, *J* = 7.1 Hz, 2H), 1.64 – 1.57 (m, 2H), 1.43 – 1.29 (m, 6H), 0.93 – 0.85 (m, 3H).

¹³C NMR (101 MHz, CDCl₃): δ 172.86, 162.27, 134.81, 129.18, 124.03, 38.34, 26.78, 23.90, 23.81, 23.61, 23.52, 22.21.

Spectral data match those previously reported.[120]

N-hexyl-2-methoxyaniline (4.6b)

Following the General Procedure C with the corresponding NHPI ester (0.4 mmol) and *o*-anisidine (0.2 mmol). The crude product was purified by preparative TLC using hexanes / EtOAc (25:1) as an eluent to afford 29 mg (70%) of the title compound **4.6b**.

¹H NMR (400 MHz, CDCl₃): δ 6.88 (td, J = 7.6, 1.4 Hz, 1H), 6.77 (dd, J = 7.9, 1.4 Hz, 1H), 6.66 (td, J = 7.7, 1.6 Hz, 1H), 6.62 (dd, J = 7.8, 1.5 Hz, 1H), 4.17 (s, 1H), 3.85 (s, 3H), 3.13 (t, J = 7.1 Hz, 2H), 1.67 (p, J = 7.2 Hz, 2H), 1.43 – 1.32 (m, 5H), 0.95 – 0.88 (m, 3H).

¹³C NMR (101 MHz, CDCl₃): δ 146.9, 138.7, 121.4, 116.2, 109.9, 109.5, 55.5, 43.9, 31.8, 29.7, 27.1, 22.8, 14.2.

Spectral data match those previously reported.[237]

N-hexyl-3-(trifluoromethyl)aniline (4.6c)

Following the General Procedure C with the corresponding NHPI ester (0.4 mmol) and 3-(trifluoromethyl)aniline (0.2 mmol). The crude product was purified by preparative TLC using hexanes / EtOAc (20:1) as an eluent to afford 27 mg (55%) of the title compound **4.6c**.

¹H NMR (400 MHz, CDCl₃): δ 7.23 (t, J = 7.9 Hz, 1H), 6.90 (d, J = 7.6 Hz, 1H), 6.78 (s, 1H), 6.72 (dd, J = 8.3, 2.3 Hz, 1H), 3.82 (s, 1H), 3.12 (t, J = 7.1 Hz, 2H), 1.68 – 1.60 (m, 2H), 1.43 – 1.29 (m, 6H), 0.95 – 0.87 (m, 3H).

¹³C NMR (101 MHz, CDCl₃): δ 148.7, 131.8, 131.5, 129.7, 125.9, 123.2, 115.8, 113.6, 108.8, 44.0, 31.7, 29.5, 26.9, 22.8, 14.2.

Spectral data match those previously reported.[238]
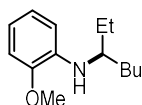
4-fluoro-*N*-hexylaniline (4.6d)

Following the General Procedure C with the corresponding NHPI ester (0.4 mmol) and 4-fluoroaniline (0.2 mmol). The crude product was purified by preparative TLC using hexanes / EtOAc (25:1) as an eluent to afford 24 mg (62%) of the title compound **4.6d**.

¹H NMR (400 MHz, CDCl₃): δ 6.93 – 6.85 (m, 2H), 6.60 – 6.53 (m, 2H), 3.06 (t, J = 7.2 Hz, 2H), 1.61 (p, J = 7.1 Hz, 2H), 1.43 – 1.28 (m, 6H), 0.92 – 0.87 (m, 3H).

¹³C NMR (101 MHz, CDCl₃): δ 156.4 (d, J = 237.4 Hz), 144.0, 115.9 (d, J = 22.2 Hz), 114.6 (d, J = 8.1 Hz), 45.6, 31.8, 29.4, 26.9, 22.8, 14.2.

Spectral data match those previously reported.[237]
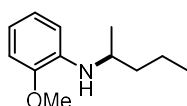
N-butyl-2-methoxyaniline (4.6e)

Following the General Procedure C with the corresponding NHPI ester (0.4 mmol) and *o*-anisidine (0.2 mmol). The crude product was purified by preparative TLC using hexanes / EtOAc (25:1) as an eluent to afford 22 mg (62%) of the title compound **4.6e**.

^{1}H NMR (400 MHz, CD$_2$Cl$_2$): δ 6.82 (td, *J* = 7.6, 1.4 Hz, 1H), 6.76 (dd, *J* = 7.9, 1.4 Hz, 1H), 6.60 (td, *J* = 7.7, 1.6 Hz, 1H), 6.56 (dd, *J* = 8.0, 1.6 Hz, 1H), 4.31 (br s, 1H), 3.83 (s, 3H), 2.94 (d, *J* = 6.8 Hz, 2H), 1.97 – 1.85 (m, 1H), 0.99 (d, *J* = 6.7 Hz, 6H).

^{13}C NMR (101 MHz, CDCl$_3$): δ 146.8, 138.7, 121.4, 116.1, 109.9, 109.5, 55.6, 51.8, 28.1, 20.7. Spectral data match those previously reported.[239]
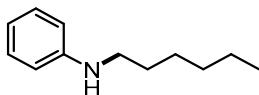
2-methoxy-*N*-pentylaniline (4.6f)
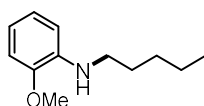
Following the General Procedure C with the corresponding NHPI ester (0.4 mmol) and *o*-anisidine (0.2 mmol). The crude product was purified by preparative TLC using hexanes / EtOAc (25:1) as an eluent to afford 22 mg (58%) of the title compound **4.6f**.

^{1}H NMR (400 MHz, CD$_2$Cl$_2$): δ 6.82 (td, *J* = 7.6, 1.4 Hz, 1H), 6.75 (dd, *J* = 7.9, 1.4 Hz, 1H), 6.63 – 6.54 (m, 2H), 4.17 (br s, 1H), 3.82 (s, 3H), 3.10 (t, *J* = 7.1 Hz, 2H), 1.68 – 1.61 (m, 2H), 1.41 – 1.33 (m, 4H), 0.96 – 0.90 (m, 3H).

^{13}C NMR (101 MHz, CDCl$_3$): δ 146.9, 138.6, 121.4, 116.2, 110.0, 109.6, 55.6, 51.8, 28.1, 20.7. Spectral data match those previously reported.[240]
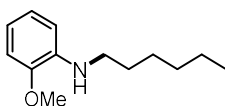
N-heptadecyl-2-methoxyaniline (4.6g)

Following the General Procedure C with the corresponding NHPI ester (0.4 mmol) and *o*-anisidine (0.2 mmol). The crude product was purified by preparative TLC using hexanes / EtOAc (20:1) as an eluent to afford 64 mg (88%) of the title compound **4.6g**.

¹H NMR (400 MHz, CDCl₃): δ 6.88 (t, *J* = 7.3 Hz, 1H), 6.78 (d, *J* = 7.6 Hz, 1H), 6.71 – 6.61 (m, 2H), 3.85 (s, 3H), 3.12 (t, *J* = 7.2 Hz, 2H), 1.70 – 1.63 (m, 3H), 1.46 – 1.27 (m, 27H), 0.89 (t, *J* = 6.6 Hz, 3H).

¹³C NMR (101 MHz, CDCl₃): δ 147.0, 138.3, 121.4, 116.6, 109.6, 110.4, 55.6, 44.1, 32.1, 29.9, 29.8, 29.8, 29.8, 29.6, 29.6, 29.5, 27.4, 22.9, 14.3.

Physical State: reddish brown solid.

HRMS (ESI): calcd for $C_{24}H_{44}NO$ $[M+H]^+$ 362.3423; found 362.3423.

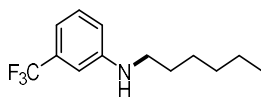### 2-methoxy-*N*-(4-phenylbutyl)aniline (4.6h)
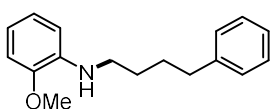
Following the General Procedure C with the corresponding NHPI ester (0.4 mmol) and *o*-anisidine (0.2 mmol). The crude product was purified by preparative TLC using hexanes / EtOAc (20:1) as an eluent to afford 38 mg (75%) of the title compound **4.6h**.

¹H NMR (400 MHz, CD₂Cl₂): δ 7.34 – 7.16 (m, 5H), 6.83 (td, *J* = 7.6, 1.5 Hz, 1H), 6.76 (dd, *J* = 7.9, 1.4 Hz, 1H), 6.61 (td, *J* = 7.6, 1.5 Hz, 1H), 6.57 (dd, *J* = 7.8, 1.5 Hz, 1H), 4.19 (br s, 1H), 3.82 (s, 3H), 3.14 (t, *J* = 6.8 Hz, 2H), 2.68 (t, *J* = 7.4 Hz, 2H), 1.79 – 1.64 (m, 4H).

¹³C NMR (101 MHz, CD₂Cl₂): δ 147.2, 143.0, 139.0, 128.8, 128.7, 126.1, 121.6, 116.3, 109.9, 109.8, 55.8, 43.9, 36.1, 29.6, 29.5.

Physical State: colorless oil.

HRMS (ESI): calcd for $C_{17}H_{22}NO$ $[M+H]^+$ 256.1701; found 256.1708.

N-(5-bromopentyl)-2-methoxyaniline (4.6i)
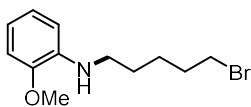
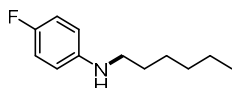

Following the General Procedure C with the corresponding NHPI ester (0.4 mmol) and *o*-anisidine (0.2 mmol). The crude product was purified by preparative TLC using hexanes / EtOAc (20:1) as an eluent to afford 22 mg (40%) of the title compound **4.6i**.

¹H NMR (400 MHz, CDCl₃): δ 7.01 – 6.88 (m, 3H), 6.85 (dd, *J* = 7.8, 1.6 Hz, 1H), 3.87 (s, 3H), 2.98 (t, *J* = 5.3 Hz, 4H), 1.76 (p, *J* = 5.6 Hz, 4H), 1.60 – 1.55 (m, 2H).

¹³C NMR (101 MHz, CDCl₃): δ 152.5, 142.9, 122.6, 121.0, 118.5, 111.2, 55.5, 52.5, 26.5, 24.6.

Physical State: colorless oil.

HRMS (ESI): calcd for C₁₂H₁₉BrNO [M+H]⁺ 272.0650; found 272.0648.

Methyl 5-((2-methoxyphenyl)amino)pentanoate (4.6j)
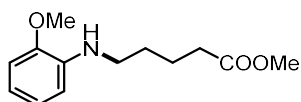
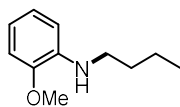

Following the General Procedure C with the corresponding NHPI ester (0.4 mmol) and *o*-anisidine (0.2 mmol). The crude product was purified by preparative TLC using hexanes / EtOAc (20:1) as an eluent to afford 19 mg (41%) of the title compound **4.6j**.

¹H NMR (400 MHz, CDCl₃): δ 6.87 (td, *J* = 7.6, 1.4 Hz, 1H), 6.77 (dd, *J* = 7.9, 1.4 Hz, 1H), 6.66 (td, *J* = 7.7, 1.5 Hz, 1H), 6.60 (dd, *J* = 7.9, 1.5 Hz, 1H), 4.18 (br s, 1H), 3.84 (s, 3H), 3.68 (s, 3H), 3.15 (t, *J* = 6.8 Hz, 2H), 2.38 (t, *J* = 7.2 Hz, 2H), 1.84 – 1.63 (m, 4H).

¹³C NMR (101 MHz, CDCl₃): δ 174.0, 146.9, 138.4, 121.4, 116.4, 109.9, 109.5, 55.5, 51.7, 43.4, 33.9, 29.1, 22.7.

Physical State: brown oil.

**HRMS (**ESI): calcd for C₁₃H₂₀NO₃ [M+H]⁺ 238.1443; found 238.1446.

N-(hex-5-yn-1-yl)-2-methoxyaniline (4.6k)
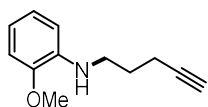
Following the General Procedure C with the corresponding NHPI ester (0.4 mmol) and *o*-anisidine (0.2 mmol). The crude product was purified by preparative TLC using hexanes / EtOAc (20:1) as an eluent to afford 12 mg (31%) of the title compound **4.6k**.

¹H NMR (400 MHz, CDCl₃): δ 6.87 (td, *J* = 7.6, 1.4 Hz, 1H), 6.77 (dd, *J* = 7.9, 1.4 Hz, 1H), 6.71 – 6.62 (m, 2H), 3.84 (s, 3H), 3.28 (t, *J* = 6.9 Hz, 2H), 2.33 (td, *J* = 7.0, 2.7 Hz, 2H), 1.99 (t, *J* = 2.7 Hz, 1H), 1.88 (p, *J* = 6.9 Hz, 2H).

¹³C NMR (101 MHz, CDCl₃): δ 147.0, 138.1, 121.4, 116.7, 110.1, 109.6, 83.9, 69.0, 55.6, 42.7, 28.2, 16.4.

Physical State: brown oil.

HRMS (ESI): calcd for C$_{12}$H$_{16}$NO [M+H]$^+$ 190.1232; found 190.1230.
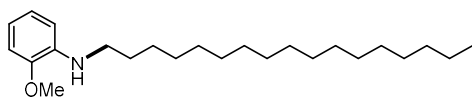
N-(3,3,4,4,5,5,6,6,7,7,8,8,9,9,10,10,10-heptadecafluorodecyl)-2-methoxyaniline (4.6l)
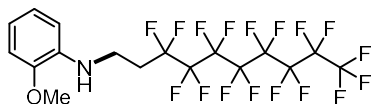
Following the General Procedure C with the corresponding NHPI ester (0.4 mmol) and *o*-anisidine (0.2 mmol). The crude product was purified by preparative TLC using hexanes / EtOAc (15:1) as an eluent to afford 57 mg (50%) of the title compound **4.6l**.

^{1}H NMR (400 MHz, CD$_2$Cl$_2$): δ 6.87 (td, *J* = 7.6, 1.4 Hz, 1H), 6.80 (dd, *J* = 8.0, 1.4 Hz, 1H), 6.69 (td, *J* = 7.7, 1.5 Hz, 1H), 6.61 (dd, *J* = 7.8, 1.5 Hz, 1H), 4.39 (br s, 1H), 3.84 (s, 3H), 3.57 – 3.52 (m, 2H), 2.51 – 2.37 (m, 2H).

^{13}C NMR (101 MHz, CD$_2$Cl$_2$): δ 147.5, 137.5, 121.7, 117.5, 110.2, 109.8, 55.9, 54.4, 54.1, 53.8, 53.6, 53.3, 35.9, 31.4, 31.2, 30.9.

^{19}F NMR (376 MHz, CD$_2$Cl$_2$): δ -81.17 (t, *J* = 10.4 Hz), -114.17 (t, *J* = 14.1 Hz), -121.90, -122.12, -122.93, -123.74, -126.3 – -126.43 (m).

Physical State: light pink solid

HRMS (ESI): calcd for C$_{17}$H$_{13}$F$_{17}$NO [M+H]$^+$ 570.0726; found 570.0729.

N-(cyclopentylmethyl)-2-methoxyaniline (4.6m)
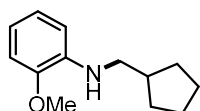
Following the General Procedure C with the corresponding NHPI ester (0.4 mmol) and *o*-anisidine (0.2 mmol). The crude product was purified by preparative TLC using hexanes / EtOAc (20:1) as an eluent to afford 24 mg (59%) of the title compound **4.6m**.

^{1}H NMR (400 MHz, CDCl$_3$): δ 6.88 (td, *J* = 7.6, 1.4 Hz, 1H), 6.77 (dd, *J* = 8.0, 1.4 Hz, 1H), 6.68 – 6.62 (m, 2H), 4.34 (br s, 1H), 3.86 (s, 3H), 3.05 (d, *J* = 7.2 Hz, 2H), 2.26 – 2.16 (m, 1H), 1.89 – 1.81 (m, 2H), 1.68 – 1.53 (m, 4H), 1.34 – 1.25 (m, 2H).

^{13}C NMR (101 MHz, CDCl$_3$): δ 146.9, 138.7, 121.4, 116.3, 110.0, 109.5, 55.6, 49.4, 39.6, 30.9, 25.4.

Physical State: pale yellow oil.

HRMS (ESI): calcd for C$_{13}$H$_{20}$NO [M+H]$^+$ 206.1545; found 206.1547.

tert-butyl (S)-(1-((2-methoxyphenyl)amino)-4-methylpentan-2-yl)carbamate (4.7a)
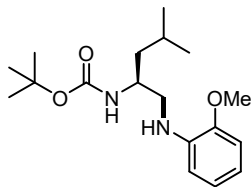
Following the General Procedure C with the corresponding NHPI ester (0.4 mmol) and *o*-anisidine (0.2 mmol). The crude product was purified by preparative TLC using hexanes / EtOAc (10:1) as an eluent to afford 38 mg (59%) of the title compound **4.7a**.

^{1}H NMR (400 MHz, CDCl$_3$): δ 6.86 (td, *J* = 7.6, 1.4 Hz, 1H), 6.76 (dd, *J* = 8.1, 1.4 Hz, 1H), 6.70 – 6.58 (m, 2H), 4.68 (br s, 1H), 4.46 (s, 1H), 3.94 (s, 1H), 3.83 (s, 3H), 3.33 – 2.94 (m, 2H), 1.82 – 1.65 (m, 1H), 1.45 (s, 9H), 1.42 – 1.32 (m, 2H), 0.99 – 0.89 (m, 6H).

^{13}C NMR (101 MHz, CDCl$_3$): δ 156.1, 147.0, 138.3, 121.4, 116.7, 110.0, 109.6, 79.4, 55.5, 49.2, 48.8, 42.5, 28.5, 25.1, 23.3, 22.3.

Physical State: pale brown solid.

HRMS (ESI): calcd for C$_{18}$H$_{31}$N$_2$O$_3$ [M+H]$^+$ 323.2335; found 323.2332.

(8R,9S,10S,13R,14S,17R)-17-((R)-4-((2-methoxyphenyl)amino)butan-2-yl)-10,13-dimethyldodecahydro-3H-cyclopenta[a]phenanthrene-3,7,12(2H,4H)-trione (4.7b)
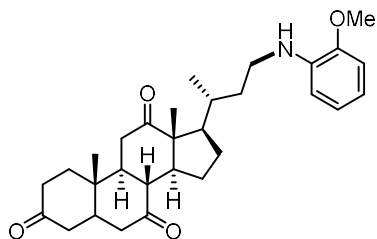
Following the General Procedure C with the corresponding NHPI ester (0.4 mmol) and *o*-anisidine (0.2 mmol). The crude product was purified by preparative TLC using hexanes / EtOAc (5:1) as an eluent to afford 41 mg (43%) of the title compound **4.7b**.

^{1}H NMR (400 MHz, CDCl$_3$): δ 6.86 (td, *J* = 7.7, 1.4 Hz, 1H), 6.75 (dd, *J* = 7.9, 1.4 Hz, 1H), 6.68 – 6.55 (m, 2H), 4.08 (br s, 1H), 3.83 (s, 3H), 3.28 – 3.13 (m, 1H), 3.07 (dt, *J* = 11.8, 7.8 Hz, 1H), 2.92 – 2.83 (m, 3H), 2.41 – 0.91 (m, 28H).

¹³C NMR (101 MHz, CDCl₃): δ 146.8, 138.6, 134.4, 121.4, 116.3, 109.9, 109.4, 57.0, 55.5, 51.9, 49.1, 49.0, 47.0, 46.1, 45.7, 45.1, 42.9, 41.6, 38.8, 36.6, 36.1, 35.5, 35.4, 34.5, 28.0, 25.3, 22.0, 19.4, 12.0.

Physical State: light brown solid.

HRMS (ESI): calcd for C₃₀H₄₂NO₄ [M+H]⁺ 480.3114; found 480.3113.

N,N-bis(2-chloroethyl)-4-(3-((2-methoxyphenyl)amino)propyl)aniline (4.7c)
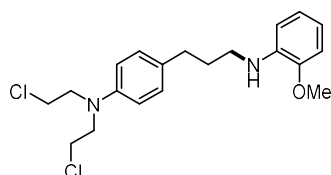
Following the General Procedure C with the corresponding NHPI ester (0.4 mmol) and *o*-anisidine (0.2 mmol). The crude product was purified by preparative TLC using hexanes / EtOAc (10:1) as an eluent to afford 38 mg (50%) of the title compound **4.7c**.

¹H NMR (400 MHz, CDCl₃): δ 7.10 (d, *J* = 8.6 Hz, 2H), 6.87 (td, *J* = 7.6, 1.5 Hz, 1H), 6.78 (dd, *J* = 8.0, 1.4 Hz, 1H), 6.73 – 6.60 (m, 4H), 3.85 (s, 3H), 3.72 – 3.60 (m, 8H), 3.16 (t, *J* = 7.1 Hz, 2H), 2.66 (t, *J* = 7.6 Hz, 2H), 1.96 (dt, *J* = 15.2, 7.3 Hz, 2H).

¹³C NMR (101 MHz, CDCl₃): δ 147.2, 144.4, 131.0, 129.8, 129.6, 121.4, 117.1, 112.4, 109.7, 55.6, 53.8, 43.7, 40.7, 32.3, 31.1.

Physical State: colorless oil.

HRMS (ESI): calcd for C₂₀H₂₇N₂OCl₂ [M+H]⁺ 381.1501; found 381.1505.

2-methoxy-*N*-(1-(6-methoxynaphthalen-2-yl)ethyl)aniline (4.7d)
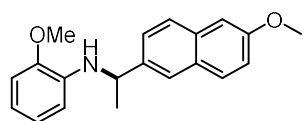
Following the General Procedure B with the corresponding NHPI ester (0.2 mmol) and *o*-anisidine (0.4 mmol). The crude product was purified by preparative TLC using hexanes / EtOAc (10:1) as an eluent to afford 34 mg (55%) of the title compound **4.7d**.

¹H NMR (400 MHz, CDCl₃): δ 7.76 (d, *J* = 1.8 Hz, 1H), 7.71 (dd, *J* = 9.0, 5.9 Hz, 2H), 7.48 (dd, *J* = 8.5, 1.8 Hz, 1H), 7.17 – 7.10 (m, 2H), 6.78 (dd, *J* = 7.8, 1.5 Hz, 1H), 6.68 (td, *J* = 7.7, 1.5 Hz, 1H), 6.61 (td, *J* = 7.7, 1.7 Hz, 1H), 6.40 (dd, *J* = 7.7, 1.7 Hz, 1H), 4.71 (s, 1H), 4.60 (q, *J* = 6.8 Hz, 1H), 3.91 (2s, *J* = 1.4 Hz, 6H), 1.62 (d, *J* = 6.7 Hz, 3H).

^{13}C NMR (101 MHz, CDCl$_3$): δ 157.5, 146.7, 140.8, 137.5, 133.9, 129.4, 129.2, 127.4, 125.1, 124.2, 121.3, 118.8, 116.5, 111.3, 109.4, 105.8, 55.6, 55.5, 53.6, 25.3.

Physical State: colorless oil.

HRMS (ESI): calcd for C$_{20}$H$_{21}$NO$_2$Na [M+H]$^+$ 330.1470; found 330.1467.

tert-butyl ((1-(((2-methoxyphenyl)amino)methyl)cyclohexyl)methyl)carbamate (4.7e)
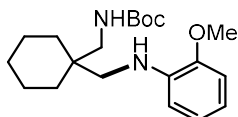
Following the General Procedure C with the corresponding NHPI ester (0.4 mmol) and *o*-anisidine (0.2 mmol). The crude product was purified by preparative TLC using hexanes / EtOAc (15:1) as an eluent to afford 33 mg (48%) of the title compound **4.7e**.

^{1}H NMR (400 MHz, CDCl$_3$): δ 6.87 (td, *J* = 7.6, 1.4 Hz, 1H), 6.77 (dd, *J* = 7.9, 1.4 Hz, 1H), 6.66 (td, *J* = 7.7, 1.5 Hz, 1H), 6.60 (dd, *J* = 7.8, 1.5 Hz, 1H), 4.74 (br s, 1H), 4.39 (br s, 1H), 3.85 (s, 3H), 3.31 (dt, *J* = 12.3, 5.5 Hz, 1H), 3.16 – 2.95 (m, 3H), 1.93 (h, *J* = 5.9 Hz, 1H), 1.72 (qd, *J* = 11.9, 10.3, 5.1 Hz, 1H), 1.45 (s, 9H), 1.21 (t, *J* = 7.1 Hz, 2H), 0.92 (dd, *J* = 6.6, 3.7 Hz, 6H).

^{13}C NMR (101 MHz, CDCl$_3$): δ 156.4, 147.1, 138.5, 121.4, 116.5, 109.9, 109.7, 79.2, 55.6, 46.3, 43.0, 40.0, 36.2, 28.5, 25.6, 23.1, 23.0.

Physical State: reddish brown oil.

HRMS (APPI): calcd for C$_{20}$H$_{33}$N$_2$O$_3$ [M+H] 349.2486; found 349.2504.

(4-chlorophenyl)(5-methoxy-3-(((2-methoxyphenyl)amino)methyl)-2-methyl-1*H*-indol-1-yl)methanone (4.7f)
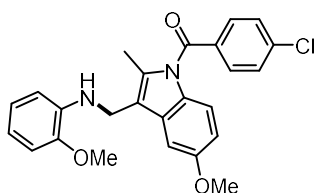
Following the General Procedure C with the corresponding NHPI ester (0.4 mmol) and *o*-anisidine (0.2 mmol). The crude product was purified by preparative TLC using hexanes / EtOAc (10:1) as an eluent to afford 35 mg (40%) of the title compound **4.7f**.

^{1}H NMR (400 MHz, CDCl$_3$): δ 7.72 – 7.65 (m, 2H), 7.52 – 7.46 (m, 2H), 7.03 (d, *J* = 2.5 Hz, 1H), 6.97 (td, *J* = 7.6, 1.5 Hz, 1H), 6.90 (d, *J* = 8.9 Hz, 1H), 6.83 (ddd, *J* = 11.0, 7.9, 1.5 Hz, 2H), 6.75

(td, J = 7.6, 1.5 Hz, 1H), 6.69 (dd, J = 9.0, 2.6 Hz, 1H), 4.37 (s, 2H), 4.31 (s, 1H), 3.81 (s, 3H), 3.80 (s, 3H), 2.44 (s, 3H).

¹³C NMR (101 MHz, CDCl₃): δ 168.5, 156.2, 147.0, 139.5, 138.5, 136.3, 134.0, 131.3, 131.1, 130.6, 129.3, 121.4, 117.0, 116.8, 115.1, 112.0, 110.0, 109.6, 101.4, 55.9, 55.5, 38.5, 13.4.

Physical State: light yellow oil.

HRMS (ESI): calcd for C₂₅H₂₃ClN₂O₃Na [M+Na]⁺ 457.1295; found 457.1290.

N-(1-(4-isobutylphenyl)ethyl)-2-methoxyaniline (4.7g)
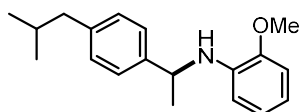
Following the General Procedure B with the corresponding NHPI ester (0.2 mmol) and *o*-anisidine (0.4 mmol). The crude product was purified by preparative TLC using hexanes / EtOAc (10:1) as an eluent to afford 23 mg (41%) of the title compound **4.7g**.

¹H NMR (400 MHz, CDCl₃): δ 7.28 – 7.24 (m, 2H), 7.09 (d, J = 7.7 Hz, 2H), 6.77 (dd, J = 7.9, 1.4 Hz, 1H), 6.72 (td, J = 7.7, 1.5 Hz, 1H), 6.61 (td, J = 7.7, 1.6 Hz, 1H), 6.38 (dd, J = 7.8, 1.6 Hz, 1H), 4.60 (br s, 1H), 4.46 (q, J = 6.7 Hz, 1H), 3.89 (s, 3H), 2.44 (d, J = 7.2 Hz, 2H), 1.84 (dp, J = 13.6, 6.8 Hz, 1H), 1.54 (d, J = 6.6 Hz, 3H), 0.89 (d, J = 6.6 Hz, 6H).

¹³C NMR (101 MHz, CDCl₃): 146.7, 142.8, 140.3, 137.5, 129.4, 125.7, 121.3, 116.3, 111.1, 109.4, 55.6, 53.1, 45.3, 30.4, 25.2, 22.6.

Physical State: colorless oil.

HRMS (ESI): calcd for C₁₉H₂₆NO [M+H]⁺ 284.2014; found 284.2017.

(*Z*)-*N*-(heptadec-8-en-1-yl)-2-methoxyaniline (4.7h)
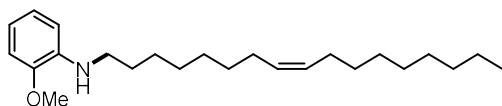
Following the General Procedure C with the corresponding NHPI ester (0.4 mmol) and *o*-anisidine (0.2 mmol). The crude product was purified by preparative TLC using hexanes / EtOAc (20:1) as an eluent to afford 29 mg (40%) of the title compound **4.7h**.

¹H NMR (400 MHz, CD₂Cl₂): δ 6.83 (td, J = 7.8, 2.6 Hz, 1H), 6.75 (dd, J = 8.0, 2.7 Hz, 1H), 6.65 – 6.50 (m, 2H), 5.47 – 5.33 (m, 2H), 4.17 (br s, 1H), 3.87 (s, 3H), 3.22 – 2.98 (m, 2H), 2.18 – 1.98 (m, 4H), 1.68 – 1.62 (m, 2H), 1.46 – 1.26 (m, 20H), 0.95 – 0.85 (m, 3H).

^{13}**C NMR** (101 MHz, CD$_2$Cl$_2$): δ 147.2, 139.1, 130.4, 130.2, 121.6, 116.2, 109.9, 109.8, 55.8, 44.1, 32.4, 30.2, 30.2, 30.0, 30.0, 29.8, 29.8, 29.7, 27.7, 27.6, 27.6, 26.0, 23.1, 14.3.

Physical State: pale yellow oil.

HRMS (ESI): calcd for C$_{24}$H$_{42}$NO [M+H]$^+$ 360.3266; found 360.3265.

(*E*)-*N*-(heptadec-8-en-1-yl)-2-methoxyaniline (4.7i)
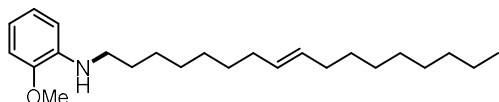
Following the General Procedure C with the corresponding NHPI ester (0.4 mmol) and *o*-anisidine (0.2 mmol). The crude product was purified by preparative TLC using hexanes / EtOAc (20:1) as an eluent to afford 23 mg (32%) of the title compound **4.7i**.

^{1}**H NMR** (400 MHz, CD$_2$Cl$_2$): δ 6.82 (td, *J* = 7.7, 2.6 Hz, 1H), 6.75 (dd, *J* = 7.5, 2.3 Hz, 1H), 6.63 – 6.55 (m, 2H), 5.42-5.31 (m, 2H), 4.17 (br s, 1H), 3.82 (s, 3H), 3.10 (t, *J* = 7.1 Hz, 2H), 2.00 – 1.96 (m, 4H), 1.66 – 1.62 (m, 2H), 1.43 – 1.28 (m, 20H), 0.89 (t, *J* = 6.9 Hz, 3H).

^{13}**C NMR** (101 MHz, CD$_2$Cl$_2$): δ 147.2, 139.1, 130.9, 130.7, 121.6, 116.2, 109.9, 109.7, 55.8, 44.1, 33.0, 33.0, 32.4, 30.1, 30.1, 30.0, 30.0, 29.8, 29.6, 29.5, 27.6, 23.1, 14.3.

Physical State: pale yellow solid.

HRMS (ESI): calcd for C$_{24}$H$_{42}$NO [M+H]$^+$ 360.3266; found 360.3268.

tert-butyl 4-((4-(trifluoromethyl)phenyl)amino)piperidine-1-carboxylate (4.8a)
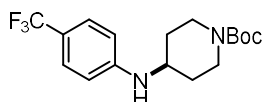
Following the General Procedure B with the corresponding NHPI ester (0.2 mmol) and 4-(trifluoromethyl)aniline (0.4 mmol). The crude product was purified by preparative TLC using hexanes / EtOAc (10:1) as an eluent to afford 52 mg (75%) of the title compound **4.8a**.

^{1}**H NMR** (400 MHz, CDCl$_3$): δ 7.40 (d, *J* = 8.5 Hz, 2H), 6.61 (d, *J* = 8.3 Hz, 2H), 4.12 – 4.00 (m, 2H), 3.46 (tt, *J* = 10.3, 4.0 Hz, 1H), 2.93 (t, *J* = 12.6 Hz, 2H), 2.06 – 1.98 (m, 2H), 1.47 (s, 9H), 1.40 – 1.33 (m, 2H).

^{13}**C NMR** (101 MHz, CDCl$_3$): δ 154.9, 134.5, 126.9 (q, *J* = 3.7 Hz), 123.7, 79.9, 32.2, 28.6, 28.6.

Physical State: white solid.

Spectral data match those previously reported.[7]

N-cyclohexylmethanesulfonamide (4.4l)
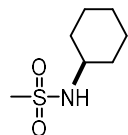
An oven-dried 15 mL vial equipped with a Teflon-coated magnetic stir bar was sequentially charged with corresponding NHPI ester (0.5 mmol), Ru(bpy)$_3$(PF$_6$)$_2$ (1 mol%), Cu(MeCN)$_4$PF$_6$ (50 mol%), **4.L26** (30 mol%), MeCN (0.1 M), methanesulfonamide (1.5 mmol), Et$_3$N (5 equiv) in the glove box. The vial was sealed with a screw cap and removed from the glove box. Then the vial was placed 3 cm away from one blue LED, and irradiated under fan cooling (maintain the temperature at room temperature) for 20 h. After the reaction, the resulting dark brown reaction mixture was acidified with saturated NH$_4$Cl solution (~1 mL) and then neutralized with saturated NaHCO$_3$ solution (~1.5 mL). The crude product in the aqueous fraction was extracted with EtOAc (~10 mL). The aqueous fraction was further washed with EtOAc (3 x ~5 mL). The combined organic fractions were concentrated *in vacuo* with the aid of a rotary evaporator. The crude product residue was purified by flash chromatography column using hexanes / EtOAc (40:1) as an eluent to afford 14 mg (16%) of the title compound **4.4l**.

¹H NMR (400 MHz, CDCl$_3$): δ 4.21 (s, 1H), 3.31 (dtt, J = 10.7, 7.6, 4.0 Hz, 1H), 2.97 (s, 3H), 2.05 – 1.88 (m, 2H), 1.73 (dt, J = 13.5, 3.9 Hz, 2H), 1.65 – 1.58 (m, 1H), 1.42 – 1.10 (m, 5H).
¹³C NMR (101 MHz, CDCl$_3$): δ 53.0, 42.3, 34.6, 25.3, 24.9.
Spectral data match those previously reported.

N-cyclohexylacetamide (4.4m)
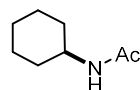
An oven-dried 15 mL vial equipped with a Teflon-coated magnetic stir bar was sequentially charged with corresponding NHPI ester (1 mmol), Ru(bpy)$_3$(PF$_6$)$_2$ (1 mol%), Cu(MeCN)$_4$PF$_6$ (50 mol%), **4.L26** (30 mol%), MeCN (0.1 M), acetamide (3 mmol), Et$_3$N (5 equiv) in the glove box. The vial was sealed with a screw cap and removed from the glove box. Then the vial was placed 3 cm away from one blue LED, and irradiated under fan cooling (maintain the temperature at room

temperature) for 20 h. After the reaction, the resulting dark brown reaction mixture was acidified with saturated NH$_4$Cl solution (~1 mL) and then neutralized with saturated NaHCO$_3$ solution (~1.5 mL). The crude product in the aqueous fraction was extracted with EtOAc (~10 mL). The aqueous fraction was further washed with EtOAc (3 x ~5 mL). The combined organic fractions were concentrated *in vacuo* with the aid of a rotary evaporator. The crude product residue was purified by flash chromatography column using hexanes / EtOAc (40:1) as an eluent to afford 13 mg (9%) of the title compound **4.4m**.

¹H NMR (400 MHz, CDCl$_3$): δ 5.33 (s, 1H), 3.84 – 3.66 (m, 1H), 1.95 (s, 5H), 1.72 – 1.57 (m, 3H), 1.44 – 1.27 (m, 2H), 1.23 – 1.02 (m, 3H).

¹³C NMR (101 MHz, CDCl$_3$): δ 169.2, 48.4, 33.4, 25.7, 25.0, 23.8.

Spectral data match those previously reported.

_N_-phenyladamantan-1-amine (4.5k)
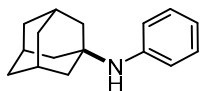
Following the General Procedure B with the corresponding NHPI ester (1.0 mmol) and 4-(trifluoromethyl)aniline (2.0 mmol). The crude product was purified by preparative TLC using hexanes / EtOAc (20:1) as an eluent to afford 21 mg (9%) of the title compound **4.5k**.

¹H NMR (400 MHz, CDCl$_3$): δ 7.20 – 7.10 (m, 2H), 6.80 (d, *J* = 7.7 Hz, 3H), 3.05 (br s, 1H), 2.15 – 2.03 (m, 3H), 1.88 (d, *J* = 2.9 Hz, 6H), 1.75 – 1.60 (m, 6H).

¹³C NMR (101 MHz, CDCl$_3$): δ 146.2, 128.9, 119.3, 119.2, 52.4, 43.6, 36.6, 29.9.

Spectral data match those previously reported.[7]

Chapter 5

Cross-coupling of Alkyl Redox-Active Esters with Benzophenone Imines via Tandem Photoredox and Copper Catalysis

Chapter 5

5.1 Introduction of the background
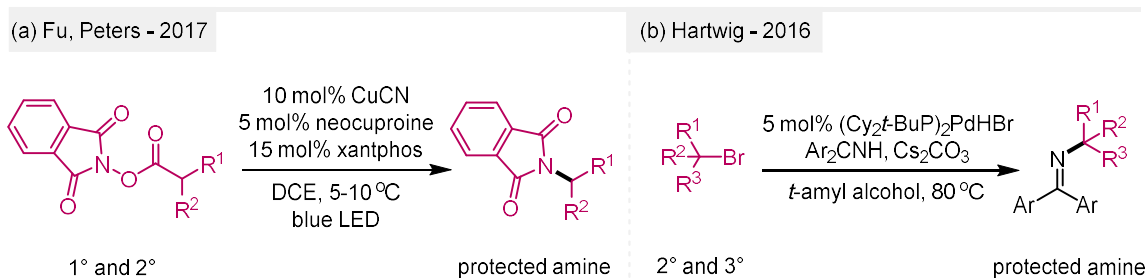
Figure 62 (a) A previous method for the intramolecular C-N coupling of alkyl NHPI esters. (b) A previous method for the cross-coupling of alkyl bromides with benzophenone imines.

Chapter 4 has described in detail the photoredox/copper dual catalytic system that was developed by us and its application in decarboxylative $C(sp^3)$-N couplings. Based on this novel catalytic system, we expected to overcome some existing limitations of such an approach and desired to address more potential challenges in coupling reactions.

Among all, we consider that one of the most urgent issues to be addressed is the development of a safe and efficient method for the synthesis of primary amines from alkyl carboxylic acids. So far, the most efficient way to achieve this transformation is the Curtius rearrangement. However, the use of equivalent amounts of azide compounds exhibits a significant safety concern and discourages experimenters. Besides, the compatibility of functional groups is another problem of the reaction that cannot be ignored. Given the importance of primary amines (see Chapter 2.4.1), chemists are always interested in exploring an alternative to the Curtius rearrangement. For example, the use of transition metal catalysis to obtain primary amines from alkyl carboxylic acids is rare but offers a potential alternative. The most representative work is an intramolecular decarboxylative $C(sp^3)$-N coupling method of NHPI esters that was developed by Fu, Peters and co-workers in 2017.[46] While this method provided an elegant way to obtain primary protected amines, the reaction did not apply to the conversion of tertiary alkyl carboxylic acids, constituting a major drawback of this method (Figure 62a).

In 2016, Hartwig and co-workers developed a palladium-catalyzed cross-coupling reaction of alkyl halides with benzophenone imines.[149] This method could efficiently convert secondary and tertiary alkyl halides into protected primary amines, providing an efficient way to access a

class of high value-added products. However, the reaction unreactive to primary alkyl halides, which has limited the broad application of this method to some extent (Figure 62b).

Inspired by the work of Hartwig and co-workers, in particular, the advantages of benzophenone imine as a nucleophilic reagent (Chapter 2.4), we speculated: could benzophenone imines be used as *N*-nucleophilic reagents in our photoredox/copper dual catalytic system? In this way, we might be able to provide a safer and credible alternative for the Curtius rearrangement, and expand the substrate applicability to primary, secondary and tertiary carboxylic acids to overcome the shortcomings of the existing methods. Based on this hypothesis, we proceeded with the reaction design (Figure 63). In the initial design shown in Figure 63, we wished to first activate the aliphatic carboxylic acids into the corresponding NHPI esters. Then, by employing benzophenone imine as *N*-nucleophiles in the established photoredox/copper bi-catalytic system, we desired to obtain protected primary amines. Finally, by a simple acidic workup, we could obtain primary alkylamines.
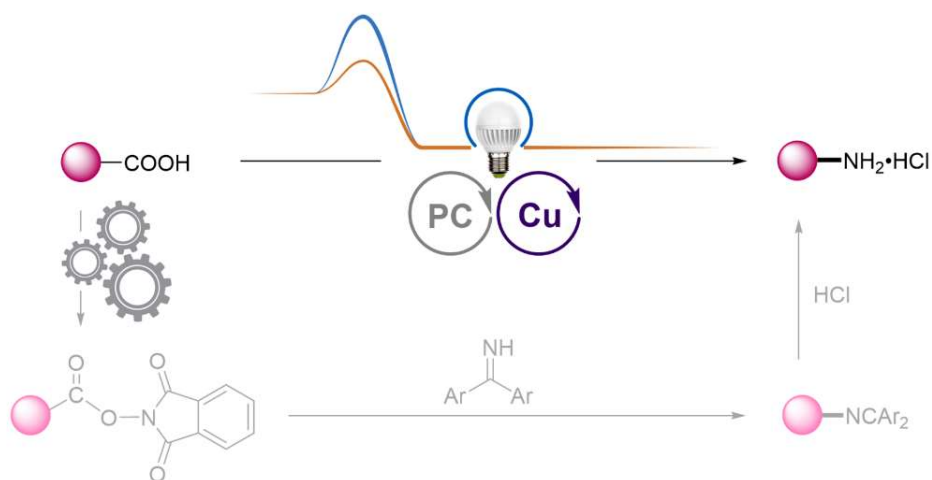
Figure 63 Our reaction design.

In this Chapter, we report the successful development of a method that enables the intermolecular coupling of alkyl NHPI esters with benzophenone imines. This method works with primary, secondary and tertiary alkyl electrophiles, which provides a clear advantage over Curtius rearrangement, reductive amination and substitution reactions.

5.2 Optimization of the reaction conditions

5.2.1 Reaction design
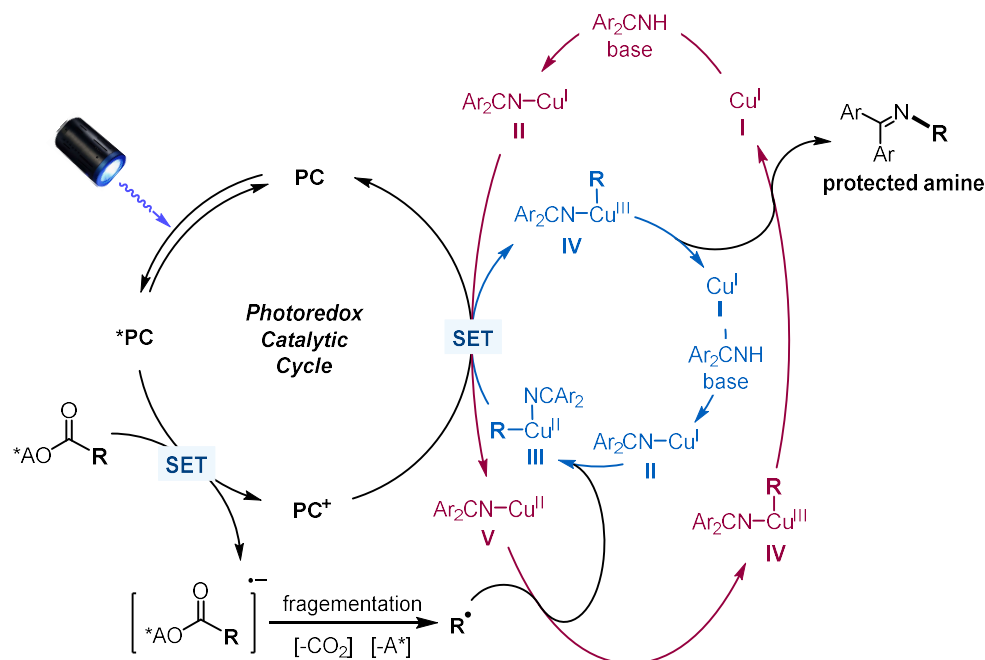
Figure 64 Proposed mechanistic pathway. Proposed copper catalytic cycle A: in blue color; proposed copper catalytic cycle B: in red color.

To start with, we proposed possible mechanistic pathways for the decarboxylative coupling of alkyl NHPI esters with benzophenone imines that were dipicted in Figure 64. Initially, the coordination of the benzophenone imines with a low-valent copper catalyst (**I**) followed by deprotonation would form the copper^I-amido species (**II**). Concurrently, the excitation of a photocatalyst (PC) would generate a photoexcited complex (PC*), which could reduce the NHPI ester through a single-electron transfer (SET), affording an alkyl radical upon fragmentation. The subsequent capture of the alkyl radical by **II** would yield intermediate (**III**). Oxidation of **III** by the oxidized photocatalyst (PC$^+$) forms a high-valent metal alkyl amido complex **IV** and regenerates the PC. **IV** is able to undergo reductive elimination to give the desired coupling product and regenerate a low-valent Cu species (**I**), closing the copper catalytic cycle (Figure 64, photoredox catalytic cycle with the copper catalytic cycle A that in blue color).

Alternatively, the copper catalytic cycle might occur via an alternative pathway where the Cu^{I}-amido species (**II**) could be directly oxidized by the oxidized photocatalyst (PC^{+}) to form a high-valent metal alkyl amido complex **V** and regenerates the PC. Then the former captures the alkyl radical from the NHPI ester to give the key Cu^{III} intermediate **IV**, which upon reductive elimination, gives the C-N coupling product (Figure 64, photoredox catalytic cycle with the copper catalytic cycle B that in red color).

5.2.2 Initial reaction conditions and results

Following the reaction design (Figure 64), we attempted to apply benzophenone imine **5.2a** as a nucleophilic reagent to the optimal reaction conditions we obtained in the decarboxylative C(sp^3)-N coupling reactions, in order to verify the feasibility of our reaction design. By trying this reaction, we found that the coupling efficiency of cyclohexyl NHPI ester **2.22** with benzophenone imine **5.2a** was not high; only 30% of the coupling product **5.3a** was afforded (Figure 65). Nevertheless, the successful obtaining of the coupling product verified the feasibility of our reaction design and laid the foundation for our further reaction optimization.
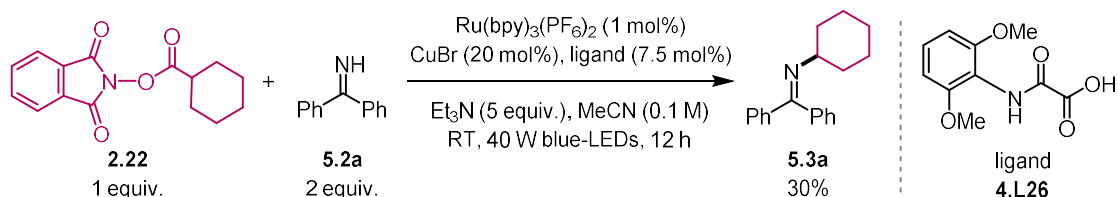
Figure 65 The first milestone in our exploration of the decarboxylative cross-coupling of NHPI ester **2.22** and benzophenone imine **5.2a**.

5.2.3 Further optimization of the reaction conditions

Optimization was conducted to search for the best conditions for this coupling (Table 19). After the screening of various ligands, it was found that ligand-less conditions gave even comparable yields (Table 19, entries 1-5). Among various copper salts, Cu(MeCN)$_4$PF$_6$ gave the best yield (Table 19, entries 5-7). Cs$_2$CO$_3$ was the best base (Table 19, entries 7-15), probably due to the coordination of the NHPI ester with Cs$_2$CO$_3$, as proposed in a previous study.[45] Dimethylacetamide (DMA) was the best solvent (Table 19, entries 9, 16-18). By changing the

photocatalyst from Ru(bpy)$_3$(PF$_6$)$_2$ (**A**) to an Ir(III) complex such as Ir[dF(CF$_3$)ppy]$_2$(dtbbpy)PF$_6$ (**B**) or Ir[(dtbbpy)(ppy)$_2$]PF$_6$ (**C**), the yield was improved (Table 19, entries 9, 19-20). An optimized yield of 49% was obtained using **1a** (0.2 mmol), benzophenone imine (**2a**, 2 equiv.), Ir[(dtbbpy)(ppy)$_2$]PF$_6$ (1 mol%), Cu(MeCN)$_4$PF$_6$ (20 mol%), Cs$_2$CO$_3$ (2 equiv.), and DMA (0.1 M) under blue LED irradiation for 20 h at room temperature (Table 19, entry 20). Interestingly, when the Cu(I) complex Cu(MeCN)$_4$PF$_6$ (20 mol%) was replaced by either a Cu metal (100 mol%) or a Cu(II) salt CuCl$_2$ (20 mol%), the coupling product was also obtained, but with lower yields (Table 19, entries 20-22).

Table 19   Summary of the effects of reaction parameters on the reaction efficiency of secondary acids
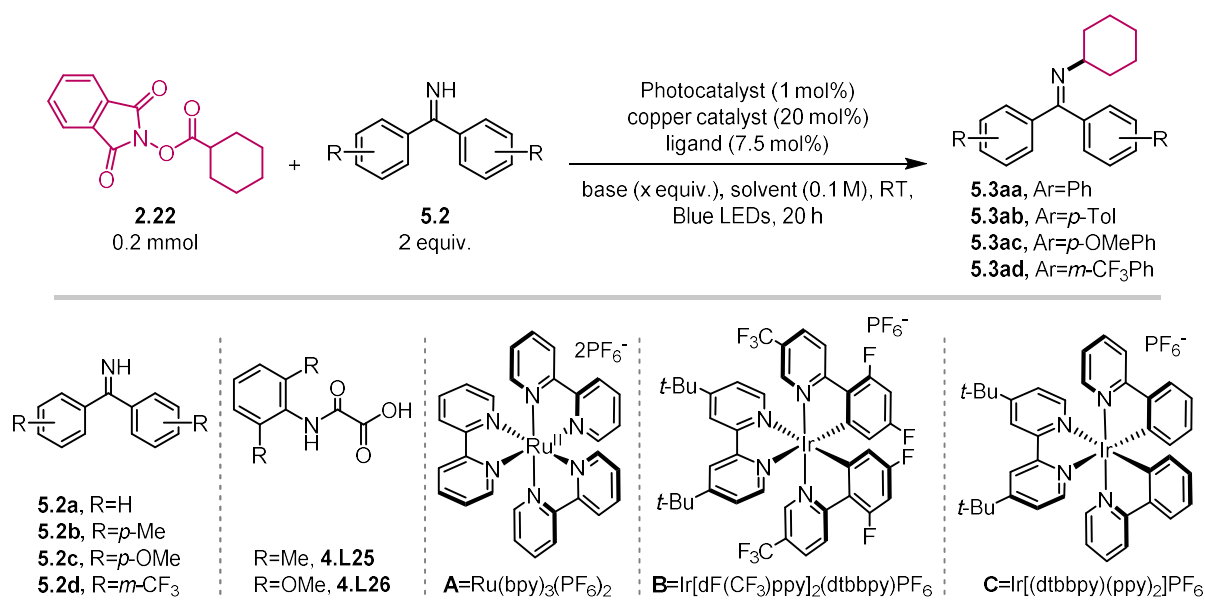
entry	imine	PC	copper catalyst	base (x equiv.)	solvent	yield (%)^a
1	**5.2a**	A	CuBr/**4.L25**	Et$_3$N (5 equiv.)	MeCN	20
2^b	**5.2a**	A	CuBr/**4.L26**	Et$_3$N (5 equiv.)	MeCN	30
3	**5.2a**	A	CuBr/PCy$_3$	Et$_3$N (5 equiv.)	MeCN	31
4	**5.2a**	A	CuBr/dtbpy	Et$_3$N (5 equiv.)	MeCN	12
5	**5.2a**	A	CuBr	Et$_3$N (5 equiv.)	MeCN	25
6	**5.2a**	A	CuCl	Et$_3$N (5 equiv.)	MeCN	30
7	**5.2a**	A	Cu(MeCN)$_4$PF$_6$	Et$_3$N (5 equiv.)	MeCN	32
8	**5.2a**	A	Cu(MeCN)$_4$PF$_6$	Cs$_2$CO$_3$ (2 equiv.)	MeCN	19
9	**5.2a**	A	Cu(MeCN)$_4$PF$_6$	Cs$_2$CO$_3$ (2 equiv.)	DMA	39

10	**5.2a**	A	Cu(MeCN)$_4$PF$_6$	K$_2$CO$_3$ (2 equiv.)	DMA	trace
11	**5.2a**	A	Cu(MeCN)$_4$PF$_6$	K^{t}OBu (2 equiv.)	DMA	trace
12	**5.2a**	A	Cu(MeCN)$_4$PF$_6$	DIPEA (2 equiv.)	MeCN	16
13	**5.2a**	A	Cu(MeCN)$_4$PF$_6$	DBU (2 equiv.)	MeCN	trace
14	**5.2a**	A	Cu(MeCN)$_4$PF$_6$	BTMG (2 equiv.)	MeCN	14%
15	**5.2a**	A	Cu(MeCN)$_4$PF$_6$	DIPA (2 equiv.)	MeCN	33%
16	**5.2a**	A	Cu(MeCN)$_4$PF$_6$	Cs$_2$CO$_3$ (2 equiv.)	DMF	27
17	**5.2a**	A	Cu(MeCN)$_4$PF$_6$	Cs$_2$CO$_3$ (2 equiv.)	DCM	19
18	**5.2a**	A	Cu(MeCN)$_4$PF$_6$	Cs$_2$CO$_3$ (2 equiv.)	THF	trace
19	**5.2a**	B	Cu(MeCN)$_4$PF$_6$	Cs$_2$CO$_3$ (2 equiv.)	DMA	40
20	**5.2a**	C	Cu(MeCN)$_4$PF$_6$	Cs$_2$CO$_3$ (2 equiv.)	DMA	49
21	**5.2a**	C	Cu (100 mol%)	Cs$_2$CO$_3$ (2 equiv.)	DMA	24
22	**5.2a**	C	CuCl$_2$	Cs$_2$CO$_3$ (2 equiv.)	DMA	28
23	**5.2b**	C	Cu(MeCN)$_4$PF$_6$	Cs$_2$CO$_3$ (2 equiv.)	DMA	33
24	**5.2c**	C	Cu(MeCN)$_4$PF$_6$	Cs$_2$CO$_3$ (2 equiv.)	DMA	29
25	**5.2d**	C	Cu(MeCN)$_4$PF$_6$	Cs$_2$CO$_3$ (2 equiv.)	DMA	70
26	**5.2d**	none	Cu(MeCN)$_4$PF$_6$	Cs$_2$CO$_3$ (2 equiv.)	DMA	trace
27	**5.2d**	C	none	Cs$_2$CO$_3$ (2 equiv.)	DMA	trace
28[f]	**5.2d**	C	Cu(MeCN)$_4$PF$_6$	Cs$_2$CO$_3$ (2 equiv.)	DMA	trace

[a]Corrected GC yield using *n*-dodecane as an internal standard. [b]Same condition as the optimized reaction condition in entry 1, Table 16, Chapter 4. Reaction was carried out with **2.22** (0.2 mmol), **5.2a** (2 equiv.), Ru(bpy)$_3$(PF$_6$)$_2$ (1 mol%), CuBr (20 mol%), **4.L26** (7.5 mol%), Et$_3$N (5 equiv.) and MeCN (2.0 mL). [c]MeCN (0.1 M). [d]K$_2$CO$_3$ (2 equiv.) as the base. [e]KO^{t}Bu (2 equiv.) as the base. [f]No light. **PC**=photocatalyst; **A**=Ru(bpy)$_3$(PF$_6$)$_2$; **B**=Ir[dF(CF$_3$)ppy]$_2$(dtbbpy)PF$_6$; **C** =Ir[(dtbbpy)(ppy)$_2$]PF$_6$; DMA=*N,N*-dimethylacetamide. DIPEA=*N,N*-diisopropylethylamine; DBU=1,8-diazabicyclo(5.4.0)undec-7-ene; BTMG: 2-tert-butyl-1,1,3,3-tetramethylguanidine; DIPA=diisopropylamine; DMF=Dimethylformamide.

Different substituted benzophenone imines were then explored as the imine partners (Table 19, entries 19, 23-25). The coupling of the electron-deficient imine **5.2d** (Table 19, entry 25) gave higher yield (70%) than that of electron-rich imines **5.2b** and **5.2c,** as well as **5.2a** (Table 19, entry 19). Notably, an added advantage of using **5.2d** is that the products are less sensitive to silica gel chromatography than using **5.2a-5.2c**. Thus, **5.2d** was chosen as the preferred nitrogen nucleophile for the following optimization. Control experiments showed that photocatalyst, copper catalyst, and light are all essential for the coupling. Without any one of the three elements, no coupling was obtained (Table 19, entries 26-28).

5.2.4 Optimization of reaction parameters for primary alkyl NHPI esters

Based on our previous experience, the activity of the secondary NHPI ester and the primary NHPI ester differs greatly in the decarboxylative coupling reaction. Therefore, we performed a second-round screening of the reaction conditions for primary NHPI esters (Table 20). As expected, when adopting the optimal conditions of secondary NHPI ester **2.22** to primary NHPI ester **4.1a**, the efficiency of the reaction was very low, only 12% (Table 20, entry 1). After adjusting the ratio of NHPI ester to benzophenone imine **5.2d**, the yield of the reaction increased slightly to 20% (Table 20, entry 2).

Based on the optimization results of the secondary NHPI ester **2.22**, we found that different bases are very crucial for the efficiency of the reactions (Table 19, entries 7-15). Therefore, we tested different organic bases and inorganic bases (Table 20, entries 3-6). To our delight, when using triethylamine as a base and acetonitrile as a solvent, the yield of the reaction could be boosted to 50% (entry 4). Further optimization of the bases showed that although *N,N*-diisopropylethylamine (DIPEA) could not provide a better yield (entry 5), diisopropylamine (DIPA) was able to increase the yield significantly to 99% (entry 6).

We attributed the success of DIPA to 3 key factors. (1) Its stability in photoredox reactions, as DIPA is more difficult to oxidize than tertiary amines, such as triethylamine and DIPEA.[78] Moreover, (2) DIPA itself can be used as a ligand to coordinate with copper salts to enhance the reactivity.

Table 20 Summary of the effects of reaction parameters on the reaction efficiency of primary acids
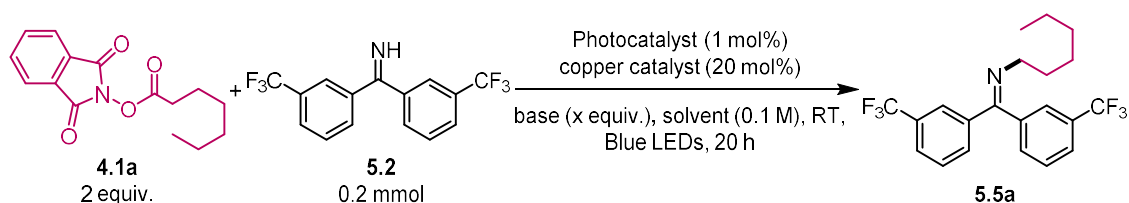
entry	imine	PC	copper catalyst	base (x equiv.)	solvent	yield (%)^a
1^b	**5.2d**	C	Cu(MeCN)$_4$PF$_6$	Cs$_2$CO$_3$ (2 equiv.)	DMA	12
2	**5.2d**	C	Cu(MeCN)$_4$PF$_6$	Cs$_2$CO$_3$ (2 equiv.)	DMA	20
3	**5.2d**	C	Cu(MeCN)$_4$PF$_6$	K$_2$CO$_3$ (2 equiv.)	DMA	trace
4	**5.2d**	C	Cu(MeCN)$_4$PF$_6$	Et$_3$N (2 equiv.)	MeCN	50
5	**5.2d**	C	Cu(MeCN)$_4$PF$_6$	DIPEA (2 equiv.)	MeCN	34

| 6 | **5.2d** | **C** | Cu(MeCN)$_4$PF$_6$ | DIPA (2 equiv.) | MeCN | 99 |

[a]Corrected GC yield using *n*-dodecane as an internal standard. [b]Reaction was carried out with **4.1a** (0.2 mmol), **5.2d** (2 equiv.), Ir[(dtbbpy)(ppy)$_2$]PF$_6$ (1 mol%), Cu(MeCN)$_4$PF$_6$ (20 mol%), Cs$_2$CO$_3$ (2 equiv.) and DMA (2.0 mL). **C** =Ir[(dtbbpy)(ppy)$_2$]PF$_6$; DMA=*N,N*-dimethylacetamide; DIPEA=*N,N*-diisopropylethylamine; DIPA=diisopropylamine.

5.3   Investigation of the substrate scope

5.3.1   Scope of alkyl NHPI esters that derived from secondary and tertiary carboxylic acids

The optimal reaction conditions in Table 19 (entry 25) could be applied to the coupling of a
wide range of secondary and tertiary alkyl NHPI esters (Figure 66). Cyclic alkyl groups, including
small and large rings (**5.3ad**-**5.3c**), indane group (**5.3d**), and heterocyclic alkyl group (**5.3e** and
5.3f), as well as acyclic secondary alkyl groups (**5.3g** and **5.3h**), were all successfully coupled.
Tertiary alkyl electrophiles are challenging substrates in cross-coupling reactions due to their steric
bulkiness. To our delight, tertiary alkyl NHPI esters are viable substrates as well (Figure 66).
Protected amines substituted by acyclic (**5.4a**-**5.4b**), cyclic (**5.4c**) alkyl groups as well as those
containing relatively complex skeletons such as adamantane (**5.4d** and **5.4e**) and a bridged bicyclic
structure (**5.4f**) could be obtained in synthetically useful yields.
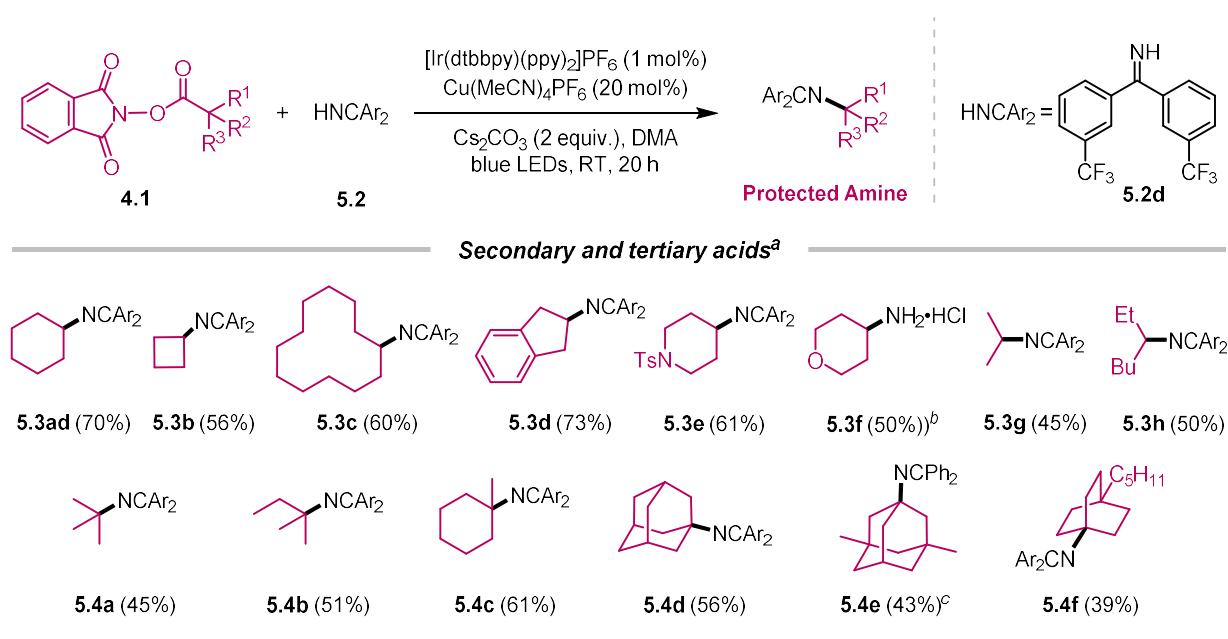
Figure 66 Scope of the coupling of secondary and tertiary alkyl NHPI esters with benzophenone imines.
[a]General conditions for secondary and tertiary NHPI esters: NHPI ester (1 equiv.), **5.2d** (2 equiv.),
Ir[(dtbbpy)(ppy)$_2$]PF$_6$ (1 mol%), Cu(MeCN)$_4$PF$_6$ (20 mol%), and Cs$_2$CO$_3$ (2 equiv.) in DMA (0.1 M),
irradiated at room temperature for 20 h, isolated yield. [b]Following acidic work-up was conducted. [c]**5.2a** as
the *N*-nucleophile.

5.3.2 Scope of alkyl NHPI esters that derived from primary carboxylic acids

Primary alkyl carboxylic acids represent one of the simplest class of reaction feedstocks that are readily available and inexpensive, and the optimum reaction conditions in Table 20 (entry 6) can be applied to the coupling of many primary alkyl NHPI esters in moderate to excellent yields (Figure 67). Functional groups such as aryl, ester, and bromo groups were tolerated (**5.5d-5.5f**). A polyfluorinated alkyl ester could also be coupled (**5.5g**), providing a convenient route to a polyfluorinated alkyl amine, which can be difficult to access otherwise. Coupling of the esters derived from 6-heptenoic acid and cyclopropyl acetic acid, which served as radical-clock probes, were able to give the 5-exo-trig cyclized and ring-opening products **5.5h** and **5.5i**, respectively. These results indicated the intermediacy of alkyl radicals.
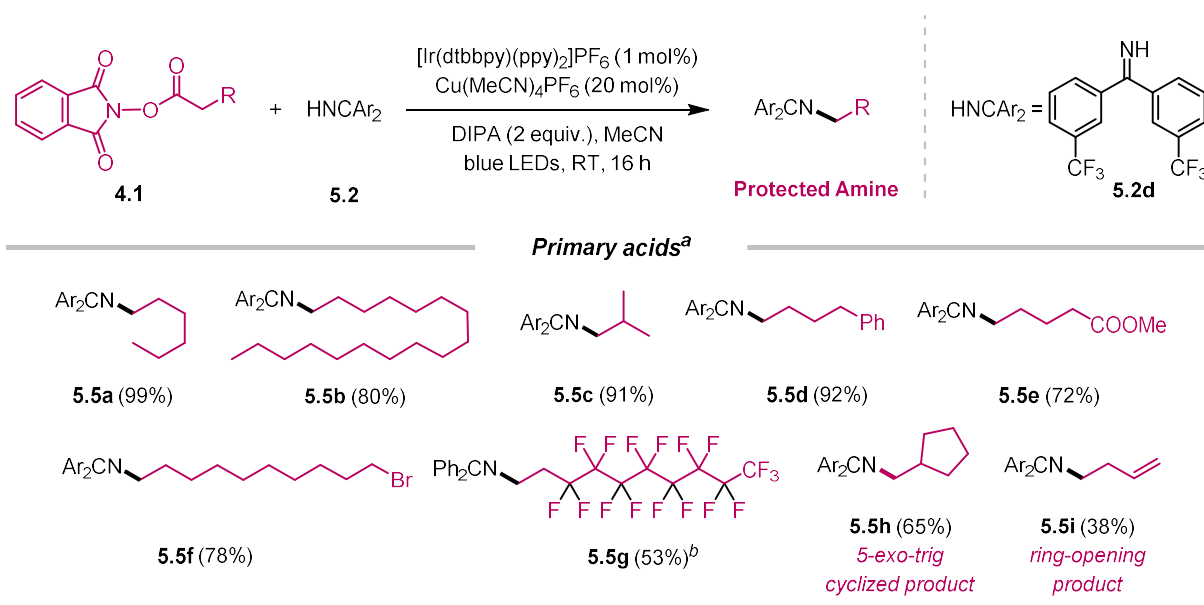
Figure 67 Scope of the coupling of primary alkyl NHPI esters with benzophenone imines. [a]General conditions for primary NHPI ester: NHPI ester (2 equiv.), **5.2d** (1 equiv.), Ir[(dtbbpy)(ppy)$_2$]PF$_6$ (1 mol%), Cu(MeCN)$_4$PF$_6$ (20 mol%) and diisopropylamine (DIPA, 2 equiv.) in MeCN (0.1 M), irradiated at room temperature for 16 h, isolated yield. [b]**5.2a** as the N-nucleophile.

5.4 Synthetic applications

5.4.1 Late-stage functionalization of natural products and drugs
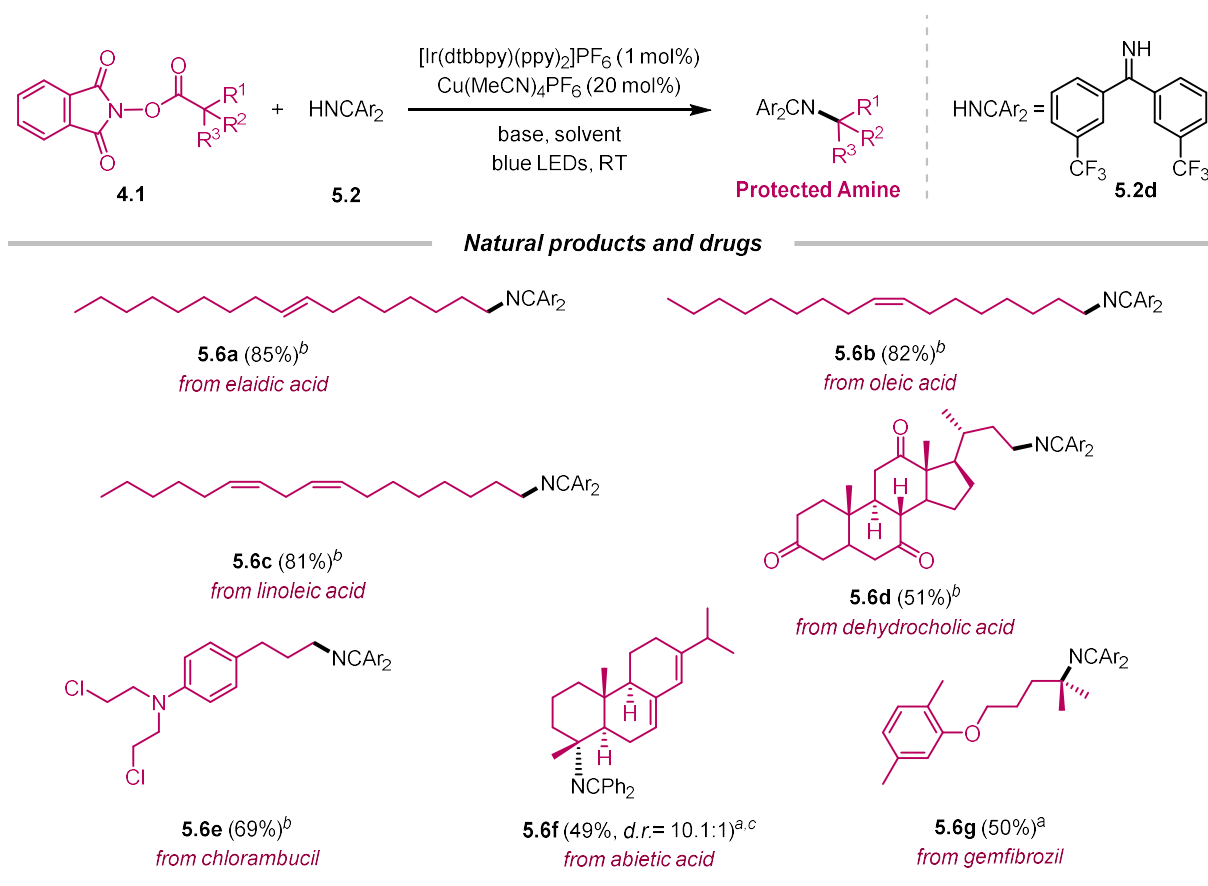
Figure 68 Late-stage functionalization of natural products and drugs. [a]General conditions for secondary and tertiary NHPI esters: NHPI ester (1 equiv.), **5.2d** (2 equiv.), Ir[(dtbbpy)(ppy)$_2$]PF$_6$ (1 mol%), Cu(MeCN)$_4$PF$_6$ (20 mol%), and Cs$_2$CO$_3$ (2 equiv.) in DMA (0.1 M), irradiated at room temperature for 20 h, isolated yield. [b]Following acidic work-up was conducted. [b]General conditions for primary NHPI ester: NHPI ester (2 equiv.), **5.2d** (1 equiv.), Ir[(dtbbpy)(ppy)$_2$]PF$_6$ (1 mol%), Cu(MeCN)$_4$PF$_6$ (20 mol%) and diisopropylamine (DIPA, 2 equiv.) in MeCN (0.1 M), irradiated at room temperature for 16 h, isolated yield. [c]**5.2a** as the N-nucleophile.

This decarboxylative amination method also enabled the synthesis of protected primary amines substituted by complex alkyl groups that derived from natural resources and drug molecules (Figure 68). For example, NHPI esters from fatty acids such as elaidic acid, oleic acid, and linoleic acid could be used to give the corresponding coupling products in good yields (**5.6a-5.6c**), without isomerization or oxidation of the olefin group. Drugs and natural products such as

dehydrocholic acid (**5.6d**), chlorambucil (**5.6e**), abietic acid (**5.6f**), and gemfibrozil (**5.6g**) were easily transformed into their protected amine derivatives, demonstrating the potential of the method in late-stage functionalizations. The cases of **5.5f, 5.6d** and **5.6e** highlight the orthogonal functional group compatibility of the present method compared to direct alkylation and reductive amination: **5.5f** has a bromo group and **5.6e** has two chloro groups which are incompatible with direct alkylation; **5.6d** has three keto groups which are incompatible with reductive amination. It is important to note that multiple stereocenters are conserved in **5.6d** and **5.6f**.

5.4.2   Synthesis of primary amine drugs using the present coupling method.
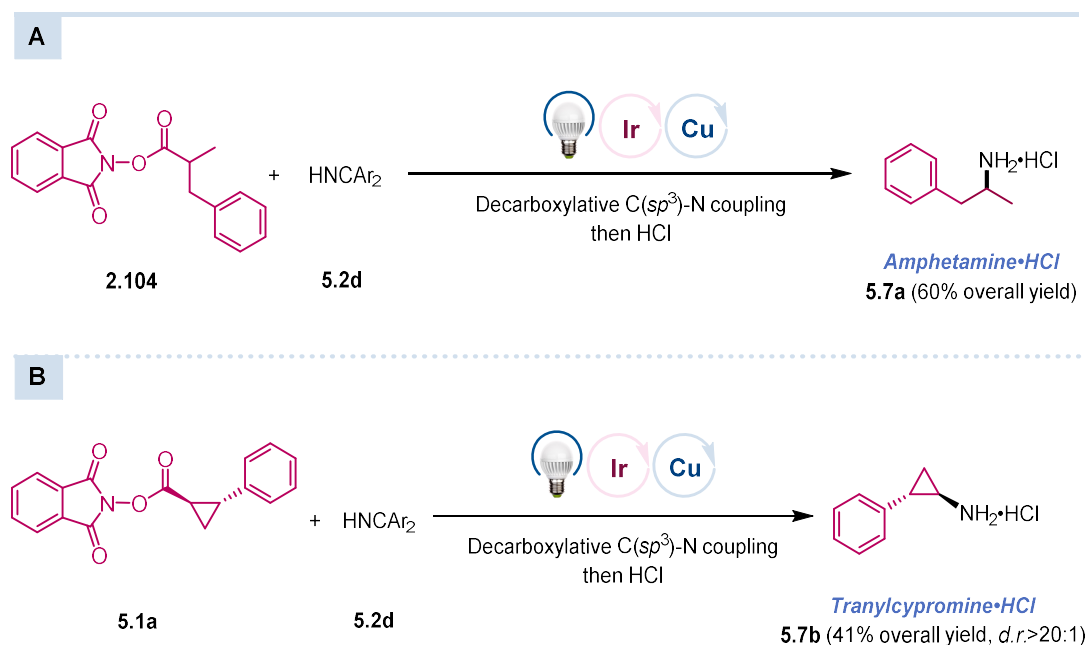
Figure 69 Synthesis of amine drugs using the present coupling method.

To further demonstrate the synthetic utility of the present coupling method, this method was applied for the synthesis of two drugs: amphetamine and tranylcypromine. As shown in Figure 69, both cases were successful. After simply acidic deprotection of the imine group, amphetamine•HCl and tranylcypromine•HCl were obtained in 60% (**5.7a**) and 41% (**5.7b**, *d.r.* > 20:1) overall yields (one-pot), respectively.

5.5 Conclusion

In summary, tandem photoredox/Cu catalysis has been developed to enable the cross-coupling of alkyl NHPI esters with benzophenone imines. The method allows for the rapid transformation of readily available alkyl carboxylic acids into alkylated primary amines, which are vital compounds in medicinal and materials chemistry. Compared to the decarboxylative amination method we presented in Chapter 4, this work further extended the scope of $C(sp^3)$-N coupling, making the amination reaction of tertiary carboxylic acids no longer difficult. Besides, compared to the classical Curtius rearrangement, this method provided a milder and safer way of converting alkyl carboxylic acids to protected primary amines.

5.6   Experimental section

5.6.1   Preparation of benzophenone imine derivatives

Note: The imines prepared below are sensitive to hydrolysis and contain small amounts of the corresponding ketones as impurities. To prevent further hydrolysis, these compounds were stored in a nitrogen-filled glovebox. Benzophenone imine **5.2a** is commercially available from Tokyo Chemical Industry (TCI) Co., Ltd, catalogue number: B1912.

4,4'-Dimethylbenzophenone imine (5.2b)
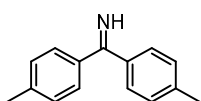
Dry magnesium turnings (365 mg, 15.0 mmol, 1.50 equiv), dry THF (20 ml), and a magnetic stir bar were placed in a nitrogen-filled flask, and the flask was connected to a reflux condenser. 4-bromotoluene (1.84 ml, 2.57 g, 15.0 mmol, 1.50 equiv) was dissolved in THF (3 ml), and a small amount of this solution was transferred to the reaction flask. The reaction was initiated with a single iodine crystal. The remaining aryl bromide solution was slowly transferred to the reaction flask. The syringe was rinsed with THF (3 ml), and the mixture was stirred at ambient temperature for 2.5 h at which time the majority of the magnesium was visibly consumed. The reaction mixture was then cooled to 0 ºC. A solution of *p*-tolunitrile (1.20 ml, 1.17 g, 9.99 mmol) in THF (7 ml) was added to the flask, and the syringe rinsed with THF (3 ml). The reaction mixture was heated at reflux for 20 h, then cooled to 0 ºC, and then quenched with dry methanol (3 ml). The reaction mixture was diluted with hexanes (30 ml), filtered through a pad of Celite, and concentrated at reduced pressure. The yellow oil was purified by column chromatography (5 % ethyl acetate gradient and 5% triethylamine in hexanes on pre-neutralized silica) to give the title compound as a pale-yellow oil (1.54 g, 74% yield). The ^{1}H NMR spectrum was consistent with the spectrum reported in the literature.[149]

4,4′-Dimethoxybenzophenone imine(5.2c)
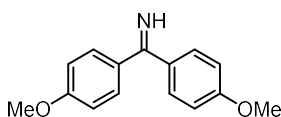
Methoxyphenylmagnesium bromide (16 ml, 1.0M, 16 mmol, 1.1 equiv) in THF was transferred to a 100 ml nitrogen-filled flask fitted with a reflux condenser, and the solution was cooled to 0 ºC. A solution of 4-methoxyobenzonitrile (2.00 g, 15.0 mmol) in dry THF (9 ml) was added to the flask, and the syringe rinsed with THF (3 ml). The reaction mixture was heated at reflux for 17 h, then cooled to 0 ºC, and then quenched with dry methanol (3 ml). The reaction mixture was diluted with hexanes (20 ml), filtered through a pad of Celite, and concentrated at reduced pressure. The yellow solid was purified by column chromatography (0 to 50% ethyl acetate gradient and 5% triethylamine in hexanes on prebasified silica) to give the title compound as an off-white powder (2.19 g, 61% yield). The ¹H NMR spectrum was consistent with the spectrum reported in the literature.[149]

Bis(3-(trifluoromethyl)phenyl)methanimine (5.2d)
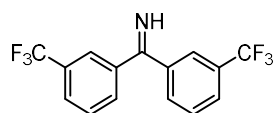
Dry magnesium turnings (370 mg, 15.2 mmol, 1.49 equiv), dry THF (10 ml), and a magnetic stir bar were placed in a nitrogen-filled flask, and the flask was connected to a reflux condenser. 3-Bromobenzotrifluoride (2.10 ml, 3.38 g, 15.0 mmol, 1.47 equiv) was dissolved in THF (3 ml), and a small amount of this solution was transferred to the reaction flask. The reaction was initiated with a single iodine crystal. The remaining aryl bromide solution was slowly transferred to the reaction flask. The syringe was rinsed with THF (3 ml) and the mixture was heated at reflux until the majority of the magnesium was visibly consumed. The reaction mixture was then cooled to 0 ºC. A solution of 3-trifluoromethylbenzonitrile (1.37 ml, 1.75 g, 10.2 mmol) in THF (2 ml) was added to the flask, and the syringe rinsed twice with THF (2 ml). The reaction mixture was heated at reflux for 4 h, then cooled to 0 ºC, and then quenched with dry methanol (2 ml). The reaction mixture was diluted with hexanes (50 ml), neutralized with sodium bicarbonate, filtered through a pad of Celite, and concentrated at reduced pressure. The red oil was purified by short path distillation (vapor temperature 110-130 ºC at approximately 0.20 Torr) as a colorless oil (2.39 g, 75% yield).

¹H NMR (400 MHz, Chloroform-*d*): δ 7.86 (s, 2H), 7.77 (d, *J* = 7.8 Hz, 2H), 7.72 (d, *J* = 7.8 Hz, 2H), 7.59 (t, *J* = 7.8 Hz, 2H).

^{13}C NMR (101 MHz, Chloroform-*d*): δ 175.7, 139.5, 131.7, 131.4 (q, *J* = 32.3 Hz), 129.4, 127.5 (q, *J* = 4.0 Hz), 125.2, 123.8 (q, *J* = 273.7 Hz).

^{19}F NMR (376 MHz, Chloroform-*d*): δ -62.8.

Physical State: pale yellow oil.

HRMS (ESI/QTOF) m/z: [M + H]$^+$ Calcd for $C_{15}H_{10}F_6N^+$ 318.0712; Found 318.0715.

The spectral data was consistent with the data reported in the literature.[149]

5.6.2 General Procedure for the synthesis of NHPI esters (General Procedure A)

A round-bottom flask or culture tube was charged with carboxylic acid (if solid, 1.0 equiv), nucleophile (*N*-hydroxyphthalimide, 1.0 equiv) and DMAP (0.1 equiv.). dichloromethane (DCM) was added (0.2 M-0.5 M) and the mixture was stirred vigorously. Carboxylic acid (if liquid, 1.0 equiv.) was added via syringe. DIC (1.1 equiv.) was then added dropwise via syringe and the mixture was allowed to stir until the carboxylic acid or the *N*-hydroxyphthalimide was fully consumed (determined by TLC). Typical reaction times were between 0.5 h and 12 h. Afterwards, the mixture was filtered over Celite and rinsed with additional CH_2Cl_2. The solvent was removed under reduced pressure, and purified by column chromatography to give the corresponding NHPI esters. Most NHPI esters are solid, which could be recrystallized (ethyl acetate and hexanes system) after column chromatography. Unless otherwise stated, NHPI esters were prepared following the General Procedure A. The preparation and spectral data of all NHPI esters used have been reported before.[46-47, 53, 241]

5.6.3 General procedure for visible-light-mediated decarboxylative amination of benzophenone imines with secondary and tertiary NHPI esters (General Procedure B)

An oven-dried 15 mL re-sealable screw-cap test tube equipped with a Teflon-coated magnetic stir bar was sequentially charged with secondary or tertiary NHPI ester (1 equiv.), **5.2a** or **5.2d** (2 equiv), [Ir(dtbbpy)(ppy)$_2$]PF$_6$ (1 mol%), Cu(MeCN)$_4$PF$_6$ (20 mol%), dimethylacetamide (DMA, 0.1 M), Cs$_2$CO$_3$ (2 equiv) in the glove box. The vial was sealed with a screw cap and removed from the glove box. Then the vial was placed 3 cm away from one blue LED, and

irradiated under fan cooling (maintain the temperature at room temperature) for 20 h. After the reaction, the resulting reaction mixture was directly purified by column chromatography (notably, the silica gel used for the purification were pre-neutralized with 5% triethylamine in hexanes solution prior to the usage, in order to minimize the product loss).

5.6.4 General procedure for visible-light-mediated decarboxylative amination of benzophenone imines with primary NHPI esters (General Procedure C)

An oven-dried 15 mL re-sealable screw-cap test tube equipped with a Teflon-coated magnetic stir bar was sequentially charged with primary NHPI ester (2 equiv.), **5.2a** or **5.2d** (1 equiv), [Ir(dtbbpy)(ppy)$_2$]PF$_6$ (1 mol%), Cu(MeCN)$_4$PF$_6$ (20 mol%), MeCN (0.1 M), diisopropylamine (2 equiv) in the glove box. The vial was sealed with a screw cap and removed from the glove box. Then the vial was placed 3 cm away from one blue LED, and irradiated under fan cooling (maintain the temperature at room temperature) for 16 h. After the reaction, the resulting reaction mixture was directly purified by column chromatography (notably, the silica gel used for the purification were pre-neutralized with 5% triethylamine in hexanes solution prior to the usage, in order to minimize the product loss).

5.6.5 General procedure for acid hydrolysis of imine products to corresponding ammonium chloride salt (General Procedure D)

An 25 mL falsk equipped with a Teflon-coated magnetic stir bar, imine product (0.2 mmol) was dissolved in methanol (3 ml). HCl$_{(aq)}$ (1.0 M, 1.5 equiv) was added dropwise to the reaction mixture with stirring. After 1 h, the reaction mixture was diluted with ether (~5 ml) and filtered through a plug of glass wool, which was rinsed with ether (1 ml) for 3 times. The volatile materials were evaporated at reduced pressure. Ether and water (~5 ml each) were added to residue, the organic layer was removed, the aqueous layer was washed again with ether (2 ml), and the combined organic layers were extracted with water (2 ml). The volatile materials were removed from the combined aqueous layers at reduced pressure. The crude ammonium chloride salt was dissolved in DCM (3 ml) and filtered through a plug of Na$_2$SO$_4$. Addition of hexanes (~8 ml) at 0 °C caused a precipitate to form, which was collected by filtration, washed with cold hexanes (2 ml) for 2 times, and dried under vacuum to give the desired compound.

5.6.6 Characterization of the reaction product

***N*-cyclohexyl-3,3'-bis(trifluoromethyl)benzophenone imine (5.3a)**
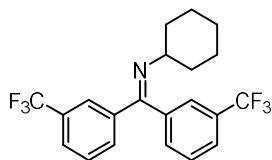
Following the General Procedure B with the corresponding NHPI ester (0.2 mmol) and **5.2d** (0.4 mmol). The crude product was purified by column chromatography (with pre-neutralized silica gel) using hexanes as an eluent to afford 56 mg (70%) of the title compound **5.3a**.

^{1}H NMR (400 MHz, Chloroform-*d*): δ 7.95 (s, 1H), 7.74 (d, *J* = 7.9 Hz, 1H), 7.67 – 7.58 (m, 3H), 7.47 – 7.40 (m, 2H), 7.36 (d, *J* = 7.6 Hz, 1H), 3.14 (tt, *J* = 9.4, 4.5 Hz, 1H), 1.83 – 1.72 (m, 2H), 1.69 – 1.54 (m, 5H), 1.27 – 1.12 (m, 3H).

^{13}C NMR (101 MHz, Chloroform-*d*): δ 162.5, 140.5, 137.3, 131.8, 131.2, 129.5, 128.8, 131.4 (q, *J* = 32.6 Hz), 130.9 (q, *J* = 32.4 Hz), 126.6 (q, *J* = 3.7 Hz), 125.6 (q, *J* = 3.8 Hz), 124.9 (q, *J* = 3.8 Hz), 124.5 (q, *J* = 3.8 Hz), 124.2 (q, *J* = 272.3 Hz), 124.0 (q, *J* = 272.5 Hz), 62.0, 34.0, 25.7, 24.3.

^{19}F NMR (376 MHz, Chloroform-*d*): δ -62.63, -62.74.

Physical State: colorless oil.

HRMS (ESI/QTOF) m/z: [M + H]$^+$ Calcd for $C_{21}H_{20}F_6N^+$ 400.1494; Found 400.1495.

***N*-cyclobutyl-3,3'-bis(trifluoromethyl)benzophenone imine (5.3b)**
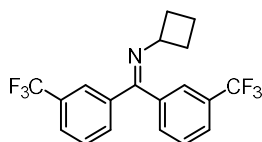
Following the General Procedure B with the corresponding NHPI ester (0.2 mmol) and **5.2d** (0.4 mmol). The crude product was purified by column chromatography (with pre-neutralized silica gel) using hexanes as an eluent to afford 42 mg (56%) of the title compound **5.3b**.

^{1}H NMR (400 MHz, Chloroform-*d*): δ 7.98 (s, 1H), 7.74 (d, *J* = 7.9 Hz, 1H), 7.68 – 7.57 (m, 3H), 7.45 (t, *J* = 7.8 Hz, 1H), 7.39 (s, 1H), 7.32 (d, *J* = 7.6 Hz, 1H), 3.93 (p, *J* = 7.7 Hz, 1H), 2.38 – 2.21 (m, 2H), 2.15 – 2.03 (m, 2H), 1.96 – 1.82 (m, 1H), 1.79 – 1.64 (m, 1H).

^{13}C NMR (101 MHz, Chloroform-*d*): δ 163.47, 140.13, 137.47, 131.85, 131.32 (q, *J* = 32.7 Hz), 131.28, 130.97 (q, *J* = 32.5 Hz), 129.37, 128.84, 126.82 (q, *J* = 3.8 Hz), 125.82 (q, *J* = 3.7 Hz),

124.92 (q, J = 3.8 Hz), 124.71 (q, J = 3.8 Hz), 124.12 (q, J = 272.5 Hz), 123.93 (q, J = 272.6 Hz), 57.52, 31.43, 16.23.

^{19}F NMR (376 MHz, Chloroform-d): δ -62.66, -62.77.

Physical State: colorless oil.

HRMS (ESI/QTOF) m/z: $[M + H]^+$ Calcd for $C_{19}H_{16}F_6N^+$ 372.1181; Found 372.1176.

N-cyclododecyl-3,3'-bis(trifluoromethyl)benzophenone imine (5.3c)
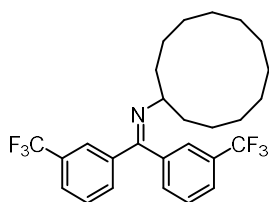
Following the General Procedure B with the corresponding NHPI ester (0.2 mmol) and **5.2d** (0.4 mmol). The crude product was purified by column chromatography (with pre-neutralized silica gel) using hexanes as an eluent to afford 58 mg (60%) of the title compound **5.3c**.

^{1}H NMR (400 MHz, Chloroform-d): δ 7.96 (s, 1H), 7.73 (d, J = 7.9 Hz, 1H), 7.70 – 7.58 (m, 3H), 7.49 – 7.39 (m, 2H), 7.35 (d, J = 7.6 Hz, 1H), 3.53 – 3.25 (m, 1H), 1.88 – 1.73 (m, 2H), 1.41 – 1.08 (m, 17H), 0.90 – 0.75 (m, 3H).

^{13}C NMR (101 MHz, Chloroform-d): δ 163.44, 140.28, 137.87, 131.78, 131.41 (q, J = 32.6 Hz), 131.30, 130.91 (q, J = 32.4 Hz), 129.48, 128.82, 126.68 (q, J = 3.6 Hz), 125.56 (q, J = 3.5 Hz), 124.85 (q, J = 3.9 Hz), 124.75 (q, J = 3.9 Hz), 124.14 (q, J = 272.6 Hz), 123.94 (q, J = 272.6 Hz), 58.13, 31.83, 23.99, 23.73, 23.21, 22.34, 22.04.

^{19}F NMR (376 MHz, Chloroform-d): δ -62.59, -62.83.

Physical State: pale yellow oil.

HRMS (ESI/QTOF) m/z: $[M + H]^+$ Calcd for $C_{27}H_{32}F_6N^+$ 484.2433; Found 484.2428.

N-(2,3-dihydro-1H-inden-2-yl)-3,3'-bis(trifluoromethyl)benzophenone imine (5.3d)
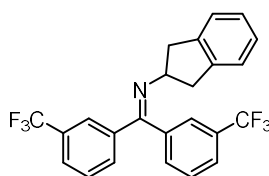
Following the General Procedure B with the corresponding NHPI ester (0.2 mmol) and **5.2d** (0.4 mmol). The crude product was purified by column chromatography (with pre-neutralized silica gel) using hexanes as an eluent to afford 63 mg (73%) of the title compound **5.3d**.

¹H NMR (400 MHz, Chloroform-*d*): δ 7.98 (d, *J* = 2.1 Hz, 1H), 7.74 (d, *J* = 8.0 Hz, 1H), 7.67 (dd, *J* = 7.8, 5.4 Hz, 3H), 7.50 – 7.39 (m, 3H), 7.23 – 7.13 (m, 4H), 4.19 (q, *J* = 7.3 Hz, 1H), 3.21 (dd, *J* = 15.5, 7.0 Hz, 2H), 3.02 (dd, *J* = 15.5, 7.6 Hz, 2H).

¹³C NMR (101 MHz, Chloroform-*d*): δ 164.43, 141.93, 139.95, 137.25, 131.94, 131.57 (q, *J* = 32.8 Hz), 131.20, 130.98 (q, *J* = 32.5 Hz), 129.61, 128.88, 126.95 (q, *J* = 4.0 Hz), 126.67, 125.89 (q, *J* = 3.7 Hz), 125.01 (q, *J* = 4.0 Hz), 124.58, 124.10 (q, *J* = 272.5 Hz), 123.90 (q, *J* = 272.5 Hz), 63.65, 41.33.

¹⁹F NMR (376 MHz, Chloroform-*d*): δ -62.64, -62.72.

Physical State: colorless oil.

HRMS (ESI/QTOF) m/z: [M + H]⁺ Calcd for $C_{24}H_{18}F_6N^+$ 434.1338; Found 434.1333.

N-(1-tosylpiperidin-4-yl)-3,3'-bis(trifluoromethyl)benzophenone imine (5.3e)
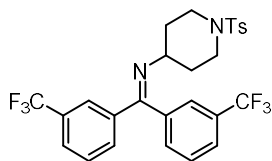
Following the General Procedure B with the corresponding NHPI ester (0.2 mmol) and **5.2d** (0.4 mmol). The crude product was purified by column chromatography (with pre-neutralized silica gel) using 0 to 30% ethyl acetate gradient in hexanes as an eluent to afford 68 mg (61%) of the title compound **5.3e**.

¹H NMR (400 MHz, Chloroform-*d*): δ 7.87 (s, 1H), 7.72 (d, *J* = 7.9 Hz, 1H), 7.68 – 7.57 (m, 4H), 7.49 (d, *J* = 7.9 Hz, 1H), 7.41 (t, *J* = 7.8 Hz, 1H), 7.36 – 7.26 (m, 4H), 3.57 (dt, *J* = 10.6, 4.7 Hz, 2H), 3.21 (s, 1H), 2.64 (ddd, *J* = 12.1, 9.3, 3.2 Hz, 2H), 2.43 (s, 3H).

¹³C NMR (101 MHz, Chloroform-*d*): δ 163.73, 143.54, 139.57, 136.56, 133.21, 131.75, 131.52 (q, *J* = 32.9 Hz), 130.87 (q, *J* = 29.8 Hz), 130.73, 129.62, 129.59, 128.76, 127.71, 126.94 (q, *J* = 3.3 Hz), 125.83 (q, *J* = 3.6 Hz), 124.59 (q, *J* = 3.5 Hz), 124.03 (q, *J* = 3.8 Hz), 123.85 (q, *J* = 272.5 Hz), 123.65 (q, *J* = 272.5 Hz), 57.23, 43.66, 32.18, 21.50.

¹⁹F NMR (376 MHz, Chloroform-*d*): -62.75, -62.80.

Physical State: white solid.

HRMS (ESI/QTOF) m/z: [M + H]$^+$ Calcd for C$_{27}$H$_{25}$F$_6$N$_2$O$_2$S$^+$ 555.1535; Found 555.1546.

(Tetrahydro-2*H*-pyran-4-yl)amine hydrochloride (5.3f)
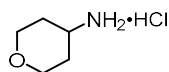
The corresponding NHPI ester (0.5 mmol) and **5.2d** (1.0 mmol) was directly transformed to the amine hydrochloride following the General Procedure B and D, the title compound **5.3f** was obtained in 50% (34 mg) overall yield.

^{1}H NMR (400 MHz, Methanol-d_4): δ 4.92 (s, 3H), 4.03 (dd, *J* = 12.0, 4.7 Hz, 2H), 3.52 – 3.34 (m, 3H), 2.11 – 1.82 (m, 2H), 1.68 (qd, *J* = 12.2, 4.7 Hz, 2H).

^{13}C NMR (101 MHz, Methanol-d_4): δ 67.74, 49.60, 32.79.

Physical State: white solid.

The ^{1}H NMR and ^{13}C NMR spectra were consistent with the spectrum reported in the literature.[242]

N-isopropyl-3,3'-bis(trifluoromethyl)benzophenone imine (5.3g)
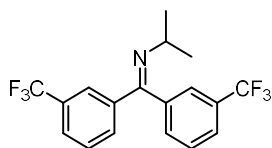
Following the General Procedure B with the corresponding NHPI ester (0.3 mmol) and **5.2d** (0.6 mmol). The crude product was purified by column chromatography (with pre-neutralized silica gel) using hexanes as an eluent to afford 48 mg (45%) of the title compound **5.3g**.

^{1}H NMR (400 MHz, Chloroform-*d*): δ 7.96 (s, 1H), 7.73 (d, *J* = 8.0 Hz, 1H), 7.68 – 7.57 (m, 3H), 7.47 – 7.39 (m, 2H), 7.36 (d, *J* = 7.6 Hz, 1H), 3.47 (p, *J* = 6.2 Hz, 1H), 1.19 (s, 3H), 1.17 (s, 3H).

^{13}C NMR (101 MHz, Chloroform-*d*): δ 162.37, 140.36, 137.32, 131.81, 131.46 (q, *J* = 32.7 Hz), 131.10, 130.93 (q, *J* = 33.6 Hz), 129.50, 128.81, 126.71 (q, *J* = 3.9 Hz), 125.66 (q, *J* = 3.8 Hz), 124.87 (q, *J* = 4.0 Hz), 124.41 (q, *J* = 3.8 Hz), 124.14 (q, *J* = 272.4 Hz), 123.94 (q, *J* = 272.4 Hz), 53.62, 23.96.

^{19}F NMR (376 MHz, Chloroform-*d*): δ -62.63, -62.75.

Physical State: yellow oil.

HRMS (ESI/QTOF) m/z: [M + H]$^+$ Calcd for C$_{18}$H$_{16}$F$_6$N$^+$ 360.1181; Found 360.1176.

N-(heptan-3-yl)-3,3'-bis(trifluoromethyl)benzophenone imine (5.3h)
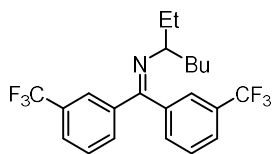
Following the General Procedure B with the corresponding NHPI ester (0.3 mmol) and **5.2d** (0.6 mmol). The crude product was purified by column chromatography (with pre-neutralized silica gel) using hexanes as an eluent to afford 62 mg (50%) of the title compound **5.3h**.

^{1}H NMR (400 MHz, Chloroform-d): δ 7.95 (s, 1H), 7.72 (d, J = 7.9 Hz, 1H), 7.70 – 7.57 (m, 3H), 7.48 – 7.39 (m, 2H), 7.34 (d, J = 7.6 Hz, 1H), 3.09 (dt, J = 11.8, 5.8 Hz, 1H), 1.67 – 1.52 (m, 4H), 1.26 – 1.09 (m, 4H), 0.85 (t, J = 7.0 Hz, 3H), 0.80 (t, J = 7.4 Hz, 3H).

^{13}C NMR (101 MHz, Chloroform-d): δ 163.19, 140.44, 137.70, 131.77, 131.50, 131.27 (q, J = 32.7 Hz), 130.92 (q, J = 32.4 Hz), 129.30, 128.83, 126.65 (q, J = 3.7 Hz), 125.45 (q, J = 3.7 Hz), 124.99 (q, J = 3.8 Hz), 124.87 (q, J = 3.9 Hz), 124.10 (q, J = 260.2 Hz), 123.97 (q, J = 272.5 Hz), 77.48, 77.16, 76.84, 64.13, 36.09, 29.51, 28.98, 22.95, 14.15, 11.20.

^{19}F NMR (376 MHz, Chloroform-d): δ -62.61, -62.83.

Physical State: colorless oil.

HRMS (ESI/QTOF) m/z: [M + H]$^+$ Calcd for C$_{22}$H$_{24}$F$_6$N$^+$ 416.1807; Found 416.1814.

N-tert-butyl-3,3'-bis(trifluoromethyl)benzophenone imine (5.4a)
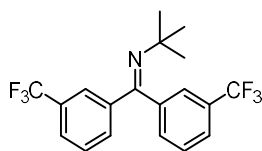
Following the General Procedure B with the corresponding NHPI ester (0.3 mmol) and **5.2d** (0.6 mmol). The crude product was purified by column chromatography (with pre-neutralized silica gel) using hexanes as an eluent to afford 50 mg (45%) of the title compound **5.4a**.

^{1}H NMR (400 MHz, Chloroform-d): δ 7.94 (s, 1H), 7.71 (d, J = 8.0 Hz, 1H), 7.64 – 7.53 (m, 2H), 7.52 (d, J = 8.0 Hz, 1H), 7.47 (s, 1H), 7.41 (d, J = 7.7 Hz, 2H), 1.17 (s, 9H).

^{13}C NMR (101 MHz, Chloroform-d): δ 160.23, 142.01, 139.97, 131.80, 131.51, 130.90 (q, J = 32.7 Hz), 130.76 (q, J = 32.3 Hz), 128.85, 128.65, 126.38 (q, J = 3.7 Hz), 125.35 (q, J = 3.8 Hz), 125.23 (q, J = 3.8 Hz), 124.59 (q, J = 4.0 Hz), 124.21 (q, J = 272.4 Hz), 123.89 (q, J = 272.4 Hz), 57.71, 31.65.

19F NMR (376 MHz, Chloroform-*d*): δ -62.65, -62.79.

Physical State: colorless oil.

HRMS (ESI/QTOF) m/z: [M + H]$^+$ Calcd for C$_{19}$H$_{18}$F$_6$N$^+$ 374.1338; Found 374.1340.

N-tert-pentyl-3,3'-bis(trifluoromethyl)benzophenone imine (5.4b)
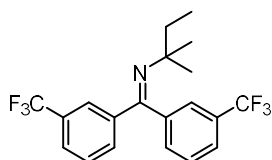
Following the General Procedure B with the corresponding NHPI ester (0.3 mmol) and **5.2d** (0.6 mmol). The crude product was purified by column chromatography (with pre-neutralized silica gel) using hexanes as an eluent to afford 59 mg (51%) of the title compound **5.4b**.

1H NMR (400 MHz, Chloroform-*d*): δ 7.92 (s, 1H), 7.71 (d, *J* = 7.9 Hz, 1H), 7.64 – 7.51 (m, 3H), 7.47 (s, 1H), 7.40 (t, *J* = 7.4 Hz, 2H), 1.61 (q, *J* = 7.4 Hz, 2H), 1.02 (s, 6H), 0.96 (t, *J* = 7.4 Hz, 3H).

13C NMR (101 MHz, Chloroform-*d*): 160.26, 142.12, 140.18, 131.73, 131.44, 130.85 (q, *J* = 32.7 Hz), 130.74 (q, *J* = 32.3 Hz), 128.81, 128.65, 126.33, 125.33, 125.17 (q, *J* = 3.8 Hz), 124.55 (q, *J* = 3.7 Hz), 124.21 (q, *J* = 272.4 Hz), 123.89 (q, *J* = 272.4 Hz), 60.12, 38.50, 28.48, 9.18.

19F NMR (376 MHz, Chloroform-*d*): δ -62.69, -62.79.

Physical State: colorless oil.

HRMS (ESI/QTOF) m/z: [M + H]$^+$ Calcd for C$_{20}$H$_{20}$F$_6$N$^+$ 388.1494; Found 388.1506.

N-(1-methylcyclohexyl)-3,3'-bis(trifluoromethyl)benzophenone imine (5.4c)
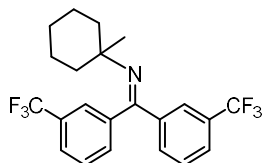
Following the General Procedure B with the corresponding NHPI ester (0.2 mmol) and **5.2d** (0.4 mmol). The crude product was purified by column chromatography (with pre-neutralized silica gel) using hexanes as an eluent to afford 50 mg (61%) of the title compound **5.4c**.

1H NMR (400 MHz, Chloroform-*d*): δ 7.93 (s, 1H), 7.71 (d, *J* = 7.9 Hz, 1H), 7.58 (dd, *J* = 18.6, 7.6 Hz, 3H), 7.48 (s, 1H), 7.44 – 7.37 (m, 2H), 1.70 – 1.52 (m, 5H), 1.45 (ddd, *J* = 14.3, 6.7, 3.3 Hz, 2H), 1.30 (td, *J* = 10.0, 5.3 Hz, 3H), 1.02 (s, 3H).

¹³C NMR (101 MHz, Chloroform-*d*): δ 160.40, 142.17, 140.34, 131.45, 131.40, 130.85 (q, *J* = 32.7 Hz), 130.75 (q, *J* = 32.3 Hz), 128.83, 128.66, 125.37 (q, *J* = 3.7 Hz), 125.33 (q, *J* = 3.7 Hz), 124.92 (q, *J* = 3.7 Hz), 124.52 (q, *J* = 3.7 Hz), 124.20 (q, *J* = 272.4 Hz), 123.94 (q, *J* = 272.4 Hz), 59.44, 40.49, 28.30, 26.00, 22.96.

¹⁹F NMR (376 MHz, Chloroform-*d*): δ -62.67, -62.79.

Physical State: pale yellow oil.

HRMS (ESI/QTOF) m/z: [M + H]⁺ Calcd for $C_{22}H_{22}F_6N^+$ 414.1651; Found 414.1650.

N-(adamantan-1-yl)-3,3'-bis(trifluoromethyl)benzophenone imine (5.4d)
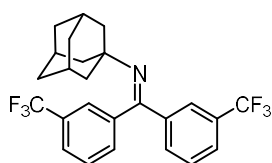
Following the General Procedure B with the corresponding NHPI ester (0.2 mmol) and **5.2d** (0.4 mmol). The crude product was purified by column chromatography (with pre-neutralized silica gel) using hexanes as an eluent to afford 51 mg (56%) of the title compound **5.4d**.

¹H NMR (400 MHz, Chloroform-*d*): δ 7.94 (s, 1H), 7.70 (d, *J* = 8.0 Hz, 1H), 7.63 – 7.48 (m, 3H), 7.47 (s, 1H), 7.39 (t, *J* = 8.0 Hz, 2H), 1.99 (q, *J* = 3.2 Hz, 3H), 1.70 – 1.51 (m, 12H).

¹³C NMR (101 MHz, Chloroform-*d*): δ 159.46, 142.21, 140.48, 131.68, 131.50, 130.72 (q, *J* = 32.3 Hz), 130.73 (q, *J* = 32.6 Hz), 128.74, 128.61, 126.31 (q, *J* = 3.4 Hz), 125.29 (q, *J* = 4.2 Hz), 125.14 (q, *J* = 3.8 Hz), 124.58 (q, *J* = 4.1 Hz), δ 124.22 (q, *J* = 272.7.2 Hz), 123.97 (q, *J* = 272.7.2 Hz), 58.84, 44.36, 36.43, 29.77.

¹⁹F NMR (376 MHz, Chloroform-*d*): δ -62.63, -62.73.

Physical State: colorless oil.

HRMS (ESI/QTOF) m/z: [M + H]⁺ Calcd for $C_{25}H_{24}F_6N^+$ 452.1807; Found 452.1810.

N-(3,5-dimethyladamantan-1-yl)-benzophenone imine (5.4e)
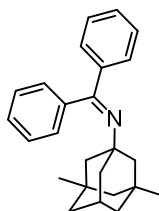
Following the General Procedure B with the corresponding NHPI ester (0.3 mmol) and **5.2a** (0.6 mmol). The crude product was purified by column chromatography (with pre-neutralized silica gel) using hexanes as an eluent to afford 44 mg (43%) of the title compound **5.4e**.

¹H NMR (400 MHz, Chloroform-*d*): δ 7.58 – 7.49 (m, 2H), 7.42 – 7.33 (m, 3H), 7.33 – 7.22 (m, 4H), 7.23 – 7.13 (m, 2H), 2.06 – 1.97 (m, 1H), 1.51 (d, *J* = 3.3 Hz, 2H), 1.39 (s, 4H), 1.20 (d, *J* = 3.1 Hz, 4H), 1.05 (s, 2H), 0.76 (s, 6H).

¹³C NMR (101 MHz, Chloroform-*d*): δ 163.14, 142.29, 140.45, 129.38, 128.45, 128.17, 127.97, 127.90, 127.76, 60.02, 50.73, 50.67, 42.85, 42.47, 32.50, 30.67, 30.57.

Physical State: colorless oil.

HRMS (APCI/QTOF) m/z: [M + H]⁺ Calcd for $C_{25}H_{30}N^+$ 344.2373; Found 344.2369.

N-(4-pentylbicyclo[2.2.2]octan-1-yl)-3,3'-bis(trifluoromethyl)benzophenone imine (5.4f)
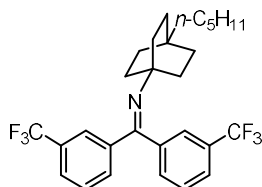
Following the General Procedure B with the corresponding NHPI ester (0.3 mmol) and **5.2d** (0.6 mmol). The crude product was purified by column chromatography (with pre-neutralized silica gel) using 0 to 20% ethyl acetate gradient in hexanes as an eluent to afford 58 mg (39%) of the title compound **5.4f**.

¹H NMR (400 MHz, Chloroform-*d*): δ 7.91 (s, 1H), 7.70 (d, *J* = 7.8 Hz, 1H), 7.61 – 7.53 (m, 2H), 7.50 – 7.45 (m, 1H), 7.42 (s, 1H), 7.38 (t, *J* = 7.5 Hz, 2H), 1.65 – 1.55 (m, 6H), 1.40 – 1.31 (m, 6H), 1.26 (q, *J* = 7.3 Hz, 2H), 1.21 – 1.09 (m, 4H), 1.04 – 0.96 (m, 2H), 0.85 (t, *J* = 7.2 Hz, 3H).

¹³C NMR (101 MHz, Chloroform-*d*): δ 160.14, 142.11, 140.56, 131.85, 131.47, 130.80 (q, *J* = 32.6 Hz), 130.71 (q, *J* = 32.3 Hz), 128.81, 128.60, 126.30 (q, *J* = 3.8 Hz), 125.26 (q, *J* = 3.4 Hz), 125.16 (q, *J* = 3.4 Hz), 124.56 (q, *J* = 4.1 Hz), 124.20 (q, *J* = 272.4 Hz), 123.96 (q, *J* = 272.4 Hz), 58.74, 41.38, 33.82, 32.94, 31.71, 30.80, 23.54, 22.81, 14.21.

¹⁹F NMR (376 MHz, Chloroform-*d*): δ -62.65, -62.70.

Physical State: colorless oil.

HRMS (ESI/QTOF) m/z: [M + H]⁺ Calcd for $C_{28}H_{32}F_6N^+$ 496.2433; Found 496.2432.

N-hexyl-3,3'-bis(trifluoromethyl)benzophenone imine (5.5a)
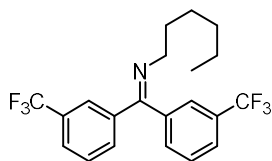
Following the General Procedure C with the corresponding NHPI ester (0.4 mmol) and **5.2d** (0.2 mmol). The crude product was purified by column chromatography (with pre-neutralized silica gel) using hexanes as an eluent to afford 79 mg (99%) of the title compound **5.5a**.

^{1}H NMR (400 MHz, Chloroform-*d*): δ 7.95 (s, 1H), 7.74 (d, *J* = 7.9 Hz, 1H), 7.64 (t, *J* = 7.7 Hz, 3H), 7.49 – 7.40 (m, 2H), 7.36 (d, *J* = 7.6 Hz, 1H), 3.35 (t, *J* = 7.0 Hz, 2H), 1.75 – 1.65 (m, 2H), 1.31 – 1.23 (m, 6H), 0.87 (t, *J* = 6.9 Hz, 3H).

^{13}C NMR (101 MHz, Chloroform-*d*): δ 164.70, 140.19, 137.04, 131.72, 131.64, 131.33, 131.15, 130.82, 129.52, 128.86, 126.79 (q, *J* = 4.6 Hz), 125.76 (q, *J* = 3.6 Hz), 125.47, 125.28, 124.80 (q, *J* = 3.8 Hz), 124.68 (q, *J* = 3.8 Hz), 122.76, 122.57, 54.36, 31.74, 31.13, 27.30, 22.71, 14.15.

^{19}F NMR (376 MHz, Chloroform-*d*): δ -62.67, -62.74.

Physical State: colorless oil.

HRMS (ESI/QTOF) m/z: [M + H]$^+$ Calcd for $C_{21}H_{22}F_6N^+$ 402.1651; Found 402.1658.

N-heptadecyl-3,3'-bis(trifluoromethyl)benzophenone imine (5.5b)
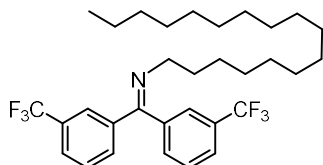
Following the General Procedure C with the corresponding NHPI ester (0.4 mmol) and **5.2d** (0.2 mmol). The crude product was purified by column chromatography (with pre-neutralized silica gel) using hexanes as an eluent to afford 89 mg (80%) of the title compound **5.5b**.

^{1}H NMR (400 MHz, Chloroform-*d*): δ 7.95 (s, 1H), 7.74 (d, *J* = 7.9 Hz, 1H), 7.64 (t, *J* = 7.4 Hz, 3H), 7.50 – 7.39 (m, 2H), 7.36 (d, *J* = 7.6 Hz, 1H), 3.35 (t, *J* = 7.0 Hz, 2H), 1.69 (p, *J* = 7.1 Hz, 2H), 1.33 – 1.20 (m, 28H), 0.88 (t, *J* = 6.7 Hz, 3H).

^{13}C NMR (101 MHz, Chloroform-*d*): δ 164.68, 140.20, 137.05, 131.72, 131.49 (q, *J* = 32.4 Hz), 131.33, 130.99 (q, *J* = 32.5 Hz), 129.52, 128.85, 126.78 (q, *J* = 3.9 Hz), 125.76 (q, *J* = 3.8 Hz), 124.80 (q, *J* = 3.9 Hz), 124.69 (q, *J* = 3.8 Hz), 124.12 (q, *J* = 272.5 Hz), 123.93 (q, *J* = 272.6 Hz), 54.37, 32.09, 31.18, 29.86, 29.82, 29.77, 29.72, 29.56, 29.53, 27.63, 22.85, 14.27.

¹⁹F NMR (376 MHz, Chloroform-*d*): δ -62.67, -62.74.

Physical State: colorless oil.

HRMS (ESI/QTOF) m/z: [M + H]⁺ Calcd for $C_{32}H_{44}F_6N^+$ 556.3372; Found 556.3376.

N-isobutyl-3,3'-bis(trifluoromethyl)benzophenone imine (5.5c)
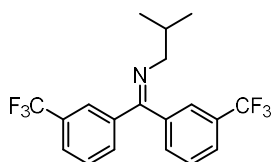
Following the General Procedure C with the corresponding NHPI ester (0.4 mmol) and **5.2d** (0.2 mmol). The crude product was purified by column chromatography (with pre-neutralized silica gel) using hexanes as an eluent to afford 68 mg (91%) of the title compound **5.5c**.

¹H NMR (400 MHz, Chloroform-*d*): δ 7.95 (s, 1H), 7.73 (d, *J* = 7.9 Hz, 1H), 7.65 (d, *J* = 7.9 Hz, 3H), 7.45 (t, *J* = 7.8 Hz, 1H), 7.41 (s, 1H), 7.35 (d, *J* = 7.6 Hz, 1H), 3.17 (d, *J* = 6.6 Hz, 2H), 2.13 – 1.97 (m, 1H), 0.95 (s, 3H), 0.93 (s, 3H).

¹³C NMR (101 MHz, Chloroform-*d*): δ 137.11, 131.71, 131.41, 131.32, 131.14, 130.82, 129.53, 128.86, 125.47, 125.29, 124.77, 124.73, 122.76, 122.58, 61.94, 30.28, 20.89.

¹⁹F NMR (376 MHz, Chloroform-*d*): δ -62.69, -62.73.

Physical State: colorless oil.

HRMS (ESI/QTOF) m/z: [M + H]⁺ Calcd for $C_{19}H_{18}F_6N^+$ 374.1338; Found 374.1332.

N-(5-phenylpentyl)-3,3'-bis(trifluoromethyl)benzophenone imine (5.5d)
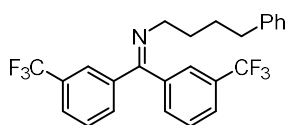
Following the General Procedure C with the corresponding NHPI ester (0.4 mmol) and **5.2d** (0.2 mmol). The crude product was purified by column chromatography (with pre-neutralized silica gel) using hexanes as an eluent to afford 83 mg (92%) of the title compound **5.5d**.

¹H NMR (400 MHz, Chloroform-*d*): δ 7.99 (s, 1H), 7.77 (d, *J* = 7.9 Hz, 1H), 7.72 – 7.61 (m, 3H), 7.48 (t, *J* = 7.8 Hz, 1H), 7.45 (s, 1H), 7.37 (d, *J* = 7.6 Hz, 1H), 7.32 – 7.27 (m, 2H), 7.25 – 7.15 (m, 3H), 3.41 (t, *J* = 6.6 Hz, 2H), 2.65 (t, *J* = 7.3 Hz, 2H), 1.84 – 1.66 (m, 4H).

¹³C NMR (101 MHz, Chloroform-*d*): δ 164.85, 142.47, 140.12, 136.98, 131.72, 131.50 (q, *J* = 32.9 Hz), 131.30, 130.98 (q, *J* = 32.4 Hz), 129.56, 128.86, 128.51, 128.42, 126.82 (q, *J* = 3.7 Hz),

125.85, 125.79 (q, J = 3.8 Hz), 124.78 (q, J = 3.9 Hz), 124.64 (q, J = 3.8 Hz), 124.11 (q, J = 272.4 Hz), 123.91 (q, J = 272.4 Hz), 54.12, 35.79, 30.76, 29.33.

19F NMR (376 MHz, Chloroform-*d*): δ -62.65, -62.70.

Physical State: yellow oil.

HRMS (ESI/QTOF) m/z: [M + H]$^+$ Calcd for $C_{25}H_{22}F_6N^+$ 450.1651; Found 450.1657.

Methyl 6-((bis(3-(trifluoromethyl)phenyl)methylene)amino)hexanoate (5.5e)
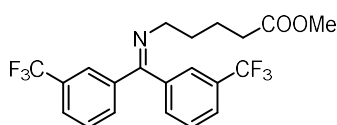
Following the General Procedure C with the corresponding NHPI ester (0.4 mmol) and **5.2d** (0.2 mmol). The crude product was purified by column chromatography (with pre-neutralized silica gel) using 0 to 30% ethyl acetate gradient in hexanes as an eluent to afford 62 mg (72%) of the title compound **5.5e**.

1H NMR (400 MHz, Chloroform-*d*): δ 7.95 (s, 1H), 7.74 (d, J = 7.9 Hz, 1H), 7.64 (t, J = 8.3 Hz, 3H), 7.45 (t, J = 7.7 Hz, 1H), 7.42 (s, 1H), 7.36 (d, J = 7.6 Hz, 1H), 3.65 (d, J = 1.2 Hz, 3H), 3.36 (t, J = 6.3 Hz, 2H), 2.32 (t, J = 7.0 Hz, 2H), 1.80 – 1.65 (m, 4H).

13C NMR (101 MHz, Chloroform-*d*): δ 174.09, 165.13, 139.99, 136.90, 131.74, 131.57 (q, J = 34.4 Hz), 131.26, 131.00 (q, J = 32.5 Hz), 129.62, 128.89, 125.87 (q, J = 3.9 Hz), 124.79 (q, J = 4.2 Hz), 124.58 (q, J = 3.8 Hz), 124.09 (q, J = 272.5 Hz), 123.89 (q, J = 272.5 Hz), 53.76, 51.65, 33.97, 30.61, 23.03.

19F NMR (376 MHz, Chloroform-*d*): δ -62.68, -62.73.

Physical State: colorless oil.

HRMS (ESI/QTOF) m/z: [M + H]$^+$ Calcd for $C_{21}H_{20}F_6NO_2^+$ 432.1393; Found 432.1388.

N-(10-bromodecyl)-3,3'-bis(trifluoromethyl)benzophenone imine (5.5f)
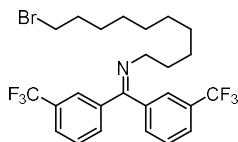
Following the General Procedure C with the corresponding NHPI ester (0.4 mmol) and **5.2d** (0.2 mmol). The crude product was purified by column chromatography (with pre-neutralized silica gel) using hexanes as an eluent to afford 83 mg (78%) of the title compound **5.5f**.

¹H NMR (400 MHz, Chloroform-*d*): δ 7.96 (s, 1H), 7.74 (d, *J* = 7.9 Hz, 1H), 7.64 (t, *J* = 8.1 Hz, 3H), 7.49 – 7.40 (m, 2H), 7.36 (d, *J* = 7.6 Hz, 1H), 3.40 (t, *J* = 6.8 Hz, 2H), 3.35 (t, *J* = 7.0 Hz, 2H), 1.84 (p, *J* = 6.9 Hz, 2H), 1.73 – 1.65 (m, 2H), 1.28 (d, *J* = 10.8 Hz, 12H).

¹³C NMR (101 MHz, Chloroform-*d*): δ 164.68, 140.19, 137.04, 131.72, 131.47 (q, *J* = 30.4 Hz), 131.32, 130.97 (q, *J* = 32.4 Hz), 129.52, 128.85, 126.76 (q, *J* = 3.7 Hz), 125.74 (q, *J* = 3.7 Hz), 124.76 (q, *J* = 3.9 Hz), 124.66 (q, *J* = 3.8 Hz), 124.11 (q, *J* = 272.5 Hz), 123.92 (q, *J* = 272.5 Hz), 54.33, 34.15, 32.96, 31.14, 29.54, 29.49, 29.47, 28.87, 28.29, 27.58.

¹⁹F NMR (376 MHz, Chloroform-*d*): δ -62.66, -62.72.

Physical State: colorless oil.

HRMS (ESI/QTOF) m/z: [M + H]⁺ Calcd for $C_{25}H_{29}BrF_6N^+$ 536.1382; Found 536.1387.

N-(3,3,4,4,5,5,6,6,7,7,8,8,9,9,10,10,10-heptadecafluorodecyl)-benzophenone imine (5.5g)
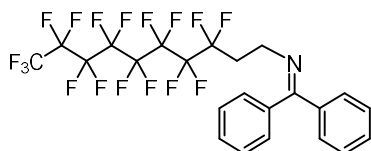
Following the General Procedure C with the corresponding NHPI ester (0.4 mmol) and **5.2a** (0.2 mmol). The crude product was purified by column chromatography (with pre-neutralized silica gel) using hexanes as an eluent to afford 66 mg (53%) of the title compound **5.5g**.

¹H NMR (400 MHz, Chloroform-*d*): δ 7.66 – 7.57 (m, 2H), 7.54 – 7.30 (m, 6H), 7.22 – 7.12 (m, 2H), 3.66 (t, *J* = 7.5 Hz, 2H), 2.72 – 2.40 (m, 2H).

¹³C NMR (101 MHz, Chloroform-*d*): δ 170.10, 139.57, 136.48, 130.43, 128.90, 128.86, 128.57, 128.29, 127.64, 45.72 (t, *J* = 3.9 Hz), 32.86 (t, *J* = 21.1 Hz).

¹⁹F NMR (376 MHz, Chloroform-*d*): δ -80.84 (t, *J* = 10.0 Hz), -113.70 (t, *J* = 13.1 Hz), -121.70, -121.96, -122.76, -123.67, -126.15.

Physical State: yellow oil.

HRMS (ESI/QTOF) m/z: [M + H]⁺ Calcd for $C_{23}H_{15}F_{17}N^+$ 628.0928; Found 628.0928.

N-(cyclopentylmethyl)-3,3'-bis(trifluoromethyl)benzophenone imine (5.5h)
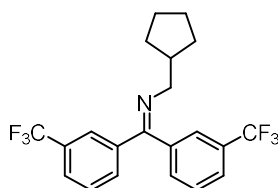
Following the General Procedure C with the corresponding NHPI ester (derived from 6-heptenoic acid, 0.4 mmol) and **5.2d** (0.2 mmol). The crude product was purified by column chromatography (with pre-neutralized silica gel) using hexanes as an eluent to afford 52 mg (65%) of the title compound **5.5h**.

^{1}H NMR (400 MHz, Chloroform-*d*): δ 7.95 (s, 1H), 7.73 (d, *J* = 7.9 Hz, 1H), 7.64 (d, *J* = 7.8 Hz, 3H), 7.45 (t, *J* = 7.8 Hz, 1H), 7.42 (s, 1H), 7.36 (d, *J* = 7.6 Hz, 1H), 3.31 (d, *J* = 6.9 Hz, 2H), 2.27 (hept, *J* = 7.5 Hz, 1H), 1.90 – 1.69 (m, 2H), 1.61 – 1.50 (m, 4H), 1.29 – 1.14 (m, 2H).

^{13}C NMR (101 MHz, Chloroform-*d*): δ 164.43, 140.29, 137.16, 131.71, 131.47 (q, *J* = 32.6 Hz), 131.44, 130.96 (q, *J* = 32.4 Hz), 129.52, 128.84, 126.74 (q, *J* = 3.8 Hz), 125.72 (q, *J* = 3.7 Hz), 124.13 (q, *J* = 272.5 Hz), 123.94 (q, *J* = 272.5 Hz), 59.40, 41.56, 30.84, 25.30.

^{19}F NMR (376 MHz, Chloroform-*d*): δ -62.68, -62.72.

Physical State: colorless oil.

HRMS (ESI/QTOF) m/z: [M + H]$^+$ Calcd for $C_{21}H_{20}F_6N^+$ 400.1494; Found 400.1505.

N-(but-3-en-1-yl)-3,3'-bis(trifluoromethyl)benzophenone imine (5.5i)
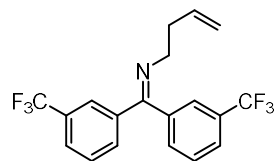
Following the General Procedure C with the corresponding NHPI ester (derived from cyclopropylacetic acid, 0.4 mmol) and **5.2d** (0.2 mmol). The crude product was purified by column chromatography (with pre-neutralized silica gel) using hexanes as an eluent to afford 28 mg (38%) of the title compound **5.5i**.

^{1}H NMR (400 MHz, Chloroform-*d*): δ 7.95 (s, 1H), 7.74 (d, *J* = 8.0 Hz, 1H), 7.64 (td, *J* = 7.7, 3.9 Hz, 3H), 7.51 – 7.39 (m, 2H), 7.37 (d, *J* = 7.7 Hz, 1H), 5.80 (ddt, *J* = 17.0, 10.2, 6.8 Hz, 1H), 5.14 – 4.92 (m, 2H), 3.44 (t, *J* = 7.0 Hz, 2H), 2.48 (q, *J* = 7.0 Hz, 2H).

^{13}C NMR (101 MHz, Chloroform-*d*): δ 165.23, 140.09, 136.90, 136.40, 131.76, 131.67, 131.34, 131.16, 130.84, 129.56, 128.87, 126.94, 126.91, 126.87, 125.87, 125.83, 125.45, 125.26, 124.87, 124.83, 124.78, 124.74, 124.70, 122.74, 122.55, 116.38, 53.84, 35.51.

^{19}F NMR (376 MHz, Chloroform-*d*): δ -62.69, -62.75.

Physical State: light yellow oil.

HRMS (APCI/QTOF) m/z: [M + H]$^+$ Calcd for $C_{19}H_{16}F_6N^+$ 372.1181; Found 372.1187.

(*E*)-*N*-(heptadec-8-en-1-yl)-3,3'-bis(trifluoromethyl)benzophenone imine (5.6a)
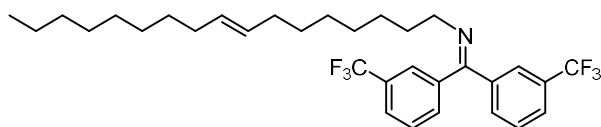
Following the General Procedure C with the corresponding NHPI ester (0.4 mmol) and **5.2d** (0.2 mmol). The crude product was purified by column chromatography (with pre-neutralized silica gel) using hexanes as an eluent to afford 94 mg (85%) of the title compound **5.6a**.

¹H NMR (400 MHz, Chloroform-*d*): δ 7.95 (s, 1H), 7.74 (d, *J* = 7.9 Hz, 1H), 7.64 (t, *J* = 7.6 Hz, 3H), 7.49 – 7.41 (m, 2H), 7.36 (d, *J* = 7.6 Hz, 1H), 5.37 (t, *J* = 4.0 Hz, 2H), 3.35 (t, *J* = 7.0 Hz, 2H), 1.95 (p, *J* = 5.1, 4.4 Hz, 4H), 1.75 – 1.63 (m, 2H), 1.33 – 1.23 (m, 20H), 0.87 (t, *J* = 6.6 Hz, 3H).

¹³C NMR (101 MHz, Chloroform-*d*): δ 164.69, 140.20, 137.05, 131.71, 131.48 (q, *J* = 32.7 Hz), 131.32, 130.98 (q, *J* = 32.5 Hz), 130.59, 130.39, 129.91 (q, *J* = 272.5 Hz), 129.52, 128.85, 126.78 (q, *J* = 3.6 Hz), 125.75 (q, *J* = 3.7 Hz), 124.79 (q, *J* = 3.8 Hz), 124.68 (q, *J* = 3.8 Hz), 124.11 (q, *J* = 272.5 Hz), 54.36, 32.76, 32.72, 32.05, 31.17, 29.85, 29.81, 29.73, 29.64, 29.47, 29.42, 29.34, 29.20, 27.60, 22.83, 14.26.

¹⁹F NMR (376 MHz, Chloroform-*d*): δ -62.67, -62.73.

Physical State: colorless oil.

HRMS (ESI/QTOF) m/z: [M + H]⁺ Calcd for $C_{32}H_{42}F_6N^+$ 554.3216; Found 554.3212.

(*Z*)-*N*-(heptadec-8-en-1-yl)-3,3'-bis(trifluoromethyl)benzophenone imine (5.6b)
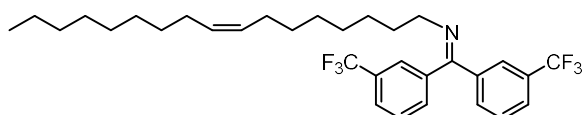
Following the General Procedure C with the corresponding NHPI ester (0.4 mmol) and **5.2d** (0.2 mmol). The crude product was purified by column chromatography (with pre-neutralized silica gel) using hexanes as an eluent to afford 90 mg (82%) of the title compound **5.6b**.

¹H NMR (400 MHz, Chloroform-*d*): δ 7.96 (s, 1H), 7.74 (d, *J* = 7.9 Hz, 1H), 7.64 (t, *J* = 6.4 Hz, 3H), 7.49 – 7.40 (m, 2H), 7.36 (d, *J* = 7.6 Hz, 1H), 5.42 – 5.24 (m, 2H), 3.36 (t, *J* = 7.0 Hz, 2H), 2.01 (q, *J* = 6.6 Hz, 4H), 1.70 (p, *J* = 7.0 Hz, 2H), 1.28 (d, *J* = 11.5 Hz, 20H), 0.88 (t, *J* = 6.7 Hz, 3H).

¹³C NMR (101 MHz, Chloroform-*d*): δ 164.68, 140.20, 137.07, 131.71, 131.49 (q, *J* = 34.6 Hz), 131.33, 130.99 (q, *J* = 32.5 Hz), 130.11, 129.92, 129.52, 128.85, 126.77 (q, *J* = 3.7 Hz), 125.75 (q, *J* = 3.7 Hz), 124.79 (q, *J* = 3.9 Hz), 124.68 (q, *J* = 3.8 Hz), 124.12 (q, *J* = 272.5 Hz), 123.92 (q, *J* = 272.5 Hz), 54.36, 32.06, 31.19, 29.93, 29.87, 29.68, 29.48, 29.36, 27.62, 27.37, 27.34, 22.84, 14.24.

¹⁹F NMR (376 MHz, Chloroform-*d*): δ -62.68, -62.75.

Physical State: colorless oil.

HRMS (ESI/QTOF) m/z: $[M + H]^+$ Calcd for $C_{32}H_{42}F_6N^+$ 554.3216; Found 554.3213.

N-((8Z,11Z)-heptadeca-8,11-dien-1-yl)-3,3'-bis(trifluoromethyl)benzophenone imine (5.6c)
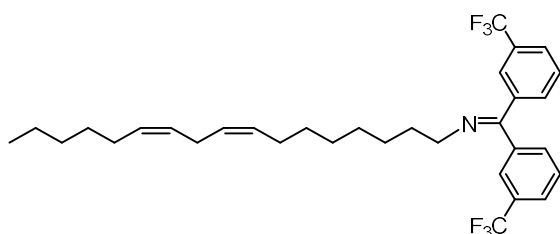
Following the General Procedure C with the corresponding NHPI ester (0.4 mmol) and **5.2d** (0.2 mmol). The crude product was purified by column chromatography (with pre-neutralized silica gel) using hexanes as an eluent to afford 89 mg (81%) of the title compound **5.6c**.

¹H NMR (400 MHz, Chloroform-*d*): δ 7.97 (s, 1H), 7.74 (d, *J* = 7.9 Hz, 1H), 7.64 (t, *J* = 6.4 Hz, 3H), 7.49 – 7.40 (m, 2H), 7.37 (d, *J* = 7.6 Hz, 1H), 5.35 (m, 4H), 3.36 (t, *J* = 7.0 Hz, 2H), 2.77 (t, *J* = 6.3 Hz, 2H), 2.05 (q, *J* = 7.1 Hz, 4H), 1.69 (q, *J* = 7.1 Hz, 2H), 1.43 – 1.15 (m, 17H), 0.89 (t, *J* = 6.8 Hz, 3H).

¹³C NMR (101 MHz, Chloroform-*d*): δ 164.69, 140.19, 131.71, 131.50 (q, *J* = 32.5 Hz), 131.32, 130.99 (q, *J* = 32.5 Hz), 130.34, 130.21, 129.52, 128.85, 128.16, 128.06, 126.78 (q, *J* = 3.7 Hz), 125.75 (q, *J* = 3.6 Hz), 124.79 (q, *J* = 3.8 Hz), 124.67 (q, *J* = 3.8 Hz), 124.13 (q, *J* = 272.5 Hz), 123.93 (q, *J* = 272.5 Hz), 54.35, 31.68, 31.18, 29.86, 29.76, 29.50, 29.47, 29.36, 27.61, 27.35, 25.78, 22.72, 14.20.

¹⁹F NMR (376 MHz, Chloroform-*d*): δ -62.68, -62.74.

Physical State: pale yellow oil.

HRMS (APPI/LTQ-Orbitrap) m/z: $[M + H]^+$ Calcd for $C_{32}H_{40}F_6N^+$ 552.3059; Found 552.3072.

(8R,9S,10S,13R,14S,17R)-17-((R)-4-((bis(3-(trifluoromethyl)phenyl)methylene)amino)butan-2-yl)-10,13-dimethyldodecahydro-3H-cyclopenta[a]phenanthrene-3,7,12(2H,4H)-trione (5.6d)
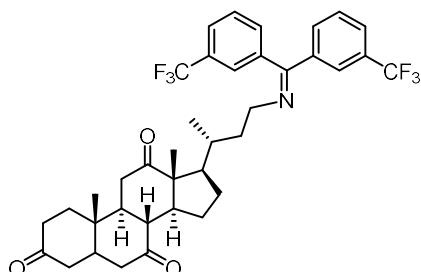
Following the General Procedure C with the corresponding NHPI ester (0.4 mmol) and **5.2d** (0.2 mmol). The crude product was purified by column chromatography (with pre-neutralized silica gel) using hexanes as an eluent to afford 69 mg (51%) of the title compound **5.6d**.

¹H NMR (400 MHz, Chloroform-*d*): δ 7.96 (s, 1H), 7.73 (d, *J* = 7.9 Hz, 1H), 7.63 (t, *J* = 7.6 Hz, 2H), 7.58 (d, *J* = 7.9 Hz, 1H), 7.48 – 7.39 (m, 2H), 7.36 (d, *J* = 7.6 Hz, 1H), 3.55 – 3.37 (m, 1H), 3.39 – 3.21 (m, 1H), 2.95 – 2.75 (m, 3H), 2.39 – 1.74 (m, 16H), 1.60 (td, *J* = 14.3, 5.1 Hz, 1H), 1.50 – 1.20 (m, 8H), 1.12 (d, *J* = 6.5 Hz, 2H), 1.05 (s, 3H), 0.75 (d, *J* = 6.4 Hz, 3H).

¹³C NMR (101 MHz, Chloroform-*d*): δ 164.76, 156.99, 140.13, 136.89, 131.69, 131.42 (q, *J* = 31.0 Hz), 131.27, 130.91 (q, *J* = 32.4 Hz), 129.54, 128.85, 126.74 (q, *J* = 3.7 Hz), 125.79 (q, *J* = 3.7 Hz), 124.69 (q, *J* = 3.9 Hz), 124.54 (q, *J* = 3.8 Hz), 124.07 (d, *J* = 272.5 Hz), 123.87 (d, *J* = 272.5 Hz), 60.49, 57.02, 51.97, 51.81, 49.08, 46.94, 45.92, 45.62, 45.09, 42.89, 42.25, 38.72, 36.72, 36.59, 36.11, 35.37, 34.36, 27.76, 25.22, 23.61, 21.99, 19.21, 14.30, 11.91.

¹⁹F NMR (376 MHz, Chloroform-*d*): δ -62.68, -62.69.

Physical State: white solid.

HRMS (ESI/QTOF) m/z: $[M + H]^+$ Calcd for $C_{38}H_{42}F_6NO_3^+$ 674.3063; Found 674.3066.

(3-(4-(bis(2-chloroethyl)amino)phenyl)propyl) 3,3'-bis(trifluoromethyl)benzophenone imine (5.6e)
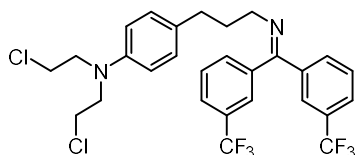
Following the General Procedure C with the corresponding NHPI ester (0.4 mmol) and **5.2d** (0.2 mmol). The crude product was purified by column chromatography (with pre-neutralized silica gel) using hexanes as an eluent to afford 79 mg (69%) of the title compound **5.6e**.

¹H NMR (400 MHz, Chloroform-*d*): δ 7.97 (s, 1H), 7.74 (d, *J* = 7.9 Hz, 1H), 7.64 (dt, *J* = 15.8, 7.6 Hz, 3H), 7.47 (t, *J* = 7.8 Hz, 1H), 7.41 (s, 1H), 7.34 (d, *J* = 7.6 Hz, 1H), 7.05 (d, *J* = 8.4 Hz, 2H), 6.60 (d, *J* = 8.6 Hz, 2H), 3.73 – 3.57 (m, 8H), 3.38 (t, *J* = 6.8 Hz, 2H), 2.61 (t, *J* = 7.6 Hz, 2H), 2.00 (p, *J* = 7.2 Hz, 2H).

¹³C NMR (101 MHz, Chloroform-*d*): δ 164.98, 144.34, 140.11, 136.96, 131.71, 131.45 (q, *J* = 32.5 Hz), 131.29, 131.19, 130.99 (q, *J* = 32.5 Hz), 129.73, 129.52, 128.88, 126.84 (q, *J* = 3.8 Hz), 125.76 (q, *J* = 3.8 Hz), 124.78 (q, *J* = 3.9 Hz), 124.60 (q, *J* = 3.8 Hz), 124.10 (q, *J* = 272.5 Hz), 123.89 (q, *J* = 272.5 Hz), 112.31, 53.77, 53.55, 40.67, 32.83, 32.55.

¹⁹F NMR (376 MHz, Chloroform-*d*): δ -62.65, -62.66.

Physical State: yellow oil.

HRMS (ESI/QTOF) m/z: [M + H]⁺ Calcd for $C_{28}H_{27}Cl_2F_6N_2^+$ 575.1450; Found 575.1457.

N-((1*R*,4a*R*,4b*R*,10a*R*)-7-isopropyl-1,4a-dimethyl-1,2,3,4,4a,4b,5,6,10,10a-decahydrophenanthren-1-yl)-1,1-diphenylmethanimine (5.6f)
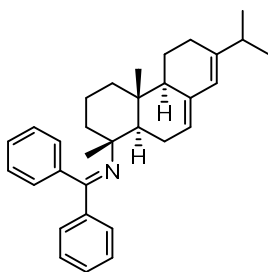
Following the General Procedure B with the corresponding NHPI ester (0.2 mmol) and **5.2a** (0.4 mmol). The crude product was purified by column chromatography (with pre-neutralized silica gel) using hexanes as an eluent to afford 43 mg (49%, *d.r.*=10.1:1) of the title compound **5.6f**.

¹H NMR (400 MHz, Chloroform-*d*): δ 7.54 – 7.46 (m, 2H), 7.41 – 7.32 (m, 3H), 7.27 (q, *J* = 6.6 Hz, 4H), 7.20 – 7.11 (m, 2H), 5.84 (s, 1H), 5.54 (d, *J* = 5.1 Hz, 1H), 2.61 (dd, *J* = 12.6, 4.6 Hz, 1H), 2.24 (p, *J* = 7.0 Hz, 1H), 2.04 (td, *J* = 19.5, 9.8 Hz, 5H), 1.83 – 1.74 (m, 2H), 1.56 – 1.02 (m, 12H), 0.98 (s, 3H), 0.82 (s, 3H).

13C NMR (101 MHz, Chloroform-*d*): δ 162.19, 145.10, 142.54, 140.48, 135.53, 129.31, 128.66, 128.14, 127.94, 127.90, 127.85, 127.81, 127.74, 122.71, 122.37, 61.84, 53.54, 51.52, 40.39, 38.40, 35.62, 35.07, 27.74, 27.72, 24.81, 22.85, 21.77, 21.59, 21.04, 19.70, 14.01.

Physical State: colorless oil.

HRMS (ESI/QTOF) m/z: $[M + H]^+$ Calcd for $C_{32}H_{40}N^+$ 438.3155; Found 438.3158.

N-(5-(2,5-dimethylphenoxy)-2-methylpentan-2-yl)-3,3'-bis(trifluoromethyl)benzophenone imine (5.6g)
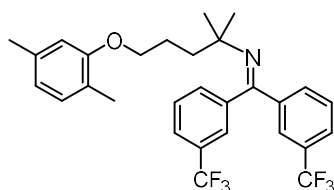
Following the General Procedure B with the corresponding NHPI ester (0.2 mmol) and **5.2d** (0.4 mmol). The crude product was purified by column chromatography (with pre-neutralized silica gel) using hexanes as an eluent to afford 52 mg (50%) of the title compound **5.6g**.

1H NMR (400 MHz, Chloroform-*d*): δ 7.90 (s, 1H), 7.72 (d, *J* = 7.9 Hz, 1H), 7.64 – 7.55 (m, 3H), 7.49 (s, 1H), 7.42 (d, *J* = 8.0 Hz, 2H), 7.02 (d, *J* = 7.4 Hz, 1H), 6.70 – 6.61 (m, 2H), 3.99 (t, *J* = 6.3 Hz, 2H), 2.31 (s, 3H), 2.20 (s, 3H), 2.02 – 1.89 (m, 2H), 1.84 – 1.73 (m, 2H), 1.08 (s, 6H).

13C NMR (101 MHz, Chloroform-*d*): δ 160.52, 157.21, 141.94, 140.01, 136.61, 131.70, 131.41, 130.42, 131.00 (q, *J* = 16.0 Hz), 130.67 (q, *J* = 15.7 Hz), 128.90, 128.69, 126.45 (q, *J* = 3.7 Hz), 125.52, 125.40 (q, *J* = 3.8 Hz), 125.28, 125.16 (q, *J* = 3.8 Hz), 124.56 (q, *J* = 4.0 Hz), 123.73, 122.82, 122.57, 120.78, 112.17, 68.49, 59.69, 42.91, 28.91, 25.12, 21.54, 15.92.

19F NMR (376 MHz, Chloroform-*d*): δ -62.66, -62.75.

Physical State: colorless oil.

HRMS (ESI/QTOF) m/z: $[M + H]^+$ Calcd for $C_{29}H_{30}F_6NO^+$ 522.2226; Found 522.2231.

Amphetamine hydrochloride (5.7a)
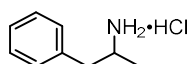
Following the General Procedure B and D with the corresponding NHPI ester (0.4 mmol) and **5.2d** (0.8 mmol), the title compound **5.7a** was obtained in 60% (41 mg) overall yield.

1H NMR (400 MHz, Chloroform-*d*): δ 8.50 (s, 3H), 7.46 – 7.04 (m, 5H), 3.75 – 3.41 (m, 1H), 3.27 (dd, *J* = 13.4, 5.4 Hz, 1H), 2.89 (dd, *J* = 13.4, 9.1 Hz, 1H), 1.41 (d, *J* = 6.5 Hz, 3H).

13C NMR (101 MHz, Chloroform-*d*): δ 135.87, 129.46, 129.03, 127.43, 49.94, 41.27, 18.32.

Physical State: white solid.

The ¹H NMR and ¹³C NMR spectra were consistent with the spectrum reported in the literature.[243]

trans-2-Phenylcyclopropylamine hydrochloride (5.7b)
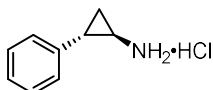
Following the General Procedure B and D with the corresponding NHPI ester (0.5 mmol) and **5.2d** (1.0 mmol), the title compound **5.7b** was obtained in 41% (35 mg) overall yield.

¹H NMR (400 MHz, Chloroform-*d*): δ 8.76 (s, 3H), 7.36 – 7.08 (m, 5H), 2.94 – 2.79 (m, 1H), 2.68 (ddd, *J* = 10.3, 6.7, 3.5 Hz, 1H), 1.69 (ddd, *J* = 10.6, 6.7, 4.3 Hz, 1H), 1.26 (q, *J* = 6.8 Hz, 1H).

¹³C NMR (101 MHz, Chloroform-*d*): δ 138.06, 128.76, 127.04, 126.85, 31.01, 21.99, 13.57.

Physical State: white solid.

The ¹H NMR and ¹³C NMR spectra were consistent with the spectrum reported in the literature.[244]

Chapter 6

Decarboxylative C(sp³)-O Cross-Coupling via Synergetic Photoredox and Copper Catalysis

Chapter 6

6.1   Introduction of the background
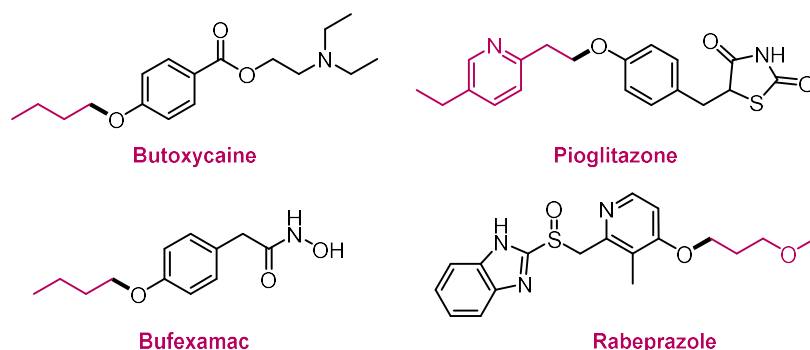
Figure 70 Examples of drug molecules containing alkyl aryl ether moieties.

In Chapter 2.3, we have outlined the importance of ethers in natural products, pharmaceuticals and agrochemicals.[111, 245] Alkaryl ethers, in particular, accounted for about 20% of the top 200 drugs in 2018. (Figure 70).[144] For this reason, the construction of alkyl aryl ethers is of great interest to chemists. In the last two decades, transition metal-catalyzed *O*-arylation of aliphatic alcohols have become one of the most important methods for the synthesis of alkyl aryl ethers.[116, 123-124, 246-247] By virtue of its wide range and good functional group tolerance, this method has significant advantages over conventional methods such as nucleophilic substitution (S$_N$2)[127-128] and nucleophilic aryl substitution (S$_N$Ar).[129] However, according to a generally accepted catalytic cycle for transition metal-catalyzed C–O cross-coupling of aryl halides and primary alcohols (Figure 71), such approach typically requires harsh conditions, including strong bases and high temperatures. Besides, activated electrophiles are critical for the success to undergo oxidative elimination (the process of **I** to **II**, Figure 71), which somewhat limits the choice of electrophiles. Furthermore, in contrast to analogous processes in metal-catalyzed C-N cross-couplings, reductive elimination from the high-valence complex [L$_n$M(Ar)(alkoxy)] in C-O couplings is sluggish (the process of **IV** to **I**, Figure 71), so that competitive β-hydride elimination may occur (the process of **IV** to **V**, Figure 71), leading to an overall reduction of the aryl halide to generate arene ArH.[248-249] Therefore, a mild and robust method for the preparation of alkyl aryl ethers will aid in the advancement of this field.
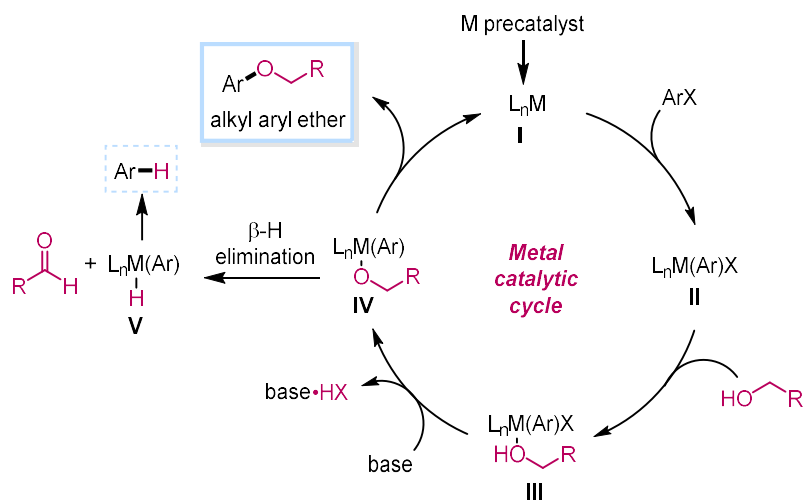
Figure 71 General catalytic cycle for transition metal (M)-catalyzed C–O cross-coupling of aryl halides and primary alcohols.

Catalytic $C(sp^3)$-O coupling of alkyl electrophiles with phenols, on the other hand, is an attractive alternative for the synthesis of alkyl aryl ethers (Figure 72b). A catalytic version of Williamson ether synthesis has the potential to overcome some intrinsic deficiencies of classical Williamson ether synthesis such as harsh conditions, restricted scope, and poor functional group tolerance.[127] More importantly, if applying alkyl NHPI esters, other than alkyl halides or aryl halides, to the coupling reactions, base-promoted elimination from alkyl electrophiles or reduction of aryl halides (the process of **IV** to **V**, Figure 71) will no longer be concerned (Figure 71, Figure 72a).[248-249] [248-249]
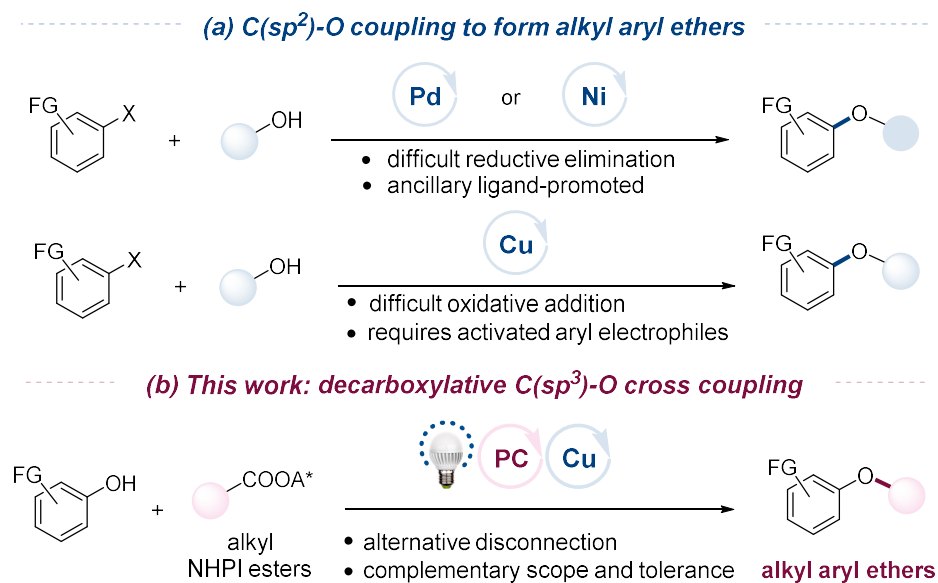
Figure 72 (a) Comparison of C-O cross-coupling methodologies for the transition metal-catalyzed synthesis of alkyl aryl ethers. (b) This work: decarboxylative C(sp^3)-O cross-coupling.

Chapter 4 and Chapter 5 have elaborated on the successful development of synergetic photoredox and copper catalysis for decarboxylative C(sp^3)-N cross-coupling. In this regard, we reasoned our established tandem photoredox/copper catalysis system might also offer an alternative method for the construction of C(sp^3)-O bonds, thus facilitating the synthesis of alkyl aryl ethers (Figure 72b).

6.2   Screening of reaction conditions

6.2.1   Optimization of reaction parameters for secondary alkyl NHPI esters

We began our investigation by subjecting cyclohexyl NHPI ester **2.22** and guaiacol **5.2a** to the conditions previously employed for decarboxylative C(sp^3)-N cross-coupling of NHPI esters with anilines[250] (Chapter 4, Table 16, entry 1). To our delight, the desired ether **5.3a** was formed, albeit in a low yield (16%, Table 21, entry 1).

It is noteworthy that we chose guaiacol **5.2a** as a nucleophilic reagent for the template reaction. There are two reasons for this: (1) the traditional transition metal-catalyzed synthesis of alkyl aryl ethers relies heavily on activated aryl halides. For this reason, the coupling effect is usually poor for aryl halides containing electron-donating groups, especially those containing neighboring electron-donating substituent groups (with sterically bulky effect). Therefore, we hope that by using guaiacol **5.2a**, which is a monomethoxybenzene that consists of phenol with a methoxy substituent at the ortho position, as the nucleophilic reagent to explore the advantages of the current approach over others. (2) At the same time, guaiacol can also act as an *O, O*-type ligand. This property may avoid relying on an external ligand to modulate the activity of the catalytic system, thus simplifying the screening process and speeding up the discovery of optimal reaction conditions.

Table 21 Summary of the effects of reaction parameters and conditions on the reaction efficiency of secondary alkyl NHPI ester
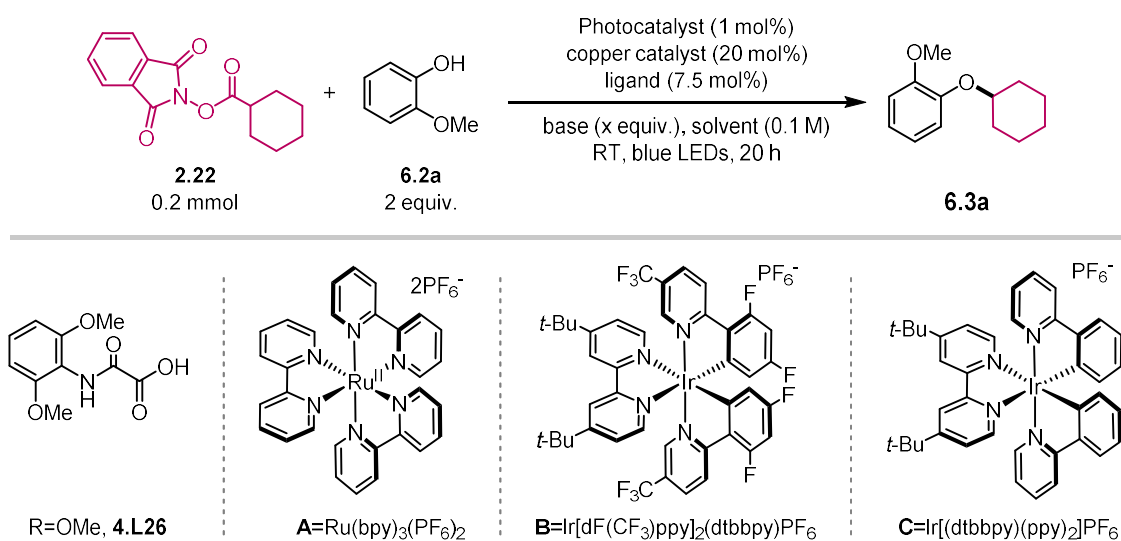
entry	PC	copper catalyst	base (x equiv.)	solvent	yield (%)^a
1^b	**A**	CuBr/**4.L26**	Et$_3$N (5 equiv.)	MeCN	16%
2	**A**	CuBr	Et$_3$N (2 equiv.)	MeCN	19%
3	**A**	CuCl	Et$_3$N (2 equiv.)	MeCN	22%
4^c	**A**	Cu	Et$_3$N (5 equiv.)	MeCN	5%
5	**A**	CuCl$_2$	Et$_3$N (5 equiv.)	MeCN	9%
6^d	**A**	CuCl	Cs$_2$CO$_3$ (2 equiv.)	MeCN	trace
7	**A**	CuCl	Et$_3$N (5 equiv.)	DMF	trace
8	**A**	CuCl	Et$_3$N (5 equiv.)	DCM	32%
9	**A**	CuCl	Et$_3$N (2 equiv.)	DCM	44%
10	**B**	CuCl	Et$_3$N (2 equiv.)	DCM	21%
11	**C**	CuCl	Et$_3$N (2 equiv.)	DCM	62%
12^e	**C**	(CuOTf)$_2$•C$_6$H$_6$	Et$_3$N (2 equiv.)	DCM	82%
13^{e,f}	**C**	(CuOTf)$_2$•C$_6$H$_6$	Et$_3$N (2 equiv.)	DCM	94%
14^{e,g}	**C**	(CuOTf)$_2$•C$_6$H$_6$	Et$_3$N (2 equiv.)	DCM	0%
15^e	none	(CuOTf)$_2$•C$_6$H$_6$	Et$_3$N (2 equiv.)	DCM	0%
16	**C**	none	Et$_3$N (2 equiv.)	DCM	0%

^{a}Corrected GC yield using n-dodecane as an internal standard. ^{b}Same condition as the optimized reaction condition in Chapter 4, Table 16, entry 1. Reaction was carried out with **2.22** (0.2 mmol), **6.2a** (2 equiv.), Ru(bpy)$_3$(PF$_6$)$_2$ (1 mol%), CuBr (20 mol%), **4.L26** (7.5 mol%), Et$_3$N (5 equiv.) and MeCN (2.0 mL). ^{c}Cu (100 mol%). ^{d}Yield of the O-acylation product is 85%. ^{e}(CuOTf)$_2$•C$_6$H$_6$ (10 mol%). ^{f}DCM (0.05 M). ^{g}No light.

The coupling was then optimized by varying reaction parameters and a summary of key observations is shown in Table 21. As mentioned earlier, guaiacol can also act as a bidentate ligand in cross-coupling reactions, so we attempted reactions without the addition of auxiliary ligands. To our surprise, the omission of the ligand was feasible (Table 21, entry 2), giving a 19% yield. CuCl is slightly better than CuBr, raising the reaction yield to 22% (Table 21, entry 3). By comparing copper catalysts in different valence states, we found that Cu(I) catalysts were the best, while Cu(II) and Cu(0) catalysts gave lower yields (Table 21, entries 2-5). When Et$_3$N was replaced by an inorganic base - Cs$_2$CO$_3$ - O-acylation of phenol instead of O-alkylation (up to 85%) was observed (Table 21, entry 6). CH$_2$Cl$_2$ was the best solvent (Table 21, entries 6-8), and decreasing the amount of base was able to increase the yield (Table 21, entry 9). Changing the photocatalyst from [Ru(bpy)$_3$](PF$_6$)$_2$ to an Ir-based photocatalyst could be beneficial (Table 21, entries 9-11), and the best photocatalyst was [Ir(dtbbpy)(ppy)$_2$]PF$_6$ (Table 21, entry 11). Further

optimization indicated that using (CuOTf)$_2$•C$_6$H$_6$ (10 mol%) as the copper catalyst and decreasing the concentration could further improve the yields (Table 21, entries 12 and 13). The best conditions were [Ir(dtbbpy)(ppy)$_2$]PF$_6$ (1 mol%) as the photocatalyst, (CuOTf)$_2$•C$_6$H$_6$ (10 mol%) as the copper catalyst, triethylamine (2 equiv.) as the base, and CH$_2$Cl$_2$ (0.05 M) as the solvent, blue LED irradiation, 20 h. A yield of 94% was obtained under these conditions (Table 21, entry 13). Control experiments disclosed the essential roles of light, photocatalyst, and copper catalyst for the coupling (Table 21, entries 14-16).

6.2.2   Optimization of reaction parameters for primary alkyl NHPI esters

For the coupling of primary alkyl NHPI esters, a modification of reaction conditions was necessary (Table 22). To start with, we tested the coupling efficiency of NHPI ester **6.1a** and guaiacol **5.2a** under the standard conditions of secondary NHPI ester (Table 21, entry 13); however, only a 9% yield was obtained (Table 22, entry 1).

Considering the high activity of primary radicals, setting the nucleophilic reagent **6.2a** as a limiting reagent while adjusting **6.1a** from 1 equivalent to 2 equivalents may be helpful. As expected, the yield of the reaction could be increased to 16% (Table 22, entry 2). Furthermore, the yield of the reaction was slightly increased when the copper catalyst loading was raised from 10 mol% to 20 mol% (Table 22, entry 3). Various copper catalysts were then screened and the results showed that Cu(MeCN)$_4$OTf was the most suitable copper catalyst (25% yield, Table 22, entries 3-6), probably due to its good solubility in DCM. Besides, the efficiency of the reaction did not decrease significantly when the equivalence of triethylamine was reduced from 2 equivalents to 1 equivalent.

It is noteworthy that during the study of the photoredox/copper-catalyzed decarboxylation system, we found that bases play a crucial role in promoting the construction of different types of bonds (see Table 14, Table 19 and Table 20). Therefore, we carefully screened a variety of bases and presented representative results in Table 22, entries 7-14. The results showed that inorganic bases were not applicable to this reaction. Amine-based organic bases, on the other hand, could give better results. More importantly, after comparing different amine-based organic bases, we found that tertiary amines with sterically bulky groups were able to give satisfactory yields (Table 22, entries 10-14). As a result, *N*-isopropyl-*N*-methyl-*tert*-butylamine (1 eq.) proved to be the best

base to boost the yield to 43% (Table 22, entry 14). Furthermore, increasing copper catalyst loading could further increase the reaction yield to 65% (Table 22, entry 15). Interestingly, the reaction yield could be further enhanced to 79% when the reaction was carried out at 0 °C - room temperature (Table 22, entry 16). The optimized conditions for the coupling of primary alkyl NHPI esters were NHPI ester (2 equiv.), phenol (1 equiv.), [Ir(dtbbpy)(ppy)$_2$]PF$_6$ (1 mol%) as the photocatalyst, Cu(MeCN)$_4$OTf (40 mol%) as the copper catalyst, and *N*-isopropyl-*N*-methyl-*tert*-butylamine (1 equiv.) as the base in CH$_2$Cl$_2$ (0.05 M), irradiated at 0-R.T. for 20 h.

Table 22 Summary of the effects of reaction parameters and conditions on the reaction efficiency of primary alkyl NHPI ester
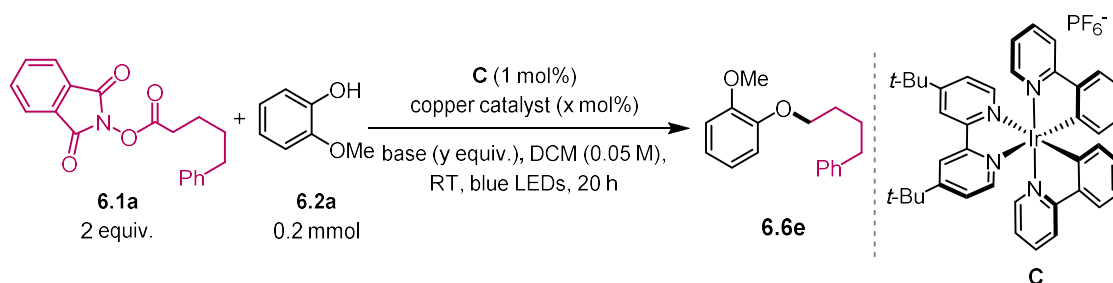
entry	copper catalyst (x mol%)	base (y equiv.)	yield (%)^a
1^b	(CuOTf)$_2$•C$_6$H$_6$ (10 mol%)	Et$_3$N (2 equiv.)	9%
2	(CuOTf)$_2$•C$_6$H$_6$ (10 mol%)	Et$_3$N (2 equiv.)	16%
3	(CuOTf)$_2$•C$_6$H$_6$ (20 mol%)	Et$_3$N (2 equiv.)	20%
4	CuCl (20 mol%)	Et$_3$N (2 equiv.)	17%
5	Cu(MeCN)$_4$PF$_6$ (20 mol%)	Et$_3$N (2 equiv.)	21%
6	Cu(MeCN)$_4$OTf (20 mol%)	Et$_3$N (2 equiv.)	25%
7	Cu(MeCN)$_4$OTf (20 mol%)	Et$_3$N (1 equiv.)	20%
8	Cu(MeCN)$_4$OTf (20 mol%)	Cs$_2$CO$_3$ (1 equiv.)	trace
9	Cu(MeCN)$_4$OTf (20 mol%)	K$_2$CO$_3$ (1 equiv.)	trace
10	Cu(MeCN)$_4$OTf (20 mol%)	DABCO (1 equiv.)	9%
11	Cu(MeCN)$_4$OTf (20 mol%)	DIPEA (1 equiv.)	26%
12	Cu(MeCN)$_4$OTf (20 mol%)	dicyclohexylamine (1 equiv.)	21%

13	Cu(MeCN)$_4$OTf (20 mol%)	N-isopropyl-tert-butyl amine (1 equiv.)	32%
14	Cu(MeCN)$_4$OTf (20 mol%)	N-isopropyl-N-methyl-tert-butyl amine (1 equiv.)	43%
15	Cu(MeCN)$_4$OTf (40 mol%)	N-isopropyl-N-methyl-tert-butyl amine (1 equiv.)	65%
16[c]	Cu(MeCN)$_4$OTf (40 mol%)	N-isopropyl-N-methyl-tert-butyl amine (1 equiv.)	79%

[a]Corrected GC yield using n-dodecane as an internal standard. [b]Same condition as the optimized reaction condition in Table 21, entry 13. Reaction was carried out with **2.22** (0.2 mmol), **6.2a** (2 equiv.), **C** (1 mol%), (CuOTf)$_2$•C$_6$H$_6$ (10 mol%), Et$_3$N (2 equiv.) and DCM (0.05 M), RT, blue LEDs, 20 h. [c]0 ºC-RT. BTMG= 2-tert-butyl-1,1,3,3-tetramethylguanidine; DABCO=1,4-diazabicyclo[2.2. 2]octane; DIPEA= N,N-diisopropylethylamine.

6.3   Scope of the decarboxylative C(sp³)-O cross-coupling

6.3.1   Scope of phenols

With the optimal condition in hand, we next investigated the scope of the decarboxylative C(sp³)-O cross-coupling. As shown in Figure 73, a diverse range of phenols that containing electron-donating (**6.3a**, **6.3b** and **6.3d**), electron-neutral (**6.3c**), and electron-withdrawing (**6.3e**-**6.3j**) groups were coupled smoothly to deliver the corresponding ethers in moderate to excellent yields. Importantly, synthetically useful functional groups like aryl halides (**6.3e**-**6.3i**), aryl boronic ester (**6.3k**) groups were well-tolerated in the coupling, indicating its excellent chemoselectivity. Other phenols containing important functional groups such as ketone (**6.3j**), cyano (**6.3l**), trifluoromethoxy (**6.3m**) groups, and polycyclic aromatic ring (**6.3n**) were also able to couple in synthetically useful yields. Notably, although GC analysis indicated a higher calibrated GC yield (72% GC yield) of **6.3m**, its volatile nature led to a diminished isolated yield (54%).
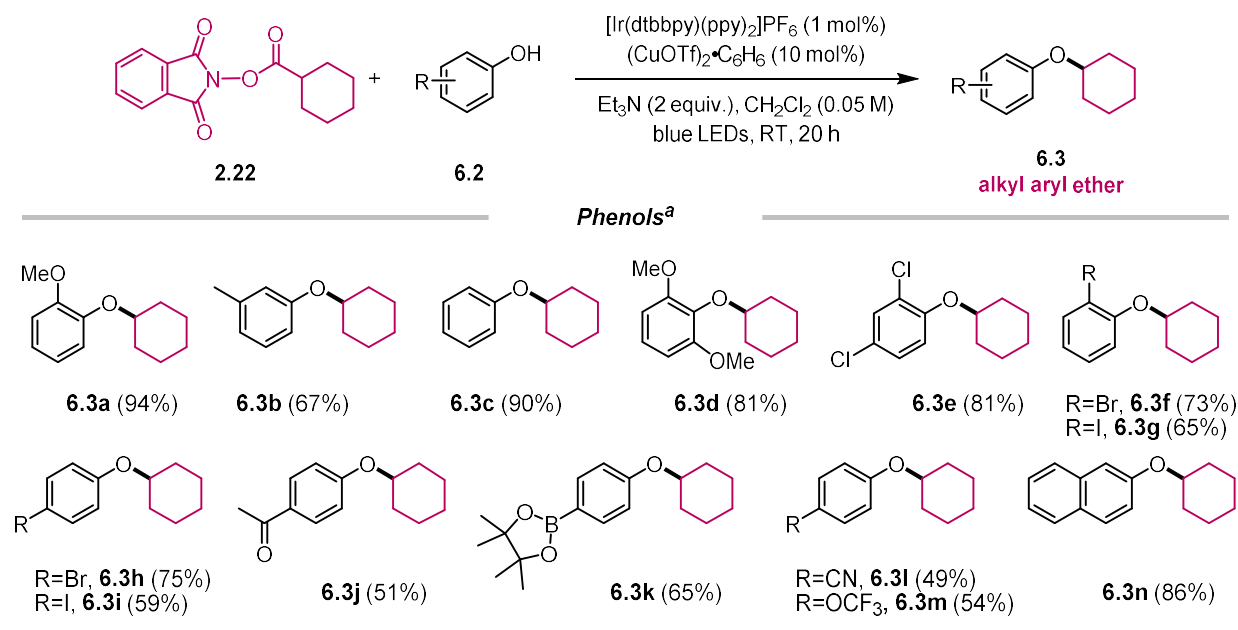
Figure 73 Scope of phenols. ᵃNHPI ester (1 equiv.), phenol (2 equiv.), [Ir(dtbbpy)(ppy)₂]PF₆ (1 mol%), (CuOTf)₂•C₆H₆ (10 mol%) and Et₃N (2 equiv.) in CH₂Cl₂ (0.05 M), irradiated at room temperature for 20 h, isolated yield.

6.3.2   Scope of secondary and tertiary alkyl NHPI esters

We then tested various secondary alkyl NHPI esters, including those containing cyclic alkyl groups (Figure 74, **6.4a-6.4c**), heterocyclic alkyl group (**6.4d**), and acyclic alkyl groups (**6.4e-6.4g**). To our delight, all these alkyl NHPI esters were coupled with ease. In our previously reported decarboxylative C(sp³)-N cross-coupling reaction, tertiary alkyl NHPI esters could not be coupled effectively.[251] In contrast, some tertiary NHPI esters, which generated non-planarizable radicals via a SET process, could be coupled in good to excellent yields (Figure 74, **6.5a-6.5f**). These sterically bulky ether products are difficult to access otherwise using classic Williamson ether synthesis, underscoring the importance of this method in complementing conventional syntheses.
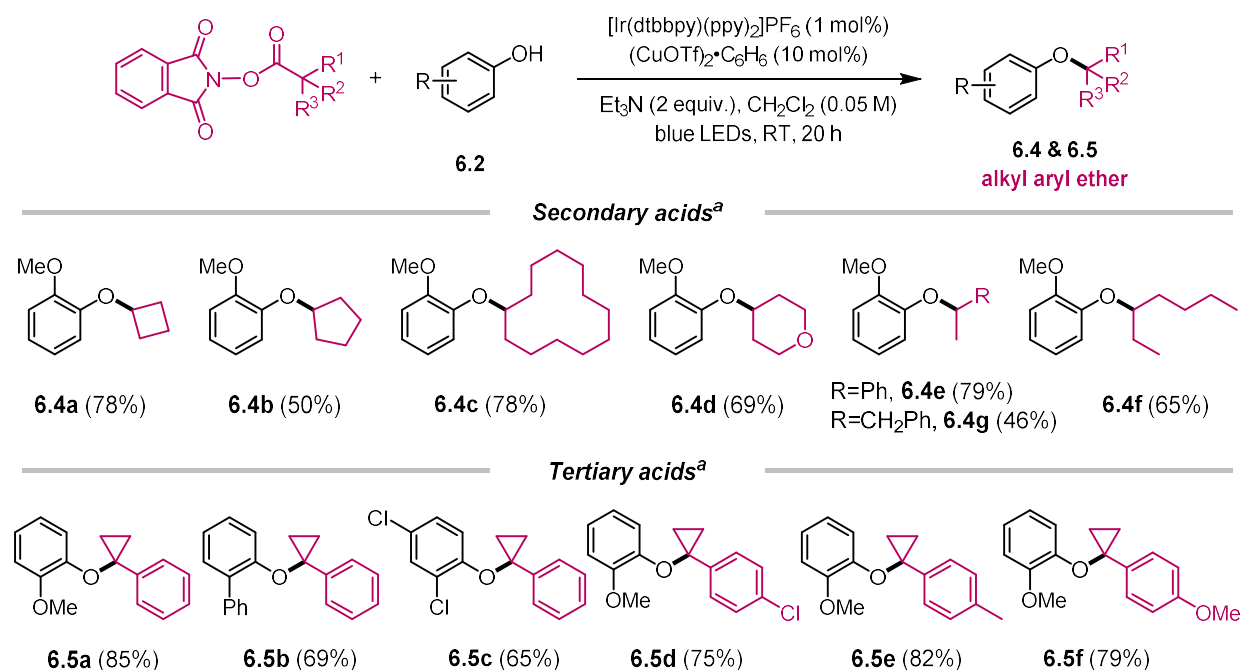
Figure 74 Scope of secondary and tertiary alkyl NHPI esters. ^{a}NHPI ester (1 equiv.), phenol (2 equiv.), [Ir(dtbbpy)(ppy)$_2$]PF$_6$ (1 mol%), (CuOTf)$_2$•C$_6$H$_6$ (10 mol%) and Et$_3$N (2 equiv.) in CH$_2$Cl$_2$ (0.05 M), irradiated at room temperature for 20 h, isolated yield.

6.3.3   Scope of primary alkyl NHPI esters

Primary aliphatic carboxylic acids stand for a class of the most readily available feedstocks; the transformation of them into high value-added alkyl aryl ethers would be highly desirable. Thus

we examined the reactivity of the corresponding NHPI esters derived from primary aliphatic carboxylic acids.

A variety of primary alkyl NHPI esters are reliable coupling partners. (Figure 75, **6.6a-6.6m**). Both non-activated alkyl (**6.6a-6.6f**) and activated benzyl groups (**6.6g-6.6j**) were tolerated. To our surprise, functional groups such as alkyl bromide (**6.6k**) and perfluorinated alkyl (**6.6l**) groups were also compatible under the standard conditions, highlighting the mildness of the conversion, in contrast to the S$_N$2 reaction. Note that alkyl aryl ethers containing sterically bulky *ortho*, *ortho*-disubstituted aryl groups (Figure 75, **6.6a**, **6.6c**, **6.6d**, **6.6f**, **6.6k-6.6m**) were readily obtained using the current method. These products are difficult to obtain using conventional C(sp^2)-O synthesis methods, which are very dependent on activated electrophiles, illustrating the advantages of our method. Coupling of the NHPI ester of 6-heptenoic acid, a radical-clock probe, was able to give the 5-*exo-trig* cyclized product (Figure 75, **6.6m**), suggesting the intermediacy of alkyl radical.
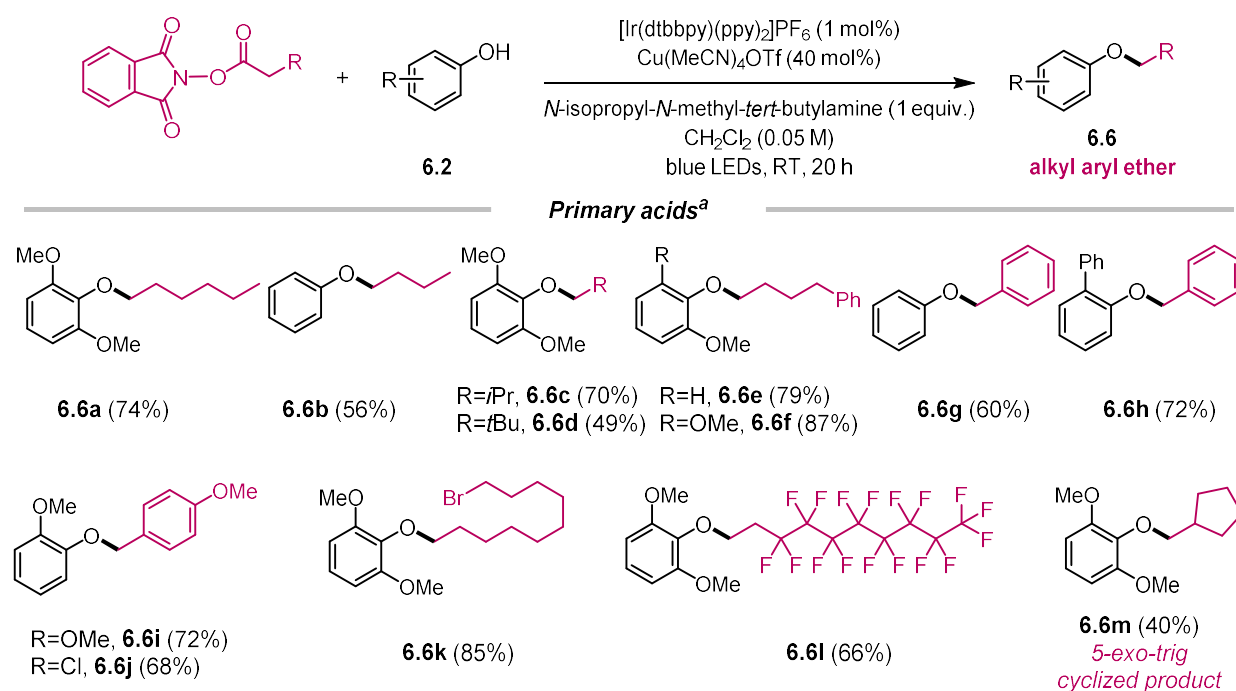
Figure 75 Scope of primary alkyl NHPI esters. ^{a}NHPI ester (2 equiv.), phenol (1 equiv.), [Ir(dtbbpy)(ppy)$_2$]PF$_6$ (1 mol%), Cu(MeCN)$_4$OTf (40 mol%) and *N*-isopropyl-*N*-methyl-*tert*-butylamine (1 equiv.) in CH$_2$Cl$_2$ (0.05 M), irradiated at 0 °C-RT for 20 h, isolated yield.

6.4   Synthetic applications

6.4.1   Late-stage functionalization of natural products and drugs
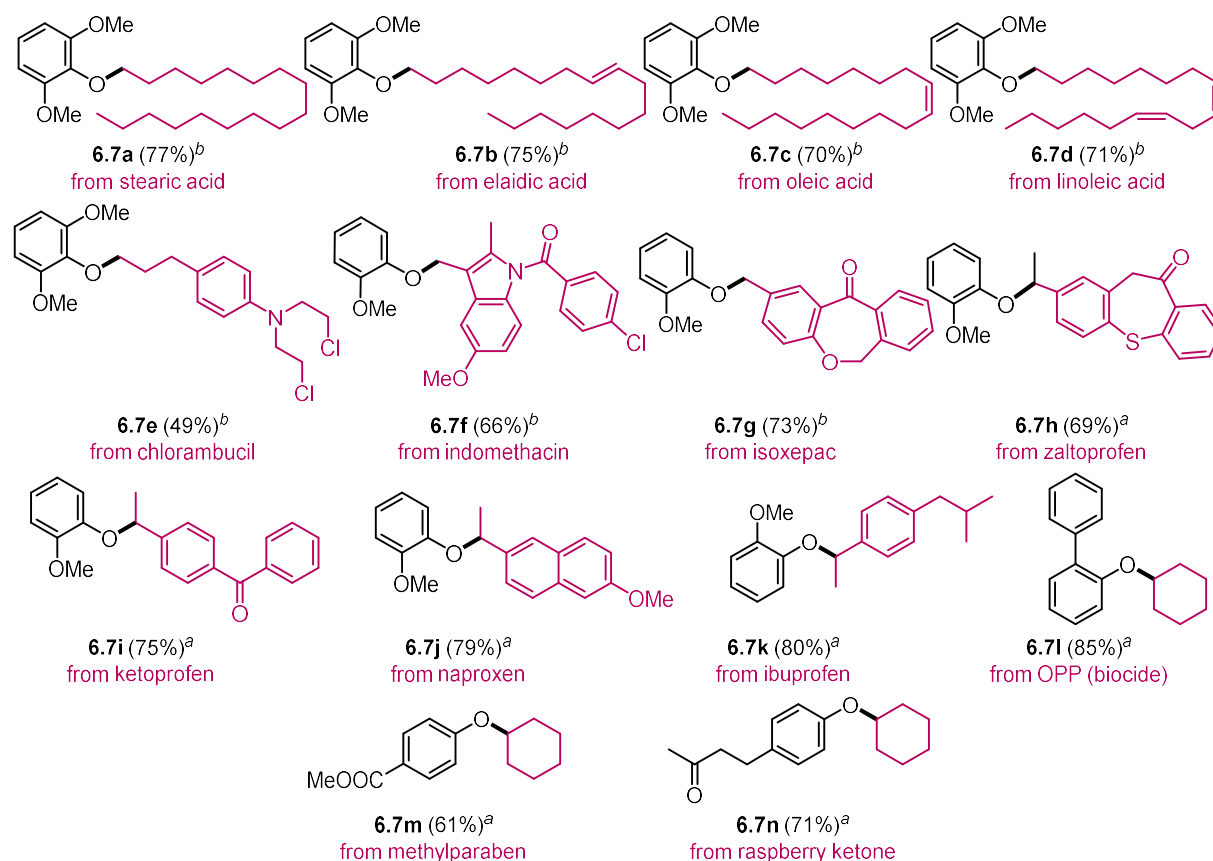
Figure 76 Late-Stage decarboxylative etherification of natural products and drugs containing carboxylic acids. [a]NHPI ester (1 equiv.), phenol (2 equiv.), [Ir(dtbbpy)(ppy)$_2$]PF$_6$ (1 mol%), (CuOTf)$_2 \cdot$C$_6$H$_6$ (10 mol%) and Et$_3$N (2 equiv.) in CH$_2$Cl$_2$ (0.05 M), irradiated at RT for 20 h, isolated yield. [b]NHPI ester (2 equiv.), phenol (1 equiv.), [Ir(dtbbpy)(ppy)$_2$]PF$_6$ (1 mol%), Cu(MeCN)$_4$OTf (40 mol%) and N-Isopropyl-N-Methyl-*tert*-butylamine (1 equiv.) in CH$_2$Cl$_2$ (0.05 M), irradiated at 0-RT for 20 h, isolated yield.

Aliphatic carboxylic acid moieties widely exist in various natural products and drugs. The use of aliphatic carboxylic acid derivatives as electrophiles enables the current method to rapidly functionalize carboxylic acid-containing complex molecules (Figure 76). Indeed, fatty acids such as stearic acid (Figure 76, **6.7a**), elaidic acid (**6.7b**), oleic acid (**6.7c**), and linoleic acid (**6.7d**) were etherified smoothly. Furthermore, drugs such as chlorambucil (**6.7e**), indomethacin (**6.7f**), isoxepac (**6.7g**), zaltoprofen (**6.7h**), ketoprofen (**6.7i**), naproxen (**6.7j**) and ibuprofen (**6.7k**) underwent esterification with ease as well. Natural phenolic compounds such as O-phenyl phenol

(OPP, **6.7l**), methylparaben (**6.7m**), and raspberry ketone (**6.7n**) could also be used as creditable coupling partners. Most of these natural products and drug molecules contain sensitive functional groups such as alkenes, carbonyl, halides and heterocyclic groups, and their late-stage functionalizations demonstrate the high chemoselectivity and functional group tolerance of the current method.

6.5   Mechanistic investigations

6.5.1   Fluorescence quenching experiments
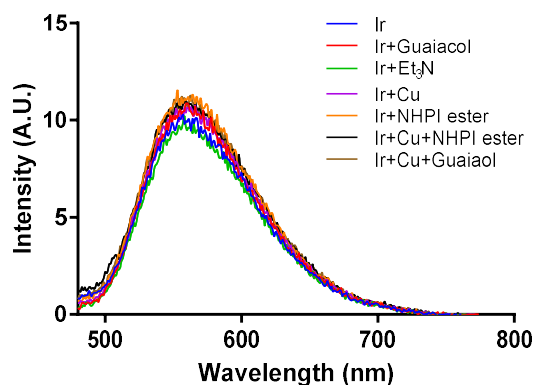
Figure 77 Fluorescence quenching experiment I. All solutions were prepared inside the glovebox before analyzing. The solutions were irradiated at 410 nm and the luminescence was measured at 581 nm. Fluorescence quenching studies were carried out using a 1.0×10^{-6} M solution of [Ir(dtbbpy)(ppy)$_2$]PF$_6$ in CH$_2$Cl$_2$, upon addition of a 1.0×10^{-3} M solution of guaiacol, Et$_3$N, Cu(MeCN)$_4$PF$_6$, NHPI ester **2.22**, mixture of Cu(MeCN)$_4$PF$_6$ and NHPI ester **2.22**, or mixture of Cu(MeCN)$_4$PF$_6$ and guaiacol **6.2a**. Under these conditions, no obvious fluorescence quenching were detected.
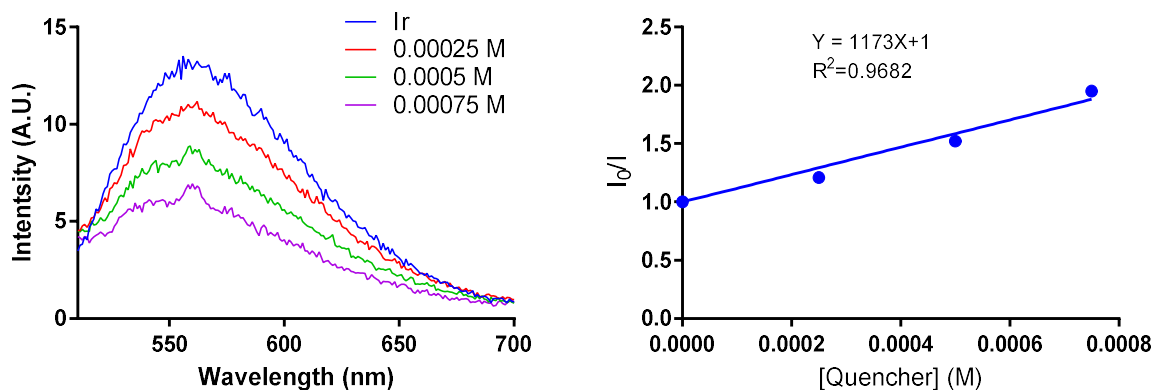
Figure 78 Left:fluorescence quenching experiment II; Fluorescence quenching studies were carried out using a 1.0×10^{-6} M solution of [Ir(dtbbpy)(ppy)$_2$]PF$_6$ in CH$_2$Cl$_2$, upon addition of variable concentration of the mixture of Cu(MeCN)$_4$PF$_6$ and Et$_3$N (1:1 molar ratio). Under these conditions, obvious fluorescence quenching were detected, depending on the concentration of the solution. Right: Stern-Volmer kinetic analysis, Stern-Volmer constant of 1173 M^{-1}S^{-1}.

To have an insight into the mechanism of this method, we carried out some experiments (Figure 77, Figure 78 and Figure 79) and hypothesized a plausible mechanistic pathway (Figure

80). In our previously decarboxylative C(sp^3)-N cross-coupling reaction,[251] we evidenced the complex of a Cu(I) catalyst with an NHPI ester could serve as an effective oxidative quencher. However, we observed the fluorescence of [Ir(dtbbpy)(ppy)$_2$]PF$_6$ was not quenched by the mixture of the complex of Cu(MeCN)$_4$PF$_6$ and NHPI ester (**2.22**), guaiacol (**6.2a**), triethylamine (Et$_3$N), Cu(MeCN)$_4$PF$_6$, NHPI ester (**2.22**), or the mixture of Cu(MeCN)$_4$PF$_6$ and guaiacol (**6.2a**) (Figure 77). To our surprise, the fluorescence was quenched by the mixture of Cu(MeCN)$_4$PF$_6$ and Et$_3$N (Figure 78 left) with defined Stern-Volmer kinetics (Figure 78 right). These results indicated that variations in the photocatalyst (Ru vs. Ir) and solvent (MeCN vs. CH$_2$Cl$_2$) resulted in different quenching processes for similar cross-coupling methods (C-N vs. C-O).[250]

6.5.2 Validation of radical intermediates
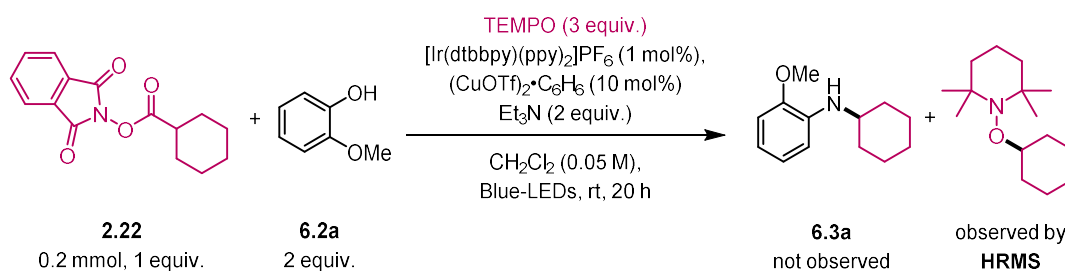
Figure 79 TEMPO trapping experiment. A reaction under the standard conditions was conducted in the presence of 3.0 equivalents of TEMPO (2,2,6,6-Tetramethylpiperidin-1-yl)oxyl) as a radical scavenger. Under such conditions, the ether product **6.3a** was not observed. TEMPO-adduct product was formed and characterized by HR-MS (ESI). HRMS (ESI/QTOF) m/z: [M + H]$^+$ Calcd for C$_{15}$H$_{30}$NO$^+$ 240.2322; Found 240.2328.

Then, we performed a radical clock experiment as well as a TEMPO trapping experiment. The free radical clock experiment allowed us to successfully obtain the product from the radical clock probe substrate (Figure 75, **6.6m**), thus verifying the intermediacy of alkyl radicals. Also, by conducting the TEMPO trapping experiment, we could completely inhibit the reaction by adding three equivalents of TEMPO under the standard conditions (Figure 79). At the same time, by HRMS, we could observe the generation of alkyl-TEMPO adduct (Figure 79), demonstrating the production of alkyl radicals.

6.5.3 Proposed mechanistic pathway
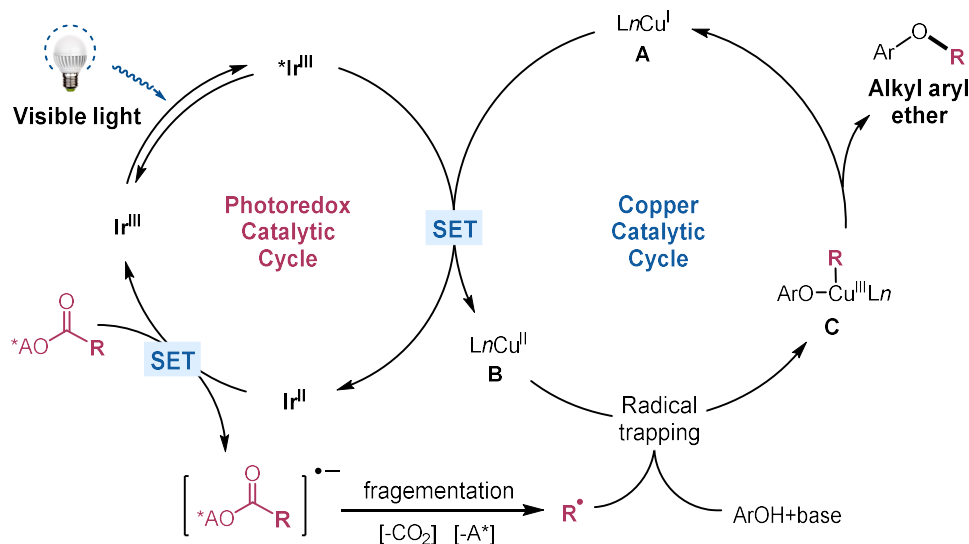
Figure 80 Proposed catalytic cycle

After analyzing the obtained results, we proposed that the excited state $*Ir^{III}$ complex ($E_{1/2}$ [$*Ir^{III}/Ir^{II}$] = +0.66 vs. SCE in MeCN)[78] first oxidizes a Cu^{I}-Et$_3$N complex **A** to give Cu^{II} species **B** (Figure 80). The exceptional function of Et$_3$N compared to other bases is evident here. Notably, as illustrated before, the steric hindrance of the amine-based base could be tuned to fit different types of alkyl radicals, facilitating the cross-coupling. The NHPI ester ($E_{1/2}^{red}$ < -1.28 vs. SCE in MeCN)[252] would then be reduced by the newly formed highly reducing Ir^{II} species ($E_{1/2}$ [Ir^{II}/Ir^{III}] = -1.51 vs. SCE in MeCN), promoting the generation of the ground-state photocatalyst and delivering a carboxyl radical to give an alkyl radical upon fragmentation. Cu^{II} complex **B** traps the alkyl radical and coordinates with phenol to yield a Cu^{III} alkyl aryloxide intermediate **C** upon deprotonation. Reductive elimination can then occur to furnish the Cu^{I} catalyst **A** and etherified products. (Figure 80).

6.6 Conclusions

In summary, decarboxylative C(sp^3)-O coupling of alkyl NHPI esters has been achieved using synergistic photoredox and Cu catalysis. This cross-coupling method enables the rapid

conversion of earth-abundant, inexpensive, and environmentally benign aliphatic carboxylic acid to valuable alkyl aryl ethers, which are crucial moieties in pharmaceutical, material, agricultural sciences. This method fills a gap and provides an alternative to the traditional C(sp^2)-O coupling and S$_N$2 reactions, nicely complementing the existing substrate scope, and improving the current functional group tolerance.

6.7 Experimental section

6.7.1 General manipulation considerations

All manipulations for the decarboxylative $C(sp^3)$-O cross-coupling via synergetic photoredox and copper-catalyzed reactions were set up in a 15 mL Teflon-screw capped test tubes (unless otherwise noted) under an inert nitrogen (N_2) atmosphere using glove-box techniques. The test tubes were then sealed with airtight electrical tapes and the reaction mixtures were stirred under irradiation of blue LEDs with a fan cooling down the temperature (approximately room temperature). Blue LEDs were purchased from Kessil Co., Ltd. (40 W max., product No. A160WE). Table fan was purchased from Galaxus Co., Ltd. (35 W max.). Flash column chromatography was performed using silica gel (Silicycle, ultra-pure grade). Preparative Thin Layer Chromatography (PTLC) was performed using glass plates from Merck KGaA, Darmstadt, Germany. The eluents for column chromatography and PTLC were presented as ratios of solvent volumes. Yields reported in the publication are of isolated materials unless otherwise noted.

6.7.2 Stern-Volmer kinetic analysis

All solutions were prepared inside the glovebox before analyzing. The solutions were irradiated at 410 nm and the luminescence was measured at 581 nm.

Stern-Volmer constants were determined using Stern–Volmer kinetics (eq 1).

$$I_0/I = 1 + K_{sv}[\text{Quencher}] \quad (1)$$

$$K_{sv} = k_q \tau_0 \quad (2)$$

As shown in equation (1), I_0 is the luminescence intensity without the quencher, I is the intensity in the presence of the quencher, K_{sv} is the Stern-Volmer constant.

As shown in equation (2), the actual bimolecular rate of quenching (k_q) can be calculated from K_{sv} using the lifetime (τ_0) of $[\text{Ir(dtbbpy)(ppy)}_2]\text{PF}_6$.

Under these conditions, the mixture of $Cu(MeCN)_4PF_6$ and Et_3N (1:1, concentration) was the only species that quenched the photoexcited catalyst with the Stern-Volmer constant of 1173 $M^{-1}S^{-1}$ (Figure 78).

6.7.3   General Procedure for the synthesis of NHPI esters (General Procedure A)

$$R^1\underset{R^2}{\overset{O}{\|}}OH \xrightarrow[\substack{DIC\ (1.1\ equiv.),\ DMAP\ (0.1\ equiv.),\\ DCM\ (0.2\text{ - }0.5\ M)}]{R^3OH\ (1.0\ equiv.)} R^1\underset{R^2}{\overset{O}{\|}}OR^3$$

A round-bottom flask or culture tube was charged with carboxylic acid (if solid, 1.0 equiv), nucleophile (*N*-hydroxyphthalimide, 1.0 equiv) and DMAP (0.1 equiv.). dichloromethane (DCM) was added (0.2 M-0.5 M) and the mixture was stirred vigorously. Carboxylic acid (if liquid, 1.0 equiv.) was added via syringe. DIC (1.1 equiv.) was then added dropwise via syringe and the mixture was allowed to stir until the carboxylic acid or the *N*-hydroxyphthalimide was fully consumed (determined by TLC). Typical reaction times were between 0.5 h and 12 h. Afterwards, the mixture was filtered over Celite and rinsed with additional CH_2Cl_2. The solvent was removed under reduced pressure, and purified by column chromatography to give the corresponding NHPI esters. Most NHPI esters are solid, which could be recrystallized (ethyl acetate and hexanes system) after column chromatography. Unless otherwise stated, NHPI esters were prepared following the General Procedure A. The preparation and spectral data of all NHPI esters used have been reported before.[46-47, 49, 53, 241, 250-251]

6.7.4   General procedure for visible-light-mediated decarboxylative etherification of phenols with secondary or tertiary NHPI esters (General Procedure B)

An oven-dried 15 mL re-sealable screw-cap test tube equipped with a Teflon-coated magnetic stir bar was sequentially charged with a secondary or tertiary NHPI ester (1 equiv.), phenol (2 equiv), [Ir(dtbbpy)(ppy)$_2$]PF$_6$ (1 mol%), (CuOTf)$_2$•C$_6$H$_6$ (10 mol%), CH_2Cl_2 (0.05 M), Et$_3$N (2 equiv) in the glove box. The vial was sealed with a screw cap and removed from the glove box. Then the vial was placed 3 cm away from one blue LED, and irradiated under fan cooling (maintain the temperature at room temperature) for 20 h. After which time the vial was removed from the light source. The crude reaction mixture was then diluted with EtOAc or diethyl ether (20 mL), washed with brine (2 x 10 mL), and separated. The aqueous layer was subsequently extracted with EtOAc or diethyl ether (2 x 10 mL), and separated. The organic fractions were combined, dried over Na$_2$SO$_4$, filtered, and concentrated under reduced pressure. The crude product residue was purified by preparative TLC using a solvent mixture (EtOAc, hexanes) as an eluent to afford the purified product. See Figure 60 for the reaction setup.

6.7.5 General procedure for visible-light-mediated decarboxylative etherification of phenols with primary NHPI esters (General Procedure C)

An oven-dried 15 mL re-sealable screw-cap test tube equipped with a Teflon-coated magnetic stir bar was sequentially charged with a primary NHPI ester (2 equiv.), phenol (1 equiv), [Ir(dtbbpy)(ppy)$_2$]PF$_6$ (1 mol%), Cu(MeCN)$_4$OTf (40 mol%), CH$_2$Cl$_2$ (0.05 M), *N*-isopropyl-*N*-methyl-*tert*-butylamine (1 equiv.) in the glove box. The vial was sealed with a screw cap and removed from the glove box. Then the vial was placed 3 cm away from one blue LED, and irradiated at 0-RT (ice bath and fan cooling) for 20 h. After which time the vial was removed from the light source. The crude reaction mixture was then diluted with EtOAc or diethyl ether (20 mL), washed with brine (2 x 10 mL), and separated. The aqueous layer was subsequently extracted with EtOAc or diethyl ether (2 x 10 mL), and separated. The organic fractions were combined, dried over Na$_2$SO$_4$, filtered, and concentrated under reduced pressure. The crude product residue was purified by preparative TLC using a solvent mixture (EtOAc, hexanes) as an eluent to afford the purified product. See Figure 81 for the reaction setup.
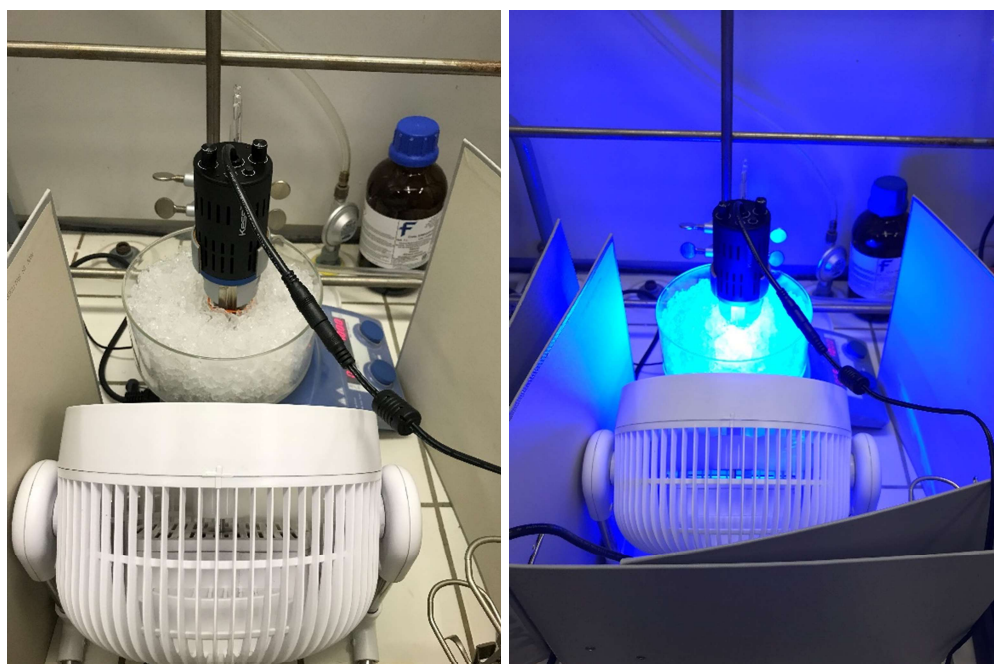
Figure 81 Reaction setup for decarboxylative C(sp^3)-O cross-coupling of primary alkyl NHPI esters.

6.7.6   Characterization of the reaction product

1-(cyclohexyloxy)-2-methoxybenzene (6.3a)
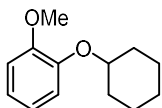
Following the General Procedure B with the corresponding phenol (2 equiv.) and NHPI ester (0.3 mmol). The crude product was purified by preparative TLC, using hexanes/EA = 40/1 (v/v) as an eluent, to yield the title compound **6.3a** (58 mg) in 94%.

^{1}H NMR (400 MHz, Chloroform-*d*): δ 7.07 – 6.70 (m, 4H), 4.18 (tt, *J* = 9.5, 3.9 Hz, 1H), 3.85 (s, 3H), 2.12 – 1.93 (m, 2H), 1.93 – 1.72 (m, 2H), 1.70 – 1.47 (m, 3H), 1.44 – 1.19 (m, 3H).

^{13}C NMR (101 MHz, Chloroform-*d*): δ 150.83, 147.36, 121.51, 120.87, 116.80, 112.45, 77.45, 56.12, 32.19, 25.79, 24.28.

The ^{1}H NMR and ^{13}C NMR spectra were consistent with the spectrum reported in the literature.[253]

1-(cyclohexyloxy)-3-methylbenzene (6.3b)

Following the General Procedure B with the corresponding phenol (2 equiv.) and NHPI ester (0.3 mmol). The crude product was purified by preparative TLC, using hexanes/EA = 40/1 (v/v) as an eluent, to yield the title compound **6.3b** (38 mg) in 67%.

^{1}H NMR (400 MHz, Chloroform-*d*): δ 7.15 (t, *J* = 8.0, 1H), 6.74 (d, *J* = 6.3 Hz, 3H), 4.23 (tt, *J* = 8.8, 4.2 Hz, 1H), 2.33 (d, *J* = 3.1 Hz, 3H), 2.11 – 1.89 (m, 2H), 1.89 – 1.72 (m, 2H), 1.63 – 1.47 (m, 3H), 1.42 – 1.27 (m, 3H).

^{13}C NMR (101 MHz, Chloroform-*d*): δ 157.93, 139.56, 129.26, 121.45, 117.13, 112.98, 75.40, 32.06, 25.82, 23.98, 21.67.

The ^{1}H NMR and ^{13}C NMR spectra were consistent with the spectrum reported in the literature.[254]

Cyclohexyl phenyl ether (6.3c)

Following the General Procedure B with the corresponding phenol (2 equiv.) and NHPI ester (0.3 mmol). The crude product was purified by preparative TLC, using hexanes/EA = 40/1 (v/v) as an eluent, to yield the title compound **6.3c** (48 mg) in 90%.

¹H NMR (400 MHz, Chloroform-*d*): δ 7.29 – 7.24 (m, 2H), 6.96 – 6.86 (m, 3H), 4.24 (tt, *J* = 9.0, 3.8 Hz, 1H), 2.06 – 1.93 (m, 2H), 1.87 – 1.74 (m, 2H), 1.62 – 1.48 (m, 3H), 1.42 – 1.27 (m, 3H).

¹³C NMR (101 MHz, Chloroform-*d*): δ 157.92, 129.55, 120.60, 116.22, 75.50, 32.02, 25.81, 23.97. The ¹H NMR and ¹³C NMR spectra were consistent with the spectrum reported in the literature.[255]

2-(cyclohexyloxy)-1,3-dimethoxybenzene (6.3d)

Following the General Procedure B with the corresponding phenol (2 equiv.) and NHPI ester (0.3 mmol). The crude product was purified by preparative TLC, using hexanes/EA = 30/1 (v/v) as an eluent, to yield the title compound **6.3d** (57 mg) in 81%.

¹H NMR (400 MHz, Chloroform-*d*): δ 6.96 (t, *J* = 8.3 Hz, 1H), 6.64 – 6.49 (m, 2H), 4.04 – 3.92 (m, 1H), 3.84 (s, 3H), 3.82 (s, 3H), 2.02 – 1.93 (m, 2H), 1.84 – 1.76 (m, 2H), 1.62 – 1.51 (m, 3H), 1.29 – 1.19 (m, 3H).

¹³C NMR (101 MHz, Chloroform-*d*): δ 154.29, 136.43, 123.27, 105.54, 81.07, 56.26, 32.74, 25.85, 24.52.

Physical State: white solid.

HRMS (APPI/LTQ-Orbitrap) m/z: [M + H]⁺ Calcd for $C_{14}H_{21}O_3^+$ 237.1485; Found 237.1487.

2,4-dichloro-1-(cyclohexyloxy)benzene (6.3e)
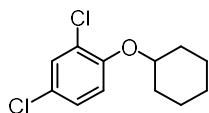
Following the General Procedure B with the corresponding phenol (2 equiv.) and NHPI ester (0.3 mmol). The crude product was purified by preparative TLC, using hexanes/EA = 30/1 (v/v) as an eluent, to yield the title compound **6.3e** (59 mg) in 81%.

¹H NMR (400 MHz, Chloroform-*d*): δ 7.35 (d, *J* = 2.6 Hz, 1H), 7.14 (dd, *J* = 8.8, 2.6 Hz, 1H), 6.87 (d, *J* = 8.8 Hz, 1H), 4.25 (tt, *J* = 8.3, 3.6 Hz, 1H), 2.02 – 1.87 (m, 2H), 1.88 – 1.75 (m, 2H), 1.67 – 1.50 (m, 3H), 1.41 – 1.26 (m, 3H).

^{13}C NMR (101 MHz, Chloroform-d): δ 152.47, 130.23, 127.52, 125.82, 125.37, 117.06, 77.63, 31.65, 25.68, 23.56.

Physical State: white solid.

HRMS (APPI/LTQ-Orbitrap) m/z: [M + H]$^+$ Calcd for C$_{12}$H$_{15}$Cl$_2$O$^+$ 245.0494; Found 245.0499.

1-bromo-2-(cyclohexyloxy)benzene (6.3f)
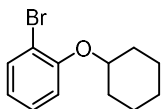
Following the General Procedure B with the corresponding phenol (2 equiv.) and NHPI ester (0.3 mmol). The crude product was purified by preparative TLC, using hexanes/EA = 30/1 (v/v) as an eluent, to yield the title compound **6.3f** (56 mg) in 73%.

^{1}H NMR (400 MHz, Chloroform-d): δ 7.53 (dd, J = 7.9, 1.7 Hz, 1H), 7.22 (td, J = 7.8, 1.7 Hz, 1H), 6.92 (dd, J = 8.3, 1.4 Hz, 1H), 6.80 (td, J = 7.6, 1.5 Hz, 1H), 4.32 (tt, J = 8.1, 3.6 Hz, 1H), 2.00 – 1.88 (m, 2H), 1.89 – 1.80 (m, 2H), 1.73 – 1.60 (m, 2H), 1.58 – 1.49 (m, 1H), 1.42 – 1.32 (m, 3H).

^{13}C NMR (101 MHz, Chloroform-d): δ 154.51, 133.63, 128.31, 121.96, 116.02, 114.01, 77.01, 31.69, 25.78, 23.53.

Physical State: colorless oil.

HRMS (APPI/LTQ-Orbitrap) m/z: [M]$^+$ Calcd for C$_{12}$H$_{15}$BrO$^+$ 254.0301; Found 254.2479.

1-(cyclohexyloxy)-2-iodobenzene (6.3g)
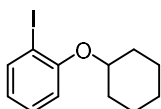
Following the General Procedure B with the corresponding phenol (2 equiv.) and NHPI ester (0.3 mmol). The crude product was purified by preparative TLC, using hexanes/EA = 30/1 (v/v) as an eluent, to yield the title compound **6.3g** (59 mg) in 65%.

^{1}H NMR (400 MHz, Chloroform-d): δ 7.77 (dd, J = 7.8, 1.7 Hz, 1H), 7.26 (td, J = 8.1, 7.5, 1.7 Hz, 1H), 6.83 (dd, J = 8.3, 1.4 Hz, 1H), 6.68 (td, J = 7.6, 1.4 Hz, 1H), 4.36 (tt, J = 7.8, 3.2 Hz, 1H), 1.94 – 1.81 (m, 4H), 1.76 – 1.64 (m, 2H), 1.57 – 1.50 (m, 1H), 1.47 – 1.35 (m, 3H).

^{13}C NMR (101 MHz, Chloroform-d): δ 156.65, 139.70, 129.31, 122.48, 114.39, 88.65, 76.65, 31.56, 25.80, 23.36.

Physical State: colorless oil.

HRMS (APPI/LTQ-Orbitrap) m/z: [M]$^+$ Calcd for $C_{12}H_{15}IO^+$ 302.0162; Found 302.0165.

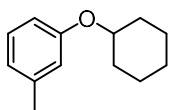**1-bromo-4-(cyclohexyloxy)benzene (6.3h)**
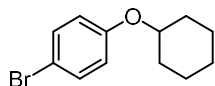
Following the General Procedure B with the corresponding phenol (2 equiv.) and NHPI ester (0.3 mmol). The crude product was purified by preparative TLC, using hexanes/EA = 30/1 (v/v) as an eluent, to yield the title compound **6.3h** (57 mg) in 75%.

^{1}H NMR (400 MHz, Chloroform-d): δ 7.41 – 7.29 (m, 2H), 7.15 – 6.86 (m, 2H), 2.57 (tt, J = 11.2, 3.6 Hz, 1H), 2.12 – 1.96 (m, 2H), 1.90 – 1.76 (m, 2H), 1.77 – 1.66 (m, 1H), 1.64 – 1.55 (m, 2H), 1.45 – 1.25 (m, 3H).

^{13}C NMR (101 MHz, Chloroform-d): δ 157.03, 132.36, 118.01, 112.64, 75.89, 31.80, 25.71, 23.83.

Physical State: pale brown oil.

HRMS (APPI/LTQ-Orbitrap) m/z: [M]$^+$ Calcd for $C_{12}H_{15}BrO^+$ 254.0301; Found 254.0304.
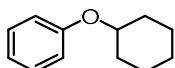
1-(cyclohexyloxy)-4-iodobenzene (6.3i)
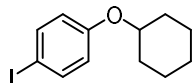
Following the General Procedure B with the corresponding phenol (2 equiv.) and NHPI ester (0.3 mmol). The crude product was purified by preparative TLC, using hexanes/EA = 30/1 (v/v) as an eluent, to yield the title compound **6.3i** (53 mg) in 59%.

^{1}H NMR (400 MHz, Chloroform-d): δ 7.53 (dd, J = 8.9, 2.0 Hz, 2H), 6.68 (dd, J = 8.7, 2.0 Hz, 2H), 4.26 – 4.09 (m, 1H), 2.00 – 1.91 (m, 2H), 1.84 – 1.70 (m, 2H), 1.60 – 1.47 (m, 3H), 1.39 – 1.27 (m, 3H).

^{13}C NMR (101 MHz, Chloroform-d): δ 157.81, 138.33, 118.57, 82.46, 75.71, 31.78, 25.71, 23.82.

Physical State: brown oil.

The ^{1}H NMR and ^{13}C NMR spectra were consistent with the spectrum reported in the literature.[256]

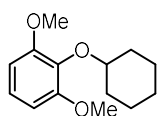**1-(4-(cyclohexyloxy)phenyl)ethan-1-one (6.3j)**
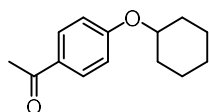
Following the General Procedure B with the corresponding phenol (2 equiv.) and NHPI ester (0.3 mmol). The crude product was purified by preparative TLC, using hexanes/EA = 20/1 (v/v) as an eluent, to yield the title compound **6.3j** (33 mg) in 51%.

¹H NMR (400 MHz, Chloroform-*d*): δ 7.98 – 7.83 (m, 2H), 6.95 – 6.81 (m, 2H), 4.35 (tt, *J* = 9.0, 4.2 Hz, 1H), 2.54 (s, 3H), 2.04 – 1.91 (m, 2H), 1.85 – 1.77 (m, 2H), 1.62 – 1.48 (m, 3H), 1.46 – 1.31 (m, 3H).

¹³C NMR (101 MHz, Chloroform-*d*): δ 196.86, 162.08, 130.73, 130.03, 115.30, 75.58, 31.74, 26.44, 25.64, 23.77.

Physical State: white solid.

HRMS (APPI/LTQ-Orbitrap) m/z: [M + H]⁺ Calcd for $C_{14}H_{19}O_2^+$ 219.1380; Found 219.1382.

2-(4-(cyclohexyloxy)phenyl)-4,4,5,5-tetramethyl-1,3,2-dioxaborolane (6.3k)
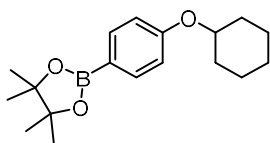
Following the General Procedure B with the corresponding phenol (2 equiv.) and NHPI ester (0.3 mmol). The crude product was purified by preparative TLC, using hexanes/EA = 30/1 (v/v) as an eluent, to yield the title compound **6.3k** (59 mg) in 65%.

¹H NMR (400 MHz, Chloroform-*d*): δ 7.83 – 7.60 (m, 2H), 6.97 – 6.73 (m, 2H), 4.31 (tt, *J* = 8.8, 3.8 Hz, 1H), 2.09 – 1.88 (m, 2H), 1.84 – 1.70 (m, 2H), 1.61 – 1.48 (m, 3H), 1.45 – 1.23 (m, 15H).

¹³C NMR (101 MHz, Chloroform-*d*): δ 160.62, 136.63, 115.30, 83.63, 75.09, 31.87, 25.77, 25.01, 23.86.

Physical State: colorless oil.

HRMS (APPI/LTQ-Orbitrap) m/z: [M + H]⁺ Calcd for $C_{18}H_{28}BO_3^+$ 303.2126; Found 303.2125.

4-(cyclohexyloxy)benzonitrile (6.3l)
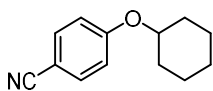
Following the General Procedure B with the corresponding phenol (2 equiv.) and NHPI ester (0.3 mmol). The crude product was purified by preparative TLC, using hexanes/EA = 30/1 (v/v) as an eluent, to yield the title compound **6.3l** (30 mg) in 49%.

¹H NMR (400 MHz, Chloroform-*d*): δ 7.63 – 7.43 (m, 2H), 7.03 – 6.81 (m, 2H), 4.32 (tt, *J* = 8.5, 3.7 Hz, 1H), 2.01 – 1.91 (m, 2H), 1.80 (m, 2H), 1.59 – 1.52 (m, 3H), 1.41 – 1.30 (m, 3H).

¹³C NMR (101 MHz, Chloroform-*d*): δ 161.44, 134.11, 119.54, 116.30, 103.45, 75.85, 31.62, 25.57, 23.71.

Physical State: pale yellow oil.

HRMS (APPI/LTQ-Orbitrap) m/z: $[M + H]^+$ Calcd for $C_{13}H_{16}NO^+$ 202.1226; Found 202.1228.

1-(cyclohexyloxy)-4-(trifluoromethoxy)benzene (6.3m)
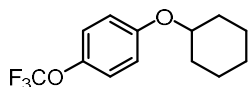
Following the General Procedure B with the corresponding phenol (2 equiv.) and NHPI ester (0.3 mmol). The crude product was purified by preparative TLC, using hexanes/EA = 30/1 (v/v) as an eluent, to yield the title compound **6.3m** (42 mg) in 54%.

¹H NMR (400 MHz, Chloroform-*d*): δ 7.11 (d, *J* = 8.4 Hz, 2H), 6.98 – 6.73 (m, 2H), 4.20 (tt, *J* = 8.3, 3.9 Hz, 1H), 2.04 – 1.91 (m, 2H), 1.87 – 1.72 (m, 2H), 1.62 – 1.46 (m, 3H), 1.39 – 1.32 (m, 2H), 0.93 – 0.74 (m, 1H).

¹³C NMR (101 MHz, Chloroform-*d*): δ 156.47, 142.62, 122.50, 120.74 (q, *J* = 255.8 Hz), 116.86, 76.13, 31.85, 25.72, 23.85.

¹⁹F NMR (376 MHz, Chloroform-*d*): δ -58.38.

Physical State: colorless oil.

HRMS (APPI/LTQ-Orbitrap) m/z: $[M + H]^+$ Calcd for $C_{13}H_{16}F_3O_2^+$ 261.1097; Found 261.1095.

2-(cyclohexyloxy)naphthalene (6.3n)
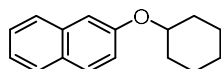
Following the General Procedure B with the corresponding phenol (2 equiv.) and NHPI ester (0.3 mmol). The crude product was purified by preparative TLC, using hexanes/EA = 30/1 (v/v) as an eluent, to yield the title compound **6.3n** (58 mg) in 86%.

¹H NMR (400 MHz, Chloroform-*d*): δ 7.93 – 7.71 (m, 3H), 7.52 (td, *J* = 7.4, 6.7, 1.3 Hz, 1H), 7.41 (td, *J* = 7.5, 6.8, 1.3 Hz, 1H), 7.30 – 7.19 (m, 4H), 4.51 (tt, *J* = 8.6, 3.8 Hz, 1H), 2.23 – 2.10 (m, 2H), 2.03 – 1.87 (m, 2H), 1.76 – 1.61 (m, 3H), 1.60 – 1.38 (m, 3H).

¹³C NMR (101 MHz, Chloroform-*d*): δ 155.75, 134.76, 129.50, 128.99, 127.73, 126.77, 126.34, 123.57, 119.97, 108.80, 75.53, 31.91, 25.84, 23.97.

Physical State: yellow oil.

HRMS (APPI/LTQ-Orbitrap) m/z: [M]⁺ Calcd for $C_{16}H_{18}O^+$ 226.1352; Found 226.1357.

1-cyclobutoxy-2-methoxybenzene (6.4a)
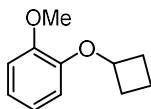
Following the General Procedure B with the corresponding phenol (2 equiv.) and NHPI ester (0.3 mmol). The crude product was purified by preparative TLC, using hexanes/EA = 40/1 (v/v) as an eluent, to yield the title compound **6.4a** (42 mg) in 78%.

¹H NMR (400 MHz, Chloroform-*d*): δ 6.98 – 6.79 (m, 3H), 6.79 – 6.65 (m, 1H), 4.66 (p, *J* = 7.3 Hz, 1H), 3.87 (s, 3H), 2.54 – 2.39 (m, 2H), 2.37 – 2.18 (m, 2H), 1.91 – 1.78 (m, 1H), 1.77 – 1.59 (m, 1H).

¹³C NMR (101 MHz, Chloroform-*d*): δ 149.31, 147.17, 120.93, 120.87, 113.50, 111.72, 72.21, 55.99, 30.95, 13.31.

Physical State: pale yellow oil.

HRMS (APPI/LTQ-Orbitrap) m/z: [M]⁺ Calcd for $C_{11}H_{14}O_2^+$ 178.0988; Found 178.0991.

1-(cyclopentyloxy)-2-methoxybenzene (6.4b)
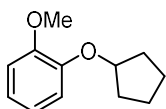
Following the General Procedure B with the corresponding phenol (2 equiv.) and NHPI ester (0.3 mmol). The crude product was purified by preparative TLC, using hexanes/EA = 40/1 (v/v) as an eluent, to yield the title compound **6.4b** (29 mg) in 50%.

¹H NMR (400 MHz, Chloroform-*d*): δ 6.91 (s, 4H), 4.86 – 4.73 (m, 1H), 3.87 (s, 3H), 1.99 – 1.79 (m, 6H), 1.66 – 1.58 (m, 2H).

¹³C NMR (101 MHz, Chloroform-*d*): δ 150.23, 147.92, 120.94, 120.92, 115.29, 112.31, 80.54, 56.18, 33.00, 24.23.

Physical State: pale yellow oil.

HRMS (APPI/LTQ-Orbitrap) m/z: [M + H]⁺ Calcd for $C_{12}H_{17}O_2^+$ 193.1223; Found 193.1227.

(2-methoxyphenoxy)cyclododecane (6.4c)

Following the General Procedure B with the corresponding phenol (2 equiv.) and NHPI ester (0.3 mmol). The crude product was purified by preparative TLC, using hexanes/EA = 40/1 (v/v) as an eluent, to yield the title compound **6.4c** (68 mg) in 78%.

¹H NMR (400 MHz, Chloroform-*d*): δ 6.99 – 6.81 (m, 4H), 4.42 (tt, *J* = 7.4, 4.3 Hz, 1H), 3.84 (s, 3H), 1.88 – 1.74 (m, 2H), 1.75 – 1.60 (m, 2H), 1.50 – 1.28 (m, 18H).

¹³C NMR (101 MHz, Chloroform-*d*): δ 150.73, 147.99, 121.22, 120.98, 116.25, 112.59, 76.95, 56.19, 29.13, 24.58, 24.20, 23.45, 23.39, 21.11.

Physical State: colorless oil.

HRMS (APPI/LTQ-Orbitrap) m/z: [M + H]$^+$ Calcd for C$_{19}$H$_{31}$O$_2{}^+$ 291.2319; Found 291.2324.

4-(2-methoxyphenoxy)tetrahydro-2*H*-pyran (6.4d)

Following the General Procedure B with the corresponding phenol (2 equiv.) and NHPI ester (0.3 mmol). The crude product was purified by preparative TLC, using hexanes/EA = 20/1 (v/v) as an eluent, to yield the title compound **6.4d** (43 mg) in 69%.

¹H NMR (400 MHz, Chloroform-*d*): δ 7.06 – 6.79 (m, 4H), 4.41 (tt, *J* = 8.3, 4.0 Hz, 1H), 4.02 (dt, *J* = 11.8, 4.6 Hz, 2H), 3.86 (s, 3H), 3.53 (ddd, *J* = 11.8, 9.0, 3.0 Hz, 2H), 2.10 – 1.90 (m, 2H), 1.92 – 1.76 (m, 2H).

¹³C NMR (101 MHz, Chloroform-*d*): δ 151.21, 146.61, 122.47, 120.93, 117.98, 112.60, 74.04, 65.59, 56.08, 32.32.

Physical State: yellow oil.

HRMS (APPI/LTQ-Orbitrap) m/z: [M + H]$^+$ Calcd for C$_{12}$H$_{17}$O$_3{}^+$ 209.1172; Found 209.1172.

1-methoxy-2-(1-phenylethoxy)benzene (6.4e)

Following the General Procedure B with the corresponding phenol (2 equiv.) and NHPI ester (0.3 mmol). The crude product was purified by preparative TLC, using hexanes/EA = 20/1 (v/v) as an eluent, to yield the title compound **6.4e** (54 mg) in 79%.

¹H NMR (400 MHz, Chloroform-*d*): δ 7.41 (d, *J* = 6.9 Hz, 2H), 7.37 – 7.30 (m, 2H), 7.27 – 7.23 (m, 1H), 6.88 (dd, *J* = 4.4, 3.0 Hz, 2H), 6.75 (dd, *J* = 4.1, 2.0 Hz, 2H), 5.32 (q, *J* = 6.5 Hz, 1H), 3.90 (s, 3H), 1.70 (d, *J* = 6.4 Hz, 3H).

¹³C NMR (101 MHz, Chloroform-*d*): δ 150.29, 147.61, 143.37, 128.62, 127.52, 125.82, 121.53, 120.82, 116.51, 112.27, 77.43, 56.16, 24.43.

Physical State: colorless oil.

HRMS (APPI/LTQ-Orbitrap) m/z: [M + Na]⁺ Calcd for $C_{15}H_{16}NaO_2^+$ 251.1043; Found 251.1045

1-(heptan-3-yloxy)-2-methoxybenzene (6.4f)
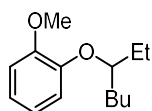
Following the General Procedure B with the corresponding phenol (2 equiv.) and NHPI ester (0.3 mmol). The crude product was purified by preparative TLC, using hexanes/EA = 30/1 (v/v) as an eluent, to yield the title compound **6.4f** (43 mg) in 65%.

¹H NMR (400 MHz, Chloroform-*d*): δ 6.89 (m, 4H), 4.14 (p, *J* = 5.9 Hz, 1H), 3.85 (s, 3H), 1.75 – 1.57 (m, 4H), 1.43 – 1.27 (m, 4H), 0.97 (t, *J* = 7.4 Hz, 3H), 0.90 (t, *J* = 6.8 Hz, 3H).

¹³C NMR (101 MHz, Chloroform-*d*): δ 150.73, 148.46, 121.17, 120.94, 116.25, 112.51, 81.13, 56.15, 33.44, 27.83, 26.86, 22.97, 14.23, 9.85.

Physical State: colorless oil.

HRMS (APPI/LTQ-Orbitrap) m/z: [M + H]⁺ Calcd for $C_{14}H_{23}O_2^+$ 223.1693; Found 223.1692.

1-methoxy-2-((1-phenylpropan-2-yl)oxy)benzene (6.4g)
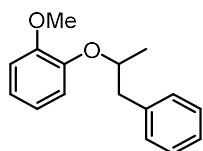
Following the General Procedure B with the corresponding phenol (2 equiv.) and NHPI ester (0.3 mmol). The crude product was purified by preparative TLC, using hexanes/EA = 30/1 (v/v) as an eluent, to yield the title compound **6.4g** (33 mg) in 46%.

^{1}H NMR (400 MHz, Chloroform-*d*): δ 7.32 – 7.20 (m, 5H), 7.04 – 6.74 (m, 4H), 4.62 – 4.45 (m, 1H), 3.85 (s, 3H), 3.21 (dd, *J* = 13.5, 5.5 Hz, 1H), 2.83 (dd, *J* = 13.6, 7.4 Hz, 1H), 1.32 (dd, *J* = 6.1, 1.3 Hz, 3H).

^{13}C NMR (101 MHz, Chloroform-*d*): δ 150.84, 147.53, 138.58, 129.68, 128.45, 126.42, 121.77, 120.99, 116.72, 112.55, 56.14, 42.96, 19.62.

Physical State: colorless oil.

HRMS (APPI/LTQ-Orbitrap) m/z: [M]$^+$ Calcd for $C_{16}H_{18}O_2^+$ 242.1301; Found 242.1306.

1-methoxy-2-(1-phenylcyclopropoxy)benzene (6.5a)
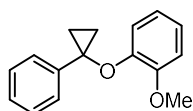
Following the General Procedure B with the corresponding phenol (2 equiv.) and NHPI ester (0.3 mmol). The crude product was purified by preparative TLC, using hexanes/EA = 20/1 (v/v) as an eluent, to yield the title compound **6.5a** (61 mg) in 85%.

^{1}H NMR (400 MHz, Chloroform-*d*): δ 7.39 – 7.18 (m, 5H), 6.97 – 6.82 (m, 3H), 6.78 – 6.68 (m, 1H), 3.91 (s, 3H), 1.57 – 1.47 (m, 2H), 1.41 – 1.30 (m, 2H).

^{13}C NMR (101 MHz, Chloroform-*d*) δ 149.25, 146.70, 141.41, 128.52, 126.36, 124.19, 121.04, 120.54, 116.07, 111.80, 60.96, 56.09, 18.33.

Physical State: colorless oil.

HRMS (ESI/QTOF) m/z: [M + Na]$^+$ Calcd for $C_{16}H_{16}NaO_2^+$ 263.1043; Found 263.1041.

2-(1-phenylcyclopropoxy)-1,1'-biphenyl (6.5b)
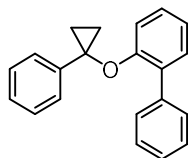
Following the General Procedure B with the corresponding phenol (2 equiv.) and NHPI ester (0.3 mmol). The crude product was purified by preparative TLC, using hexanes/EA = 20/1 (v/v) as an eluent, to yield the title compound **6.5b** (59 mg) in 69%.

¹H NMR (400 MHz, Chloroform-*d*): δ 7.62 – 7.55 (m, 2H), 7.44 (t, *J* = 7.5 Hz, 2H), 7.37 – 7.28 (m, 4H), 7.23 – 7.18 (m, 3H), 7.16 – 7.11 (m, 1H), 6.99 (t, *J* = 7.1 Hz, 2H), 1.45 – 1.37 (m, 2H), 1.34 – 1.28 (m, 2H).

¹³C NMR (101 MHz, Chloroform-*d*) δ 154.21, 141.73, 138.78, 131.02, 130.96, 129.71, 128.57, 128.15, 128.05, 126.93, 126.36, 124.17, 121.05, 115.93, 60.85, 18.40.

Physical State: colorless oil.

HRMS (APCI/QTOF) m/z: [M + H]⁺ Calcd for $C_{21}H_{19}O^+$ 287.1430; Found 287.1431.

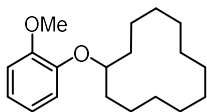### 2,4-dichloro-1-(1-phenylcyclopropoxy)benzene (6.5c)
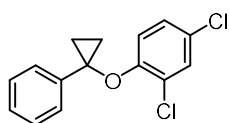
Following the General Procedure B with the corresponding phenol (2 equiv.) and NHPI ester (0.3 mmol). The crude product was purified by preparative TLC, using hexanes/EA = 20/1 (v/v) as an eluent, to yield the title compound **6.5c** (54 mg) in 65%.

¹H NMR (400 MHz, Chloroform-*d*): δ 7.35 (d, *J* = 2.5 Hz, 1H), 7.33 – 7.27 (m, 2H), 7.25 – 7.15 (m, 3H), 6.99 (dd, *J* = 8.9, 2.5 Hz, 1H), 6.86 (d, *J* = 8.9 Hz, 1H), 1.51 – 1.44 (m, 2H), 1.40 – 1.32 (m, 2H).

¹³C NMR (101 MHz, Chloroform-*d*): δ 151.99, 140.27, 130.01, 128.77, 127.27, 126.88, 125.99, 124.20, 123.58, 117.28, 62.04, 17.76.

Physical State: colorless oil.

HRMS (APCI/QTOF) m/z: [M + H]⁺ Calcd for $C_{15}H_{13}Cl_2O^+$ 279.0338; Found 279.0330.

1-(1-(4-chlorophenyl)cyclopropoxy)-2-methoxybenzene (6.5d)
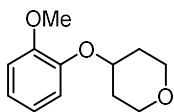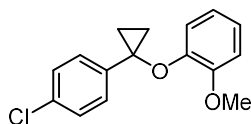

Following the General Procedure B with the corresponding phenol (2 equiv.) and NHPI ester (0.3 mmol). The crude product was purified by preparative TLC, using hexanes/EA = 20/1 (v/v) as an eluent, to yield the title compound **6.5d** (62 mg) in 75%.

¹H NMR (400 MHz, Chloroform-*d*): δ 7.31 – 7.22 (m, 2H), 7.21 – 7.10 (m, 2H), 7.01 – 6.81 (m, 3H), 6.76 (ddd, *J* = 8.1, 6.1, 2.8 Hz, 1H), 3.93 (s, 3H), 1.60 – 1.48 (m, 2H), 1.41 – 1.29 (m, 2H).

^{13}C NMR (101 MHz, Chloroform-*d*): δ 149.25, 146.37, 140.10, 132.18, 128.68, 125.69, 121.32, 120.51, 115.91, 111.83, 60.62, 56.04, 18.36.

Physical State: white solid.

HRMS (APCI/QTOF) m/z: [M + H]$^+$ Calcd for C$_{16}$H$_{16}$ClO$_2^+$ 275.0833; Found 275.0829.

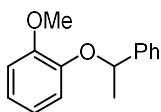**1-methoxy-2-(1-(*p*-tolyl)cyclopropoxy)benzene (6.5e)**
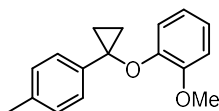
Following the General Procedure B with the corresponding phenol (2 equiv.) and NHPI ester (0.3 mmol). The crude product was purified by preparative TLC, using hexanes/EA = 20/1 (v/v) as an eluent, to yield the title compound **6.5e** (62 mg) in 82%.

^{1}H NMR (400 MHz, Chloroform-*d*): δ 7.14 – 7.07 (m, 4H), 6.93 – 6.83 (m, 3H), 6.73 (ddd, *J* = 8.0, 7.1, 2.1 Hz, 1H), 3.91 (s, 3H), 2.30 (s, 3H), 1.53 – 1.45 (m, 2H), 1.35 – 1.29 (m, 2H).

^{13}C NMR (101 MHz, Chloroform-*d*): δ 149.24, 146.78, 138.32, 135.97, 129.24, 124.24, 120.96, 120.54, 116.08, 111.77, 60.95, 56.08, 21.09, 18.01.

Physical State: colorless oil.

HRMS (ESI/QTOF) m/z: [M + Na]$^+$ Calcd for C$_{17}$H$_{18}$NaO$_2^+$ 277.1199; Found 277.1200.

1-methoxy-2-(1-(4-methoxyphenyl)cyclopropoxy)benzene (6.5f)
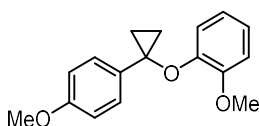
Following the General Procedure B with the corresponding phenol (2 equiv.) and NHPI ester (0.3 mmol). The crude product was purified by preparative TLC, using hexanes/EA = 20/1 (v/v) as an eluent, to yield the title compound **6.5f** (64 mg) in 79%.

^{1}H NMR (400 MHz, Chloroform-*d*): δ 7.22 – 7.10 (m, 2H), 6.95 – 6.80 (m, 5H), 6.73 (ddd, *J* = 8.0, 6.8, 2.3 Hz, 1H), 3.90 (s, 3H), 3.76 (s, 3H), 1.50 – 1.41 (m, 2H), 1.30 – 1.25 (m, 2H).

^{13}C NMR (101 MHz, Chloroform-*d*): δ 158.33, 149.30, 146.75, 133.18, 125.81, 120.99, 120.52, 116.15, 113.97, 111.77, 60.92, 56.07, 55.36, 17.41.

Physical State: colorless oil.

HRMS (ESI/QTOF) m/z: [M + Na]$^+$ Calcd for C$_{17}$H$_{18}$NaO$_3^+$ 293.1148; Found 293.1153

2-(hexyloxy)-1,3-dimethoxybenzene (6.6a)

Following the General Procedure C with the corresponding phenol (0.3 mmol) and NHPI ester (2 equiv.). The crude product was purified by preparative TLC, using hexanes/EA = 30/1 (v/v) as an eluent, to yield the title compound **6.6a** (53 mg) in 74%.

¹H NMR (400 MHz, Chloroform-*d*): δ 6.97 (t, *J* = 8.4 Hz, 1H), 6.57 (d, *J* = 8.4 Hz, 2H), 3.96 (t, *J* = 6.9 Hz, 2H), 3.84 (s, 6H), 1.76 (p, *J* = 7.0 Hz, 2H), 1.48 – 1.40 (m, 2H), 1.36 – 1.26 (m, 5H), 0.91 – 0.84 (m, 3H).

¹³C NMR (101 MHz, Chloroform-*d*): δ 153.93, 137.72, 123.46, 105.55, 73.64, 56.26, 31.83, 30.22, 25.70, 22.82, 14.23.

Physical State: pale yellow oil.

HRMS (ESI/QTOF) m/z: [M + Na]⁺ Calcd for $C_{14}H_{22}NaO_3^+$ 261.1461; Found 261.1463.

butoxybenzene (6.6b)

Following the General Procedure C with the corresponding phenol (0.3 mmol) and NHPI ester (2 equiv.). The crude product was purified by preparative TLC, using hexanes/EA = 40/1 (v/v) as an eluent, to yield the title compound **6.6b** (25 mg) in 56%.

¹H NMR (400 MHz, Chloroform-*d*): δ 7.29 (t, *J* = 7.8 Hz, 2H), 7.08 – 6.84 (m, 3H), 3.98 (t, *J* = 6.5 Hz, 2H), 1.85 – 1.71 (m, 2H), 1.51 (h, *J* = 7.4 Hz, 2H), 0.99 (t, *J* = 7.4 Hz, 3H).

¹³C NMR (101 MHz, Chloroform-*d*): δ 159.29, 129.53, 120.58, 114.64, 67.70, 31.52, 19.42, 14.01.

Physical State: colorless oil.

The ¹H NMR and ¹³C NMR spectra were consistent with the spectrum reported in the literature.[257]

2-isobutoxy-1,3-dimethoxybenzene (6.6c)

223

Following the General Procedure C with the corresponding phenol (0.3 mmol) and NHPI ester (2 equiv.). The crude product was purified by preparative TLC, using hexanes/EA = 30/1 (v/v) as an eluent, to yield the title compound **6.6c** (44 mg) in 70%.

^{1}H NMR (400 MHz, Chloroform-*d*): δ 6.96 (t, *J* = 8.4 Hz, 1H), 6.57 (d, *J* = 8.4 Hz, 2H), 3.84 (s, 6H), 3.73 (d, *J* = 6.7 Hz, 2H), 2.07 (dp, *J* = 13.4, 6.7 Hz, 1H), 1.02 (d, *J* = 6.7 Hz, 6H).

^{13}C NMR (101 MHz, Chloroform-*d*): δ 153.87, 138.16, 123.36, 105.78, 80.27, 56.34, 29.20, 19.45.

Physical State: pale yellow oil.

HRMS (ESI/QTOF) m/z: [M + Na]$^+$ Calcd for $C_{12}H_{18}NaO_3^+$ 233.1148; Found 233.1149.

1,3-dimethoxy-2-(neopentyloxy)benzene (6.6d)
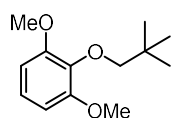
Following the General Procedure C with the corresponding phenol (0.3 mmol) and NHPI ester (2 equiv.). The crude product was purified by preparative TLC, using hexanes/EA = 30/1 (v/v) as an eluent, to yield the title compound **6.6d** (33 mg) in 49%.

^{1}H NMR (400 MHz, Chloroform-*d*): δ 6.95 (t, *J* = 8.3 Hz, 1H), 6.57 (d, *J* = 8.4 Hz, 2H), 3.83 (s, 6H), 3.62 (s, 2H), 1.06 (s, 9H).

^{13}C NMR (101 MHz, Chloroform-*d*): δ 153.90, 138.79, 123.25, 106.16, 83.59, 56.49, 32.59, 26.71.

Physical State: colorless oil.

HRMS (ESI/QTOF) m/z: [M + Na]$^+$ Calcd for $C_{13}H_{20}NaO_3^+$ 247.1305; Found 247.1304.

1-methoxy-2-(4-phenylbutoxy)benzene (6.6e)
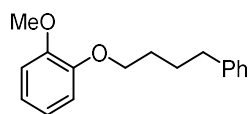
Following the General Procedure C with the corresponding phenol (0.3 mmol) and NHPI ester (2 equiv.). The crude product was purified by preparative TLC, using hexanes/EA = 30/1 (v/v) as an eluent, to yield the title compound **6.6e** (61 mg) in 79%.

^{1}H NMR (400 MHz, Chloroform-*d*): δ 7.33 – 7.27 (m, 2H), 7.24 – 7.17 (m, 3H), 6.90 (td, *J* = 5.9, 3.1 Hz, 4H), 4.05 (t, *J* = 6.5 Hz, 2H), 3.87 (s, 3H), 2.71 (t, *J* = 7.4 Hz, 2H), 1.98 – 1.75 (m, 4H).

^{13}C NMR (101 MHz, Chloroform-*d*): δ 149.63, 148.69, 142.35, 128.56, 128.41, 125.87, 121.05, 120.95, 113.36, 112.00, 68.95, 56.06, 35.72, 28.94, 27.92.

Physical State: colorless oil.

HRMS (ESI/QTOF) m/z: [M + Na]$^+$ Calcd for C$_{17}$H$_{20}$NaO$_2$$^+$ 279.1356; Found 279.1352.

1,3-dimethoxy-2-(4-phenylbutoxy)benzene (6.6f)

Following the General Procedure C with the corresponding phenol (0.3 mmol) and NHPI ester (2 equiv.). The crude product was purified by preparative TLC, using hexanes/EA = 30/1 (v/v) as an eluent, to yield the title compound **6.6f** (75 mg) in 87%.

^{1}H NMR (400 MHz, Chloroform-d): δ 7.31 – 7.26 (m, 2H), 7.22 – 7.16 (m, 3H), 6.98 (t, J = 8.4 Hz, 1H), 6.58 (d, J = 8.4 Hz, 2H), 4.04 – 3.96 (m, 2H), 3.83 (s, 6H), 2.72 – 2.65 (m, 2H), 1.86 – 1.78 (m, 4H).

^{13}C NMR (101 MHz, Chloroform-d): δ 153.92, 142.80, 137.61, 128.60, 128.36, 125.75, 123.55, 105.51, 73.22, 56.24, 35.80, 29.91, 27.90.

Physical State: colorless oil.

HRMS (APPI/LTQ-Orbitrap) m/z: [M + H]$^+$ Calcd for C$_{18}$H$_{23}$O$_3$$^+$ 287.1642; Found 287.1643.

(benzyloxy)benzene (6.6g)
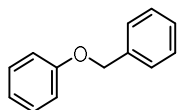
Following the General Procedure C with the corresponding phenol (0.3 mmol) and NHPI ester (2 equiv.). The crude product was purified by preparative TLC, using hexanes/EA = 30/1 (v/v) as an eluent, to yield the title compound **6.6g** (33 mg) in 60%.

^{1}H NMR (400 MHz, Chloroform-d): δ 7.50 – 7.37 (m, 4H), 7.37 – 7.27 (m, 3H), 7.04 – 6.93 (m, 3H), 5.08 (s, 2H).

^{13}C NMR (101 MHz, Chloroform-d): δ 158.93, 137.23, 129.62, 128.71, 128.07, 127.61, 121.08, 115.00, 70.06.

Physical State: colorless solid.

The ^{1}H NMR and ^{13}C NMR spectra were consistent with the spectrum reported in the literature.[258]

2-(benzyloxy)-1,1'-biphenyl (6.6h)

Following the General Procedure C with the corresponding phenol (0.3 mmol) and NHPI ester (2 equiv.). The crude product was purified by preparative TLC, using hexanes/EA = 30/1 (v/v) as an eluent, to yield the title compound **6.6h** (56 mg) in 72%.

^{1}**H NMR** (400 MHz, Chloroform-*d*): δ 7.72 – 7.54 (m, 2H), 7.51 – 7.27 (m, 10H), 7.14 – 7.00 (m, 2H), 5.12 (s, 2H).

^{13}**C NMR** (101 MHz, Chloroform-*d*): δ 155.72, 138.65, 137.38, 131.54, 131.13, 129.78, 128.69, 128.53, 128.03, 127.69, 127.02, 126.95, 121.48, 113.55, 70.58.

Physical State: colorless oil.

HRMS (ESI/QTOF) m/z: [M + H]$^+$ Calcd for C$_{19}$H$_{17}$O$^+$ 261.1274; Found 261.1278.

1-methoxy-2-((4-methoxybenzyl)oxy)benzene (6.6i)

Following the General Procedure C with the corresponding phenol (0.3 mmol) and NHPI ester (2 equiv.). The crude product was purified by preparative TLC, using hexanes/EA = 20/1 (v/v) as an eluent, to yield the title compound **6.6i** (53 mg) in 72%.

^{1}**H NMR** (400 MHz, Chloroform-*d*): δ 7.37 (d, *J* = 8.3 Hz, 2H), 6.96 – 6.84 (m, 6H), 5.08 (s, 2H), 3.88 (s, 3H), 3.81 (s, 3H).

^{13}**C NMR** (101 MHz, Chloroform-*d*): δ 159.45, 149.93, 148.37, 129.44, 129.13, 121.52, 120.90, 114.53, 114.05, 112.07, 77.36, 70.97, 56.07, 55.40.

Physical State: white solid.

HRMS (APCI/QTOF) m/z: [M + Na]$^+$ Calcd for C$_{15}$H$_{16}$NaO$_3^+$ 267.0992; Found 267.0987.

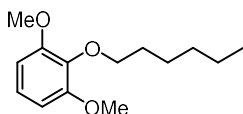**1-((4-chlorobenzyl)oxy)-2-methoxybenzene (6.6j)**

Following the General Procedure C with the corresponding phenol (0.3 mmol) and NHPI ester (2 equiv.). The crude product was purified by preparative TLC, using hexanes/EA = 20/1 (v/v) as an eluent, to yield the title compound **6.6j** (51 mg) in 68%.

^{1}H NMR (400 MHz, Chloroform-d): δ 7.43 – 7.30 (m, 4H), 7.00 – 6.82 (m, 4H), 5.12 (s, 2H), 3.89 (s, 3H).

^{13}C NMR (101 MHz, Chloroform-d): δ 149.87, 147.99, 135.87, 133.64, 128.77, 128.72, 121.85, 120.87, 114.47, 112.08, 70.40, 55.99.

Physical State: yellow oil.

HRMS (ESI/QTOF) m/z: [M + Na]$^+$ Calcd for C$_{14}$H$_{13}$ClNaO$_2^+$ 271.0496; Found 271.0497.

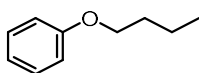### 2-((10-bromodecyl)oxy)-1,3-dimethoxybenzene (6.6k)
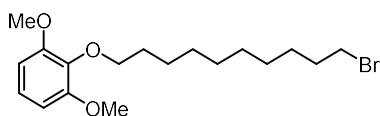
Following the General Procedure C with the corresponding phenol (0.3 mmol) and NHPI ester (2 equiv.). The crude product was purified by preparative TLC, using hexanes/EA = 30/1 (v/v) as an eluent, to yield the title compound **6.6k** (95 mg) in 85%.

^{1}H NMR (400 MHz, Chloroform-d): δ 6.97 (t, J = 8.4 Hz, 1H), 6.57 (d, J = 8.3 Hz, 2H), 3.96 (t, J = 6.8 Hz, 2H), 3.84 (s, 6H), 3.40 (t, J = 6.9 Hz, 2H), 1.85 (p, J = 7.0 Hz, 2H), 1.75 (p, J = 7.0 Hz, 2H), 1.49 – 1.27 (m, 12H).

^{13}C NMR (101 MHz, Chloroform-d): δ 153.90, 137.67, 123.46, 105.52, 73.58, 56.25, 34.17, 32.97, 30.22, 29.63, 29.52, 28.90, 28.31, 25.98.

Physical State: pale yellow oil.

HRMS (ESI/QTOF) m/z: [M + Na]$^+$ Calcd for C$_{18}$H$_{29}$BrNaO$_3^+$ 395.1192; Found 395.1196.

2-((3,3,4,4,5,5,6,6,7,7,8,8,9,9,10,10,10-heptadecafluorodecyl)oxy)-1,3-dimethoxybenzene (6.6l)
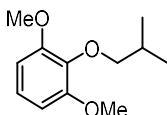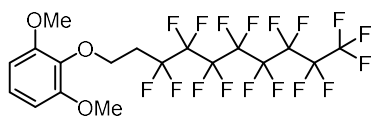

Following the General Procedure C with the corresponding phenol (0.3 mmol) and NHPI ester (2 equiv.). The crude product was purified by preparative TLC, using hexanes/EA = 20/1 (v/v) as an eluent, to yield the title compound **6.6l** (119 mg) in 66%.

¹H NMR (400 MHz, Chloroform-*d*): δ 7.15 (t, *J* = 8.4 Hz, 1H), 6.62 (d, *J* = 8.5 Hz, 2H), 3.82 (s, 6H), 3.02 – 2.84 (m, 2H), 2.61 (tt, *J* = 18.1, 8.0 Hz, 2H).

¹³C NMR (101 MHz, Chloroform-*d*): δ 169.23, 152.36, 128.62, 126.68, 104.97, 56.23, 26.90 (t, *J* = 22.2 Hz), 25.35 (t, *J* = 4.1 Hz).

¹⁹F NMR (376 MHz, Chloroform-*d*): δ -80.81 (t, *J* = 10.0 Hz), -114.66 (t, *J* = 14.1 Hz), -121.68, -121.91, -122.72, -123.45, -126.12.

Physical State: colorless oil.

HRMS (ESI/QTOF) m/z: [M + H]⁺ Calcd for $C_{18}H_{14}F_{17}O_3^+$ 601.0666; Found 601.0661.

2-(cyclopentylmethoxy)-1,3-dimethoxybenzene (6.6m)
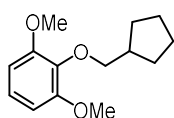
Following the General Procedure C with the corresponding phenol (0.3 mmol) and NHPI ester (2 equiv.). The crude product was purified by preparative TLC, using hexanes/EA = 20/1 (v/v) as an eluent, to yield the title compound **6.6m** (28 mg) in 40%.

¹H NMR (400 MHz, Chloroform-*d*): δ 6.96 (t, *J* = 8.3 Hz, 1H), 6.57 (d, *J* = 8.3 Hz, 2H), 3.88 – 3.78 (m, 8H), 2.37 (hept, *J* = 7.6 Hz, 1H), 1.87 – 1.77 (m, 2H), 1.63 – 1.54 (m, 4H), 1.45 – 1.35 (m, 2H).

¹³C NMR (101 MHz, Chloroform-*d*): δ 153.92, 137.99, 123.41, 105.71, 77.92, 56.33, 39.99, 29.57, 25.68.

Physical State: colorless oil.

HRMS (ESI/QTOF) m/z: [M + Na]⁺ Calcd for $C_{14}H_{20}NaO_3^+$ 259.1305; Found 259.1307.

2-(heptadecyloxy)-1,3-dimethoxybenzene (6.7a)
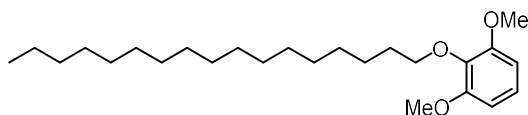
Following the General Procedure C with the corresponding phenol (0.3 mmol) and NHPI ester (2 equiv.). The crude product was purified by preparative TLC, using hexanes/EA = 20/1 (v/v) as an eluent, to yield the title compound **6.7a** (91 mg) in 77%.

¹H NMR (400 MHz, Chloroform-*d*): δ 6.97 (t, *J* = 8.4 Hz, 1H), 6.57 (d, *J* = 8.4 Hz, 2H), 3.96 (t, *J* = 6.9 Hz, 2H), 3.84 (s, 6H), 1.76 (p, *J* = 7.0 Hz, 2H), 1.26 (m, 30H), 0.87 (d, *J* = 7.0 Hz, 3H).

¹³C NMR (101 MHz, Chloroform-*d*): δ 153.92, 137.70, 123.45, 105.53, 73.63, 56.24, 32.07, 30.25, 29.84, 29.80, 29.61, 29.51, 26.02, 22.83, 14.25.

Physical State: white solid.

HRMS (ESI/QTOF) m/z: [M + Na]⁺ Calcd for $C_{25}H_{44}NaO_3^+$ 415.3183; Found 415.3180.

(E)-2-(heptadec-8-en-1-yloxy)-1,3-dimethoxybenzene (6.7b)
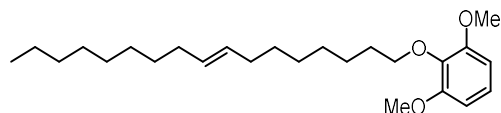
Following the General Procedure C with the corresponding phenol (0.3 mmol) and NHPI ester (2 equiv.). The crude product was purified by preparative TLC, using hexanes/EA = 20/1 (v/v) as an eluent, to yield the title compound **6.7b** (88 mg) in 75%.
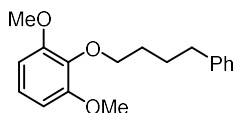
¹H NMR (400 MHz, Chloroform-*d*): δ 6.97 (t, *J* = 8.4 Hz, 1H), 6.57 (d, *J* = 8.4 Hz, 2H), 5.39 (td, *J* = 3.8, 1.9 Hz, 2H), 3.96 (t, *J* = 6.8 Hz, 2H), 3.84 (s, 6H), 1.96 (dt, *J* = 8.0, 4.2 Hz, 4H), 1.75 (p, *J* = 7.0 Hz, 2H), 1.51 – 1.22 (m, 20H), 0.88 (t, *J* = 6.5 Hz, 3H).

¹³C NMR (101 MHz, Chloroform-*d*): δ 153.93, 137.71, 130.53, 130.45, 123.46, 105.54, 73.61, 56.26, 32.76, 32.05, 30.25, 29.81, 29.78, 29.64, 29.47, 29.34, 29.30, 25.99, 22.83, 14.26.

Physical State: pale yellow oil.

HRMS (ESI/QTOF) m/z: [M + Na]⁺ Calcd for $C_{25}H_{42}NaO_3^+$ 413.3026; Found 413.3028.

(Z)-2-(heptadec-8-en-1-yloxy)-1,3-dimethoxybenzene (6.7c)
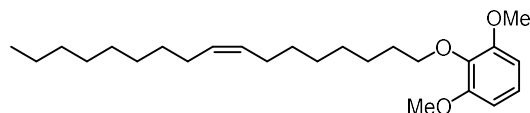
Following the General Procedure C with the corresponding phenol (0.3 mmol) and NHPI ester (2 equiv.). The crude product was purified by preparative TLC, using hexanes/EA = 20/1 (v/v) as an eluent, to yield the title compound **6.7c** (82 mg) in 70%.

¹H NMR (400 MHz, Chloroform-*d*): δ 6.97 (t, *J* = 8.4 Hz, 1H), 6.57 (d, *J* = 8.4 Hz, 2H), 5.42 – 5.27 (m, 2H), 3.96 (t, *J* = 6.9 Hz, 2H), 3.84 (s, 6H), 2.06 – 1.94 (m, 4H), 1.76 (p, *J* = 7.0 Hz, 2H), 1.48 – 1.19 (m, 20H), 0.88 (t, *J* = 6.5 Hz, 3H).

¹³C NMR (101 MHz, Chloroform-*d*): δ 153.92, 137.70, 130.07, 129.98, 123.46, 105.53, 73.60, 56.25, 32.05, 30.23, 29.92, 29.90, 29.85, 29.67, 29.50, 29.47, 29.45, 27.37, 25.99, 22.82, 14.25.

Physical State: colorless oil.

HRMS (ESI/QTOF) m/z: [M + Na]$^+$ Calcd for C$_{25}$H$_{42}$NaO$_3$$^+$ 413.3026; Found 413.3028.

2-(((8Z,11Z)-heptadeca-8,11-dien-1-yl)oxy)-1,3-dimethoxybenzene (6.7d)
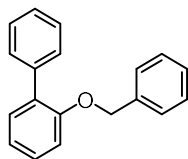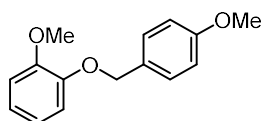

Following the General Procedure C with the corresponding phenol (0.3 mmol) and NHPI ester (2 equiv.). The crude product was purified by preparative TLC, using hexanes/EA = 20/1 (v/v) as an eluent, to yield the title compound **6.7d** (83 mg) in 71%.

^{1}H NMR (400 MHz, Chloroform-*d*): δ 6.97 (t, *J* = 8.4 Hz, 1H), 6.57 (d, *J* = 8.4 Hz, 2H), 5.35 (tq, *J* = 10.9, 6.8, 5.4 Hz, 4H), 3.96 (t, *J* = 6.8 Hz, 2H), 3.84 (s, 6H), 2.78 (t, *J* = 6.5 Hz, 2H), 2.09 – 2.00 (m, 4H), 1.76 (p, *J* = 7.0 Hz, 2H), 1.51 – 1.24 (m, 13H), 0.89 (t, *J* = 6.7 Hz, 3H).

^{13}C NMR (101 MHz, Chloroform-*d*): δ 153.91, 137.69, 130.33, 130.27, 128.11, 128.07, 123.46, 105.53, 73.58, 56.24, 31.66, 30.23, 29.79, 29.49, 29.44, 27.39, 27.34, 25.98, 25.77, 22.71, 14.20.

Physical State: colorless oil.

HRMS (ESI/QTOF) m/z: [M + Na]$^+$ Calcd for C$_{25}$H$_{40}$NaO$_3$$^+$ 411.2870; Found 411.2879.

N,N-bis(2-chloroethyl)-4-(3-(2,6-dimethoxyphenoxy)propyl)aniline (6.7e)
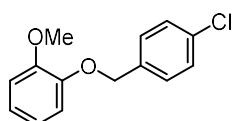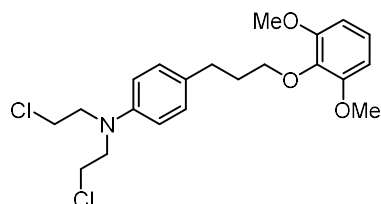

Following the General Procedure C with the corresponding phenol (0.3 mmol) and NHPI ester (2 equiv.). The crude product was purified by preparative TLC, using hexanes/EA = 10/1 (v/v) as an eluent, to yield the title compound **6.7e** (60 mg) in 49%.

^{1}H NMR (400 MHz, Chloroform-*d*): δ 7.18 – 7.07 (m, 2H), 6.98 (t, *J* = 8.4 Hz, 1H), 6.60 (dd, *J* = 18.0, 8.5 Hz, 4H), 4.01 (t, *J* = 6.4 Hz, 2H), 3.85 (s, 6H), 3.74 – 3.66 (m, 4H), 3.62 (m, 4H), 2.80 – 2.68 (m, 2H), 2.08 – 1.95 (m, 2H).

^{13}C NMR (101 MHz, Chloroform-*d*): δ 153.90, 144.27, 137.57, 131.74, 129.88, 123.57, 112.32, 105.54, 72.85, 56.26, 53.81, 40.71, 32.24, 31.24.

Physical State: light brown oil.

HRMS (ESI/QTOF) m/z: [M + Na]$^+$ Calcd for C$_{21}$H$_{27}$Cl$_2$NNaO$_3$$^+$ 434.1260; Found 434.1264

(4-chlorophenyl)(5-methoxy-3-((2-methoxyphenoxy)methyl)-2-methyl-*1H*-indol-1-yl)methanone (6.7f)

Following the General Procedure C with the corresponding phenol (0.3 mmol) and NHPI ester (2 equiv.). The crude product was purified by preparative TLC, using hexanes/EA = 10/1 (v/v) as an eluent, to yield the title compound **6.7f** (86 mg) in 66%.

^{1}H NMR (400 MHz, Chloroform-*d*): δ 7.68 – 7.61 (m, 2H), 7.50 – 7.44 (m, 2H), 7.17 (d, *J* = 2.6 Hz, 1H), 7.05 – 6.96 (m, 2H), 6.96 – 6.88 (m, 2H), 6.83 (d, *J* = 9.0 Hz, 1H), 6.67 (dd, *J* = 9.0, 2.6 Hz, 1H), 5.22 (s, 2H), 3.87 (s, 3H), 3.83 (s, 3H), 2.42 (s, 3H).

^{13}C NMR (101 MHz, Chloroform-*d*): δ 168.56, 156.20, 150.66, 148.18, 139.52, 137.17, 133.90, 131.40, 131.12, 130.58, 129.26, 122.37, 120.96, 116.05, 115.39, 114.93, 112.27, 112.15, 101.85, 63.11, 56.03, 55.82, 13.41.

Physical State: bright yellow oil.

HRMS (APPI/LTQ-Orbitrap) m/z: [M + H]$^+$ Calcd for C$_{25}$H$_{23}$ClNO$_4$$^+$ 436.1310; Found 436.1300.

2-((2-methoxyphenoxy)methyl)dibenzo[b,e]oxepin-11(*6H*)-one (6.7g)
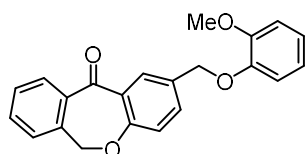
Following the General Procedure C with the corresponding phenol (0.3 mmol) and NHPI ester (2 equiv.). The crude product was purified by preparative TLC, using hexanes/EA = 10/1 (v/v) as an eluent, to yield the title compound **6.7g** (76 mg) in 73%.

^{1}H NMR (400 MHz, Chloroform-*d*): δ 8.29 (d, *J* = 2.3 Hz, 1H), 7.90 (dd, *J* = 7.7, 1.4 Hz, 1H), 7.63 (dd, *J* = 8.5, 2.4 Hz, 1H), 7.56 (td, *J* = 7.4, 1.4 Hz, 1H), 7.47 (td, *J* = 7.6, 1.3 Hz, 1H), 7.39 – 7.34 (m, 1H), 7.06 (d, *J* = 8.4 Hz, 1H), 6.96 – 6.84 (m, 4H), 5.19 (s, 2H), 5.14 (s, 2H), 3.89 (s, 3H).

^{13}**C NMR** (101 MHz, Chloroform-*d*): δ 190.95, 161.16, 150.00, 148.15, 140.59, 135.67, 134.94, 132.90, 131.20, 129.61, 129.41, 127.94, 125.20, 121.86, 121.30, 120.94, 114.74, 112.12, 73.78, 70.60, 56.07.

Physical State: pale yellow oil.

HRMS (ESI/QTOF) m/z: [M + Na]$^+$ Calcd for $C_{22}H_{18}NaO_4^+$ 369.1097; Found 369.1095.

2-(1-(2-methoxyphenoxy)ethyl)dibenzo[b,f]thiepin-10(11*H*)-one (6.7h)
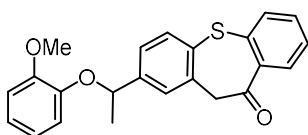
Following the General Procedure B with the corresponding phenol (2 equiv.) and NHPI ester (0.3 mmol). The crude product was purified by preparative TLC, using hexanes/EA = 10/1 (v/v) as an eluent, to yield the title compound **6.7h** (78 mg) in 69%.

^{1}**H NMR** (400 MHz, Chloroform-*d*): δ 8.22 (dd, *J* = 8.0, 1.6 Hz, 1H), 7.75 – 7.56 (m, 2H), 7.52 (d, *J* = 1.9 Hz, 1H), 7.44 (td, *J* = 7.6, 1.7 Hz, 1H), 7.38 – 7.27 (m, 2H), 7.00 – 6.82 (m, 2H), 6.82 – 6.61 (m, 2H), 5.33 (q, *J* = 6.5 Hz, 1H), 4.39 (s, 2H), 3.91 (s, 3H), 1.66 (d, *J* = 6.5 Hz, 3H).

^{13}**C NMR** (101 MHz, Chloroform-*d*): δ 191.49, 150.36, 147.23, 145.77, 140.37, 137.93, 136.30, 133.50, 132.61, 131.64, 131.58, 130.97, 126.94, 126.89, 124.67, 121.97, 120.82, 116.69, 112.28, 76.93, 56.09, 51.27, 24.28.

Physical State: pale yellow oil.

HRMS (APPI/LTQ-Orbitrap) m/z: [M + Na]$^+$ Calcd for $C_{23}H_{20}NaO_3S^+$ 399.1025; Found 399.1037.

(4-(1-(2-methoxyphenoxy)ethyl)phenyl)(phenyl)methanone (6.7i)
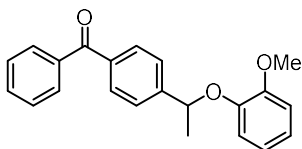
Following the General Procedure B with the corresponding phenol (2 equiv.) and NHPI ester (0.3 mmol). The crude product was purified by preparative TLC, using hexanes/EA = 10/1 (v/v) as an eluent, to yield the title compound **6.7i** (75 mg) in 75%.

¹H NMR (400 MHz, Chloroform-*d*): δ 7.82 (s, 1H), 7.77 – 7.63 (m, 4H), 7.62 – 7.54 (m, 1H), 7.45 (td, *J* = 7.6, 3.6 Hz, 3H), 6.94 – 6.82 (m, 2H), 6.82 – 6.69 (m, 2H), 5.40 (q, *J* = 6.5 Hz, 1H), 3.84 (s, 3H), 1.71 (d, *J* = 6.5 Hz, 3H).

¹³C NMR (101 MHz, Chloroform-*d*): δ 196.72, 150.45, 147.21, 143.62, 137.87, 137.69, 132.52, 130.21, 129.96, 129.40, 128.74, 128.40, 127.68, 121.99, 120.82, 116.92, 112.36, 77.06, 56.07, 24.20.

Physical State: white solid.

HRMS (APPI/LTQ-Orbitrap) m/z: [M + H]⁺ Calcd for $C_{22}H_{21}O_3^+$ 333.1485; Found 333.1485.

2-methoxy-6-(1-(2-methoxyphenoxy)ethyl)naphthalene (6.7j)
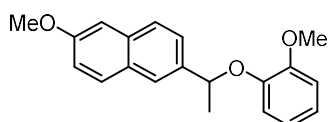
Following the General Procedure B with the corresponding phenol (2 equiv.) and NHPI ester (0.3 mmol). The crude product was purified by preparative TLC, using hexanes/EA = 10/1 (v/v) as an eluent, to yield the title compound **6.7j** (73 mg) in 79%.

¹H NMR (400 MHz, Chloroform-*d*): δ 7.77 (d, *J* = 1.7 Hz, 1H), 7.72 (t, *J* = 8.5 Hz, 2H), 7.54 (dd, *J* = 8.4, 1.8 Hz, 1H), 7.18 – 7.10 (m, 2H), 6.93 – 6.83 (m, 2H), 6.81 (dd, *J* = 8.0, 1.5 Hz, 1H), 6.72 (ddd, *J* = 8.2, 6.9, 2.1 Hz, 1H), 5.45 (q, *J* = 6.4 Hz, 1H), 3.92 (s, 3H), 3.91 (s, 3H), 1.77 (d, *J* = 6.4 Hz, 3H).

¹³C NMR (101 MHz, Chloroform-*d*): δ 157.75, 150.33, 147.66, 138.57, 134.15, 129.53, 128.89, 127.32, 124.56, 124.51, 121.55, 120.82, 118.97, 116.69, 112.24, 105.81, 77.68, 56.16, 55.42, 24.46.

Physical State: white solid.

HRMS (ESI/QTOF) m/z: [M + Na]⁺ Calcd for $C_{20}H_{20}NaO_3^+$ 331.1305; Found 331.1311.

1-(1-(4-isobutylphenyl)ethoxy)-2-methoxybenzene (6.7k)
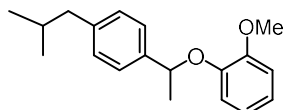
Following the General Procedure B with the corresponding phenol (2 equiv.) and NHPI ester (0.3 mmol). The crude product was purified by preparative TLC, using hexanes/EA = 10/1 (v/v) as an eluent, to yield the title compound **6.7k** (68 mg) in 80%.

¹H NMR (400 MHz, Chloroform-*d*): δ 7.35 – 7.27 (m, 2H), 7.15 – 7.07 (m, 2H), 6.93 – 6.82 (m, 2H), 6.81 – 6.72 (m, 2H), 5.29 (q, *J* = 6.4 Hz, 1H), 3.89 (s, 3H), 2.45 (d, *J* = 7.2 Hz, 2H), 1.85 (dp, *J* = 13.5, 6.7 Hz, 1H), 1.68 (d, *J* = 6.4 Hz, 3H), 0.90 (s, 3H), 0.88 (s, 3H).

¹³C NMR (101 MHz, Chloroform-*d*): δ 150.34, 147.74, 140.95, 140.58, 129.33, 125.62, 121.44, 120.82, 116.60, 112.27, 77.41, 56.18, 45.28, 30.31, 24.31, 22.54, 22.53.

Physical State: yellow oil.

HRMS (APPI/LTQ-Orbitrap) m/z: $[M]^+$ Calcd for $C_{19}H_{24}O_2^+$ 284.1771; Found 284.1774.

2-(cyclohexyloxy)-1,1'-biphenyl (6.7l)
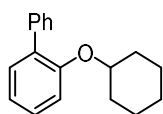
Following the General Procedure B with the corresponding phenol (2 equiv.) and NHPI ester (0.3 mmol). The crude product was purified by preparative TLC, using hexanes/EA = 30/1 (v/v) as an eluent, to yield the title compound **6.7l** (64 mg) in 85%.
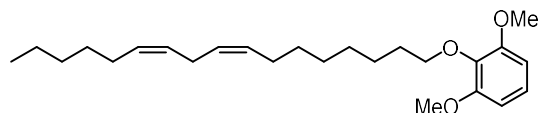
¹H NMR (400 MHz, Chloroform-*d*): δ 7.60 – 7.52 (m, 2H), 7.41 – 7.25 (m, 6H), 7.01 (t, *J* = 7.5 Hz, 2H), 4.20 (tt, *J* = 8.1, 3.7 Hz, 1H), 1.91 – 1.77 (m, 2H), 1.70 – 1.60 (m, 2H), 1.53 – 1.44 (m, 3H), 1.33 – 1.23 (m, 4H).

¹³C NMR (101 MHz, Chloroform-*d*): δ 154.89, 139.06, 132.23, 131.19, 129.78, 128.46, 127.85, 126.75, 121.00, 115.19, 76.14, 31.75, 25.77, 23.57.

Physical State: colorless oil.

HRMS (APPI/LTQ-Orbitrap) m/z: $[M + H]^+$ Calcd for $C_{18}H_{21}O^+$ 253.1587; Found 253.1589.

methyl 4-(cyclohexyloxy)benzoate (6.7m)
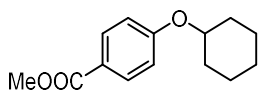
Following the General Procedure B with the corresponding phenol (2 equiv.) and NHPI ester (0.3 mmol). The crude product was purified by preparative TLC, using hexanes/EA = 20/1 (v/v) as an eluent, to yield the title compound **6.7m** (43 mg) in 61%.

¹H NMR (400 MHz, Chloroform-*d*): δ 7.96 (d, *J* = 8.8 Hz, 2H), 6.89 (d, *J* = 8.8 Hz, 2H), 4.33 (tt, *J* = 8.7, 3.8 Hz, 1H), 3.87 (s, 3H), 2.06 – 1.90 (m, 2H), 1.87 – 1.74 (m, 2H), 1.54 (td, *J* = 12.6, 11.3, 7.8 Hz, 3H), 1.43 – 1.27 (m, 3H).

^{13}C NMR (101 MHz, Chloroform-d): δ 167.06, 161.90, 131.71, 122.21, 115.27, 75.54, 51.94, 31.76, 25.66, 23.80.

Physical State: colorless oil.

HRMS (ESI/QTOF) m/z: [M + H]$^+$ Calcd for C$_{14}$H$_{19}$O$_3^+$ 235.1329; Found 235.1327.

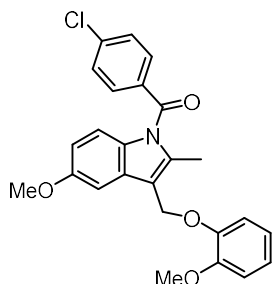**4-(4-(cyclohexyloxy)phenyl)butan-2-one (6.7n)**
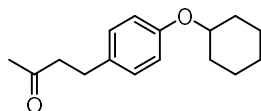
Following the General Procedure B with the corresponding phenol (2 equiv.) and NHPI ester (0.3 mmol). The crude product was purified by preparative TLC, using hexanes/EA = 20/1 (v/v) as an eluent, to yield the title compound **6.7n** (52 mg) in 71%.

^{1}H NMR (400 MHz, Chloroform-d): δ 7.06 (d, J = 8.5 Hz, 2H), 6.81 (d, J = 8.5 Hz, 2H), 4.18 (tt, J = 8.8, 3.8 Hz, 1H), 2.82 (t, J = 7.4 Hz, 2H), 2.72 (t, J = 7.8 Hz, 2H), 2.13 (s, 3H), 2.05 – 1.89 (m, 2H), 1.89 – 1.70 (m, 2H), 1.59 – 1.41 (m, 3H), 1.39 – 1.25 (m, 3H).

^{13}C NMR (101 MHz, Chloroform-d): δ 156.27, 132.99, 129.30, 116.31, 75.69, 45.61, 32.02, 30.24, 29.07, 25.78, 23.95.

Physical State: white solid.

HRMS (ESI/QTOF) m/z: [M + Na]$^+$ Calcd for C$_{16}$H$_{22}$NaO$_2^+$ 269.1512; Found 269.1512.

Chapter 7

Deoxygenative Trifluoromethylthiolation of Carboxylic Acids

7.1 Introduction of the background

In Chapter 2.5, we have introduced in detail the existing methodologies for the synthesis of trifluoromethylthioesters as well as their shortcomings. Based on the issues with the existing methods, we desired to develop a strategy for the synthesis of trifluoromethylthioesters so that (1) simple, readily available, inexpensive and environmentally friendly raw materials can be used as reactants. (2) a strategy to slow-release the trifluoromethylthio anion (SCF_3^-) could be developed, thus avoiding its decomposition during the reaction process.[185, 201]

We ventured to hypothesize whether or not carboxylic acids could be used directly for the synthesis of trifluoromethylthioester. By using carboxylic acids as substrates, we could not only generate trifluoromethylthioester straightforwardly. More importantly, we have repeatedly mentioned the advantages of using carboxylic acids as feedstocks in the previous sections, and such advantages will undoubtedly broaden the range of substrate scope.
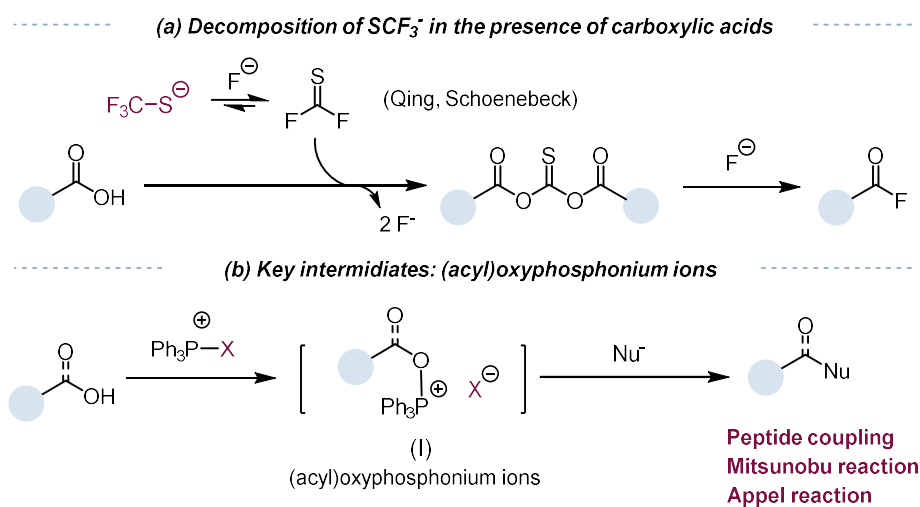
Figure 82 (a) Reaction of SCF_3^- with carboxylic acids to give acyl fluorides; (b) key intermidiates: (acyl)oxyphosphonium ions.

Using carboxylic acids as starting materials and undergoing tandem carboxylic acid activation/nucleophilic substitution processes seem to be a potential solution to deliver trifluoromethylthioesters. However, in 2017, a study by Schoenebeck and co-workers seemed to prove the infeasibility of this hypothesis (Figure 82a).[201] Their study showed that after in-situ

activation of the carboxylic acid, the nucleophilic trifluoromethylthio anion (SCF$_3^-$) was not able to attack the activated intermediate effectively. In contrast to the generation of trifluoromethylthioester, this method only yielded acyl fluoride compounds in high yield (Figure 82a).
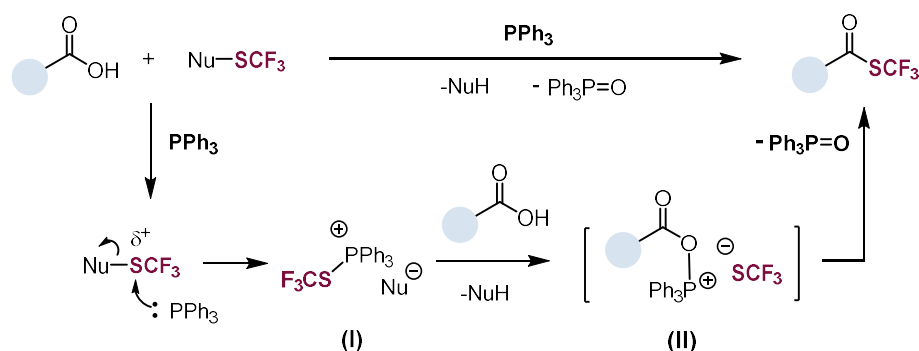
Figure 83 This work: deoxygenative trifluoromethylthiolation of carboxylic acids.

Inspired by the rich chemistry of phosphorus reagents and (acyl)oxyphosphonium ions **I** (Figure 82b) in peptide coupling,[259] Mitsunobu,[260-261] and Appel[262] reactions, we assumed that such intermediates could be possibly transformed into trifluoromethylthioesters from carboxylic acids via a deoxygenative process.

Here we describe a "umpolung" strategy that allows for the deoxygenative trifluoromethylthiolation of carboxylic acids via the use of electrophilic trifluoromethylthiolating reagents. This method is featured by its controllable release of CF$_3$S$^-$ anion and its mildness, chemoselectivity and efficiency (Figure 83). An initial reaction design is depicted in Figure 83. The "umpolung" is achieved with triphenylphosphine (PPh$_3$), which first captures a CF$_3$S$^+$ cation to form a SCF$_3$-phosphonium salt (**I**), followed by a methathesis reaction with a carboxylate to give an oxyphosphonium intermediate (**II**), which is probe to deoxygenative trifluoromethylthiolation to give a trifluoromethylthioester while eliminating triphenylphosphine oxide (PPh$_3$=O) (Figure 83).

7.2   Screening of reaction conditions

We began our investigation by optimizing the reaction of 4-phenylbenzoic acid (**7.1a**) with *N*-(trifluoromethylthio)phthalimide (**7.2a**). To our delight, the reaction proceeded in the presence of 1.1 equiv of Ph$_3$P in tetrahydrofuran (THF, 0.2 M) with a yield of 40% to give the desired trifluoromethylthioester (**7.3a**) (Figure 84).
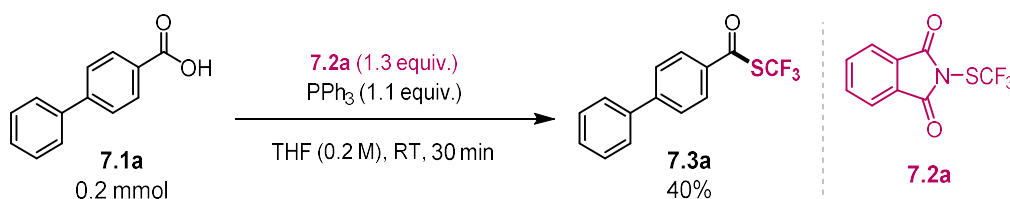
Figure 84   First milestone in the exploration of deoxygenative trifluoromethylthiolation of carboxylic acids

After obtaining this exciting result, we then proceeded to a systematic screening of the reaction conditions. The reaction was then optimized by varying reaction parameters. A summary of key observations is shown in Table 23. Notably, a small amount of Lewis acid could significantly enhance the reactivity of **7.2a** (Table 23, entries 1-6). We assumed that the coordination of Lewis acid with the phthalimide group could facilitate polarizing **7.2a**, promoting the nucleophilic attack of PPh$_3$ to **7.2a** and smoothing the generation of the key intermediate SCF$_3$-phosphonium salt (Figure 82b, **I**). Anhydrous FeCl$_3$ (5 mol%) was the best Lewis acid to boost the yield to 95% (Table 23, entry 2). THF was the best solvent (Table 23, entries 2, 7-12), probably due to the good solubility of the system in THF.

Further optimization indicated Ph$_3$P was the best mediator among several phosphine reagents (Table 23, entries 2, 13-15). It is worth noting that the phosphine reagents played a vital role in the transformation. When conducting the reaction in the absence of such reagents, no target product was produced (Table 23, entry 16). **7.2a** proved to be superior to other electrophilic trifluoromethylthiolating reagents **7.2b-7.2d** (Table 23, entries 17-20). When the nucleophilic NMe$_4$SCF$_3$ (**7.2e**) was employed, no product was formed (Table 23, entry 10). The reliance on electrophilic trifluoromethylating reagents demonstrates that this conversion is different from the carboxylic acid activation/nucleophilic substitution process (see Figure 82a). The external bases

were shown to be ineffective in promoting the transformation (Table 23, entries 21-24). It was worthy to note that the reaction was completed within 30 minutes at room temperature.

Table 23 Summary of the effects of reaction parameters and conditions on the reaction efficiency

entry	SCF3⁻ reagent	Lewis acid	PR$_3$	base (x equiv.)	solvent	yield (%)^a
1	**7.2a**	-	PPh$_3$	-	THF	40%
2	**7.2a**	FeCl$_3$	PPh$_3$	-	THF	95%
3	**7.2a**	FeCl$_3$·6H$_2$O	PPh$_3$	-	THF	71%
4^b	**7.2a**	BF$_3$·OEt$_2$	PPh$_3$	-	THF	64%
5	**7.2a**	AlCl$_3$	PPh$_3$	-	THF	39%
6	**7.2a**	Sc(OTf)$_3$	PPh$_3$	-	THF	71%
7	**7.2a**	FeCl$_3$	PPh$_3$	-	MeCN	36%
8	**7.2a**	FeCl$_3$	PPh$_3$	-	DCM	29%
9	**7.2a**	FeCl$_3$	PPh$_3$	-	DMF	18%
10	**7.2a**	FeCl$_3$	PPh$_3$	-	PhMe	70%
11	**7.2a**	FeCl$_3$	PPh$_3$	-	PhCF$_3$	81%
12	**7.2a**	FeCl$_3$	PPh$_3$	-	Et$_2$O	55%
13	**7.2a**	FeCl$_3$	PCy$_3$	-	THF	39%
14	**7.2a**	FeCl$_3$	P(OEt)$_3$	-	THF	12%
15	**7.2a**	FeCl$_3$	P(OEt)P	-	THF	35%
16	**7.2a**	FeCl$_3$	-	-	THF	ND
17	**7.2b**	FeCl$_3$	PPh$_3$	-	THF	19%
18	**7.2c**	FeCl$_3$	PPh$_3$	-	THF	51%
19	**7.2d**	FeCl$_3$	PPh$_3$	-	THF	7%

20	**7.2e**	$FeCl_3$	PPh_3	-	THF	ND
21	**7.2a**	$FeCl_3$	PPh_3	$NaHCO_3$	THF	69%
22	**7.2a**	$FeCl_3$	PPh_3	Cs_2CO_3	THF	40%
23	**7.2a**	$FeCl_3$	PPh_3	2,6-lutidine	THF	68%
24	**7.2a**	$FeCl_3$	PPh_3	NaH_2PO_4	THF	42%

[a]Yield determined by ^{19}F NMR spectroscopy of the crude reaction mixture using a,a,a-trifluorotoluene as an internal standard. [b]$BF_3 \cdot OEt_2$ (10 mol%).

7.3 Scope of the deoxygenative trifluoromethylthiolation of carboxylic aicds

7.3.1 Scope of aromatic carboxylic acids
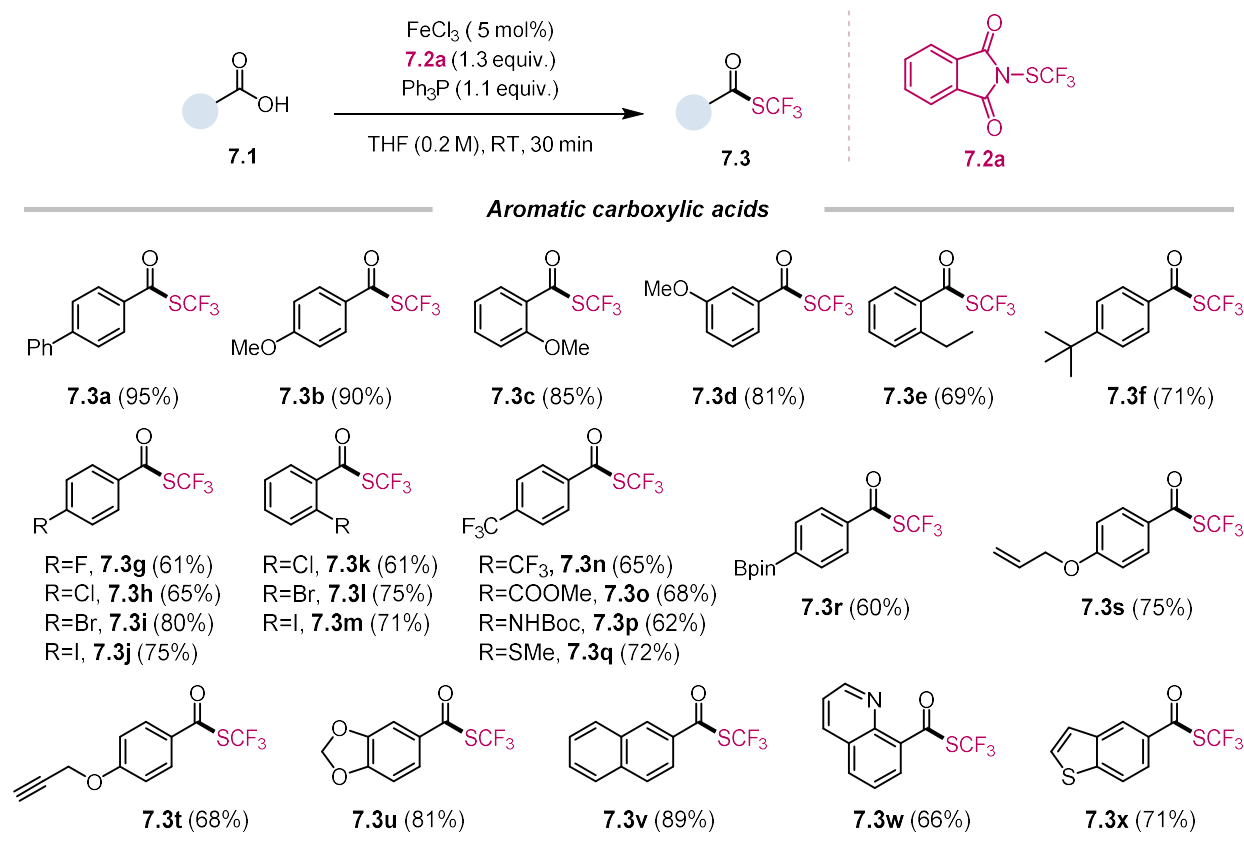
Figure 85 Scope of the trifluoromethylthiolation of aromatic carboxylic acids. [a]Carboxylic acid (1.0 equiv.), triphenylphosphine (Ph₃P, 1.1 equiv.), N-(trifluoromethylthio)phthalimide **7.2a** (1.3 equiv.), FeCl₃ (5 mol%) in THF (0.2 M), room temperature, 30 min, isolated yield.

With the optimized conditions in hands (Table 23, entry 2), we next examined the scope of our methodology (Figure 85). A range of aromatic carboxylic acids with electron-donating (**7.3b-7.3f**) and electron-withdrawing (**7.3g-7.3o**) substituents was coupled with **7.2a** to give the corresponding trifluoromethylthioesters in moderate to good yields. Importantly, aromatic carboxylic acids with aryl halides (**7.3g-7.3m**), even reactive iodide groups (**7.3j**, **7.3m**), were tolerated in the reaction. Synthetically useful functional groups such as trifluoromethyl (**7.3n**), ester (**7.3o**), (*tert*-butoxycarbonyl)amino (**7.3p**), thiomethyl (**7.3q**), boronic ester (**7.3r**), alkene (**7.3s**), alkyne (**7.3t**), 1,3-benzodioxole (**7.3u**) and naphthalene (**7.3v**) groups were all compatible.

The reactions also enabled the transformations of a diverse set of heteroaryl carboxylic acids, thus affording the desired products (**7.3w**−**7.3x**) in satisfactory yields.

7.3.2 Scope of aliphatic and cinnamic carboxylic acids
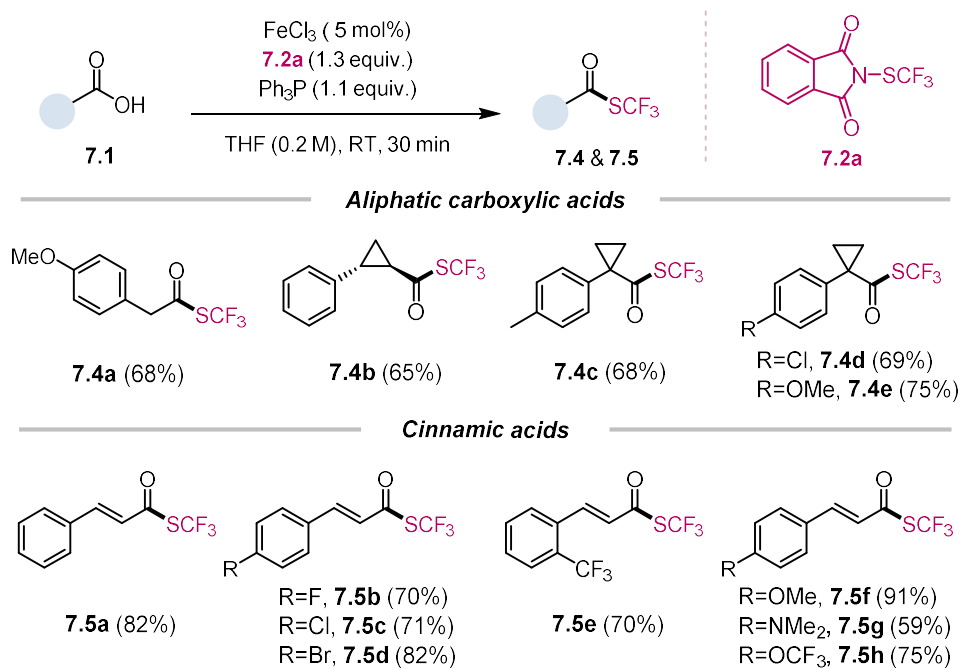
Figure 86 Scope of the trifluoromethylthiolation of aliphatic and cinnamic carboxylic acids. [a]Carboxylic acid (1.0 equiv.), triphenylphosphine (Ph₃P, 1.1 equiv.), *N*-(trifluoromethylthio)phthalimide **7.2a** (1.3 equiv.), FeCl₃ (5 mol%) in THF (0.2 M), room temperature, 30 min, isolated yield.

The reactions could transform aliphatic carboxylic acids and cinnamic acids to the corresponding trifluoromethylthioesters smoothly (Figure 86). These substrates were previously unreactive using other methods.[187, 193, 196, 198-199] Primary, secondary and tertiary carboxylic acids were all suitable starting materials to furnish the desired trifluoromethylthioester products (**7.4a**-**7.4e**) in decent yields. The functionalization was also robust for a range of cinnamic acids containing electron-neutral (**7.5a**), electron-withdrawing (**7.5b**-**7.5e, 7.5h**), and electron-donating (**7.5f**-**7.5g**) substituents. Notably, most of the trifluoromethylthioester molecules were hitherto unknown compounds.

7.3.3 Unsuccessful substrate
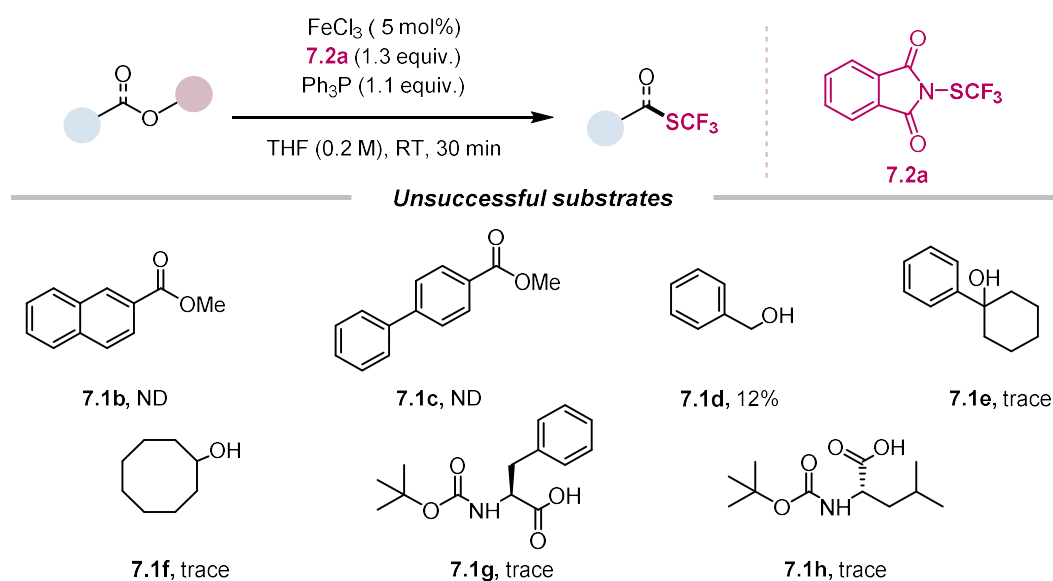
Figure 87 Unsuccessful substrates for the deoxygenative trifluoromethylthiolation reaction. *Carboxylic acid (1.0 equiv.), triphenylphosphine (Ph₃P, 1.1 equiv.), *N*-(trifluoromethylthio)phthalimide **7.2a** (1.3 equiv.), FeCl₃ (5 mol%) in THF (0.2 M), room temperature. Reactions were monitored using GC-MS after 30 minutes, yields mentioned here are GC yields, *n*-dodecane was used as an internal standard. ND (not detected).

Besides, a variety of aliphatic alcohols and substituted methyl benzoates (Figure 87, **7.1b-7.1h**) were examined (Figure 87). Methyl benzoates (**7.1b-7.1c**) gave no desired products under the optimal condition. While some aliphatic alcohols, such as primary ones (**7.1d**), could give desired products in meager yields, the messy products made it hard to obtain the desired product. Several amino acids were also tested (**7.1g-7.1h**); nevertheless, they gave nearly no desired products (Figure 87), possibly owing to the competition of multiple nucleophilic sites.

7.4 Synthetic applications

7.4.1 Late-Stage trifluoromethylthiolation of natural products and drugs
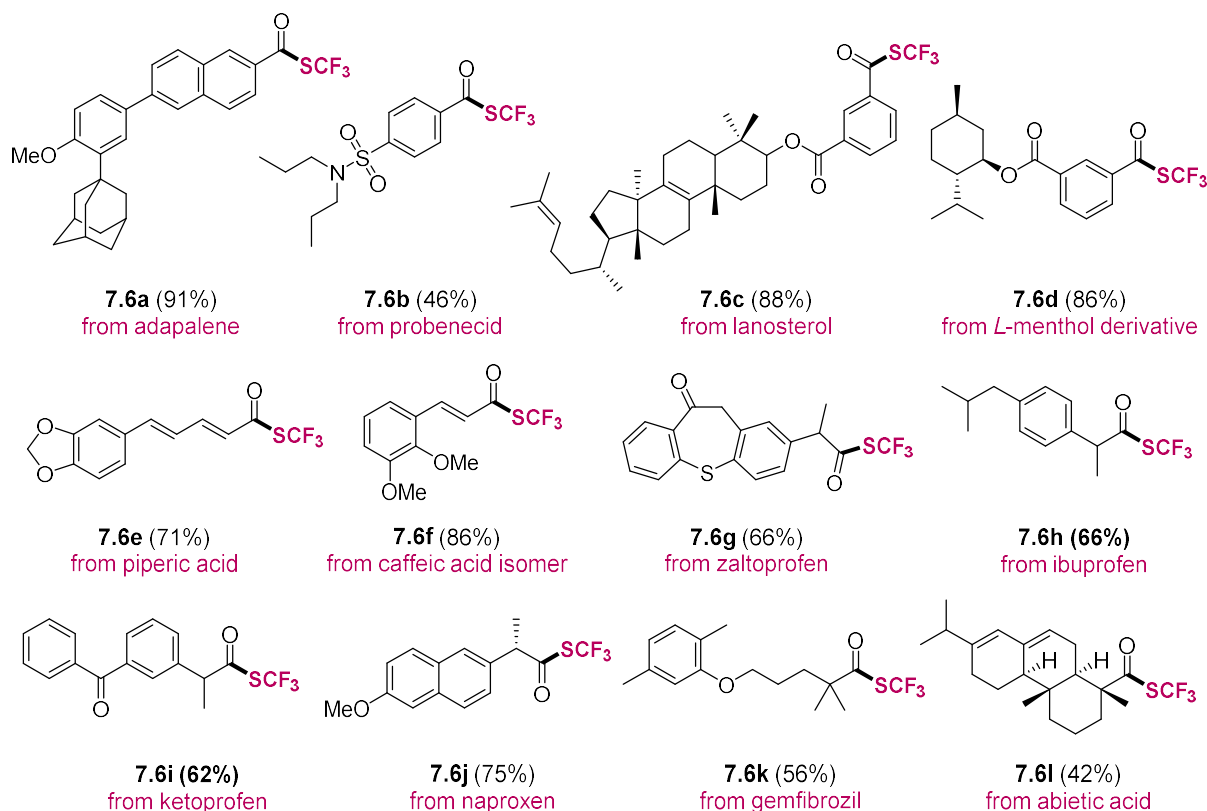
Figure 88 Late-Stage trifluoromethylthiolation of natural products and drugs containing a carboxylic group. [a]Carboxylic acid (1.0 equiv.), triphenylphosphine (Ph$_3$P, 1.1 equiv.), N-(trifluoromethylthio)phthalimide **7.2a** (1.3 equiv.), FeCl$_3$ (5 mol%) in THF (0.2 M), room temperature, 30 min, isolated yield.

Owing to the ubiquity of carboxylic acid-containing moieties in natural products and drug molecules, the direct use of carboxylic acids as substrates enables a facile, rapid, and late-stage functionalization of bio-active molecules (Figure 88). Indeed, aromatic carboxylic acids, such as adapalene (**7.6a**), probenecid (**7.6b**), lanosterol (**7.6c**), and L-menthol derivative (**7.6d**), were converted with ease. Moreover, natural-occurring cinnamic acids, such as piperic acid, with a conjugated double bond (**7.6e**); caffeic acid isomer, with an isolated double bond (**7.6f**), were reliable coupling partners as well. To date, there are no reported methods that could convert drugs and natural products with an aliphatic carboxylic acid group to their corresponding trifluoromethylthioesters, showcasing the efficiency of our method. To further expand the scope,

we then transformed zaltoprofen (**7.6g**), ibuprofen (**7.6h**), ketoprofen (**7.6i**), naproxen (**7.6j**), gemfibrozil (**7.6k**) and abietic acid (**7.6l**) to the corresponding products.

The successful late-stage modification of these natural products and drug molecules, many of which contain sensitive sulfonamide, alkene, carbonyl, and heterocyclic groups, highlights the mild condition, high chemoselectivity and functional group tolerance of the current method.

7.4.2 Palladium-catalyzed decarbonylative cross-coupling of trifluoromethylthioesters

Trifluoromethylthioethers are widely-existing in pharmaceutical and agrochemical compounds,[178] the transformation of trifluoromethylthioesters that derived from carboxylic acids to trifluoromethylthioethers could provide a valuable disconnection.

In 2017, the group of Sanford reported a palladium-catalyzed decarbonylative cross-coupling of aroyl chlorides.[263] Considering the strong electron-withdrawing nature of the trifluoromethylthio group, we anticipated that a similar strategy could also be feasible in the decarbonylation of trifluoromethylthioesters. To our delight, as shown in Figure 89, **7.3a** could be transformed into trifluoromethylthioether **7.7a** in 91% yield. This conversion provides a novel approach of synthesizing trifluoromethylthioethers from inexpensive, environmentally benign, and readily available carboxylic acids, providing a novel synthetic disconnection and nicely complementing existing methods to synthesize trifluoromethylthioethers.
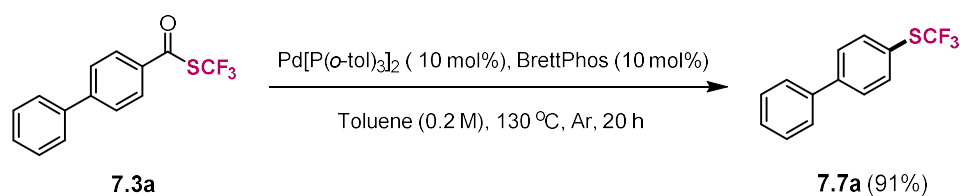
Figure 89 Pd-catalyzed decarbonylative trifluoromethyl thiolation of trifluoromethylthioester.

7.5   Proposed mechanism

We tentatively proposed a mechanism for the deoxygenative trifluoromethylthiolation of carboxylic acids (Figure 90). Nucleophilic attack of PPh$_3$ to **7.2a** could form a trifluoromethylthiophosphonium ion **II** (Figure 90). Meanwhile, carboxylic acid attacks **II** to generate acyloxyphosphonium intermediate **III** and release a CF$_3$S$^-$ anion simultaneously. The nucleophilic CF$_3$S$^-$ anion could then attack at the C−acyl moiety to give trifluoromethylthioester products and Ph$_3$PO.
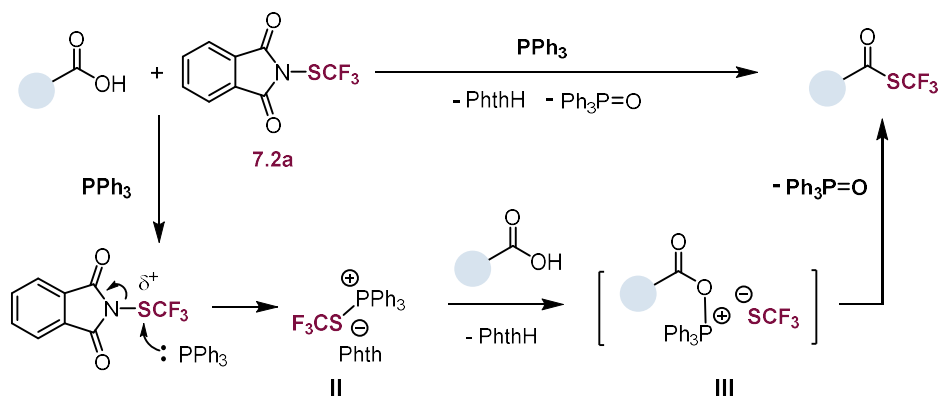
Figure 90 Proposed mechanism.

7.6   Conclusion

In summary, we have developed for the first time a deoxygenative trifluoromethylthiolation method to synthesize trifluoromethylthioesters.

In this transformation process, PPh$_3$ can be used as a mediator to "umpolung" the electrophilic trifluoromethylthiolating agent *N*-(trifluoromethylthio)phthalimide (**7.2a**) to yield trifluoromethylthioesters from readily available carboxylic acids. The reactions are facile, rapid, and mildness. The current method enables rapid access to a wide range of trifluoromethylthioesters from earth-abundant, inexpensive, and environmentally benign carboxylic acids. This method can modify a diversity of natural products and drug molecules to their corresponding trifluoromethylthioesters. Besides, with the aid of palladium catalysis, the trifluoromethylthioesters can be further converted to the corresponding trifluoromethylthioethers.

We foresee this method can expedite drug discovery by providing novel synthetic disconnections and offering facile access to potentially bio-active moieties.

7.7   Experimental section

7.7.1   General procedure for deoxygenative trifluoromethylthiolation of carboxylic acids

Two oven-dried 15 mL re-sealable screw-cap vials (oven-dried) were both equipped with a Teflon-coated magnetic stirring bar (oven-dried), and were transferred into glovebox. One vial was sequentially charged with carboxylic acid (1.0 equiv., 0.30 mmol), triphenylphosphine (Ph$_3$P, 1.1 equiv., 0.33 mmol, 87 mg) and anhydrous Tetrahydrofuran (THF, 0.5 mL) in glovebox and the mixture was stirred vigorously. Another vial was sequentially charged with *N*-(trifluoromethylthio)phthalimide (1.3 equiv., 0.39 mmol, 96 mg), anhydrous FeCl$_3$ (5 mol%, 2.4 mg), and anhydrous THF (1 mL) in the glovebox. Then the 2 vials were transferred out of the glovebox. The solution of the second vial was added into the first one dropwise under nitrogen at room temperature. The resulting mixture was stirred at room temperature for 30 minutes during which time the color of the mixture change from red to bright yellow. After the reaction, the solvent was blown away by dry air and the reaction mixture was diluted with dichloromethane and was purified by flash column chromatography using a solvent mixture (ethyl acetate, hexanes or diethyl ether, *n*-pentane) as an eluent to afford the purified product. Notice: Because of the high volatility of certain products, their isolated yields were low.

7.7.2   Characterization of the reaction product

S-(trifluoromethyl) [1,1'-biphenyl]-4-carbothioate (7.3a)
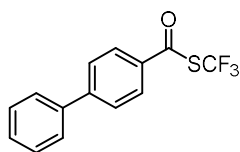
Following the General Procedure with the corresponding carboxylic acid (0.3 mmol). The crude product purified by flash column chromatography, using hexanes/EA = 30/1 (v/v) as an eluent, to yield the title compound **7.3a** (80 mg) in 95%.

^{1}H NMR (400 MHz, Chloroform-d): δ 7.98 – 7.88 (m, 2H), 7.75 – 7.70 (m, 2H), 7.65 – 7.60 (m, 2H), 7.52 – 7.42 (m, 3H).

^{13}C NMR (101 MHz, Chloroform-d): δ 183.25, 148.40, 139.64, 134.24 (q, *J* = 2.7 Hz), 129.64, 129.32, 128.77, 128.61 (q, *J* = 309.6 Hz), 128.26, 127.83.

^{19}F NMR (376 MHz, Chloroform-d): δ -39.50.

Physical State: white solid.

HRMS (EI) m/z: [M]$^+$ Calcd for C$_{14}$H$_9$F$_3$OS$^+$ 282.0321, Found 282.0321.

The spectra were consistent with the spectrum reported in the literature.[187]

S-(trifluoromethyl) 4-methoxybenzothioate (7.3b)
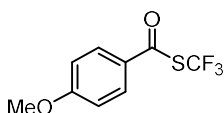
Following the General Procedure with the corresponding carboxylic acid (0.3 mmol). The crude product purified by flash column chromatography, using hexanes/EA = 30/1 (v/v) as an eluent, to yield the title compound **7.3b** (64 mg) in 90%.

^{1}H NMR (400 MHz, Chloroform-d): δ 7.82 (d, *J* = 8.9 Hz, 2H), 6.96 (d, *J* = 8.9 Hz, 2H), 3.89 (s, 3H).

^{13}C NMR (101 MHz, Chloroform-d): δ 181.48, 165.07, 130.09, 128.20 (q, *J* = 309.2 Hz), 127.82 (q, *J* = 2.7 Hz), 114.41, 55.70.

^{19}F NMR (376 MHz, Chloroform-d): δ -39.43.

Physical State: pale brown oil.

HRMS (ESI/QTOF) m/z: [M + H]$^+$ Calcd for C$_{10}$H$_7$F$_3$O$_2$S$^+$ 237.0192, Found 237.0193.

The spectra were consistent with the spectrum reported in the literature.[187]

S-(trifluoromethyl) 2-methoxybenzothioate (7.3c)
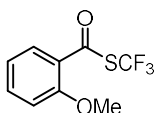
Following the General Procedure with the corresponding carboxylic acid (0.3 mmol). The crude product purified by flash column chromatography, using *n*-pentane/diethyl ether = 30/1 (v/v) as an eluent, to yield the title compound **7.3c** (60 mg) in 85%.

^{1}H NMR (400 MHz, Chloroform-d): δ 7.89 (dd, *J* = 7.9, 1.8 Hz, 1H), 7.58 (ddd, *J* = 8.2, 7.3, 1.8 Hz, 1H), 7.10 – 7.05 (m, 1H), 7.03 (d, *J* = 8.4 Hz, 1H), 3.99 (s, 3H).

^{13}C NMR (101 MHz, Chloroform-d): δ 182.01, 159.32, 136.03, 130.37, 128.31 (q, *J* = 310.1 Hz), 124.09 (q, *J* = 2.6 Hz), 121.29, 112.30, 56.01.

^{19}F NMR (376 MHz, Chloroform-d): δ -42.13.

Physical State: colorless oil.

HRMS (ESI/QTOF) m/z: [M + H]$^+$ Calcd for C$_{10}$H$_7$F$_3$O$_2$S$^+$ 237.0192, Found 237.0192.

The spectra were consistent with the spectrum reported in the literature.[196]

S-(trifluoromethyl) 2-methoxybenzothioate (7.3d)
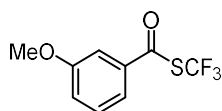
Following the General Procedure with the corresponding carboxylic acid (0.3 mmol). The crude product purified by flash column chromatography, using *n*-pentane/diethyl ether = 30/1 (v/v) as an eluent, to yield the title compound **7.3d** (57 mg) in 81%.

^{1}H NMR (400 MHz, Chloroform-d): δ 7.46 – 7.39 (m, 2H), 7.36 (s, 1H), 7.22 – 7.18 (m, 1H), 3.86 (s, 3H).

^{13}C NMR (101 MHz, Chloroform-d): δ 183.36, 160.27, 136.54, 130.36, 128.14 (q, J = 309.6 Hz), 121.67, 120.28, 111.93, 55.74.

^{19}F NMR (376 MHz, Chloroform-d): δ -39.77.

Physical State: colorless oil.

HRMS (ESI/QTOF) m/z: [M + Na]$^+$ Calcd for C$_9$H$_7$F$_3$O$_2$SNa$^+$ 259.0017, Found 259.0018.

The spectra were consistent with the spectrum reported in the literature.[196]

S-(trifluoromethyl) 2-ethylbenzothioate (7.3e)
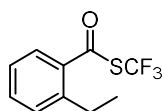
Following the General Procedure with the corresponding carboxylic acid (0.3 mmol). The crude product purified by flash column chromatography, using *n*-pentane/diethyl ether = 30/1 (v/v) as an eluent, to yield the title compound **7.3e** (48 mg) in 69%.

^{1}H NMR (400 MHz, Chloroform-d): δ 7.67 (dd, J = 7.8, 1.4 Hz, 1H), 7.52 (td, J = 7.6 Hz, 1.4 Hz, 1H), 7.32 (ddd, J = 15.2, 7.7, 1.2 Hz, 2H), 2.88 (q, J = 7.5 Hz, 2H), 1.24 (td, J = 7.5, 1.1 Hz, 4H).

^{13}C NMR (101 MHz, Chloroform-d): δ 184.84, 144.67, 134.65 (q, J = 2.7 Hz), 133.67, 130.94, 128.74, 128.05 (q, J = 309.9 Hz), 126.36, 26.97, 15.81.

^{19}F NMR (376 MHz, Chloroform-d): δ -40.61.

Physical State: yellowish oil.

HRMS (APPI/LTQ-Orbitrap) m/z: [M + H]$^+$ Calcd for C$_{10}$H$_{10}$F$_3$OS$^+$ 235.0399, Found 235.0399.

The spectra were consistent with the spectrum reported in the literature.[187]

S-(trifluoromethyl) 4-(tert-butyl)benzothioate (7.3f)
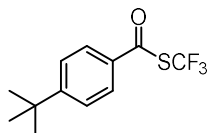
Following the General Procedure with the corresponding carboxylic acid (0.3 mmol). The crude product purified by flash column chromatography, using n-pentane/diethyl ether = 30/1 (v/v) as an eluent, to yield the title compound **7.3f** (56 mg) in 71%.

^{1}H NMR (400 MHz, Chloroform-d): δ 7.87 – 7.72 (m, 2H), 7.59 – 7.45 (m, 2H), 1.35 (s, 9H).

^{13}C NMR (101 MHz, Chloroform-d): δ 182.73, 159.30, 132.51 (q, J = 2.8 Hz), 128.15 (q, J = 309.3 Hz), 127.65, 126.19, 35.42, 30.96.

^{19}F NMR (376 MHz, Chloroform-d): δ -39.57.

Physical State: yellowish oil.

HRMS (ESI/QTOF) m/z: [M + Na]$^+$ Calcd for $C_{12}H_{13}F_3OSNa^+$ 285.0537, Found 285.0534.

The spectra were consistent with the spectrum reported in the literature.[187]

S-(trifluoromethyl) 4-fluorobenzothioate (7.3g)
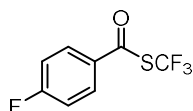
Following the General Procedure with the corresponding carboxylic acid (0.3 mmol). The crude product purified by flash column chromatography, using n-pentane/diethyl ether = 30/1 (v/v) as an eluent, to yield the title compound **7.3g** (41 mg) in 61%.

^{1}H NMR (400 MHz, Chloroform-d): δ 7.90 (dd, J = 8.5, 5.1 Hz, 2H), 7.20 (t, J = 8.3 Hz, 2H).

^{13}C NMR (101 MHz, Chloroform-d): δ 181.91, 168.23, 165.66, 131.62, 130.61, 130.51, 128.00 (q, J = 309.8 Hz), 116.84, 116.62.

^{19}F NMR (376 MHz, Chloroform-d): δ -39.56, -101.01.

Physical State: yellowish oil.

HRMS (APPI/LTQ-Orbitrap) m/z: [M + H]$^+$ Calcd for $C_8H_5F_4OS^+$ 224.9992; Found 224.9994.

The spectra were consistent with the spectrum reported in the literature.[187]

S-(trifluoromethyl) 4-chlorobenzothioate (7.3h)
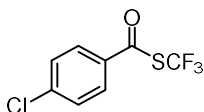
Following the General Procedure with the corresponding carboxylic acid (0.3 mmol). The crude product purified by flash column chromatography, using *n*-pentane/diethyl ether = 30/1 (v/v) as an eluent, to yield the title compound **7.3h** (47 mg) in 65%.

¹H NMR (400 MHz, Chloroform-d): δ 7.80 (d, *J* = 8.2 Hz, 2H), 7.50 (d, *J* = 8.2 Hz, 2H).

¹³C NMR (101 MHz, Chloroform-d): δ 182.32, 141.90, 133.56 (q, *J* = 2.7 Hz), 129.75, 129.09, 127.95 (q, *J* = 310.0 Hz).

¹⁹F NMR (376 MHz, Chloroform-d): δ -39.53.

Physical State: yellowish oil.

HRMS (APPI/LTQ-Orbitrap) m/z: [M + H]⁺ Calcd for $C_8H_5F_3ClOS^+$ 240.9696; Found 240.9698.

The spectra were consistent with the spectrum reported in the literature.[187]

S-(trifluoromethyl) 4-bromobenzothioate (7.3i)
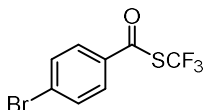
Following the General Procedure with the corresponding carboxylic acid (0.3 mmol). The crude product purified by flash column chromatography, using *n*-pentane/diethyl ether = 30/1 (v/v) as an eluent, to yield the title compound **7.3i** (68 mg) in 80%.

¹H NMR (400 MHz, Chloroform-d): δ 7.75 – 7.62 (m, 4H).

¹³C NMR (101 MHz, Chloroform-d): δ 182.54, 133.98 (q, *J* = 2.7 Hz), 132.73, 130.63, 129.09, 127.91 (q, *J* = 309.9 Hz).

¹⁹F NMR (376 MHz, Chloroform-d): δ -39.54.

Physical State: yellowish solid.

HRMS (APPI/LTQ-Orbitrap) m/z: [M + H]⁺ Calcd for $C_8H_5BrF_3OS^+$ 284.9191; Found 284.9192.

The spectra were consistent with the spectrum reported in the literature.[187]

S-(trifluoromethyl) 4-iodobenzothioate (7.3j)
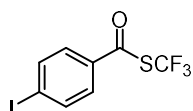
Following the General Procedure with the corresponding carboxylic acid (0.3 mmol). The crude product purified by flash column chromatography, using *n*-pentane/diethyl ether = 30/1 (v/v) as an eluent, to yield the title compound **7.3j** (75 mg) in 75%.

^{1}H NMR (400 MHz, Chloroform-d): δ 7.95 – 7.87 (m, 2H), 7.63 – 7.55 (m, 2H).

^{13}C NMR (101 MHz, Chloroform-d): δ 182.77, 138.57, 134.42, 134.39, 129.27, 128.71, 126.19, 103.38.

^{19}F NMR (376 MHz, Chloroform-d): δ -39.53.

Physical State: white solid.

HRMS (APPI/LTQ-Orbitrap) m/z: [M + H]$^+$ Calcd for $C_8H_5F_3IOS^+$ 332.9052; Found 332.9059.

S-(trifluoromethyl) 2-chlorobenzothioate (7.3k)
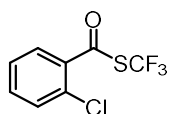
Following the General Procedure with the corresponding carboxylic acid (0.3 mmol). The crude product purified by flash column chromatography, using *n*-pentane/diethyl ether = 30/1 (v/v) as an eluent, to yield the title compound **7.3k** (44 mg) in 61%.

^{1}H NMR (400 MHz, Chloroform-d): δ 7.73 – 7.64 (m, 1H), 7.56 – 7.48 (m, 2H), 7.45 – 7.35 (m, 1H).

^{13}C NMR (101 MHz, Chloroform-d): δ 182.67, 134.78 (q, *J* = 2.6 Hz), 134.12, 131.91, 131.68, 129.67, 127.60 (q, *J* = 310.9 Hz), 127.28.

^{19}F NMR (376 MHz, Chloroform-d): δ -40.55.

Physical State: yellowish oil.

HRMS (APPI/LTQ-Orbitrap) m/z: [M + H]$^+$ Calcd for $C_8H_5F_3ClOS^+$ 240.9696; Found 240.9697.

The spectra were consistent with the spectrum reported in the literature.[196]

S-(trifluoromethyl) 2-bromobenzothioate (7.3l)
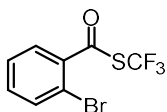
Following the General Procedure with the corresponding carboxylic acid (0.3 mmol). The crude product purified by flash column chromatography, using *n*-pentane/diethyl ether = 30/1 (v/v) as an eluent, to yield the title compound **7.3l** (64 mg) in 75%.

¹H NMR (400 MHz, Chloroform-d): δ 7.79 – 7.67 (m, 1H), 7.67 – 7.58 (m, 1H), 7.48 – 7.40 (m, 2H).

¹³C NMR (101 MHz, Chloroform-d): δ 183.55 (q, *J* = 1.3 Hz), 136.84 (q, *J* = 2.8 Hz), 134.95, 134.02, 129.53, 127.80, 127.54 (q, *J* = 311.1 Hz), 119.62.

¹⁹F NMR (376 MHz, Chloroform-d): δ -40.51.

Physical State: yellowish oil.

HRMS (APPI/LTQ-Orbitrap) m/z: [M + H]⁺ Calcd for $C_8H_5BrF_3OS^+$ 284.9191; Found 284.9193.

S-(trifluoromethyl) 2-iodobenzothioate (7.3m)
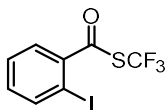
Following the General Procedure with the corresponding carboxylic acid (0.3 mmol). The crude product purified by flash column chromatography, using *n*-pentane/diethyl ether = 30/1 (v/v) as an eluent, to yield the title compound **7.3m** (71 mg) in 71%.

¹H NMR (400 MHz, Chloroform-d): δ 8.01 (d, *J* = 8.0 Hz, 1H), 7.59 (dd, *J* = 7.9, 1.6 Hz, 1H), 7.51 – 7.41 (m, 1H), 7.27 – 7.23 (m, 1H).

¹³C NMR (101 MHz, Chloroform-d): δ 184.66, 141.86, 139.85 (q, *J* = 2.7 Hz), 134.00, 129.22, 128.48, 127.55 (q, *J* = 311.0 Hz), 91.58.

¹⁹F NMR (376 MHz, Chloroform-d): δ -40.46.

Physical State: yellowish oil.

HRMS (APPI/LTQ-Orbitrap) m/z: [M + H]⁺ Calcd for $C_8H_5F_3IOS^+$ 332.9052; Found 332.9059.

S-(trifluoromethyl) 4-(trifluoromethyl)benzothioate (7.3n)
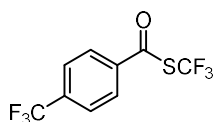
Following the General Procedure with the corresponding carboxylic acid (0.3 mmol). The crude product purified by flash column chromatography, using hexanes/EA = 30/1 (v/v) as an eluent, to yield the title compound **7.3n** (53 mg) in 65%.

¹H NMR (400 MHz, Chloroform-d): δ 8.12 – 7.92 (m, 2H), 7.92 – 7.73 (m, 2H).

¹³C NMR (101 MHz, Chloroform-d): δ 182.77, 137.95, 136.42 (q, J = 33.2 Hz), 128.16, 127.79 (q, J = 310.2 Hz), 126.50 (q, J = 3.7 Hz), 123.29 (q, J = 273.1 Hz).

¹⁹F NMR (376 MHz, Chloroform-d): δ -39.60, -63.42.

Physical State: white solid.

HRMS (EI) m/z: [M - F]⁺ Calcd for 254.9903; Found: 254.9904.

The spectra were consistent with the spectrum reported in the literature.[196]

4-((trifluoromethylthio)carbonyl)benzoate (7.3o)
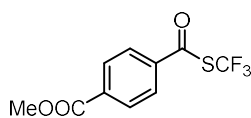
Following the General Procedure with the corresponding carboxylic acid (0.3 mmol). The crude product purified by flash column chromatography, using hexanes/EA = 20/1 (v/v) as an eluent, to yield the title compound **7.3o** (54 mg) in 68%.

¹H NMR (400 MHz, Chloroform-d): δ 8.23 – 8.07 (m, 2H), 7.99 – 7.84 (m, 2H), 3.96 (s, 3H).

¹³C NMR (101 MHz, Chloroform-d): δ 183.06, 165.69, 138.32 (q, J = 2.7 Hz), 135.83, 130.47, 127.89 (d, J = 310.1 Hz), 127.70, 52.85.

¹⁹F NMR (376 MHz, Chloroform-d): δ -39.65.

Physical State: off-white solid.

HRMS (APPI/LTQ-Orbitrap) m/z: [M + H]⁺ Calcd for $C_{10}H_8F_3O_3S^+$ 265.0141; Found 265.0140.

The spectra were consistent with the spectrum reported in the literature.[187]

S-(trifluoromethyl) 4-((*tert*-butoxycarbonyl)amino)benzothioate (7.3p)
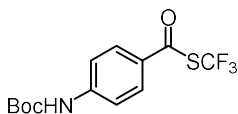
Following the General Procedure with the corresponding carboxylic acid (0.3 mmol). The crude product purified by flash column chromatography, using hexanes/EA = 30/1 (v/v) as an eluent, to yield the title compound **7.3p** (60 mg) in 62%.

¹H NMR (400 MHz, Chloroform-d): δ 7.86 – 7.76 (m, 2H), 7.58 – 7.49 (m, 2H), 6.88 (s, 1H), 1.55 (s, 9H).

¹³C NMR (101 MHz, Chloroform-d): δ 151.88, 144.83, 129.31, 128.16 (q, J = 309.3 Hz), 117.71, 81.82, 28.21.

¹⁹F NMR (376 MHz, Chloroform-d): δ -39.43.

Physical State: pale grey solid.

HRMS (APPI/LTQ-Orbitrap) m/z: [M + H]⁺ Calcd for $C_{13}H_{15}F_3NO_3S^+$ 322.0719; Found 322.0710.

S-(trifluoromethyl) 4-(methylthio)benzothioate (7.3q)
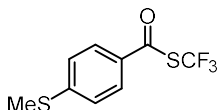
Following the General Procedure with the corresponding carboxylic acid (0.3 mmol). The crude product purified by flash column chromatography, using hexanes/EA = 30/1 (v/v) as an eluent, to yield the title compound **7.3q** (54 mg) in 72%.

¹H NMR (400 MHz, Chloroform-d): δ 7.88 – 7.69 (m, 2H), 7.40 – 7.24 (m, 2H), 2.55 (s, 3H).

¹³C NMR (101 MHz, Chloroform-d): δ 182.14, 149.30, 131.17 (q, J = 2.9 Hz), 128.24 (q, J = 309.5 Hz), 128.05, 125.25, 14.73.

¹⁹F NMR (376 MHz, Chloroform-d): δ -39.43.

Physical State: white solid.

HRMS (APPI/LTQ-Orbitrap) m/z: [M + H]⁺ Calcd for $C_9H_8F_3OS_2^+$ 252.9963; Found 252.9958.

S-(trifluoromethyl) 4-(4,4,5,5-tetramethyl-1,3,2-dioxaborolan-2-yl)benzothioate (7.3r)
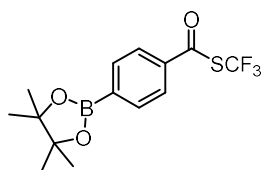
Following the General Procedure with the corresponding carboxylic acid (0.2 mmol). The crude product purified by flash column chromatography, using *n*-pentane/diethyl ether = 30/1 (v/v) as an eluent, to yield the title compound **7.3r** (40 mg) in 60%.

¹H NMR (400 MHz, Chloroform-d): δ 8.04 – 7.90 (m, 2H), 7.90 – 7.79 (m, 2H), 1.38 (s, 12H).

¹³C NMR (101 MHz, Chloroform-d): δ 183.69, 137.06 (q, J = 2.6 Hz), 135.52, 128.16 (q, J = 309.6 Hz), 126.69, 84.65, 25.03.

¹⁹F NMR (376 MHz, Chloroform-d): δ -39.68.

Physical State: yellow oil.

HRMS (APPI/LTQ-Orbitrap) m/z: [M + H]⁺ Calcd for $C_{14}H_{17}BF_3O_3S^+$ 333.0938; Found 333.0939.

S-(trifluoromethyl) 4-(allyloxy)benzothioate (7.3s)
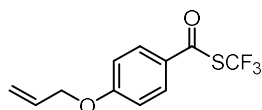
Following the General Procedure with the corresponding carboxylic acid (0.3 mmol). The crude product purified by flash column chromatography, using hexanes/EA = 30/1 (v/v) as an eluent, to yield the title compound **7.3s** (59 mg) in 75%.

¹H NMR (400 MHz, Chloroform-d): δ 7.91 – 7.71 (m, 2H), 7.04 – 6.91 (m, 2H), 6.14 – 5.92 (m, 1H), 5.47 – 5.27 (m, 2H), 4.62 (dt, J = 5.3, 1.6 Hz, 2H).

¹³C NMR (101 MHz, Chloroform-d): δ 181.57, 164.20, 132.12, 130.19, 128.34 (q, J = 309.2 Hz), 128.01 (q, J = 2.9 Hz), 118.69, 115.23, 69.27.

¹⁹F NMR (376 MHz, Chloroform-d): δ -39.43.

Physical State: white solid.

HRMS (APPI/LTQ-Orbitrap) m/z: [M + H]⁺ Calcd for $C_{11}H_{10}F_3O_2S^+$ 263.0348; Found 263.0347.

S-(trifluoromethyl) 4-(allyloxy)benzothioate (7.3t)
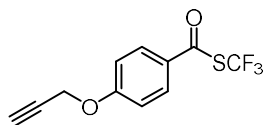
Following the General Procedure with the corresponding carboxylic acid (0.3 mmol). The crude product purified by flash column chromatography, using hexanes/EA = 30/1 (v/v) as an eluent, to yield the title compound **7.3t** (53 mg) in 68%.

**^{1}H NMR** (400 MHz, Chloroform-d): δ 7.89 – 7.80 (m, 2H), 7.10 – 7.01 (m, 2H), 4.78 (d, *J* = 2.4 Hz, 2H), 2.57 (t, *J* = 2.4 Hz, 1H).

^{13}C NMR (101 MHz, Chloroform-d): δ 181.69, 162.94, 130.66, 130.13, 128.71 (q, *J* = 2.8 Hz), 128.27 (q, *J* = 309.3 Hz), 115.44, 56.20.

^{19}F NMR (376 MHz, Chloroform-d): δ -39.44.

Physical State: white solid.

HRMS (APPI/LTQ-Orbitrap) m/z: [M + H]$^+$ Calcd for $C_{11}H_8F_3O_2S^+$ 261.0192; Found 261.0190.

S-(trifluoromethyl) benzo[1,3]dioxole-5-carbothioate (7.3u)
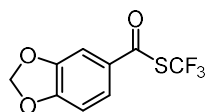
Following the General Procedure with the corresponding carboxylic acid (0.3 mmol). The crude product purified by flash column chromatography, using *n*-pentane/diethyl ether = 20/1 (v/v) as an eluent, to yield the title compound **7.3u** (61 mg) in 81%.

^{1}H NMR (400 MHz, Chloroform-d): δ 7.46 (ddd, *J* = 8.2, 1.9, 0.7 Hz, 1H), 7.28 (dd, *J* = 12.7, 1.2 Hz, 1H), 6.88 (d, *J* = 8.2 Hz, 1H), 6.09 (s, 2H).

^{13}C NMR (101 MHz, Chloroform-d): δ 181.40, 153.66, 148.81, 129.64 (q, *J* = 2.8 Hz), 128.20 (q, *J* = 309.3 Hz), 124.60, 108.58, 107.39, 102.61.

^{19}F NMR (376 MHz, Chloroform-d): δ -39.58.

Physical State: off-white solid.

HRMS (APPI/LTQ-Orbitrap) m/z: [M + H]$^+$ Calcd for $C_9H_6F_3O_3S^+$ 250.9984; Found 250.9983.

S-(trifluoromethyl) naphthalene-2-carbothioate (7.3v)
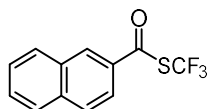
Following the General Procedure with the corresponding carboxylic acid (0.3 mmol). The crude product purified by flash column chromatography, using *n*-pentane/diethyl ether = 20/1 (v/v) as an eluent, to yield the title compound **7.3v** (68 mg) in 89%.

**¹H NMR** (400 MHz, Chloroform-d): δ 8.39 (s, 1H), 8.05 – 7.76 (m, 4H), 7.64 (m, 2H).

¹³C NMR (101 MHz, Chloroform-d): δ 183.14, 136.37, 132.40 (q, J = 2.8 Hz), 132.25, 129.86, 129.72, 129.59, 129.28, 128.13 (q, J = 309.6 Hz), 127.97, 127.56, 122.57.

¹⁹F NMR (376 MHz, Chloroform-d): δ -39.50.

Physical State: white solid.

HRMS (APPI/LTQ-Orbitrap) m/z: [M + H]$^+$ Calcd for $C_{12}H_8F_3OS^+$ 257.0243; Found 257.0244. The spectra were consistent with the spectrum reported in the literature.[187]

S-(trifluoromethyl) quinoline-8-carbothioate (7.3w)
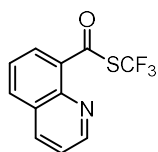
Following the General Procedure with the corresponding carboxylic acid (0.3 mmol). The crude product purified by flash column chromatography, using hexanes/EA = 20/1 (v/v) as an eluent, to yield the title compound **7.3w** (51 mg) in 66%.

¹H NMR (400 MHz, Chloroform-d): δ 9.01 (dd, J = 4.2, 1.8 Hz, 1H), 8.44 (dd, J = 7.4, 1.5 Hz, 1H), 8.28 (dd, J = 8.3, 1.8 Hz, 1H), 8.10 (dd, J = 8.2, 1.5 Hz, 1H), 7.68 (t, J = 7.7 Hz, 1H), 7.56 (dd, J = 8.4, 4.2 Hz, 1H).

¹³C NMR (101 MHz, Chloroform-d): δ 149.95, 145.01, 136.90, 134.32, 132.10 (q, J = 9.9 Hz), 131.92, 128.52 (q, J = 12.3 Hz), 128.29 (q, J = 313.1 Hz), 128.06, 126.34, 122.14.

¹⁹F NMR (376 MHz, Chloroform-d): δ -43.85.

Physical State: off-white solid.

HRMS (APPI/LTQ-Orbitrap) m/z: [M + H]$^+$ Calcd for $C_{11}H_7F_3NOS^+$ 258.0195; Found 258.019.

S-(trifluoromethyl) benzothiophene-5-carbothioate (7.3x)
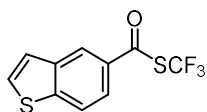
Following the General Procedure with the corresponding carboxylic acid (0.3 mmol). The crude product purified by flash column chromatography, using hexanes/EA = 20/1 (v/v) as an eluent, to yield the title compound **7.3x** (56 mg) in 71%.

^{1}H NMR (400 MHz, Chloroform-d): δ 8.33 (d, *J* = 1.8 Hz, 1H), 7.97 (dd, *J* = 8.4, 0.9 Hz, 1H), 7.79 (dd, *J* = 8.5, 1.8 Hz, 1H), 7.60 (d, *J* = 5.5 Hz, 1H), 7.46 (dd, *J* = 5.5, 0.8 Hz, 1H).

^{13}C NMR (101 MHz, Chloroform-d): δ 183.07, 146.08, 139.44, 131.61 (q, *J* = 2.8 Hz), 129.03, 128.11 (q, *J* = 309.5 Hz), 124.52, 123.71, 123.28, 122.25.

^{19}F NMR (376 MHz, Chloroform-d): δ -39.51.

Physical State: yellowish solid.

HRMS (APPI/LTQ-Orbitrap) m/z: $[M + H]^+$ Calcd for $C_{10}H_6F_3OS_2^+$ 262.9807; Found 262.9806.

S-(trifluoromethyl) 2-(4-methoxyphenyl)ethanethioate (7.4a)
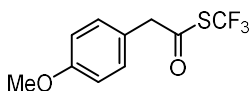
Following the General Procedure with the corresponding carboxylic acid (0.3 mmol). The crude product purified by flash column chromatography, using hexanes/EA = 30/1 (v/v) as an eluent, to yield the title compound **7.4a** (51 mg) in 68%.

^{1}H NMR (400 MHz, Chloroform-d): δ 7.23 – 7.16 (m, 2H), 6.97 – 6.85 (m, 2H), 3.82 (s, 3H), 3.81 (s, 2H).

^{13}C NMR (101 MHz, Chloroform-d): δ 190.03, 159.99, 131.52, 127.93 (q, *J* = 310.2 Hz), 122.62, 114.68, 55.43, 50.12 (q, *J* = 2.8 Hz).

^{19}F NMR (376 MHz, Chloroform-d): δ -40.69.

Physical State: colorless oil.

HRMS (nanochip-ESI/LTQ-Orbitrap) m/z: $[M]^+$ Calcd for $C_{10}H_9F_3O_2S^+$ 250.0270; Found 250.0267.

S-(trifluoromethyl) (1R,2R)-2-phenylcyclopropane-1-carbothioate (7.4b)
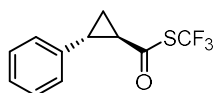
Following the General Procedure with the corresponding carboxylic acid (0.3 mmol). The crude product purified by flash column chromatography, using *n*-pentane/diethyl ether = 30/1 (v/v) as an eluent, to yield the title compound **7.4b** (48 mg) in 65%.

¹H NMR (400 MHz, Chloroform-*d*): δ 7.41 – 7.23 (m, 3H), 7.21 – 7.09 (m, 2H), 2.86 (ddd, *J* = 9.5, 7.1, 4.0 Hz, 1H), 2.17 (dt, *J* = 8.6, 4.6 Hz, 1H), 1.94 (dt, *J* = 9.6, 5.0 Hz, 1H), 1.65 (td, *J* = 7.6, 4.8 Hz, 1H).

¹³C NMR (101 MHz, Chloroform-*d*): δ 188.73, 138.41, 128.86, 127.72 (q, *J* = 310.0 Hz), 127.41, 126.42, 33.92 (q, *J* = 3.7 Hz), 30.30, 19.79.

¹⁹F NMR (376 MHz, Chloroform-*d*): δ -40.02.

Physical State: pale yellow oil.

HRMS (APPI/LTQ-Orbitrap) m/z: [M]⁺ Calcd for $C_{11}H_9F_3OS^+$ 246.0321; Found 246.0317.

S-(trifluoromethyl) 1-(4-methylphenyl)cyclopropane-1-carbothioate (7.4c)
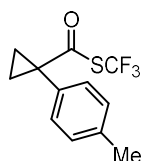
Following the General Procedure with the corresponding carboxylic acid (0.3 mmol). The crude product purified by flash column chromatography, using *n*-pentane/diethyl ether =30/1 (v/v) as an eluent, to yield the title compound **7.4c** (53 mg) in 68%.

¹H NMR (400 MHz, Chloroform-*d*): δ 7.34 (d, *J* = 7.7 Hz, 2H), 7.21 (d, *J* = 7.7 Hz, 2H), 2.40 (s, 3H), 1.83 (q, *J* = 3.6 Hz, 2H), 1.37 (q, *J* = 4.1 Hz, 2H).

¹³C NMR (101 MHz, Chloroform-*d*): δ 193.73, 139.75, 132.97, 132.42, 129.68, 128.07 (q, *J* = 310.1 Hz), 38.23 (q, *J* = 3.2 Hz), 21.45, 20.48.

¹⁹F NMR (376 MHz, Chloroform-*d*): δ -41.84.

Physical State: yellowish oil.

HRMS (APPI/LTQ-Orbitrap) m/z: [M]⁺ Calcd for $C_{12}H_{11}F_3OS^+$ 260.0477; Found 260.0478.

S-(trifluoromethyl) 1-(4-chlorophenyl)cyclopropane-1-carbothioate (7.4d)
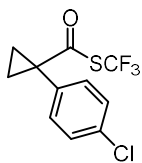
Following the General Procedure with the corresponding carboxylic acid (0.3 mmol). The crude product purified by flash column chromatography, using *n*-pentane/diethyl ether =30/1 (v/v) as an eluent, to yield the title compound **7.4d** (58 mg) in 69%.

¹H NMR (400 MHz, Chloroform-*d*): δ 7.38 (d, *J* = 2.4 Hz, 4H), 1.85 (q, *J* = 4.1 Hz, 2H), 1.36 (q, *J* = 4.1 Hz, 2H).

¹³C NMR (101 MHz, Chloroform-*d*): δ 192.73, 135.79, 134.53, 133.80, 129.27, 127.86 (q, *J* = 310.2 Hz), 38.02 (q, *J* = 3.3 Hz), 20.48.

¹⁹F NMR (376 MHz, Chloroform-*d*): δ -41.61.

Physical State: yellowish oil.

HRMS (APPI/LTQ-Orbitrap) m/z: [M]⁺ Calcd for $C_{11}H_8ClF_3OS^+$ 279.9931; Found 279.9932.

S-(trifluoromethyl) 1-(4-methoxyphenyl)cyclopropane-1-carbothioate (7.4e)
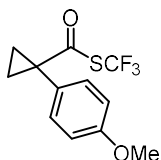
Following the General Procedure with the corresponding carboxylic acid (0.3 mmol). The crude product purified by flash column chromatography, using *n*-pentane/diethyl ether =30/1 (v/v) as an eluent, to yield the title compound **7.4e** (62 mg) in 75%.

¹H NMR (400 MHz, Chloroform-*d*): δ 7.36 (d, *J* = 8.4 Hz, 2H), 6.91 (d, *J* = 8.4 Hz, 2H), 3.84 (s, 3H), 1.81 (q, *J* = 3.9 Hz, 2H), 1.35 (q, *J* = 4.0 Hz, 2H).

¹³C NMR (101 MHz, Chloroform-*d*): δ 194.05, 160.60, 133.82, 128.10 (q, *J* = 310.1 Hz), 127.80, 114.30, 55.46, 37.80 (q, *J* = 3.3 Hz), 20.64.

¹⁹F NMR (376 MHz, Chloroform-*d*): δ -41.95.

Physical State: reddish oil.

HRMS (APPI/LTQ-Orbitrap) m/z: [M]⁺ Calcd for $C_{12}H_{11}F_3O_2S^+$ 276.0426; Found 276.0429.

S-(trifluoromethyl) (E)-3-phenylprop-2-enethioate (7.5a)
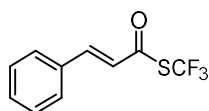
Following the General Procedure with the corresponding carboxylic acid (0.3 mmol). The crude product purified by flash column chromatography, using *n*-pentane/diethyl ether =30/1 (v/v) as an eluent, to yield the title compound **7.5a** (57 mg) in 82%.

¹H NMR (400 MHz, Chloroform-d): δ 7.65 (d, *J* = 15.8 Hz, 1H), 7.60 – 7.53 (m, 2H), 7.51 – 7.38 (m, 3H), 6.61 (d, *J* = 15.8 Hz, 1H).

¹³C NMR (101 MHz, Chloroform-d): δ 180.95, 145.18, 133.14, 131.95, 129.36, 129.01, 128.07 (q, *J* = 309.5 Hz), 122.86 (q, *J* = 3.1 Hz).

¹⁹F NMR (376 MHz, Chloroform-d): δ -39.52.

Physical State: colorless oil.

HRMS (APPI/LTQ-Orbitrap) m/z: [M + H]⁺ Calcd for $C_{10}H_8F_3OS^+$ 233.0242; Found 233.0241.

S-(trifluoromethyl) (E)-3-(4-fluorophenyl)prop-2-enethioate (7.5b)
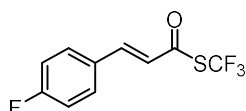
Following the General Procedure with the corresponding carboxylic acid (0.3 mmol). The crude product purified by flash column chromatography, using *n*-pentane/diethyl ether =30/1 (v/v) as an eluent, to yield the title compound **7.5b** (53 mg) in 70%.

¹H NMR (400 MHz, Chloroform-d): δ 7.71 – 7.44 (m, 3H), 7.12 (t, *J* = 8.4 Hz, 2H), 6.53 (d, *J* = 15.8 Hz, 1H).

¹³C NMR (101 MHz, Chloroform-d): δ 180.77, 164.90 (d, *J* = 254.3 Hz), 143.75, 131.08 (d, *J* = 8.8 Hz), 129.42 (d, *J* = 3.4 Hz), 128.02 (q, *J* = 309.5 Hz), 122.86 – 122.11 (m), 116.64 (d, *J* = 22.2 Hz).

¹⁹F NMR (376 MHz, Chloroform-d): δ -39.53, -106.55.

Physical State: yellowish solid.

HRMS (APPI/LTQ-Orbitrap) m/z: [M + H]⁺ Calcd for $C_{10}H_7F_4OS^+$ 251.0148; Found 251.0149.

S-(trifluoromethyl) (E)-3-(4-chlorophenyl)prop-2-enethioate (7.5c)
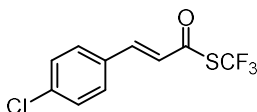
Following the General Procedure with the corresponding carboxylic acid (0.3 mmol). The crude product purified by flash column chromatography, using n-pentane/diethyl ether =30/1 (v/v) as an eluent, to yield the title compound **7.5c** (57 mg) in 71%.

^{1}H NMR (400 MHz, Chloroform-d): δ 7.59 (d, J = 15.8 Hz, 1H), 7.52 – 7.46 (m, 2H), 7.44 – 7.37 (m, 2H), 6.57 (d, J = 15.8 Hz, 1H).

^{13}C NMR (101 MHz, Chloroform-d): δ 180.77 (q, J = 1.6 Hz), 143.55, 138.04, 131.60, 130.11, 129.68, 127.97 (q, J = 309.6 Hz), 123.19 (q, J = 3.1 Hz).

^{19}F NMR (376 MHz, Chloroform-d): δ -39.52.

Physical State: white solid.

HRMS (APPI/LTQ-Orbitrap) m/z: [M + H]$^+$ Calcd for $C_{10}H_7ClF_3OS^+$ 266.9853; Found 266.9853.

S-(trifluoromethyl) (E)-3-(4-bromophenyl)prop-2-enethioate (7.5d)
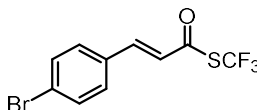
Following the General Procedure with the corresponding carboxylic acid (0.2 mmol). The crude product purified by flash column chromatography, using hexanes/EA = 30/1 (v/v) as an eluent, to yield the title compound **7.5d** (51 mg) in 82%.

^{1}H NMR (400 MHz, Chloroform-d): δ 7.64 – 7.53 (m, 3H), 7.42 (d, J = 8.5 Hz, 2H), 6.59 (d, J = 15.8 Hz, 1H).

^{13}C NMR (101 MHz, Chloroform-d): δ 180.80, 143.64, 132.68, 132.04, 130.26, 127.95 (q, J = 309.7 Hz), 126.51, 123.30 (q, J = 3.2 Hz).

^{19}F NMR (376 MHz, Chloroform-d): δ -39.52.

Physical State: white solid.

HRMS (APPI/LTQ-Orbitrap) m/z: [M + H]$^+$ Calcd for $C_{10}H_7BrF_3OS^+$ 310.9348; Found 310.9350.

S-(trifluoromethyl) (E)-3-(2-(trifluoromethyl)phenyl)prop-2-enethioate (7.5e)
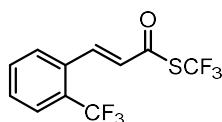
Following the General Procedure with the corresponding carboxylic acid (0.3 mmol). The crude product purified by flash column chromatography, using *n*-pentane/diethyl ether =30/1 (v/v) as an eluent, to yield the title compound **7.5e** (63 mg) in 70%.

^{1}H NMR (400 MHz, Chloroform-d): δ 8.03 (dd, *J* = 15.7, 2.1 Hz, 1H), 7.73 (dd, *J* = 14.3, 7.7 Hz, 2H), 7.59 (dt, *J* = 22.1, 7.5 Hz, 2H), 6.58 (d, *J* = 15.6 Hz, 1H).

^{13}C NMR (101 MHz, Chloroform-d): δ 180.67, 140.32 (q, *J* = 2.2 Hz), 132.33 (q, *J* = 1.1 Hz), 131.78 (q, *J* = 1.6 Hz), 130.91, 129.64 (q, *J* = 30.6 Hz), 128.00, 127.73 (q, *J* = 309.8 Hz), 126.82 – 126.32 (m), 123.70 (q, *J* = 274.1 Hz).

^{19}F NMR (376 MHz, Chloroform-d): δ -39.62, -58.73.

Physical State: yellowish oil.

HRMS (APPI/LTQ-Orbitrap) m/z: [M + H]$^+$ Calcd for $C_{11}H_7F_6OS^+$ 301.0116; Found 301.0116.

S-(trifluoromethyl) (E)-3-(4-methoxyphenyl)prop-2-enethioate (7.5f)
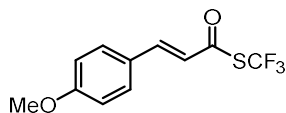
Following the General Procedure with the corresponding carboxylic acid (0.3 mmol). The crude product purified by flash column chromatography, using *n*-pentane/diethyl ether =20/1 (v/v) as an eluent, to yield the title compound **7.5f** (72 mg) in 91%.

^{1}H NMR (400 MHz, Chloroform-d): δ 7.60 (d, *J* = 15.7 Hz, 1H), 7.55 – 7.48 (m, 2H), 6.96 – 6.88 (m, 2H), 6.46 (d, *J* = 15.7 Hz, 1H), 3.86 (s, 3H).

^{13}C NMR (101 MHz, Chloroform-d): δ 180.68, 162.84, 145.00, 130.99, 128.22 (q, *J* = 309.2 Hz), 125.81, 120.31 (q, *J* = 3.1 Hz), 114.84, 55.62.

^{19}F NMR (376 MHz, Chloroform-d): δ -39.45.

Physical State: off-white solid.

HRMS (APPI/LTQ-Orbitrap) m/z: [M + H]$^+$ Calcd for $C_{11}H_{10}F_3O_2S^+$ 263.0348; Found 263.0352.

S-(trifluoromethyl) (E)-3-(4-(dimethylamino)phenyl)prop-2-enethioate (7.5g)
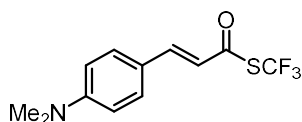
Following the General Procedure with the corresponding carboxylic acid (0.3 mmol). The crude product purified by flash column chromatography, using *n*-pentane/diethyl ether =20/1 (v/v) as an eluent, to yield the title compound **7.5g** (49 mg) in 59%.

¹H NMR (400 MHz, Chloroform-d): δ 7.58 (d, *J* = 15.4 Hz, 1H), 7.51 – 7.39 (m, 2H), 6.73 – 6.62 (m, 2H), 6.36 (d, *J* = 15.4 Hz, 1H), 3.06 (s, 6H).

¹³C NMR (101 MHz, Chloroform-d): δ 180.20, 152.91, 146.10, 131.27, 128.52 (q, *J* = 308.8 Hz), 120.69, 116.90 (q, *J* = 3.3 Hz), 111.92, 40.21.

¹⁹F NMR (376 MHz, Chloroform-d): δ -39.29.

Physical State: yellowish solid.

HRMS (APPI/LTQ-Orbitrap) m/z: [M + H]⁺ Calcd for $C_{12}H_{13}F_3NOS^+$ 276.0664; Found 276.0665.

S-(trifluoromethyl) (E)-3-(4-(trifluoromethoxy)phenyl)prop-2-enethioate (7.5h)
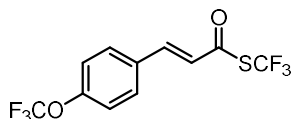
Following the General Procedure with the corresponding carboxylic acid (0.3 mmol). The crude product purified by flash column chromatography, using *n*-pentane/diethyl ether =20/1 (v/v) as an eluent, to yield the title compound **7.5h** (71 mg) in 75%.

¹H NMR (400 MHz, Chloroform-d): δ 7.64 (d, *J* = 15.8 Hz, 1H), 7.55 – 7.45 (m, 2H), 7.42 (s, 1H), 7.38 – 7.30 (m, 1H), 6.64 (d, *J* = 15.8 Hz, 1H).

¹³C NMR (101 MHz, Chloroform-d): δ 180.61, 149.80 (d, *J* = 2.1 Hz), 142.94, 135.05, 130.69, 127.75 (q, *J* = 309.8 Hz), 127.16, 124.20 (q, *J* = 3.1 Hz), 123.82, 120.71, 120.37 (q, *J* = 258.2 Hz).

¹⁹F NMR (376 MHz, Chloroform-d): δ -39.60, -57.89.

Physical State: colorless oil.

HRMS (APPI/LTQ-Orbitrap) m/z: [M + H]⁺ Calcd for $C_{11}H_7F_6O_2S^+$ 317.0066; Found 317.0069.

S-(trifluoromethyl) **6-(3-(adamantan-1-yl)-4-methoxyphenyl)naphthalene-2-carbothioate (7.6a)**
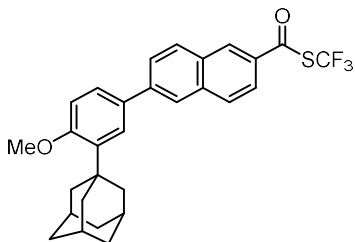
Following the General Procedure with the corresponding carboxylic acid (0.2 mmol). The crude product purified by flash column chromatography, using hexanes/EA = 30/1 (v/v) as an eluent, to yield the title compound **7.6a** (90 mg) in 91%.

**^{1}H NMR** (400 MHz, Chloroform-*d*): δ 8.41 (s, 1H), 8.07 – 7.99 (m, 2H), 7.97 (d, *J* = 8.7 Hz, 1H), 7.87 (ddd, *J* = 8.6, 4.5, 1.8 Hz, 2H), 7.61 (d, *J* = 2.4 Hz, 1H), 7.56 (dd, *J* = 8.4, 2.3 Hz, 1H), 7.01 (d, *J* = 8.5 Hz, 1H), 2.23 – 2.07 (m, 9H), 1.81 (d, *J* = 3.0 Hz, 6H).

^{13}C NMR (101 MHz, Chloroform-*d*): 182.97, 159.23, 142.80, 139.17, 136.89, 132.00, 131.90 (q, *J* = 2.6 Hz), 130.96, 130.10, 129.72, 129.28, 128.18 (q, *J* = 310.6 Hz), 127.34, 126.01, 125.83, 124.77, 122.97, 112.16, 55.19, 40.61, 37.25, 37.12, 29.11.

^{19}F NMR (376 MHz, Chloroform-*d*): δ -39.46.

Physical State: white solid.

HRMS (APPI/LTQ-Orbitrap) [M]$^+$ Calcd for $C_{29}H_{27}F_3O_2S^+$ 496.1678; Found 496.1672.

S-(trifluoromethyl) 4-(N,N-dipropylsulfamoyl)benzothioate (7.6b)
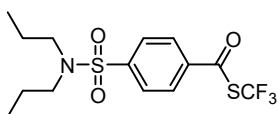
Following the General Procedure with the corresponding carboxylic acid (0.3 mmol). The crude product purified by flash column chromatography, using hexanes/EA = 20/1 (v/v) as an eluent, to yield the title compound **7.6b** (51 mg) in 46%.

**^{1}H NMR** (400 MHz, Methylene Chloride-*d*$_2$): δ 8.12 – 7.91 (m, 4H), 3.19 – 3.05 (t, *J* = 7.4 Hz, 4H), 1.57 (h, *J* = 7.4 Hz, 4H), 0.90 (t, *J* = 7.4 Hz, 6H).

^{13}C NMR (101 MHz, Methylene Chloride-*d*$_2$): δ 146.29, 137.51 (q, *J* = 2.7 Hz), 132.15 (q, *J* = 10.8 Hz), 128.48 (q, *J* = 12.5 Hz), 128.28, 127.83 (q, *J* = 309.9 Hz), 127.73, 49.90, 21.88, 10.86.

^{19}F NMR (376 MHz, Methylene Chloride-*d*$_2$): δ -40.18.

Physical State: white solid.

HRMS (APPI/LTQ-Orbitrap) m/z: [M + H]$^+$ Calcd for C$_{14}$H$_{19}$F$_3$NO$_3$S$_2$$^+$ 370.0753; Found 370.0752.

(10S,13R,14R,17R)-4,4,10,13,14-pentamethyl-17-((R)-6-methylhept-5-en-2-yl)-2,3,4,5,6,7,10,11,12,13,14,15,16,17-tetradecahydro-1H-cyclopenta[a]phenanthren-3-yl 3-(((trifluoromethyl)thio)carbonyl)benzoate (7.6c)

Following the General Procedure with the corresponding carboxylic acid (0.2 mmol). The crude product purified by flash column chromatography, using hexanes/EA = 20/1 (v/v) as an eluent, to yield the title compound **7.6c** (116 mg) in 88% (mixture of 2 diastereoisomers).

^{1}H NMR (400 MHz, Chloroform-*d*): δ 146.29, 137.51 (q, *J* = 2.7 Hz), 132.15 (q, *J* = 10.8 Hz), 128.48 (q, *J* = 12.5 Hz), 128.28, 127.83 (q, *J* = 309.9 Hz), 127.73, 49.90, 21.88, 10.86.

^{13}C NMR (101 MHz, Chloroform-*d*): δ 182.74, 164.57, 135.62, 134.68, 134.66, 134.13, 132.31, 131.25, 130.90, 129.47, 128.67, 125.25, 82.66, 50.59, 50.52, 50.41, 49.84, 44.51, 44.49, 39.54, 38.24, 36.96, 36.50, 36.37, 36.28, 35.28, 30.99, 30.85, 29.72, 28.23, 28.22, 28.14, 28.02, 26.39, 25.74, 24.94, 24.31, 24.29, 24.25, 24.13, 22.85, 22.56, 21.07, 19.22, 18.74, 18.66, 18.17, 17.65, 16.86, 15.78.

^{19}F NMR (376 MHz, Chloroform-*d*): δ -39.55.

Physical State: white solid.

HRMS (APPI/LTQ-Orbitrap) m/z: [M]$^+$ Calcd for C$_{39}$H$_{53}$F$_3$O$_3$S$^+$ 658.3662; Found 658.3661.

***S*-(trifluoromethyl) 4-(((1*R*,2*S*,5*R*)-2-isopropyl-5-methylcyclohexyl)oxy)benzothioate (7.6d)**

Following the General Procedure with the corresponding carboxylic acid (0.2 mmol). The crude product purified by flash column chromatography, using hexanes/EA = 30/1 (v/v) as an eluent, to yield the title compound **7.6d** (67 mg) in 86%.

¹H NMR (400 MHz, Chloroform-d): δ 8.49 (t, J = 1.8 Hz, 1H), 8.33 (dt, J = 7.8, 1.4 Hz, 1H), 8.03 (ddd, J = 7.9, 2.0, 1.2 Hz, 1H), 7.61 (t, J = 7.8 Hz, 1H), 4.98 (td, J = 10.9, 4.4 Hz, 1H), 2.16 – 2.08 (m, 1H), 1.92 (pd, J = 7.0, 2.8 Hz, 1H), 1.78 – 1.71 (m, 2H), 1.62 – 1.55 (m, 2H), 1.18 – 1.09 (m, 2H), 0.93 (dd, J = 6.8, 5.3 Hz, 6H), 0.80 (d, J = 6.9 Hz, 3H).

¹³C NMR (101 MHz, Chloroform-d): δ 182.98, 164.59, 135.82, 135.52 (q, J = 2.8 Hz), 132.32, 131.41, 129.58, 128.80, 127.98 (q, J = 309.9 Hz), 76.03, 47.33, 41.03, 34.36, 31.62, 26.76, 23.80, 22.15, 20.87, 16.70.

¹⁹F NMR (376 MHz, Chloroform-d): δ -39.58.

Physical State: white solid.

HRMS (APPI/LTQ-Orbitrap) m/z: [M+H]⁺ Calcd for $C_{19}H_{24}F_3O_3S^+$ 389.1393; Found 389.1394.

S-(trifluoromethyl) (2*E*,4*E*)-5-(benzo[1,3]dioxol-5-yl)penta-2,4-dienethioate (7.6e)

Following the General Procedure with the corresponding carboxylic acid (0.2 mmol). The crude product purified by flash column chromatography, using *n*-pentane/diethyl ether =20/1 (v/v) as an eluent, to yield the title compound **7.6e** (43 mg) in 71%.

¹H NMR (400 MHz, Chloroform-d): δ 7.38 (dd, J = 15.0, 11.1 Hz, 1H), 7.02 – 6.94 (m, 3H), 6.81 (d, J = 8.0 Hz, 1H), 6.67 (dd, J = 15.4, 11.1 Hz, 1H), 6.10 (d, J = 15.0 Hz, 1H), 6.01 (s, 2H).

¹³C NMR (101 MHz, Chloroform-d): δ 180.46, 149.63, 148.62, 145.39, 144.81, 130.06, 128.21 (q, J = 309.2 Hz), 124.57 (q, J = 3.1 Hz), 124.19, 123.43, 108.83, 106.17, 101.76.

¹⁹F NMR (376 MHz, Chloroform-d): δ -39.42.

Physical State: yellowish solid.

HRMS (APPI/LTQ-Orbitrap) m/z: [M + H]⁺ Calcd for $C_{13}H_{10}F_3O_3S^+$ 303.0297; Found 303.0296.

S-(trifluoromethyl) (E)-3-(2,3-dimethoxyphenyl)prop-2-enethioate (7.6f)

Following the General Procedure with the corresponding carboxylic acid (0.3 mmol). The crude product purified by flash column chromatography, using *n*-pentane/diethyl ether =20/1 (v/v) as an eluent, to yield the title compound **7.6f** (75 mg) in 86%.

¹H NMR (400 MHz, Chloroform-d): δ 7.96 (d, *J* = 16.0 Hz, 1H), 7.14 – 6.98 (m, 3H), 6.67 (d, *J* = 16.0 Hz, 1H), 3.89 (s, 6H).

¹³C NMR (101 MHz, Chloroform-d): δ 181.31, 153.31, 149.48, 140.29, 128.16 (q, *J* = 309.4 Hz), 127.19, 124.49, 124.07 (q, *J* = 3.1 Hz), 119.78, 115.59, 61.56, 56.04.

¹⁹F NMR (376 MHz, Chloroform-d): δ -39.56.

Physical State: yellowish oil.

HRMS (APPI/LTQ-Orbitrap) m/z: [M + H]$^+$ Calcd for C$_{12}$H$_{12}$F$_3$O$_3$S$^+$ 293.0454; Found 293.0447.

S-(trifluoromethyl) 2-(10-oxo-10,11-dihydrodibenzo[b,f]thiepin-2-yl)propanethioate (7.6g)

Following the General Procedure with the corresponding carboxylic acid (0.2 mmol). The crude product purified by flash column chromatography, using *n*-pentane/diethyl ether =20/1 (v/v) as an eluent, to yield the title compound **7.6g** (50 mg) in 66%.

¹H NMR (400 MHz, Chloroform-d): δ 8.21 (dd, *J* = 8.0, 1.7 Hz, 1H), 7.66 (d, *J* = 8.0 Hz, 1H), 7.60 (dd, *J* = 7.9, 1.3 Hz, 1H), 7.44 (ddd, *J* = 7.9, 7.2, 1.7 Hz, 1H), 7.39 – 7.30 (m, 2H), 7.13 (dd, *J* = 8.0, 2.0 Hz, 1H), 4.38 (d, *J* = 1.9 Hz, 2H), 3.86 (q, *J* = 7.1 Hz, 1H), 1.55 (d, *J* = 7.1 Hz, 3H).

¹³C NMR (101 MHz, Chloroform-*d*) δ 191.83, 191.06, 139.88, 139.38, 138.76, 136.19, 135.11, 132.80, 132.13, 131.70, 131.01, 129.37, 127.70 (q, *J* = 310.5 Hz), 127.14, 127.10, 54.80 (q, *J* = 2.7 Hz), 51.16, 17.91.

¹⁹F NMR (376 MHz, Chloroform-d): δ -40.31.

Physical State: yellowish oil.

HRMS (APPI/LTQ-Orbitrap) m/z: [M]$^+$ Calcd for C$_{18}$H$_{14}$F$_3$O$_2$S$_2$$^+$ 383.0382; Found 383.0380.
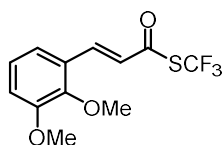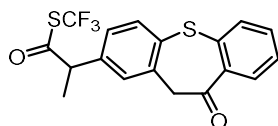
S-(trifluoromethyl) 2-(4-isobutylphenyl)propanethioate (7.6h)
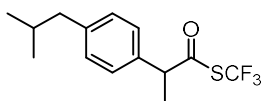
Following the General Procedure with the corresponding carboxylic acid (0.2 mmol). The crude product purified by flash column chromatography, using *n*-pentane/diethyl ether =20/1 (v/v) as an eluent, to yield the title compound **7.6h** (38 mg) in 66%.

^{1}H NMR (400 MHz, Chloroform-d): δ 7.17 (d, *J* = 2.3 Hz, 4H), 3.84 (q, *J* = 7.1 Hz, 1H), 2.49 (d, *J* = 7.2 Hz, 2H), 1.87 (dp, *J* = 13.6, 7.0 Hz, 1H), 1.57 (d, *J* = 7.1 Hz, 3H), 0.92 (d, *J* = 6.6 Hz, 6H).

^{13}C NMR (101 MHz, Chloroform-d): δ 192.87, 142.32, 134.23, 129.90, 128.24, 127.90 (q, *J* = 310.1 Hz), 54.87 (q, *J* = 2.5 Hz), 45.07, 30.16, 22.35, 17.57.

^{19}F NMR (376 MHz, Chloroform-d): δ -40.59.

Physical State: yellowish oil.

HRMS (APPI/LTQ-Orbitrap) m/z: [M]$^+$ Calcd for $C_{14}H_{17}F_3OS^+$ 290.0947; Found 290.0942.

S-(trifluoromethyl) 2-(3-benzoylphenyl)propanethioate (7.6i)
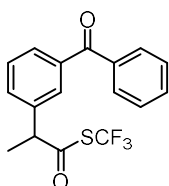
Following the General Procedure with the corresponding carboxylic acid (0.2 mmol). The crude product purified by flash column chromatography, using *n*-pentane/diethyl ether =20/1 (v/v) as an eluent, to yield the title compound **7.6i** (42 mg) in 62%.

^{1}H NMR (400 MHz, Chloroform-d): δ 7.88 – 7.68 (m, 4H), 7.63 (d, *J* = 7.5 Hz, 1H), 7.57 – 7.45 (m, 4H), 3.95 (q, *J* = 7.1 Hz, 1H), 1.61 (d, *J* = 7.1 Hz, 3H).

^{13}C NMR (101 MHz, Chloroform-d): δ 195.99, 191.93, 138.48, 137.60, 137.17, 132.77, 132.05, 130.21, 130.07, 129.88, 129.22, 128.43, 127.64 (q, *J* = 310.4 Hz), 54.94 (q, *J* = 2.6 Hz), 17.76.

^{19}F NMR (376 MHz, Chloroform-d): δ -40.33.

Physical State: yellowish oil.

HRMS (APPI/LTQ-Orbitrap) m/z: [M + H]$^+$ Calcd for $C_{17}H_{14}F_3O_2S^+$ 339.0661; Found 339.0659.

S-(trifluoromethyl) (*S*)-2-(6-methoxynaphthalen-2-yl)propanethioate (7.6j)
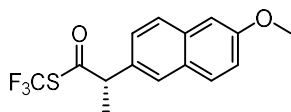
Following the General Procedure with the corresponding carboxylic acid (0.2 mmol). The crude product purified by flash column chromatography, using *n*-pentane/diethyl ether =20/1 (v/v) as an eluent, to yield the title compound **7.6j** (47 mg) in 75%.

¹H NMR (400 MHz, Chloroform-d): δ 7.76 (t, *J* = 9.4 Hz, 2H), 7.68 (d, *J* = 1.9 Hz, 1H), 7.33 (dd, *J* = 8.4, 1.8 Hz, 1H), 7.20 (dd, *J* = 8.9, 2.6 Hz, 1H), 7.15 (d, *J* = 2.5 Hz, 1H), 4.00 (q, *J* = 7.1 Hz, 1H), 3.93 (s, 3H), 1.65 (d, *J* = 7.0 Hz, 3H).

¹³C NMR (101 MHz, Chloroform-d): δ 192.84, 158.29, 134.43, 132.04, 129.43, 128.89, 127.94, 127.81, 127.62 (q, *J* = 255.3 Hz), 126.19, 119.61, 105.70, 55.38, 55.19 (q, *J* = 2.5 Hz), 17.59.

¹⁹F NMR (376 MHz, Chloroform-d): δ -40.55.

Physical State: white solide.

HRMS (APPI/LTQ-Orbitrap) m/z: $[M]^+$ Calcd for $C_{15}H_{13}F_3O_2S^+$ 314.0583; Found 314.0581.

S-(trifluoromethyl) 5-(2,5-dimethylphenoxy)-2,2-dimethylpentanethioate (7.6k)
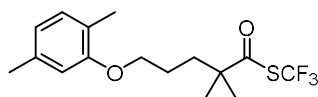
Following the General Procedure with the corresponding carboxylic acid (0.2 mmol). The crude product purified by flash column chromatography, using hexanes/EA = 30/1 (v/v) as an eluent, to yield the title compound **7.6k** (37 mg) in 56%.

¹H NMR (400 MHz, Chloroform-*d*): δ 7.02 (d, *J* = 7.4 Hz, 1H), 6.68 (d, *J* = 7.0 Hz, 1H), 6.61 (s, 1H), 3.95 (p, *J* = 2.8 Hz, 2H), 2.32 (s, 3H), 2.19 (s, 3H), 1.85 – 1.74 (m, 4H), 1.30 (s, 6H).

¹³C NMR (101 MHz, Chloroform-*d*): δ 197.30, 156.89, 136.67, 130.51, 128.43 (q, *J* = 309.4 Hz), 123.68, 121.02, 112.01, 67.46, 51.38 (q, *J* = 2.2 Hz), 37.20, 24.83, 24.72, 21.52, 15.90.

¹⁹F NMR (376 MHz, Chloroform-*d*): δ -40.08.

Physical State: white solid.

HRMS (APPI/LTQ-Orbitrap) m/z: $[M]^+$ Calcd for $C_{16}H_{21}F_3O_2S^+$ 334.1209; Found 334.1209.

S-(trifluoromethyl) (1R,4aR,4bR,10aR)-7-isopropyl-1,4a-dimethyl-1,2,3,4,4a,4b,5,6,10,10a-decahydrophenanthrene-1-carbothioate (7.6l)
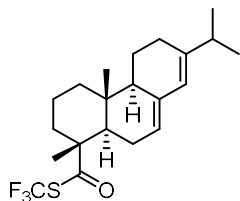
Following the General Procedure with the corresponding carboxylic acid (0.2 mmol). The crude product purified by flash column chromatography, using hexanes/EA = 30/1 (v/v) as an eluent, to yield the title compound **7.6l** (32 mg) in 42%.

^{1}H NMR (400 MHz, Chloroform-*d*): δ 5.78 (s, 1H), 5.39 – 5.32 (m, 1H), 2.23 (octet, *J* = 8.0, Hz, 1H), 2.09 – 1.62 (m, 12H), 1.32 (s, 3H), 1.23 – 1.10 (m, 3H), 1.03 (d, *J* = 3.4 Hz, 3H), 1.01 (d, *J* = 3.4 Hz, 3H), 0.84 (s, 3H).

^{13}C NMR (101 MHz, Chloroform-*d*): δ 198.61, 145.72, 128.50 (q, *J* = 309.5 Hz), 119.78, 55.86, 50.92, 45.81, 38.00, 37.51, 34.91, 27.42, 25.28, 22.53, 21.42, 20.86, 18.00, 16.87, 14.29.

^{19}F NMR (376 MHz, Chloroform-*d*): δ -40.41.

Physical State: colorless oil.

HRMS (APPI/LTQ-Orbitrap) $[M]^+$ Calcd for $C_{21}H_{29}F_3OS^+$ 386.1886; Found 386.1880.

[1,1'-biphenyl]-4-yl(trifluoromethyl)sulfane (7.7a)
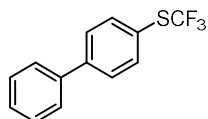
In a nitrogen-filled glovebox, **7.3a** (1 equiv, 0.1 mmol) was weighed into a 4 mL vial equipped with a 10 μm magnetic stir bar. A pre-mixed solution of Pd catalyst and ligand in toluene (0.3 mL) was added. The vial was connected to a reflux condenser, capped with a rubber septum, and this assembly was removed from the glovebox. An argon balloon was placed on top of the condenser and the reaction mixture was stirred at 130 ºC. After 20 h, the reaction mixture was cooled to room temperature and diluted with diethyl ether. The resulting solution was filtered through a silica plug and concentrated under reduced pressure. The products were purified via flash column chromatography on silica gel (hexanes/Et$_2$O=30/1, v/v).

^{1}H NMR (400 MHz, Chloroform-*d*): δ 7.79 (dd, *J* = 16.6, 8.4 Hz, 2H), 7.66 (dd, *J* = 15.0, 7.9 Hz, 4H), 7.51 (t, *J* = 7.6 Hz, 2H), 7.47 – 7.41 (m, 1H).

^{13}C NMR (101 MHz, Chloroform-*d*): δ 143.9 (s), 139.7 (s), 136.7 (s), 132.7 (q, J = 308.1 Hz), 129.0 (s), 128.2 (s), 127.2 (s), 123.1 (q, J = 1.8 Hz).

^{19}F NMR (376 MHz, Chloroform-*d*): δ -42.68 (s, 3F).

Physical State: White solid.

HRMS (APPI/LTQ-Orbitrap) [M+H]$^+$ Calcd for $C_{13}H_{10}F_3S^+$ 255.0450; Found 255.0451.

Chapter 8

General Conclusions and Outlook

8.1　General conclusions

The research work discussed in this thesis aimed to develop novel carbon-heteroatom bond-forming reactions using aliphatic carboxylic acids as versatile coupling partners, including (1) decarboxylative $C(sp^3)$-heteroatom (N, O) cross-couplings via tandem photoredox and copper catalysis; (2) deoxygenative trifluoromethylthiolation of carboxylic acids.

8.1.1　Conclusions of decarboxylative $C(sp^3)$-N and $C(sp^3)$-O cross-coupling reactions
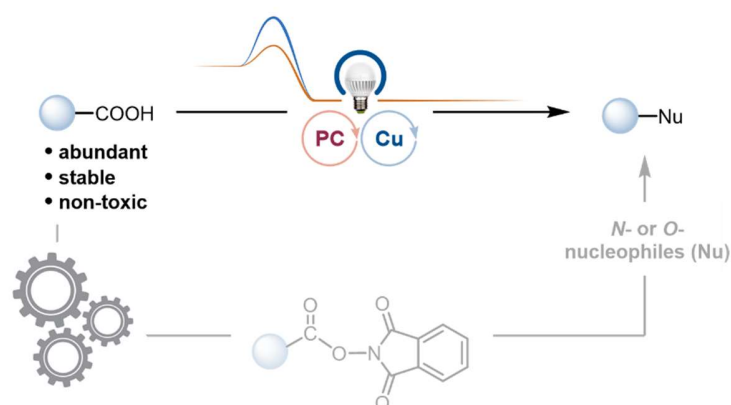
Figure 91 Decarboxylative $C(sp^3)$-N and $C(sp^3)$-O cross-couplings via synergistic photoredox and copper catalysis.

In Chapters 4-6, we describe the development of a synergistic photoredox/copper catalysis system (Figure 91) and its applications in decarboxylative amination and etherification reactions. This catalytic system enables efficient couplings of alkyl carboxylic acid-derived NHPI esters with a variety of *N*-, *O*-nucleophiles.

Each chapter in Chapters 4-6 begins with a challenging cross-coupling puzzle and then details how these puzzles can be solved using our established photoredox/copper cooperative catalytic strategy. Chapters 4 and 6 show how $C(sp^3)$-N and $C(sp^3)$-O bonds can be efficiently constructed via transition metal-catalyzed decarboxylative cross-coupling reactions, respectively, and how carboxylic acid-containing natural products and drugs can be efficiently modified. The method we developed not only fills a gap in the field of decarboxylative $C(sp^3)$-N and $C(sp^3)$-O bond-forming reactions, but also opens up more pathways for drug modifications.

Chapter 3 describes the application of benzophenone imines as a class of amine equivalents in the decarboxylative C(sp^3)-N cross-coupling reactions. This method was established to provide an efficient and safer alternative to the conventional Curtius rearrangement. By using distinctive *N*-sp^2-hybridized benzophenone amines as nucleophilic reagents, the reactions were not only efficient (up to 99% yield) but also allows for the rapid transformaiton of a wide range of primary, secondary and tertiary alkyl carboxylic acids into protected primary alkyl amines.

8.1.2 Conclusions of Deoxygenative trifluoromethylthioesterification reactions of carboxylic acids
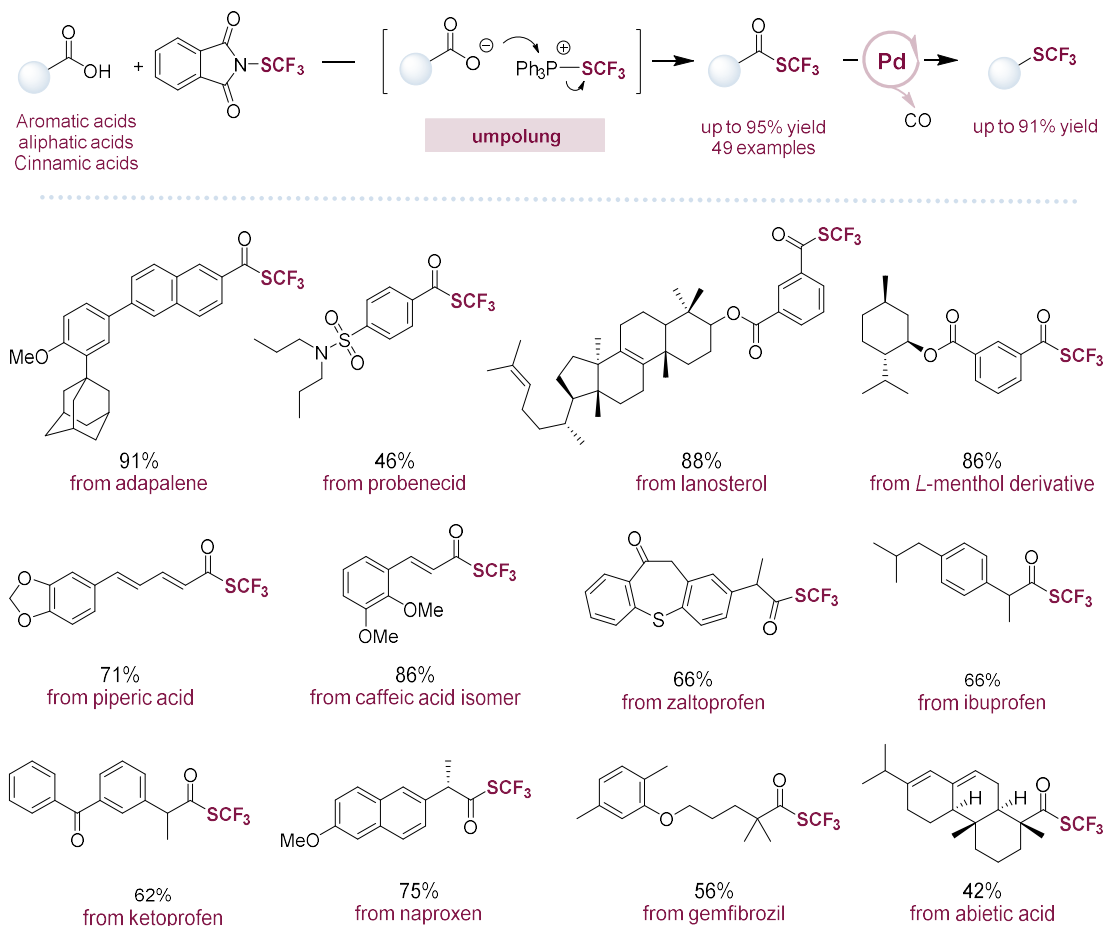
Figure 92 Deoxygenative trifluoromethylthiolation of carboxylic acids.

In Chapter 5, we describe a deoxygenative trifluoromethylthiolation method that enables the generation of trifluoromethylthioesters directly from carboxylic acids in one step (Figure 92). The method is based on a "umpolung" strategy wherein triphenylphosphine is first used to activate an electrophilic trifluoromethylthiolating (CF_3S^+) reagent and then to act as an oxygen acceptor as well as a trifluoromethylthio anion (CF_3S^-) donor. Based on this concept, the method provided a strategy for the controlled release of CF_3S^- anion, which was a long-standing challenge in synthetic fluorine chemistry. The established method (Figure 92) is mild (room temperature), rapid (30 minutes), efficient (up to 95% yield), wide-ranging (nearly 50 examples including aromatic

carboxylic acids, aliphatic acids, and cinnamic acids), and highly compatible (numerous functional groups and complexes). Most importantly, it can be applied to the late-stage functionalization of a wide range of natural products and drug molecules that containing carboxylic acid groups (Figure 92). This approach has largely expanded the library of trifluoromethylthioester molecules, most of which were reported for the first time, thus providing more candidate molecules for drug discovery.

To further demonstrate the practicality of the synthesis of trifluoromethylthioesters, we successfully achieved the facile conversion of trifluoromethylthioesters to trifluoromethylthioesters via palladium-catalyzed decarbonylation. Such an approach has offered an expedient route to achieve trifluoromethylthioethers from carboxylic acids.

8.2 Outlook

The thesis presents the development of a series of novel carbon-heteroatom bond-forming reactions using carboxylic acids as a class of inexpensive and versatile coupling partners. Following the experimental results and lines of research obtained in this thesis, we believe that more interesting questions remain to be addressed. Here, we list these topics and ideas in the hope that they will inspire more people.

8.2.1 Outlook concerning decarboxylative C(sp^3)-N and C(sp^3)-O cross-coupling reactions

(1) Although significant progress has been made in decarboxylative C(sp^3)-N and C(sp^3)-O cross-coupling reactions, how to reduce the cost of such transformations remains an important issue. For example, whether the ruthenium- and iridium-based photocatalysts can be replaced with non-precious metal-based photocatalysts or even organic photocatalysts? It is worth mentioning that the author has already identified some potential organic photocatalysts during the preparation of the thesis and showed encouraging results, and further investigations are in progress.

(2) Enantioselective decarboxylative C(sp^3)-N and C(sp^3)-O coupling method is a very intriguing and challenging topic. While the idea is conceptually feasible, the potential hurdles are considerable. For example, the types of ligands that can be applied to the reaction are limited, which poses a significant difficulty in finding suitable chiral ligands (see Figure 44, Figure 45, Figure 46). Moreover, ligands are not essential in most reactions present in this thesis, thus the high activity of the reaction would pose considerable challenges in selecting efficient chiral ligands.

(3) In order to improve the overall synthesis productivity, it would be interesting to extend the established transformations to multi-component reactions. For example, additional Michael acceptors or other acceptors could be added to the standard reaction conditions we have established. Based on this approach, we may be able to forge both C-C and C-heteroatom bonds simultaneously, thus significantly improving the reaction efficiency.

(4) The direct use of aliphatic carboxylic acids as coupling partners can avoid additional pre-functionalization, which not only improves the synthesis efficiency but also improves the atom economy. Relevant work is underway in our laboratory and some preliminary results have been obtained.

8.2.2 Outlook concerning deoxygenative trifluoromethylthioesterification reactions of carboxylic acids

(1) Although this method is compatible with a wide range of functional groups and can be applied to the late-stage functionalization of natural products and drug molecules, we did not test the reactivity of this method to functionalize peptides. We expect that this efficient and straightforward strategy may allow for the C-terminal selective bioconjugation of peptides (even proteins).

(2) To date, we only have applied the reagent *N*-trifluoromethylthiophthalimide to deoxygenative trifluoromethylthioesterification of carboxylic acids. However, more electrophilic reagents other than *N*-trifluoromethylthiophthalimide could be applied to this methodology, providing a more expansive playground for this novel strategy.

(3) As presented in chapter 7, trifluoromethylthioesters can be transformed into trifluoromethylthioethers via a palladium-catalyzed decarbonylation pathway. In this process, trifluoromethylthioesters need to be isolated. We envision the development of a one-pot reaction to convert carboxylic acids directly to trifluoromethylthioethers would be of greatly synthetic importance.

Chapter 9

References

Chapter 9

9.1 References

[1] Nicolaou, K. C. Organic synthesis: the art and science of replicating the molecules of living nature and creating others like them in the laboratory. *Proc. Math. Phys. Eng. Sci.* **2014,** *470*, 20130690.

[2] Campos, K. R.; Coleman, P. J.; Alvarez, J. C.; Dreher, S. D.; Garbaccio, R. M.; Terrett, N. K.; Tillyer, R. D.; Truppo, M. D.; Parmee, E. R. The importance of synthetic chemistry in the pharmaceutical industry. *Science* **2019,** *363*.

[3] Corey, E. J. General methods for the construction of complex molecules. *Pure Appl. Chem.* **1967,** *14*, 19-38.

[4] Meijere, A. d.; Diederich, F. *Metal-Catalyzed Cross-Coupling Reactions*. Wiley-VCH: Weinheim, 2004.

[5] Hu, X. Nickel-catalyzed cross coupling of non-activated alkyl halides: A mechanistic perspective. *Chem. Sci.* **2011,** *2*, 1867-1886.

[6] Tasker, S. Z.; Standley, E. A.; Jamison, T. F. Recent advances in homogeneous nickel catalysis. *Nature* **2014,** *509*, 299-309.

[7] Choi, J.; Fu, G. C. Transition metal-catalyzed alkyl-alkyl bond formation: Another dimension in cross-coupling chemistry. *Science* **2017,** *356*.

[8] Gooßen, L. J.; Rodríguez, N.; Gooßen, K. Carboxylic Acids as Substrates in Homogeneous Catalysis. *Angew. Chem., Int. Ed.* **2008,** *47*, 3100-3120.

[9] Rodriguez, N.; Goossen, L. J. Decarboxylative coupling reactions: a modern strategy for C-C-bond formation. *Chem. Soc. Rev.* **2011,** *40*, 5030-5048.

[10] Larrosa, I.; Cornella, J. Decarboxylative Carbon-Carbon Bond-Forming Transformations of (Hetero)aromatic Carboxylic Acids. *Synthesis* **2012,** *44*, 653-676.

[11] Dickstein, J. S.; Mulrooney, C. A.; O'Brien, E. M.; Morgan, B. J.; Kozlowski, M. C. Development of a Catalytic Aromatic Decarboxylation Reaction. *Org. Lett.* **2007,** *9*, 2441-2444.

[12] Goossen, L. J.; Deng, G.; Levy, L. M. Synthesis of biaryls via catalytic decarboxylative coupling. *Science* **2006,** *313*, 662-664.

[13] Goossen, L. J.; Rodriguez, N.; Linder, C. Decarboxylative Biaryl Synthesis from Aromatic Carboxylates and Aryl Triflates. *J. Am. Chem. Soc.* **2008,** *130*, 15248-15249.

[14] Myers, A. G.; Tanaka, D.; Mannion, M. R. Development of a Decarboxylative Palladation Reaction and Its Use in a Heck-type Olefination of Arene Carboxylates. *J. Am. Chem. Soc.* **2002,** *124*, 11250-11251.

[15] Murarka, S. N-(Acyloxy)phthalimides as Redox-Active Esters in Cross-Coupling Reactions. *Adv. Synth. Catal.* **2018,** *360*, 1735-1753.

[16] Anderson, J. M.; Kochi, J. K. Silver (I) -Catalyzed Oxidative Decarboxylation of Acids by Peroxydisulfate. The Role of Silver (II). *J. Am. Chem. Soc.* **1970,** *92*, 1651-1659.

[17] Johnson, R. G.; Ingham, R. K. The Degradation Of Carboxylic Acid Salts By Means Of Halogen - The Hunsdiecker Reaction. *Chem. Rev.* **1956,** *56*, 219-269.

[18] Kochi, J. K. A New Method for Halodecarboxylation of Acids Using Lead(IV) Acetate. *J. Am. Chem. Soc.* **1965,** *87*, 2500-2502.

[19] Kochi, J. K. Mechanisms of Organic Oxidation and Reduction by Metal Complexes. *Science* **1967,** *155*, 415-424.

[20] Wang, Z.; Zhu, L.; Yin, F.; Su, Z.; Li, Z.; Li, C. Silver-catalyzed decarboxylative chlorination of aliphatic carboxylic acids. *J. Am. Chem. Soc.* **2012,** *134*, 4258-4263.

[21]   Barton, D. H. R.; Crich, D.; Motherwell, W. B. New and improved methods for the radical decarboxylation of acids. *J. Chem. Soc., Chem. Commun.* **1983**, 939.

[22]   Barton, D. H. R.; Crich*, D.; Motherwell, W. B. A practical alternative to the hunsdiecker reaction. *Tetrahedron Lett.* **1983,** *24*, 4979-4982.

[23]   Saraiva, M. F.; Couri, M. R. C.; Le Hyaric, M.; de Almeida, M. V. The Barton ester free-radical reaction: a brief review of applications. *Tetrahedron* **2009,** *65*, 3563-3572.

[24]   Okada, K.; Okamoto, K.; Oda, M. A New and Practical Method of Decarboxylation: Photosensitized Decarboxylation of (N-Acyloxyphthalimides via Electron-Transfer Mechanism. *J. Am. Chem. Soc.* **1988,** *110*, 8736-8738.

[25]   Okada, K.; Okamoto, K.; Morita, N.; Okubo, K.; Oda, M. Photosensitized decarboxylative Michael addition through N-(acyloxy)phthalimides via an electron-transfer mechanism. *J. Am. Chem. Soc.* **1991,** *113*, 9401-9402.

[26]   Schnermann, M. J.; Overman, L. E. A concise synthesis of (-)-aplyviolene facilitated by a strategic tertiary radical conjugate addition. *Angew. Chem., Int. Ed.* **2012,** *51*, 9576-9580.

[27]   Pratsch, G.; Lackner, G. L.; Overman, L. E. Constructing Quaternary Carbons from N-(Acyloxy)phthalimide Precursors of Tertiary Radicals Using Visible-Light Photocatalysis. *J. Org. Chem.* **2015,** *80*, 6025-6036.

[28]   Hu, C.; Chen, Y. Chemoselective and fast decarboxylative allylation by photoredox catalysis under mild conditions. *Org. Chem. Front.* **2015,** *2*, 1352-1355.

[29]   Schwarz, J.; König, B. Metal-free, visible-light-mediated, decarboxylative alkylation of biomass-derived compounds. *Green Chem.* **2016,** *18*, 4743-4749.

[30]   Kong, W.; Yu, C.; An, H.; Song, Q. Photoredox-Catalyzed Decarboxylative Alkylation of Silyl Enol Ethers To Synthesize Functionalized Aryl Alkyl Ketones. *Org. Lett.* **2018,** *20*, 349-352.

[31]   Sha, W.; Ni, S.; Han, J.; Pan, Y. Access to Alkyl-Substituted Lactone via Photoredox-Catalyzed Alkylation/Lactonization of Unsaturated Carboxylic Acids. *Org. Lett.* **2017,** *19*, 5900-5903.

[32]   Zhao, Y.; Chen, J. R.; Xiao, W. J. Visible-Light Photocatalytic Decarboxylative Alkyl Radical Addition Cascade for Synthesis of Benzazepine Derivatives. *Org. Lett.* **2018,** *20*, 224-227.

[33]   Yang, J. C.; Zhang, J. Y.; Zhang, J. J.; Duan, X. H.; Guo, L. N. Metal-Free, Visible-Light-Promoted Decarboxylative Radical Cyclization of Vinyl Azides with N-Acyloxyphthalimides. *J. Org. Chem.* **2018,** *83*, 1598-1605.

[34]   Jin, Y.; Jiang, M.; Wang, H.; Fu, H. Installing amino acids and peptides on N-heterocycles under visible-light assistance. *Sci Rep* **2016,** *6*, 20068.

[35]   Cheng, W.-M.; Shang, R.; Fu, Y. Photoredox/Brønsted Acid Co-Catalysis Enabling Decarboxylative Coupling of Amino Acid and Peptide Redox-Active Esters with N-Heteroarenes. *ACS Catal.* **2016,** *7*, 907-911.

[36]   Cheng, W. M.; Shang, R.; Fu, M. C.; Fu, Y. Photoredox-Catalysed Decarboxylative Alkylation of N-Heteroarenes with N-(Acyloxy)phthalimides. *Chem. Eur. J.* **2017,** *23*, 2537-2541.

[37]   Zhang, J. J.; Yang, J. C.; Guo, L. N.; Duan, X. H. Visible-Light-Mediated Dual Decarboxylative Coupling of Redox-Active Esters with alpha,beta-Unsaturated Carboxylic Acids. *Chem. Eur. J.* **2017,** *23*, 10259-10263.

[38] Xu, K.; Tan, Z.; Zhang, H.; Liu, J.; Zhang, S.; Wang, Z. Photoredox catalysis enabled alkylation of alkenyl carboxylic acids with N-(acyloxy)phthalimide via dual decarboxylation. *Chem. Commun.* **2017,** *53*, 10719-10722.

[39] Wang, G. Z.; Shang, R.; Fu, Y. Irradiation-Induced Palladium-Catalyzed Decarboxylative Heck Reaction of Aliphatic N-(Acyloxy)phthalimides at Room Temperature. *Org. Lett.* **2018,** *20*, 888-891.

[40] Yang, J.; Zhang, J.; Qi, L.; Hu, C.; Chen, Y. Visible-light-induced chemoselective reductive decarboxylative alkynylation under biomolecule-compatible conditions. *Chem. Commun.* **2015,** *51*, 5275-5278.

[41] Zhang, H.; Zhang, P.; Jiang, M.; Yang, H.; Fu, H. Merging Photoredox with Copper Catalysis: Decarboxylative Alkynylation of alpha-Amino Acid Derivatives. *Org. Lett.* **2017,** *19*, 1016-1019.

[42] Hu, D.; Wang, L.; Li, P. Decarboxylative Borylation of Aliphatic Esters under Visible-Light Photoredox Conditions. *Org. Lett.* **2017,** *19*, 2770-2773.

[43] Fawcett, A.; Pradeilles, J.; Wang, Y.; Mutsuga, T.; Myers, E. L.; Aggarwal, V. K. Photoinduced decarboxylative borylation of carboxylic acids. *Science* **2017**.

[44] Jiang, M.; Yang, H.; Fu, H. Visible-Light Photoredox Synthesis of Chiral alpha-Selenoamino Acids. *Org. Lett.* **2016,** *18*, 1968-1971.

[45] Jin, Y.; Yang, H.; Fu, H. An N-(acetoxy)phthalimide motif as a visible-light pro-photosensitizer in photoredox decarboxylative arylthiation. *Chem. Commun.* **2016,** *52*, 12909-12912.

[46] Zhao, W.; Wurz, R. P.; Peters, J. C.; Fu, G. C. Photoinduced, copper-catalyzed decarboxylative C-N coupling to generate protected amines: An alternative to the curtius rearrangement. *J. Am. Chem. Soc.* **2017,** *139*, 12153–12156.

[47] Cornella, J.; Edwards, J. T.; Qin, T.; Kawamura, S.; Wang, J.; Pan, C. M.; Gianatassio, R.; Schmidt, M.; Eastgate, M. D.; Baran, P. S. Practical Ni-catalyzed aryl-alkyl cross-coupling of secondary redox-active esters. *J. Am. Chem. Soc.* **2016,** *138*, 2174-2177.

[48] Huihui, K. M.; Caputo, J. A.; Melchor, Z.; Olivares, A. M.; Spiewak, A. M.; Johnson, K. A.; DiBenedetto, T. A.; Kim, S.; Ackerman, L. K.; Weix, D. J. Decarboxylative cross-electrophile Coupling of N-hydroxyphthalimide esters with aryl iodides. *J. Am. Chem. Soc.* **2016,** *138*, 5016-5019.

[49] Toriyama, F.; Cornella, J.; Wimmer, L.; Chen, T. G.; Dixon, D. D.; Creech, G.; Baran, P. S. Redox-active esters in Fe-catalyzed C-C coupling. *J. Am. Chem. Soc.* **2016,** *138*, 11132-11135.

[50] Wang, J.; Qin, T.; Chen, T.-G.; Wimmer, L.; Edwards, J. T.; Cornella, J.; Vokits, B.; Shaw, S. A.; Baran, P. S. Nickel-Catalyzed Cross-Coupling of Redox-Active Esters with Boronic Acids. *Angew. Chem., Int. Ed.* **2016,** *55*, 9676 –9679.

[51] Edwards, J. T.; Merchant, R. R.; McClymont, K. S.; Knouse, K. W.; Qin, T.; Malins, L. R.; Vokits, B.; Shaw, S. A.; Bao, D. H.; Wei, F. L.; Zhou, T.; Eastgate, M. D.; Baran, P. S. Decarboxylative alkenylation. *Nature* **2017,** *545*, 213-218.

[52] Suzuki, N.; Hofstra, J. L.; Poremba, K. E.; Reisman, S. E. Nickel-Catalyzed Enantioselective Cross-Coupling of N-Hydroxyphthalimide Esters with Vinyl Bromides. *Org. Lett.* **2017,** *19*, 2150-2153.

[53] Qin, T.; Cornella, J.; Li, C.; Malins, L. R.; Edwards, J. T.; Kawamura, S.; Maxwell, B. D.; Eastgate, M. D.; Baran, P. S. A general alkyl-alkyl cross-coupling enabled by redox-active esters and alkylzinc reagents. *Science* **2016,** *352*, 801-805.

[54] Qin, T.; Malins, L. R.; Edwards, J. T.; Merchant, R. R.; Novak, A. J.; Zhong, J. Z.; Mills, R. B.; Yan, M.; Yuan, C.; Eastgate, M. D.; Baran, P. S. Nickel-Catalyzed Barton Decarboxylation and Giese Reactions: A Practical Take on Classic Transforms. *Angew. Chem., Int. Ed.* **2017,** *56,* 260-265.

[55] Lu, X.; Xiao, B.; Liu, L.; Fu, Y. Formation of C(sp(3))-C(sp(3)) Bonds through Nickel-Catalyzed Decarboxylative Olefin Hydroalkylation Reactions. *Chem. Eur. J.* **2016,** *22,* 11161-11164.

[56] Smith, J. M.; Qin, T.; Merchant, R. R.; Edwards, J. T.; Malins, L. R.; Liu, Z.; Che, G.; Shen, Z.; Shaw, S. A.; Eastgate, M. D.; Baran, P. S. Decarboxylative Alkynylation. *Angew. Chem., Int. Ed.* **2017,** *56,* 11906-11910.

[57] Huang, L.; Olivares, A. M.; Weix, D. J. Reductive Decarboxylative Alkynylation of N-Hydroxyphthalimide Esters with Bromoalkynes. *Angew. Chem., Int. Ed.* **2017,** *56,* 11901-11905.

[58] Li, C.; Wang, J.; Barton, L. M.; Yu, S.; Tian, M.; Peters, D. S.; Kumar, M.; Yu, A. W.; Johnson, K. A.; Chatterjee, A. K.; Yan, M.; Baran, P. S. Decarboxylative borylation. *Science* **2017**.

[59] Xue, W.; Oestreich, M. Copper-Catalyzed Decarboxylative Radical Silylation of Redox-Active Aliphatic Carboxylic Acid Derivatives. *Angew. Chem., Int. Ed.* **2017,** *56,* 11649-11652.

[60] Ault, A. The Nobel Prize in Chemistry for 2001. *J. Chem. Educ.* **2001,** *79,* 572-577.

[61] Casey, C. P. Development of the Olefin Metathesis Method in Organic Synthesis. *J. Chem. Educ.* **2005,** *83,* 192-195.

[62] Johansson Seechurn, C. C.; Kitching, M. O.; Colacot, T. J.; Snieckus, V. Palladium-catalyzed cross-coupling: a historical contextual perspective to the 2010 Nobel Prize. *Angew. Chem., Int. Ed.* **2012,** *51,* 5062-5085.

[63] Tsuji, J. *Palladium Reagents and Catalysts: New Perspectives for the 21st Century.* John Wiley & Sons: 2005.

[64] Jones, G. O.; Liu, P.; Houk, K. N.; Buchwald, S. L. Computational Explorations of Mechanisms and Ligand-Directed Selectivities of Copper-Catalyzed Ullmann-Type Reactions. *J. Am. Chem. Soc.* **2010,** *132,* 6205-6213.

[65] Yu, H.-Z.; Jiang, Y.-Y.; Fu, Y.; Liu, L. Alternative Mechanistic Explanation for Ligand-Dependent Selectivities in Copper-Catalyzed N- and O-Arylation Reactions. *J. Am. Chem. Soc.* **2010,** *132,* 18078-18091.

[66] Giri, R.; Brusoe, A.; Troshin, K.; Wang, J. Y.; Font, M.; Hartwig, J. F. Mechanism of the Ullmann Biaryl Ether Synthesis Catalyzed by Complexes of Anionic Ligands: Evidence for the Reaction of Iodoarenes with Ligated Anionic Cu(I) Intermediates. *J. Am. Chem. Soc.* **2018,** *140,* 793-806.

[67] Evano, G.; Blanchard, N. *Copper-Mediated Cross-Coupling Reactions.* John Wiley & Sons: 2014.

[68] Casitas, A.; Ribas, X. The role of organometallic copper(iii) complexes in homogeneous catalysis. *Chem. Sci.* **2013,** *4,* 2301.

[69] Furuya, T.; Kamlet, A. S.; Ritter, T. Catalysis for fluorination and trifluoromethylation. *Nature* **2011,** *473,* 470-477.

[70] Hickman, A. J.; Sanford, M. S. High-valent organometallic copper and palladium in catalysis. *Nature* **2012,** *484,* 177-185.

[71] Creutz, S. E.; Lotito, K. J.; Fu, G. C.; Peters, J. C. Photoinduced Ullmann C–N Coupling: Demonstrating the Viability of a Radical Pathway. *science* **2012,** *338*, 647-651.

[72] Kainz, Q. M.; Matier, C. D.; Bartoszewicz, A.; Zultanski, S. L.; Peters, J. C.; Fu, G. C. Asymmetric copper-catalyzed C-N cross-couplings induced by visible light. *Science* **2016,** *351*, 681-684.

[73] Twilton, J.; Le, C.; Zhang, P.; Shaw, M. H.; Evans, R. W.; MacMillan, D. W. C. The merger of transition metal and photocatalysis. *Nature Reviews Chemistry* **2017,** *1*.

[74] Hossain, A.; Bhattacharyya, A.; Reiser, O. Copper's rapid ascent in visible-light photoredox catalysis. *Science* **2019,** *364*.

[75] Narayanam, J. M.; Stephenson, C. R. Visible light photoredox catalysis: applications in organic synthesis. *Chem. Soc. Rev.* **2011,** *40*, 102-113.

[76] Karkas, M. D.; Porco, J. A., Jr.; Stephenson, C. R. Photochemical Approaches to Complex Chemotypes: Applications in Natural Product Synthesis. *Chem. Rev.* **2016,** *116*, 9683-9747.

[77] Bach, T.; Hehn, J. P. Photochemical reactions as key steps in natural product synthesis. *Angew. Chem., Int. Ed.* **2011,** *50*, 1000-1045.

[78] Prier, C. K.; Rankic, D. A.; MacMillan, D. W. Visible light photoredox catalysis with transition metal complexes: applications in organic synthesis. *Chem. Rev.* **2013,** *113*, 5322-5363.

[79] Lowry, M. S.; Bernhard, S. Synthetically tailored excited states: phosphorescent, cyclometalated iridium(III) complexes and their applications. **2006,** *12*, 7970-7977.

[80] Takeda, H.; Ishitani, O. Development of efficient photocatalytic systems for CO2 reduction using mononuclear and multinuclear metal complexes based on mechanistic studies. *Coord. Chem. Rev.* **2010,** *254*, 346-354.

[81] K.Kalyanasundaram; M.Grätzel Applications of functionalized transition metalcomplexes in photonic and optoelectronicdevices. *Coord. Chem. Rev.* **1998,** *77*, 347 – 414.

[82] Nicewicz, D. A.; MacMillan, D. W. C. Merging Photoredox Catalysis with Organocatalysis: The Direct Asymmetric Alkylation of Aldehydes. *Science* **2008,** *322*, 77-80.

[83] Ischay, M. A.; Anzovino, M. E.; Du, J.; Yoon, T. P. Efficient Visible Light Photocatalysis of [2+2] Enone Cycloadditions. *J. Am. Chem. Soc.* **2008,** *130*, 12886–12887.

[84] Narayanam, J. M. R.; Tucker, J. W.; Stephenson, C. R. J. Electron-Transfer Photoredox Catalysis: Development of a Tin-Free Reductive Dehalogenation Reaction. *J. Am. Chem. Soc.* **2009,** *131*, 8756–8757.

[85] Arias-Rotondo, D. M.; McCusker, J. K. The photophysics of photoredox catalysis: a roadmap for catalyst design. *Chem. Soc. Rev.* **2016,** *45*, 5803-5820.

[86] Ye, Y.; Sanford, M. S. Merging visible-light photocatalysis and transition-metal catalysis in the copper-catalyzed trifluoromethylation of boronic acids with CF3I. *J. Am. Chem. Soc.* **2012,** *134*, 9034-9037.

[87] Zhang, H. R.; Chen, D. Q.; Han, Y. P.; Qiu, Y. F.; Jin, D. P.; Liu, X. Y. Merging photoredox with copper catalysis: decarboxylative difluoroacetylation of alpha,beta-unsaturated carboxylic acids with ICF2CO2Et. *Chem. Commun.* **2016,** *52*, 11827-11830.

[88] Wang, D.; Zhu, N.; Chen, P.; Lin, Z.; Liu, G. Enantioselective Decarboxylative Cyanation Employing Cooperative Photoredox Catalysis and Copper Catalysis. *J. Am. Chem. Soc.* **2017,** *139*, 15632-15635.

[89]   Sha, W.; Deng, L.; Ni, S.; Mei, H.; Han, J.; Pan, Y. Merging Photoredox and Copper Catalysis: Enantioselective Radical Cyanoalkylation of Styrenes. *ACS Catal.* **2018,** *8*, 7489-7494.

[90]   Le, C.; Chen, T. Q.; Liang, T.; Zhang, P.; MacMillan, D. W. C. A radical approach to the copper oxidative addition problem: Trifluoromethylation of bromoarenes. *Science* **2018,** *360*, 1010–1014.

[91]   Kautzky, J. A.; Wang, T.; Evans, R. W.; MacMillan, D. W. C. Decarboxylative Trifluoromethylation of Aliphatic Carboxylic Acids. *J. Am. Chem. Soc.* **2018,** *140*, 6522-6526.

[92]   Kalyani, D.; McMurtrey, K. B.; Neufeldt, S. R.; Sanford, M. S. Room-temperature C-H arylation: merger of Pd-catalyzed C-H functionalization and visible-light photocatalysis. *J. Am. Chem. Soc.* **2011,** *133*, 18566-18569.

[93]   Griffin, J. D.; Cavanaugh, C. L.; Nicewicz, D. A. Reversing the Regioselectivity of Halofunctionalization Reactions through Cooperative Photoredox and Copper Catalysis. *Angew. Chem., Int. Ed.* **2017,** *56*, 2097-2100.

[94]   Bao, X.; Wang, Q.; Zhu, J. Dual Photoredox/Copper Catalysis for the Remote C(sp(3))-H Functionalization of Alcohols and Alkyl Halides by N-Alkoxypyridinium Salts. *Angew. Chem., Int. Ed.* **2019,** *58*, 2139-2143.

[95]   Rueping, M.; Koenigs, R. M.; Poscharny, K.; Fabry, D. C.; Leonori, D.; Vila, C. Dual catalysis: combination of photocatalytic aerobic oxidation and metal catalyzed alkynylation reactions--C-C bond formation using visible light. *Chem. Eur. J.* **2012,** *18*, 5170-5174.

[96]   Perepichka, I.; Kundu, S.; Hearne, Z.; Li, C. J. Efficient merging of copper and photoredox catalysis for the asymmetric cross-dehydrogenative-coupling of alkynes and tetrahydroisoquinolines. *Org. Biomol. Chem.* **2015,** *13*, 447-451.

[97]   Xiang, M.; Meng, Q. Y.; Li, J. X.; Zheng, Y. W.; Ye, C.; Li, Z. J.; Chen, B.; Tung, C. H.; Wu, L. Z. Activation of CH Bonds through Oxidant-Free Photoredox Catalysis: Cross-Coupling Hydrogen-Evolution Transformation of Isochromans and beta-Keto Esters. *Chem. Eur. J.* **2015,** *21*, 18080-18084.

[98]   Zhang, H.; Zhang, P.; Jiang, M.; Yang, H.; Fu, H. Merging photoredox with copper catalysis: Decarboxylative alkynylation of α-amino acid derivatives. *Org. Lett.* **2017,** *19*, 1016-1019.

[99]   Yoo, W. J.; Tsukamoto, T.; Kobayashi, S. Visible-light-mediated chan-lam coupling reactions of aryl boronic acids and aniline derivatives. *Angew. Chem., Int. Ed.* **2015,** *54*, 6587-6590.

[100]   Tao, C.; Wang, B.; Sun, L.; Liu, Z.; Zhai, Y.; Zhang, X.; Wang, J. Merging visible-light photoredox and copper catalysis in catalytic aerobic oxidation of amines to nitriles. *Org. Biomol. Chem.* **2017,** *15*, 328-332.

[101]   Bai, P.; Sun, S.; Li, Z.; Qiao, H.; Su, X.; Yang, F.; Wu, Y.; Wu, Y. Ru/Cu Photoredox or Cu/Ag Catalyzed C4-H Sulfonylation of 1-Naphthylamides at Room Temperature. *J. Org. Chem.* **2017,** *82*, 12119-12127.

[102]   Jin, R.; Chen, Y.; Liu, W.; Xu, D.; Li, Y.; Ding, A.; Guo, H. Merging photoredox catalysis with Lewis acid catalysis: activation of carbon-carbon triple bonds. *Chem. Commun.* **2016,** *52*, 9909-9912.

[103] Xia, X. F.; Zhang, G. W.; Wang, D.; Zhu, S. L. Visible-Light Induced and Oxygen-Promoted Oxidative Cyclization of Aromatic Enamines for the Synthesis of Quinolines Derivatives. *J. Org. Chem.* **2017,** *82*, 8455-8463.

[104] Hsieh, S. Y.; Bode, J. W. Lewis Acid Induced Toggle from Ir(II) to Ir(IV) Pathways in Photocatalytic Reactions: Synthesis of Thiomorpholines and Thiazepanes from Aldehydes and SLAP Reagents. *ACS. Cent. Sci.* **2017,** *3*, 66-72.

[105] Reed, N. L.; Herman, M. I.; Miltchev, V. P.; Yoon, T. P. Photocatalytic Oxyamination of Alkenes: Copper(II) Salts as Terminal Oxidants in Photoredox Catalysis. *Org. Lett.* **2018,** *20*, 7345-7350.

[106] Mao, R.-Z.; Xiong, D.-C.; Guo, F.; Li, Q.; Duan, J.; Ye, X.-S. Light-driven highly efficient glycosylation reactions. *Org. Chem. Front.* **2016,** *3*, 737-743.

[107] Lawrence, S. A. *Amines: Synthesis Properties and Applications*. Cambridge University Press: Cambridge, 2004.

[108] Ricci, A. *Amino Group Chemistry: From Synthesis to the Life Sciences*. Wiley-VCH: Weinheim, 2008.

[109] Ruiz-Castillo, P.; Buchwald, S. L. Applications of Palladium-Catalyzed C-N Cross-Coupling Reactions. *Chem. Rev.* **2016,** *116*, 12564-12649.

[110] Nakata, T. Total Synthesis of Marine Polycyclic Ethers. *Chem. Rev.* **2005,** *105*, 4314−4347.

[111] Li, J. J.; Johnson, D. S.; Sliskovic, D. R.; Roth, B. D. *Contemporary Drug Synthesis*. Wiley: Hoboken, New Jersey, 2004.

[112] Müller, F. *Agrochemicals: Composition, Production, Toxicology, Applications*. Wiley-VCH: Weinheim, Germany, 1999.

[113] Brown, D. G.; Bostrom, J. Analysis of Past and Present Synthetic Methodologies on Medicinal Chemistry: Where Have All the New Reactions Gone? *J. Med. Chem.* **2016,** *59*, 4443-4458.

[114] McMurray, L.; McGuire, T. M.; Howells, R. L. Recent Advances in Photocatalytic Decarboxylative Coupling Reactions in Medicinal Chemistry. *Synthesis* **2020**, DOI: 10.1055/s-0039-1690843.

[115] Surry, D. S.; Buchwald, S. L. Dialkylbiaryl phosphines in Pd-catalyzed amination: A user's guide. *Chem. Sci.* **2011,** *2*, 27-50.

[116] hartwig, J. F. Transition Metal Catalyzed Synthesis of Arylamines and Aryl Ethers fromAryl Halides and Triflates: Scope and Mechanism. *Angew. Chem., Int. Ed.* **1998,** *37*, 2046-2067.

[117] Hartwig, J. F. Evolution of a fourth generation catalyst for the amination and thioetherification of aryl halides. *Acc. Chem. Res.* **2008,** *41*, 1534-1544.

[118] Mann, G.; Hartwig, J. F.; Driver, M. S.; Fernandez-Rivas, C. Palladium-Catalyzed C-N(sp2) Bond Formation: N-Arylation of Aromatic and Unsaturated Nitrogen and the Reductive Elimination Chemistry of Palladium Azolyl and Methyleneamido Complexes. *J. Am. Chem. Soc.* **1998,** *120*, 827-828.

[119] Sambiagio, C.; Marsden, S. P.; Blacker, A. J.; McGowan, P. C. Copper catalysed Ullmann type chemistry: From mechanistic aspects to modern development. *Chem. Soc. Rev.* **2014,** *43*, 3525-3550.

[120] Yang, M.; Liu, F. An Ullmann Coupling of Aryl Iodides and Amines Using an Air-Stable Diazaphospholane Ligand. *J. Org. Chem.* **2007,** *72*, 8969-8971.

[121] Qiao, J.; Lam, P. Copper-Promoted Carbon-Heteroatom Bond Cross-Coupling with Boronic Acids and Derivatives. *Synthesis* **2010,** *2011*, 829-856.

[122] Enthaler, S.; Company, A. Palladium-catalysed hydroxylation and alkoxylation. *Chem. Soc. Rev.* **2011**, *40*, 4912-4924.

[123] Gowrisankar, S.; Sergeev, A. G.; Anbarasan, P.; Spannenberg, A.; Neumann, H.; Beller, M. A General and Efficient Catalyst for Palladium-Catalyzed C-O Coupling Reactions of Aryl Halides with Primary Alcohols. *J. Am. Chem. Soc.* **2010,** *132*, 11592–11598.

[124] Wu, X.; Fors, B. P.; Buchwald, S. L. A single phosphine ligand allows palladium-catalyzed intermolecular C-O bond formation with secondary and primary alcohols. *Angew. Chem., Int. Ed.* **2011,** *50*, 9943-9947.

[125] MacQueen, P. M.; Tassone, J. P.; Diaz, C.; Stradiotto, M. Exploiting Ancillary Ligation To Enable Nickel-Catalyzed C–O Cross-Couplings of Aryl Electrophiles with Aliphatic Alcohols. *J. Am. Chem. Soc.* **2018,** *140*, 5023-5027.

[126] Carey, F. A.; Sundberg, R. J. *Advanced Organic Chemistry, Part B: Reactions and Synthesis, 5th ed*. Springer: New York, 2007.

[127] Fuhrmann, E.; Talbiersky, J. Synthesis of Alkyl Aryl Ethers by Catalytic Williamson Ether Synthesis with Weak Alkylation Agents. *Org. Process Res. Dev.* **2005,** *9*, 206−211.

[128] Williamson, A. Ueber die Theorie der Aetherbildung. *Justus Liebigs Ann. Chem.* **1851**, 37-49.

[129] Caron, S.; Ghosh, A., Nucleophilic Aromatic Substitution. In *Practical Synthetic Organic Chemistry*, John Wiley & Sons: Hoboken, NJ, 2011; p 237−253.

[130] Gomez, S.; Peters, J. A.; Maschmeyer, T. The Reductive Amination of Aldehydes and Ketonesand the Hydrogenation of Nitriles:Mechanistic Aspects and Selectivity Control. *Adv. Synth. Catal.* **2002,** *344*, 1037-1057.

[131] Ghosh, A. K.; Brindisi, M.; Sarkar, A. The Curtius Rearrangement: Applications in Modern Drug Discovery and Medicinal Chemistry. *ChemMedChem* **2018,** *13*, 2351-2373.

[132] Swamy, K. C. K.; Kumar, N. N. B.; Balaraman, E.; Kumar, K. V. P. P. Mitsunobu and Related Reactions: Advances and Applications. *Chem. Rev.* **2009,** *109*, 2551–2651.

[133] Liu, Z. J.; Lu, X.; Wang, G.; Li, L.; Jiang, W. T.; Wang, Y. D.; Xiao, B.; Fu, Y. Directing group in decarboxylative cross-coupling: Copper-catalyzed site-selective C–N bond formation from nonactivated aliphatic carboxylic acids. *J. Am. Chem. Soc.* **2016,** *138*, 9714-9719.

[134] Fang, Z.; Feng, Y.; Dong, H.; Li, D.; Tang, T. Copper(I)-catalyzed radical decarboxylative imidation of carboxylic acids with N-fluoroarylsulfonimides. *Chem. Commun.* **2016,** *52*, 11120-11123.

[135] Zhu, Y.; Li, X.; Wang, X.; Huang, X.; Shen, T.; Zhang, Y.; Sun, X.; Zou, M.; Song, S.; Jiao, N. Silver-Catalyzed Decarboxylative Azidation of Aliphatic Carboxylic Acids. *Org. Lett.* **2015,** *17*, 4702-4705.

[136] Liu, C.; Wang, X.; Li, Z.; Cui, L.; Li, C. Silver-Catalyzed Decarboxylative Radical Azidation of Aliphatic Carboxylic Acids in Aqueous Solution. *J. Am. Chem. Soc.* **2015,** *137*, 9820-9823.

[137] Kong, D.; Moon, P.; Bsharat, O.; Lundgren, R. J. Direct Catalytic Decarboxylative Amination of Aryl Acetic Acids. *Angew. Chem., Int. Ed.* **2019**.

[138] Kojima, M.; Matsunaga, S. The Merger of Photoredox and Cobalt Catalysis. *Trends in Chemistry* **2020,** *2*, 410-426.

[139] Shaw, M. H.; Twilton, J.; MacMillan, D. W. Photoredox Catalysis in Organic Chemistry. *J. Org. Chem.* **2016,** *81*, 6898-6926.

[140] Kiyokawa, K.; Watanabe, T.; Fra, L.; Kojima, T.; Minakata, S. Hypervalent Iodine(III)-Mediated Decarboxylative Ritter-Type Amination Leading to the Production of alpha-Tertiary Amine Derivatives. *J. Org. Chem.* **2017,** *82*, 11711-11720.

[141] Sakakibara, Y.; Ito, E.; Fukushima, T.; Murakami, K.; Itami, K. Late-Stage Functionalization of Arylacetic Acids by Photoredox-Catalyzed Decarboxylative Carbon-Heteroatom Bond Formation. *Chem. Eur. J.* **2018,** *24*, 9254-9258.

[142] Marcote, D. C.; Street-Jeakings, R.; Dauncey, E.; Douglas, J. J.; Ruffoni, A.; Leonori, D. Photoinduced decarboxylative azidation of cyclic amino acids. *Org. Biomol. Chem.* **2019,** *17*, 1839-1842.

[143] Shibutani, S.; Kodo, T.; Takeda, M.; Nagao, K.; Tokunaga, N.; Sasaki, Y.; Ohmiya, H. Organophotoredox-Catalyzed Decarboxylative C(sp(3))-O Bond Formation. *J. Am. Chem. Soc.* **2020,** *142*, 1211-1216.

[144] njardarson.lab.arizona.edu/sites/njardarson.lab.arizona.edu/files (accessed April 23, 2020).

[145] Morandi, B.; Legnani, L.; Bhawal, B. Recent Developments in the Direct Synthesis of Unprotected Primary- Amines. *Synthesis* **2016,** *49*, 776-789.

[146] Kim, H.; Chang, S. The Use of Ammonia as an Ultimate Amino Source in the Transition Metal-Catalyzed C-H Amination. *Acc. Chem. Res.* **2017,** *50*, 482-486.

[147] Crespo, A. Benzophenone Imine. *Synlett* **2006,** *2006*, 2345-2346.

[148] Kondo, Y.; Morimoto, H.; Ohshima, T. Recent Progress towards the Use of Benzophenone Imines as an Ammonia Equivalent. *Chem. Lett.* **2020,** *49*, 497-504.

[149] Peacock, D. M.; Roos, C. B.; Hartwig, J. F. Palladium-Catalyzed Cross Coupling of Secondary and Tertiary Alkyl Bromides with a Nitrogen Nucleophile. *ACS. Cent. Sci.* **2016,** *2*, 647-652.

[150] Yue, H.; Guo, L.; Liu, X.; Rueping, M. Nickel-Catalyzed Synthesis of Primary Aryl and Heteroaryl Amines via C-O Bond Cleavage. *Org. Lett.* **2017,** *19*, 1788-1791.

[151] Mikhailine, A. A.; Grasa Mannino, G. A.; Colacot, T. J. Catalyst-Directed Chemoselective Double Amination of Bromo-chloro(hetero)arenes: A Synthetic Route toward Advanced Amino-aniline Intermediates. *Org. Lett.* **2018,** *20*, 2301-2305.

[152] Huang, H.; Chen, W.; Xu, Y.; Li, J. I−/TBHP catalyzed Csp3–N/Csp2–N bond formation via oxidative coupling with benzophenone imine in water. *Green Chem.* **2015,** *17*, 4715-4719.

[153] Kramer, S. Synthesis of alpha-Substituted Primary Benzylamines through Copper-Catalyzed Cross-Dehydrogenative Coupling. *Org. Lett.* **2019,** *21*, 65-69.

[154] Kiyokawa, K.; Okumatsu, D.; Minakata, S. Synthesis of Hypervalent Iodine(III) Reagents Containing a Transferable (Diarylmethylene)amino Group and Their Use in the Oxidative Amination of Silyl Ketene Acetals. *Angew. Chem., Int. Ed.* **2019,** *58*, 8907-8911.

[155] Mai, E.; Schneider, C. Catalytic, enantioselective synthesis of Boc-protected 1,2-amino alcohols through aminolysis of meso epoxides with benzophenone imine *ARKIVOC* **2008**, 216-222.

[156] Lim, J. J.; Leitch, D. C. Lewis Acid-Catalyzed Addition of Benzophenone Imine to Epoxides Enables the Selective Synthesis and Derivatization of Primary 1,2-Amino Alcohols. *Org. Process Res. Dev.* **2018,** *22*, 641-649.

[157] Chan-Penebre, E.; Kuplast, K. G.; Majer, C. R.; Boriack-Sjodin, P. A.; Wigle, T. J.; Johnston, L. D.; Rioux, N.; Munchhof, M. J.; Jin, L.; Jacques, S. L.; West, K. A.; Lingaraj, T.; Stickland, K.; Ribich, S. A.; Raimondi, A.; Scott, M. P.; Waters, N. J.; Pollock, R. M.; Smith, J. J.; Barbash, O.; Pappalardi, M.; Ho, T. F.; Nurse, K.; Oza, K. P.; Gallagher, K.

T.; Kruger, R.; Moyer, M. P.; Copeland, R. A.; Chesworth, R.; Duncan, K. W. A selective inhibitor of PRMT5 with in vivo and in vitro potency in MCL models. *Nat. Chem. Biol.* **2015,** *11*, 432-437.

[158] Gillingham, D.; Fei, N. Catalytic X-H insertion reactions based on carbenoids. *Chem. Soc. Rev.* **2013,** *42*, 4918-4931.

[159] zhou, S.-F.; Zhou, Q.-L. Transition-Metal-Catalyzed Enantioselective HeteroatomHydrogen Bond Insertion Reactions. *Acc. Chem. Res.* **2012,** *45*, 1365–1377

[160] Ford, A.; Miel, H.; Ring, A.; Slattery, C. N.; Maguire, A. R.; McKervey, M. A. Modern Organic Synthesis with alpha-Diazocarbonyl Compounds. *Chem. Rev.* **2015,** *115*, 9981-10080.

[161] Tan, F.; Liu, X.; Hao, X.; Tang, Y.; Lin, L.; Feng, X. Asymmetric Catalytic Insertion of α-Diazo Carbonyl Compounds into O–H Bonds of Carboxylic Acids. *ACS Catal.* **2016,** *6*, 6930-6934.

[162] Yang, J.; Ruan, P.; Yang, W.; Feng, X.; Liu, X. Enantioselective carbene insertion into the N-H bond of benzophenone imine. *Chem. Sci.* **2019,** *10*, 10305-10309.

[163] Noble, A.; Anderson, J. C. Nitro-Mannich reaction. *Chem. Rev.* **2013,** *113*, 2887-2939.

[164] Lykke, L.; Monge, D.; Nielsen, M.; Jorgensen, K. A. Asymmetric organocatalytic formal aza-Michael addition of ammonia to nitroalkenes. *Chem. Eur. J* **2010,** *16*, 13330-13334.

[165] Zhang, S.-J.; Cui, H.-L.; Jiang, K.; Li, R.; Ding, Z.-Y.; Chen, Y.-C. Enantioselective Allylic Amination of Morita-Baylis-Hillman Carbonates Catalysed by Modified Cinchona Alkaloids. *Eur. J. Org. Chem.* **2009,** *2009*, 5804-5809.

[166] Deng, H.-P.; Wei, Y.; Shi, M. Chiral Bifunctional Thiourea-Phosphane Organocatalysts in Asymmetric Allylic Amination of Morita-Baylis-Hillman Acetates. *Eur. J. Org. Chem.* **2011,** *2011*, 1956-1960.

[167] Lin, A.; Mao, H.; Zhu, X.; Ge, H.; Tan, R.; Zhu, C.; Cheng, Y. Organocatalytic enantioselective amination of Morita-Baylis-Hillman carbonates with masked ammonia: a facile method for the synthesis of unprotected alpha-methylene-beta-amino esters. *Chem. Eur. J* **2011,** *17*, 13676-13679.

[168] Fernandes, R. A.; Kattanguru, P.; Gholap, S. P.; Chaudhari, D. A. Recent advances in the Overman rearrangement: synthesis of natural products and valuable compounds. *Org. Biomol. Chem.* **2017,** *15*, 2672-2710.

[169] Xu, K.; Wang, Y. H.; Khakyzadeh, V.; Breit, B. Asymmetric synthesis of allylic amines via hydroamination of allenes with benzophenone imine. *Chem. Sci.* **2016,** *7*, 3313-3316.

[170] Ibrahem, I.; Rios, R.; Vesely, J.; Zhao, G. L.; Cordova, A. Organocatalytic asymmetric 5-hydroxyisoxazolidine synthesis: a highly enantioselective route to beta-amino acids. *Chem. Commun.* **2007**, 849-851.

[171] Chen, Y. K.; Yoshida, M.; MacMillan, D. W. C. Enantioselective Organocatalytic Amine Conjugate Addition. *J. Am. Chem. Soc.* **2006,** *128*, 9328-9329.

[172] Choubane, H.; Garrido-Castro, A. F.; Alvarado, C.; Martin-Somer, A.; Guerrero-Corella, A.; Daaou, M.; Diaz-Tendero, S.; Carmen Maestro, M.; Fraile, A.; Aleman, J. Intramolecular hydrogen-bond activation for the addition of nucleophilic imines: 2-hydroxybenzophenone as a chemical auxiliary. *Chem. Commun.* **2018,** *54*, 3399-3402.

[173] Medical gallery of Blausen Medical 2014. *WikiJournal of Medicine* **2014,** *1*.

[174] Harpere, D. B.; O'Haganb, D. The Fluorinated Natural Products *Nat. Prod. Rep.* **1994,** *11*, 123-133.

[175] Ojima, I. *Fluorine in Medicinal Chemistry and Chemical Biology*. John Wiley & Sons Ltd: Hoboken, 2009.

[176] Tressaud, A.; Haufe, G. *Fluorine and Health: Molecular Imaging, Biomedical Materials and Pharmaceuticals*. Elsevier: London, 2008.

[177] Wang, J.; Sanchez-Rosello, M.; Acena, J. L.; del Pozo, C.; Sorochinsky, A. E.; Fustero, S.; Soloshonok, V. A.; Liu, H. Fluorine in pharmaceutical industry: fluorine-containing drugs introduced to the market in the last decade (2001-2011). *Chem. Rev.* **2014,** *114*, 2432-2506.

[178] Xu, X. H.; Matsuzaki, K.; Shibata, N. Synthetic methods for compounds having CF3-S units on carbon by trifluoromethylation, trifluoromethylthiolation, triflylation, and related reactions. *Chem. Rev.* **2015,** *115*, 731-764.

[179] Bennion, B. J.; Be, N. A.; McNerney, M. W.; Lao, V.; Carlson, E. M.; Valdez, C. A.; Malfatti, M. A.; Enright, H. A.; Nguyen, T. H.; Lightstone, F. C.; Carpenter, T. S. Predicting a Drug's Membrane Permeability: A Computational Model Validated With in Vitro Permeability Assay Data. *J. Phys. Chem. B* **2017,** *121*, 5228-5237.

[180] Hansch, C.; Leo, A.; TAFT, R. W. A Survey of Hammett Substituent Constants and Resonance and Field Parameters. *Chem. Rev.* **1999,** *91*, 165-195.

[181] Leo, A. J.; Hansch, C.; Elkins, D. Partition Coefficiencts and Their Uses. *Chem. Rev.* **1971,** *71*, 525-616.

[182] L.M.Yagupol'skii; N.V.Kondratenko, A. Y. I. c. The Electronic Nature of Fluorine-containing Substituents. *Russ. Chem. Rev.* **1974,** *43*, 64-94.

[183] Boiko, V. N. Aromatic and heterocyclic perfluoroalkyl sulfides. Methods of preparation. *Beilstein J. Org. Chem.* **2010,** *6*, 880-921.

[184] He, J.; Chen, C.; Fu, G. C.; Peters, J. C. Visible-Light-Induced, Copper-Catalyzed Three-Component Coupling of Alkyl Halides, Olefins, and Trifluoromethylthiolate to Generate Trifluoromethyl Thioethers. *ACS Catal.* **2018,** *8*, 11741-11748.

[185] Liu, J. B.; Xu, X. H.; Chen, Z. H.; Qing, F. L. Direct dehydroxytrifluoromethylthiolation of alcohols using silver(I) trifluoromethanethiolate and tetra-n-butylammonium iodide. *Angew. Chem., Int. Ed.* **2015,** *54*, 897-900.

[186] Mukherjee, S.; Maji, B.; Tlahuext-Aca, A.; Glorius, F. Visible-Light-Promoted Activation of Unactivated C(sp3)-H Bonds and Their Selective Trifluoromethylthiolation. *J. Am. Chem. Soc.* **2016,** *138*, 16200-16203.

[187] Mukherjee, S.; Patra, T.; Glorius, F. Cooperative Catalysis: A Strategy To Synthesize Trifluoromethyl-thioesters from Aldehydes. *ACS Catal.* **2018,** *8*, 5842-5846.

[188] Ni, C.; Hu, J. The unique fluorine effects in organic reactions: recent facts and insights into fluoroalkylations. *Chem. Soc. Rev.* **2016,** *45*, 5441-5454.

[189] Shao, X.; Xu, C.; Lu, L.; Shen, Q. Shelf-stable electrophilic reagents for trifluoromethylthiolation. *Acc. Chem. Res.* **2015,** *48*, 1227-1236.

[190] Teverovskiy, G.; Surry, D. S.; Buchwald, S. L. Pd-catalyzed synthesis of Ar-SCF3 compounds under mild conditions. *Angew. Chem., Int. Ed.* **2011,** *50*, 7312-7314.

[191] Toulgoat, F.; Alazet, S.; Billard, T. Direct Trifluoromethylthiolatio Reactions: The "Renaissance" of an Old Concept. *Eur. J. Org. Chem.* **2014**, 2415–2428.

[192] Wu, H.; Xiao, Z.; Wu, J.; Guo, Y.; Xiao, J. C.; Liu, C.; Chen, Q. Y. Direct trifluoromethylthiolation of unactivated C(sp3)-H using silver(I) trifluoromethanethiolate and potassium persulfate. *Angew. Chem., Int. Ed.* **2015,** *54*, 4070-4074.

[193] Xu, B.; Li, D.; Lu, L.; Wang, D.; Hu, Y.; Shen, Q. Radical fluoroalkylthiolation of aldehydes with PhSO2SRf (Rf = CF3, C2F5, CF2H or CH2F): a general protocol for the preparation of fluoroalkylthioesters. *Org. Chem. Front.* **2018,** *5*, 2163-2166.

[194] Zeng, Y.; Hu, J. Silver-Mediated Trifluoromethylthiolation-Iodination of Arynes. *Org. Lett.* **2016,** *18*, 856-859.

[195] Zhang, C. P.; Vicic, D. A. Nickel-catalyzed synthesis of aryl trifluoromethyl sulfides at room temperature. *J. Am. Chem. Soc.* **2012,** *134*, 183-185.

[196] Zhang, M.; Chen, J.; Chen, Z.; Weng, Z. Copper-mediated effective synthesis of S - trifluoromethyl esters by trifluoromethylthiolation of acid chlorides. *Tetrahedron* **2016,** *72*, 3525-3530.

[197] Baert, F.; Colomb, J.; Billard, T. Electrophilic trifluoromethanesulfanylation of organometallic species with trifluoromethanesulfanamides. *Angew. Chem., Int. Ed.* **2012,** *51*, 10382-10385.

[198] E. H. Man; Coffman, D. D.; Muetterties, E. L. Synthesis and Properties of Bis-(trifluoromethylthio) -mercury. *J. Am. Chem. Soc.* **1959,** *81*, 3575-3577.

[199] Kremlev, M. M.; Tyrra, W.; Naumann, D.; Yagupolskii, Y. L. S-Trifluoromethyl esters of thiocarboxylic acids, RC(O)SCF3. *Tetrahedron Lett.* **2004,** *45*, 6101-6104.

[200] Zhang, M.; Yuan, X. A.; Zhu, C.; Xie, J. Deoxygenative Deuteration of Carboxylic Acids with D2 O. *Angew. Chem., Int. Ed.* **2019,** *58*, 312-316.

[201] Scattolin, T.; Deckers, K.; Schoenebeck, F. Direct Synthesis of Acyl Fluorides from Carboxylic Acids with the Bench-Stable Solid Reagent (Me4N)SCF3. *Org. Lett.* **2017,** *19*, 5740-5743.

[202] Zuo, Z.; Ahneman, D. T.; Chu, L.; Terrett, J. A.; Doyle, A. G.; MacMillan, D. W. C. Merging photoredox with nickel catalysis: Coupling of α-carboxyl sp3-carbons with aryl halides. *Science* **2014,** *345*, 437-440.

[203] Tellis, J. C.; Primer, D. N.; Molander, G. A. Single-electron transmetalation in organoboron cross-coupling by photoredox/nickel dual catalysis. *Science* **2014,** *345*, 433-436.

[204] Skubi, K. L.; Blum, T. R.; Yoon, T. P. Dual catalysis strategies in photochemical synthesis. *Chem. Rev.* **2016,** *116*, 10035-10074.

[205] Corcoran, E. B.; Pirnot, M. T.; Lin, S.; Dreher, S. D.; DiRocco, D. A.; Davies, I. W.; Buchwald, S. L.; MacMillan, D. W. C. Aryl amination using ligand-free Ni(II) salts and photoredox catalysis. *Science* **2016,** *353*, 279-283.

[206] Yoo, W.-J.; Tsukamoto, T.; Kobayashi, S. Visible-light-mediated Chan-Lam coupling reactions of aryl boronic acids and aniline derivatives. *Angew. Chem., Int. Ed.* **2015,** *54*, 6587–6590.

[207] Kelkar, A. A.; Patil, N. M.; Chaudhari, R. V. Copper-catalyzed amination of aryl halides: single step synthesisof triarylamines. *Tetrahedron Lett.* **2002,** *43*, 7143-7146.

[208] Daly, S.; Haddow, M. F.; Orpen, A. G.; Rolls, G. T. A.; Wass, D. F.; Wingad, R. L. Copper(I) Diphosphine Catalysts for C-N Bond Formation: Synthesis, Structure, and Ligand Effects. *Organometallics* **2008,** *27*, 3196–3202.

[209] Zhang, Y.; Yang, X.; Yao, Q.; Ma, D. CuI/DMPAO-catalyzed N-arylation of acyclic secondary amines. *Org. Lett.* **2012,** *14*, 3056-3059.

[210] Zhou, W.; Fan, M.; Yin, J.; Jiang, Y.; Ma, D. CuI/Oxalic Diamide Catalyzed Coupling Reaction of (Hetero)Aryl Chlorides and Amines. *J. Am. Chem. Soc.* **2015,** *137*, 11942-11945.

[211] Fan, M.; Zhou, W.; Jiang, Y.; Ma, D. CuI/Oxalamide Catalyzed Couplings of (Hetero)aryl Chlorides and Phenols for Diaryl Ether Formation. *Angew. Chem., Int. Ed.* **2016,** *55*, 6211-6215.

[212] Tlahuext-Aca, A.; Candish, L.; Garza-Sanchez, R. A.; Glorius, F. Decarboxylative Olefination of Activated Aliphatic Acids Enabled by Dual Organophotoredox/Copper Catalysis. *ACS Catal.* **2018,** *8*, 1715-1719.

[213] Collins, K. D.; Glorius, F. A robustness screen for the rapid assessment of chemical reactions. *Nat. Chem.* **2013,** *5*, 597-601.

[214] Griller, D.; Ingold, K. U. Free-Radical Clocks. *Acc. Chem. Res.* **1980,** *13*, 317-323.

[215] Rassi, A., Jr.; Rassi, A.; Marcondes de Rezende, J. American trypanosomiasis (Chagas disease). *Infect. Dis. Clin. North. Am.* **2012,** *26*, 275-291.

[216] Keenan, M.; Chaplin, J. H.; Alexander, P. W.; Abbott, M. J.; Best, W. M.; Khong, A.; Botero, A.; Perez, C.; Cornwall, S.; Thompson, R. A.; White, K. L.; Shackleford, D. M.; Koltun, M.; Chiu, F. C.; Morizzi, J.; Ryan, E.; Campbell, M.; von Geldern, T. W.; Scandale, I.; Chatelain, E.; Charman, S. A. Two analogues of fenarimol show curative activity in an experimental model of Chagas disease. *J. Med. Chem.* **2013,** *56*, 10158-10170.

[217] Kowa Co., Ltd. U.S. Patent 6867221 B2, 2005. *Kowa Co., Ltd. U.S. Patent 6867221 B2, 2005.*

[218] Liu, Y.; Yang, Y.; Zhu, R.; Zhang, D. Computational Clarification of Synergetic RuII/CuI-Metallaphotoredox Catalysis in C(sp3)–N Cross-Coupling Reactions of Alkyl Redox-Active Esters with Anilines. *ACS Catal.* **2020,** *10*, 5030-5041.

[219] Synthesis and Characterization of Mono and Bis 8-aminoquinoline copper(II) Complexes in Monomeric and dimeric forms. *Delta J. Sci.* **1993,** *17*, 141-155.

[220] Chen, Z.; Zeng, H.; Gong, H.; Wang, H.; Li, C.-J. Palladium-catalyzed reductive coupling of phenols with anilines and amines: efficient conversion of phenolic lignin model monomers and analogues to cyclohexylamines. *Chem. Sci.* **2015,** *6*, 4174-4178.

[221] Nakanishi, M.; Katayev, D.; Besnard, C.; Kundig, E. P. Fused indolines by palladium-catalyzed asymmetric C-C coupling involving an unactivated methylene group. *Angew. Chem., Int. Ed.* **2011,** *50*, 7438-7441.

[222] Dong, J.; Wu, Z.; Liu, Z.; Liu, P.; Sun, P. Rhodium(III)-Catalyzed Direct Cyanation of Aromatic C-H Bond to Form 2-(Alkylamino)benzonitriles Using N-Nitroso As Directing Group. *J. Org. Chem.* **2015,** *80*, 12588-12593.

[223] Wu, Z.; Zhou, L.; Jiang, Z.; Wu, D.; Li, Z.; Zhou, X. Sulfonato-Cu(salen) Complex Catalyzed N-Arylation of Aliphatic Amines with Aryl Halides in Water. *Eur. J. Org. Chem.* **2010,** *2010*, 4971-4975.

[224] Shankaraiah, N.; Markandeya, N.; Srinivasulu, V.; Sreekanth, K.; Reddy Ch, S.; Santos, L. S.; Kamal, A. A one-pot azido reductive tandem mono-N-alkylation employing dialkylboron triflates: online ESI-MS mechanistic investigation. *J. Org. Chem.* **2011,** *76*, 7017-7026.

[225] Larsen, S. B.; Bang-Andersen, B.; Johansen, T. N.; Jørgensen, M. Palladium-catalyzed monoamination of dihalogenated benzenes. *Tetrahedron* **2008,** *64*, 2938-2950.

[226] Li, J.; Cui, M.; Yu, A.; Wu, Y. Carbene adduct of cyclopalladated ferrocenylimine as an efficient catalyst for the amination of aryl chlorides. *J. Organomet. Chem.* **2007,** *692*, 3732-3742.

[227] Jang, E. S.; McMullin, C. L.; Kass, M.; Meyer, K.; Cundari, T. R.; Warren, T. H. Copper(II) anilides in sp(3) C-H amination. *J. Am. Chem. Soc.* **2014,** *136*, 10930-10940.

[228] Yang, C.-H.; Fan, W.-W.; Liu, G.-Q.; Duan, L.; Li, L.; Li, Y.-M. On the understanding of BF3·Et2O-promoted intra- and intermolecular amination and oxygenation of unfunctionalized olefins. *RSC Adv.* **2015,** *5*, 61081-61093.

[229] Bera, S. S.; Debbarma, S.; Ghosh, A. K.; Chand, S.; Maji, M. S. Cp*CoIII-Catalyzed syn-Selective C-H Hydroarylation of Alkynes Using Benzamides: An Approach Toward Highly Conjugated Organic Frameworks. *J. Org. Chem.* **2017,** *82*, 420-430.

[230] Do, H.-Q.; Bachman, S.; Bissember, A. C.; Peters, J. C.; Fu, G. C. Photoinduced, copper-catalyzed alkylation of amides with unactivated secondary alkyl halides at room temperature. *J. Am. Chem. Soc.* **2014,** *136*, 2162-2167.

[231] Tran, B. L.; Li, B.; Driess, M.; Hartwig, J. F. Copper-catalyzed intermolecular amidation and imidation of unactivated alkanes. *J. Am. Chem. Soc.* **2014,** *136*, 2555-2563.

[232] Islam, S. M.; Ghosh, K.; Roy, A. S.; Molla, R. A.; Salam, N.; Chatterjee, T.; Iqubal, M. A. Polystyrene anchored ruthenium(II) complex catalyzed carbonylation of nitrobenzene and amines for the synthesis of disubstituted ureas. *J. Organomet. Chem.* **2014,** *772-773*, 152-160.

[233] Cabrera, A.; Sharma, P.; Pérez-Flores, F. J.; Velasco, L.; Arias, J. L.; Rubio-Pérez, L. Diastereo- and enantioselective reductive amination of cycloaliphatic ketones by preformed chiral palladium complexes. *Catal. Sci. Technol.* **2014,** *4*, 2626.

[234] Santoro, F.; Psaro, R.; Ravasio, N.; Zaccheria, F. N-Alkylation of amines through hydrogen borrowing over a heterogeneous Cu catalyst. *RSC Adv.* **2014,** *4*, 2596-2600.

[235] Guo, D.; Huang, H.; Xu, J.; Jiang, H.; Liu, H. Efficient Iron-Catalyzed N-Arylation of Aryl Halides with Amines. *Org. Lett.* **2008,** *10*, 4513-4516.

[236] Tang, W.; Johnston, S.; Li, C.; Iggo, J. A.; Bacsa, J.; Xiao, J. Cooperative catalysis: combining an achiral metal catalyst with a chiral Bronsted acid enables highly enantioselective hydrogenation of imines. *Chem. Eur. J* **2013,** *19*, 14187-14193.

[237] Yin, Z.; Zeng, H.; Wu, J.; Zheng, S.; Zhang, G. Cobalt-Catalyzed Synthesis of Aromatic, Aliphatic, and Cyclic Secondary Amines via a "Hydrogen-Borrowing" Strategy. *ACS Catal.* **2016,** *6*, 6546-6550.

[238] Ferretti, A. C.; Mathew, J. S.; Ashworth, I.; Purdy, M.; Brennan, C.; Blackmond, D. G. Mechanistic Inferences Derived from Competitive Catalytic Reactions: Pd(binap)-Catalyzed Amination of Aryl Halides. *Adv. Synth. Catal.* **2008,** *350*, 1007-1012.

[239] Huang, L.; Yu, R.; Zhu, X.; Wan, Y. A recyclable Cu-catalyzed C–N coupling reaction in water and its application to synthesis of imidazo[1,2-a]quinoxaline. *Tetrahedron* **2013,** *69*, 8974-8977.

[240] Han, S.; Zhang, F. F.; Qian, H. Y.; Chen, L. L.; Pu, J. B.; Xie, X.; Chen, J. Z. Development of Quinoline-2,4(1H,3H)-diones as Potent and Selective Ligands of the Cannabinoid Type 2 Receptor. *J. Med. Chem.* **2015,** *58*, 5751-5769.

[241] Li, C.; Wang, J.; Barton, L. M.; Yu, S.; Tian, M.; Peters, D. S.; Kumar, M.; Yu, A. W.; Johnson, K. A.; Chatterjee, A. K.; Yan, M.; Baran, P. S. Decarboxylative borylation. *Science* **2017,** *356*, eaam7355.

[242] Frutos, R. P.; Tampone, T. G.; Mulder, J. A.; Rodriguez, S.; Yee, N. K.; Yang, B.-S.; Senanayake, C. H. Development of a Practical Process for the Synthesis of PDE4 Inhibitors. *Org. Process Res. Dev.* **2016,** *20*, 982-988.

[243] Kitamura, M.; Suga, T.; Chiba, S.; Narasaka, K. Synthesis of Primary Amines by the Electrophilic Amination of Grignard Reagents with 1,3-Dioxolan-2-one O-Sulfonyloxime. *Org. Lett.* **2004**, 4619–4621.

[244] Miyamura, S.; Araki, M.; Suzuki, T.; Yamaguchi, J.; Itami, K. Stereodivergent synthesis of arylcyclopropylamines by sequential C-H borylation and Suzuki-Miyaura coupling. *Angew. Chem., Int. Ed.* **2015,** *54*, 846-851.

[245] Zhang, H.; Ruiz-Castillo, P.; Buchwald, S. L. Palladium-Catalyzed C-O Cross-Coupling of Primary Alcohols. *Org. Lett.* **2018,** *20*, 1580-1583.

[246] Keerthi Krishnan, K.; Ujwaldev, S. M.; Sindhu, K. S.; Anilkumar, G. Recent advances in the transition metal catalyzed etherification reactions. *Tetrahedron* **2016,** *72*, 7393-7407.

[247] Wolter, M.; Nordmann, G.; Job, G. E.; Buchwald, S. L. Copper-Catalyzed Coupling of Aryl Iodides with Aliphatic Alcohols. *Org. Lett.* **2002,** *4*, 973-976.

[248] Hartwig, J. F. Electronic Effects on Reductive Elimination To Form Carbon-Carbon and Carbon-Heteroatom Bonds from Palladium(II) Complexes. *Inorg. Chem* **2007,** *46*, 1936-1947.

[249] Widenhoefer, R. A.; Buchwald, S. L. Electronic Dependence of C-O Reductive Elimination from Palladium (Aryl)neopentoxide Complexes. *J. Am. Chem. Soc.* **1998,** *120*, 6504-6511.

[250] Mao, R.; Frey, A.; Balon, J.; Hu, X. Decarboxylative C(sp3)–N cross-coupling via synergetic photoredox and copper catalysis. *Nat. Catal.* **2018,** *1*, 120-126.

[251] Mao, R.; Balon, J.; Hu, X. Cross Coupling of Alkyl Redox-Active Esters with Benzophenone Imines via Tandem Photoredox and Copper Catalysis. *Angew. Chem., Int. Ed.* **2018,** *57*, 9501-9504.

[252] Okada, K.; Okamoto, K.; Morita, N.; Okubo, K.; Oda, M. Photosensitized Decarboxylative Michael Addition through N-(Acyloxy) phthalimides via an Electron-Transfer Mechanism. *J. Am. Chem. Soc.* **1991,** *113*, 9401–9402.

[253] Sawatzky, R. S.; Hargreaves, B. K. V.; Stradiotto, M. A Comparative Ancillary Ligand Survey in Palladium-Catalyzed C-O Cross-Coupling of Primary and Secondary Aliphatic Alcohols. *Eur. J. Org. Chem.* **2016,** *2016*, 2444-2449.

[254] Salvador, T. K.; Arnett, C. H.; Kundu, S.; Sapiezynski, N. G.; Bertke, J. A.; Raghibi Boroujeni, M.; Warren, T. H. Copper Catalyzed sp(3) C-H Etherification with Acyl Protected Phenols. *J. Am. Chem. Soc.* **2016,** *138*, 16580-16583.

[255] Wang, M.; Gutierrez, O. Y.; Camaioni, D. M.; Lercher, J. A. Palladium-Catalyzed Reductive Insertion of Alcohols into Aryl Ether Bonds. *Angew. Chem., Int. Ed.* **2018,** *57*, 3747-3751.

[256] Shirakawa, E.; Hayashi, Y.; Itoh, K.; Watabe, R.; Uchiyama, N.; Konagaya, W.; Masui, S.; Hayashi, T. Cross-coupling of aryl Grignard reagents with aryl iodides and bromides through S(RN)1 pathway. *Angew. Chem., Int. Ed.* **2012,** *51*, 218-221.

[257] Zheng, Y. W.; Ye, P.; Chen, B.; Meng, Q. Y.; Feng, K.; Wang, W.; Wu, L. Z.; Tung, C. H. Benzene C-H Etherification via Photocatalytic Hydrogen-Evolution Cross-Coupling Reaction. *Org. Lett.* **2017,** *19*, 2206-2209.

[258] Chen, C.; Chan, K. S. Alkyl Carbon–Oxygen Bond Cleavage of Aryl Alkyl Ethers by Iridium–Porphyrin and Rhodium–Porphyrin Complexes in Alkaline Media. *Organometallics* **2017,** *36*, 3456-3464.

[259] El-Faham, A.; Albericio, F. Peptide coupling reagents, more than a letter soup. *Chem. Rev.* **2011,** *111*, 6557-6602.

[260] Mitsunobu, O. The Use of Diethyl Azodicarboxylate and Triphenylphosphine in Synthesis and Transformation of Natural Products. *Synthesis* **1981,** *1*, 1-28.

[261] Mitsunobu, O.; Yamada, M. Preparation of Esters of Carboxylic and Phosphoric Acid via Quaternary Phosphonium Salts *Bull. Chem. Soc. Jpn.* **1967,** *40*, 2380-2382.

[262] Appel, R. Tertiary Phosphane/Tetrachloromethane, a Versatile Reagent for Chlorination, Dehydration, and P-N Linkage. *Angew. Chem., Int. Ed.* **1975,** *14*, 801–811.

[263] Malapit, C. A.; Ichiishi, N.; Sanford, M. S. Pd-Catalyzed Decarbonylative Cross-Couplings of Aroyl Chlorides. *Org. Lett.* **2017,** *19*, 4142-4145.

Curriculum Vitae

Curriculum Vitae
Runze Mao

PERSONAL INFORMATION

Date of birth: 21 November 1993   **ORCID:** 0000-0003-4678-7251

E-mail: _runzemaoepfl@gmail.com_   **ResearcherID:** AAD-1836-2020

EDUCATION, EMPLOYMENT, AND RESEARCH PROJECTS

❖ **Ph.D. candidate | Chemistry | EPFL, Switzerland**   07. 2016 – 07. 2020

- Ph.D. project: Aliphatic carboxylic acids as coupling partners in carbon-heteroatom bond-forming reactions. Advisor: Prof. Xile Hu

- Marie Sklodowska-Curie Initial Training Network project (675020-MSCA-ITN-2015-ETN)

❖ **M.Sc. | Chemical Biology | Peking University, China**   09. 2013 – 07. 2016

- Master's thesis: Light-driven C-S bond cleavage of thioglycosides and glycosylation reactions. Advisor: Prof. Xin-Shan Ye

- National Scholarship for Graduate students (China), Top 5%

❖ **B.Sc. | Chemical Biology | Henan Normal University, China**   09. 2009 – 07. 2013

- Bachelor's thesis: New methodology for assembly of bioactive heterocyclic compounds. Advisors: Prof. Gui-Rong Qu & Prof. Hai-Ming Guo

- National Scholarship for Undergraduate students (China), Top 1%

PUBLICATIONS IN PEER−REVIEWED SCIENTIFIC JOURNALS

1. Bera, S.†; **Mao, R.†;** Hu, X. Enantioselective $C(sp^3)$–$C(sp^3)$ Cross-Coupling of Non-activated Alkyl Electrophiles via Nickel Hydride Catalysis. *Nat. Chem.* **2020,** accepted for publication. († contributed equally)

2. **Mao, R.;** Bera, S.; Cheseaux, A.; Hu, X. Deoxygenative Trifluoromethylthiolation of Carboxylic Acids. *Chem. Sci.* **2019,** *10*, 9555-9559.

3. **Mao, R.;** Balon, J.; Hu, X. Decarboxylative $C(sp^3)$-O Cross-Coupling. *Angew. Chem., Int. Ed.* **2018,** *57*, 13624-13628.

4. **Mao, R.;** Balon, J.; Hu, X. Cross-Coupling of Alkyl Redox-Active Esters with Benzophenone Imines: Tandem Photoredox and Copper Catalysis. *Angew. Chem., Int. Ed.* **2018,** *57*, 9501-9504.

5. **Mao, R.;** Frey, A.; Balon, J.; Hu, X. Decarboxylative C(sp^3)–N Cross-Coupling via Synergetic Photoredox and Copper Catalysis. *Nat. Catal.* **2018,** *1*, 120-126.

6. **Mao, R.;** Sun, L.; Wang, Y.-S.; Zhou, M.-M.; Xiong, D.-C.; Li, Q.; Ye, X.-S. *N*-9 Alkylation of Purines via Light-Promoted and Metal-Free Radical Relay. *Chin. Chem. Lett.* **2018,** *29*, 61-64.

7. **Mao, R;** Xiong, D.-C.; Guo, F.; Li, Q.; Duan, J.; Ye, X.-S. Light-Driven Highly Efficient Glycosylation Reactions. *Org. Chem. Front.* **2016,** *3*, 737-743.

8. **Mao, R.;** Guo, F.; Xiong, D.-C.; Li, Q.; Duan, J.; Ye, X.-S. Photoinduced C-S Bond Cleavage of Thioglycosides and Glycosylation. *Org. Lett.* **2015,** *17*, 5606-9.

9. Guo, H.-M.*; **Mao, R.** (1st author w/o the corresponding author); Wang, Q.-T.; Niu, H.-Y.; Xie, M.-S.; Qu, G.-R. Pd(II)-Catalyzed One-Pot, Three-Step Route for the Synthesis of Unsymmetrical Acridines. *Org. Lett.* **2013,** *15*, 5460–5463.

PRIZES, AWARDS, AND FELLOWSHIPS

❖ Finalist for the Reaxys Ph.D. Prize, Elsevier.　　　　　　　　　　　　　　　10. 2019

❖ Chemistry Travel Award, Swiss Academy of Sciences (SCNAT).　　　　　　　04. 2018

❖ Ph.D. fellowship | Marie Sklodowska-Curie ITN project.　　　　07.2016 – 12.2019

❖ Excellent Graduate Award, Peking University, China.　　　　　　　　　　　06. 2016

❖ Ph.D. fellowship | Clarendon scholarship, Oxford University (declined).　　　04. 2016

❖ National Scholarship for Graduate students, China.　　　　　　　　　　　　11. 2015

❖ National Scholarship for Undergraduate students, China.　　　　　　　　　11. 2012

❖ "Challenge Cup" National Science and Technology competition (2nd prize,), China　10. 2011

❖ Youth Technology Innovation Award, Henan, China　　　　　　　　　　　　10. 2011

❖ "Toshiba Cup" China Normal University Innovation (2nd prize), China　　　　10. 2011

CONTRIBUTIONS TO INTERNATIONAL CONFERENCES

1. **Mao, R.;** Hu, X.* Decarboxylative C(sp^3)–Heteroatom Cross-Coupling via Synergetic Photoredox and Copper Catalysis. **Reaxys Ph.D. Prize Symposium (oral and poster presentations).** Amsterdam, the Netherlands. October 2019.

2. **Mao, R.;** Hu, X.* Decarboxylative C(sp^3)–Heteroatom Cross-Coupling via Synergetic Photoredox and Copper Catalysis. **XXII International Conference on Organic Synthesis (poster presentation).** Florence, Italy. September 2019.

3. **Mao, R.;** Hu, X.* Decarboxylative C(sp^3)–Heteroatom Cross-Coupling via Synergetic Photoredox and Copper Catalysis. **The Swiss Chemical Society Fall Meeting (poster presentation).** Bern, Switzerland. September 2017.

SECONDMENTS

1. Electrochemical Chlorination Reaction for Activated C(sp^3)-H Bonds. 04. 2019 − 07. 2019 (3 months). **Co-supervisor: Dr. Chris Scarborough, Syngenta, Switzerland.**

2. C(sp^3)-N Cross-Coupling for Strained Rings. 03. 2019 − 04. 2019 (1 month). **Co-supervisor: Prof. Dr. Miquel Costas, Universitat de Girona, Spain.**

3. Non-precious Photocatalysts for Decarboxylative Cross Coupling. 08. 2018 − 09. 2018 (1 month). **Co-supervisor: Dr. Henrik Junge, Leibniz Institute for Catalysis, Germany**.

4. Mechanistic Study of Decarboxylative C(sp^3)-N Cross Coupling. 08. 2017 − 09. 2017 (1 month). **Co-supervisor: Prof. Dr. Martin Albrecht, University of Bern, Switzerland.**

TEACHING ACTIVITIES

❖	Advanced general chemistry (I) | EPFL, Switzerland	2019–2020 (academic year)
❖	Structural analysis | EPFL, Switzerland	2018–2019 (academic year)
❖	General and analytical chemistry (II) | EPFL, Switzerland	2018–2019 (academic year)
❖	Organic chemistry | EPFL, Switzerland	2018–2019 (academic year)
❖	Biooriented chemical chemistry | EPFL, Switzerland	2017–2018 (academic year)
❖	Organic chemistry (I) | EPFL, Switzerland	2017–2018 (academic year)
❖	Project in molecular sciences | EPFL, Switzerland	2016–2017 (academic year)

SUPERVISION OF STUDENTS AND JUNIOR RESEARCHERS

❖ **Ms. Aurélya Christelle Turla | Swiss Apprenticeship Program**   04. 2019 – 06. 2020

- Research Project: Synthesis of *N*-fluoro substituted carboxamides and sulfonamides and their application in $C(sp^3)$-H activation.

❖ **Mr. Alexis Cheseaux | Swiss Apprenticeship Program**   04. 2018 – 06. 2019

- Research Project: Fe-Catalyzed alkyl radical addition.

❖ **Mr. Jonathan Balon | Swiss Apprenticeship Program**   04. 2017 – 06. 2018

- Research Project: Synthesis of redox-active esters and their application in cross-coupling reactions.

❖ **Mr. Adrian Frey | Master Project | EPFL, Switzerland**   02. 2017 – 06. 2017

- Research Project: Synthesis of redox-active esters and their application in cross-coupling reactions.